N. A. de Ridder, P. Hondius, A. J. Hellings

Institute for Land and Water Management Research, Wageningen

Hydrogeological investigations of the Peel region and its environs

1967 Centre for Agricultural Publications and Documentation

Wageningen

This publication is also issued as Technical Bulletin 48 of the Institute for Land and Water Management Research, Wageningen

Table of contents

Introduction

The Peel region is an area which covers the greater part of the provinces of Limburg and eastern Noord-Brabant in the south-east Netherlands (Map 1).

The use of groundwater for domestic, municipal, industrial and agriculture purposes is rapidly increasing and this makes it necessary to gain a better insight in the subsurface geology and hydrology of the region, as they pertain to the replenishment, discharge, storage and additional development of the groundwater.

HELLINGS (1958) has shown that large areas of arable land in north- and middle Limburg are suffering from dessication. In order to improve the water management of these dessicating soils a water supply scheme was developed, which includes pumping water from the river Meuse into existing canals and ditches. Apart from this scheme increasing use is made of groundwater pumped from deep wells for sprinkler irrigation. Besides the quality of the groundwater, for which each user has his own standards, the problem arises as to whether or not the increasing use of groundwater eventually could exceed the average annual recharge to the groundwater reservoir and substantially lower the regional water table.

To study these problems and for possible water supply and discharge projects this survey was made. Although many deep wells were made the work done was of a reconnaissance type. It includes studies of the subsurface geological conditions, geological structure, water-bearing formations aquicludes, formation constants, groundwater movement and quality.

Owing to the character of these investigations and the complex geological structure of the investigated region several detail problems could not be studied. Such problems can only be solved by making additional borings.

The authors are much indebted to all those who gave their help at the time these investigations were carried on. We are much indebted to our field assistents Mr. H. J. MEIJER and Mr. W. B. VERHAEGH who carried out the borings and pumping tests, and to Mr. E. VAN REES VELLINGA who described many samples lithologically.

During the course of the investigations we were kindly assisted by several institutions and surveys. The Geological Survey at Haarlem provided much aid by making many heavy mineral-, and palynological analyses. Grain size analyses were carried out by the Institute for Soil Fertility at Groningen. The Water Table Record Office TNO provided filter pipes so that nearly all borings could be installed as observation wells. The Governmental Institution for Drinking Water Supply at The Hague carried out the chemical analyses of many groundwater samples.

1 Stratigraphy

The Peel region is underlain by Neogene deposits, which during the Pleistocene period became covered by large sand- and gravel cones of the Rhine and the Meuse. These sediments of Pleistocene age have been the subject of several investigations for many years (ZONNEVELD, 1947; ZAGWIJN, 1957, 1960; ZONNEVELD, 1956). As a result of these investigations, the stratigraphy, petrology and palynology of this sedimentary mass are relatively well known. However the new borings have thrown more light on the occurrence distribution, and thickness of the various formations and in particular on the geological structure of the region. To distinguish the different formations such sedimentary characteristics as grain size, heavy mineral- and gravel composition, and lime content were studied. A number of palynological analyses enabled some of these formations to be dated more exactly.

Table 1 shows the various distinguished formations and the time-stratigraphic division of the Neogene and Quarternary as introduced by the above mentioned authors. Appendix I (A-Q) shows the geological sections.

1.1 Middle Miocene

The Middle Miocene transgression covered the greater part of the Netherlands. The coastline must have been in the neighbourhood of Roermond. North of this line Middle Miocene is present in marine facies and it consists of glauconite- and mica-bearing fine sand and clay.

Heavy minerals which are numerically important in the Middle Miocene sediments are garnet, epidote, green hornblende, and especially zircon (Fig. 1, borings P10, P27 and P122).

Owing to tectonic movements the top of this series is found at various depths. In certain areas on the Peelhorst it lies directly under the Pleistocene at 15 to 20 m above sea level. On the down-thrown blocks it lies much deeper ('Venlo graben'), whereas in the Roervalley graben Middle Miocene is found at 300 to 400 m below sea level.

The thickness of the series varies from 100 to 200 m on the Peelhorst till over 300 m in the Roervalley graben and 'Venlo graben'.

In the south-eastern part of the region Middle Miocene is present in continental facies, mainly developed as sand and clay with lignite measures. This series crops out east of Roermond, near Herkenbosch.

Table 1. Lithostratigraphy and chronology of the Pleistocene and Upper Tertiary according to Zagwijn *(1957, 1960) and* Zonneveld *(1958)*

<table>
<tr><th></th><th></th><th colspan="2">Lithostratigraphy</th><th>Chronology</th><th>Climate</th></tr>
<tr><td>Holocene</td><td></td><td></td><td rowspan="3">'Sand Diluvium'</td><td>Holocene</td><td>W</td></tr>
<tr><td rowspan="10">Pleistocene</td><td rowspan="4">Upper Pleistocene</td><td>'Well sands'</td><td>Weichselian</td><td>C</td></tr>
<tr><td>Grubbenvorst formation</td><td>Eemian</td><td>W</td></tr>
<tr><td colspan="2">Veghel formation</td><td>Saalian</td><td>C</td></tr>
<tr><td colspan="2">Rosmalen zone</td><td>Holsteinian</td><td>W</td></tr>
<tr><td rowspan="2">Middle Pleistocene</td><td colspan="2" rowspan="2">Sterksel formation
(Budel, Woensel, Weert
and Sterksel zones)</td><td>Elsterian</td><td>C</td></tr>
<tr><td>Cromerian</td><td>W</td></tr>
<tr><td rowspan="4">Lower Pleistocene</td><td colspan="2" rowspan="2">Kedichem formation</td><td>Menapian</td><td>C</td></tr>
<tr><td>Waalian</td><td>W</td></tr>
<tr><td rowspan="2">Tegelen formation</td><td>Tegelen clay</td><td>Eburonian</td><td>C</td></tr>
<tr><td></td><td>Tiglian</td><td>W</td></tr>
<tr><td rowspan="3">Tertiary</td><td rowspan="2">Pliocene</td><td colspan="2" rowspan="2">Kieseloolite
formation</td><td>Praetiglian</td><td>C</td></tr>
<tr><td>Reuverian
Brunssumian
Susterian</td><td>W</td></tr>
<tr><td>Middle Miocene</td><td colspan="2">Reinbeker Stufe
Hemmoorer Stufe</td><td>Tortonian
Helvetian/
Burdigalian</td><td></td></tr>
</table>

MINERALS

garnet	volcanic minerals (augite, basaltic hornblende titanite, hypersthene, olivine)
epidote	topaz
saussurite + alterite	other minerals
hornblende (green, brown, alkali)	staurolite
hornblende (vosges)	metamorphic minerals
chloritoid	tourmaline

LITHOLOGY	CLAY AND SILT (< 16μ)	
very fine sand	0– 2%	peat
fine sand	2– 5%	plant remains
coarse sand	5–10%	humus
very coarse sand	10–20%	peaty
gravel	20–40%	wood
	> 40%	charcoal lumps of browncoal

Sa = Sand Diluvium
Well = Well sands
Grub = Grubbenvorst formation
Veg = Veghel formation
Ros = Rosmalen zone
Ste = Sterksel zone }
Bud = Budel zone } Sterksel formation
Woe = Woensel zone }
Wee = Weert zone }
Ked = Kedichem formation

Teg = Tegelen formation
Praetigl = Praetiglian
Kies = Kieseloolite formation
Mio = Miocene (marine + continental)

N.A.P. = mean sea level
P10 well number, archives I.C.W. Wageningen
52B/21 well number, archives Geol. Survey Haarlem

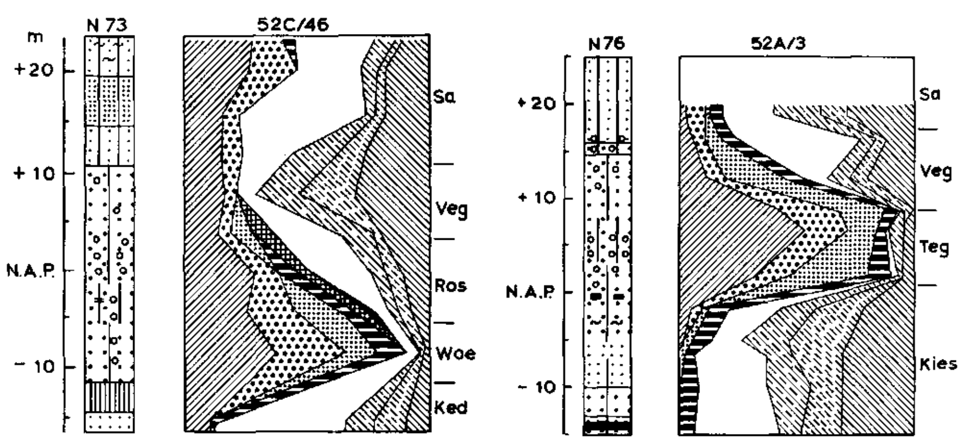

Fig. 1a Heavy mineral composition and lithology of borings N73 and N76.

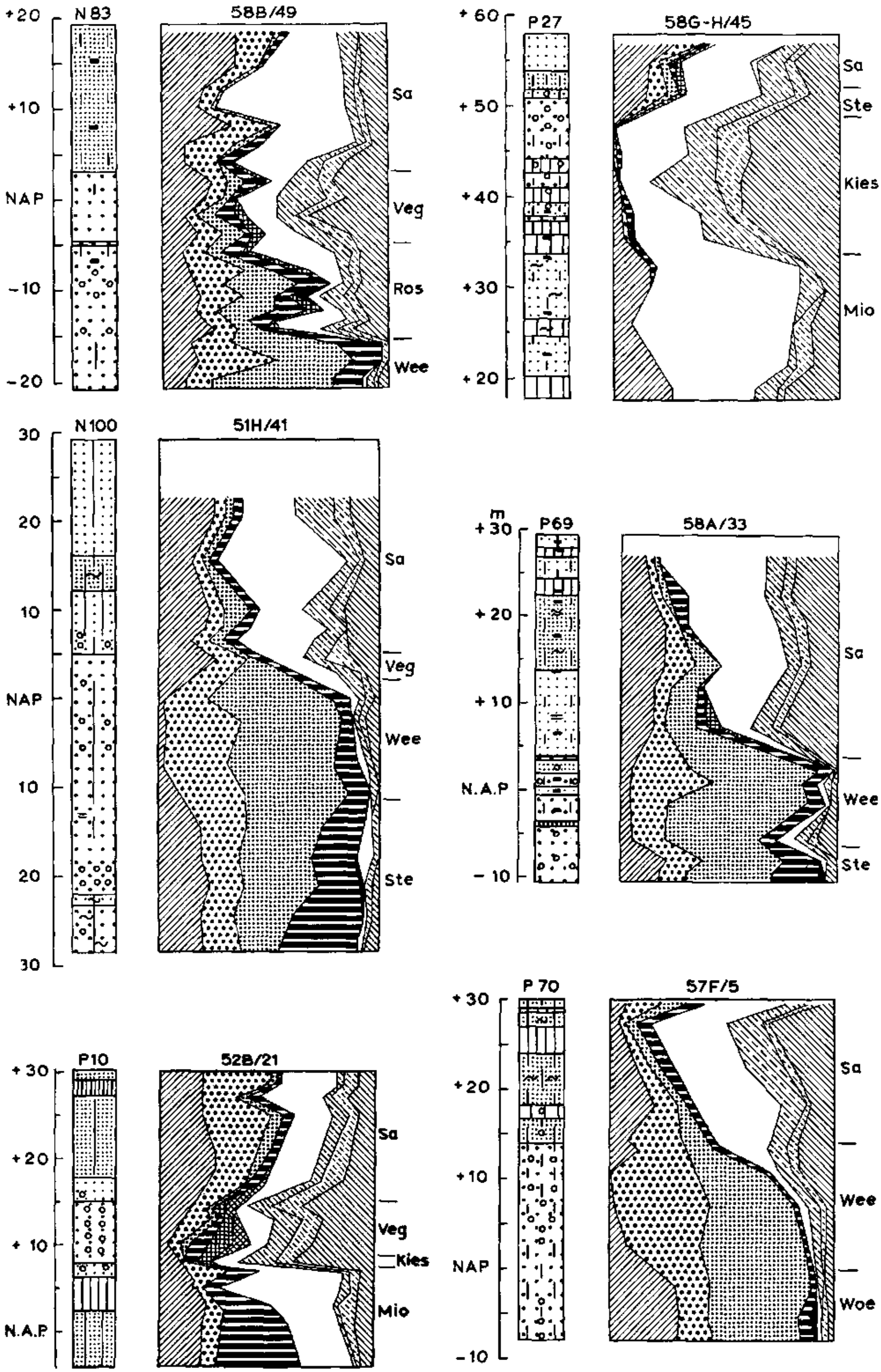

Fig. 1b Heavy mineral composition and lithology of borings N83, N100, P10, P27, P69 and P70.

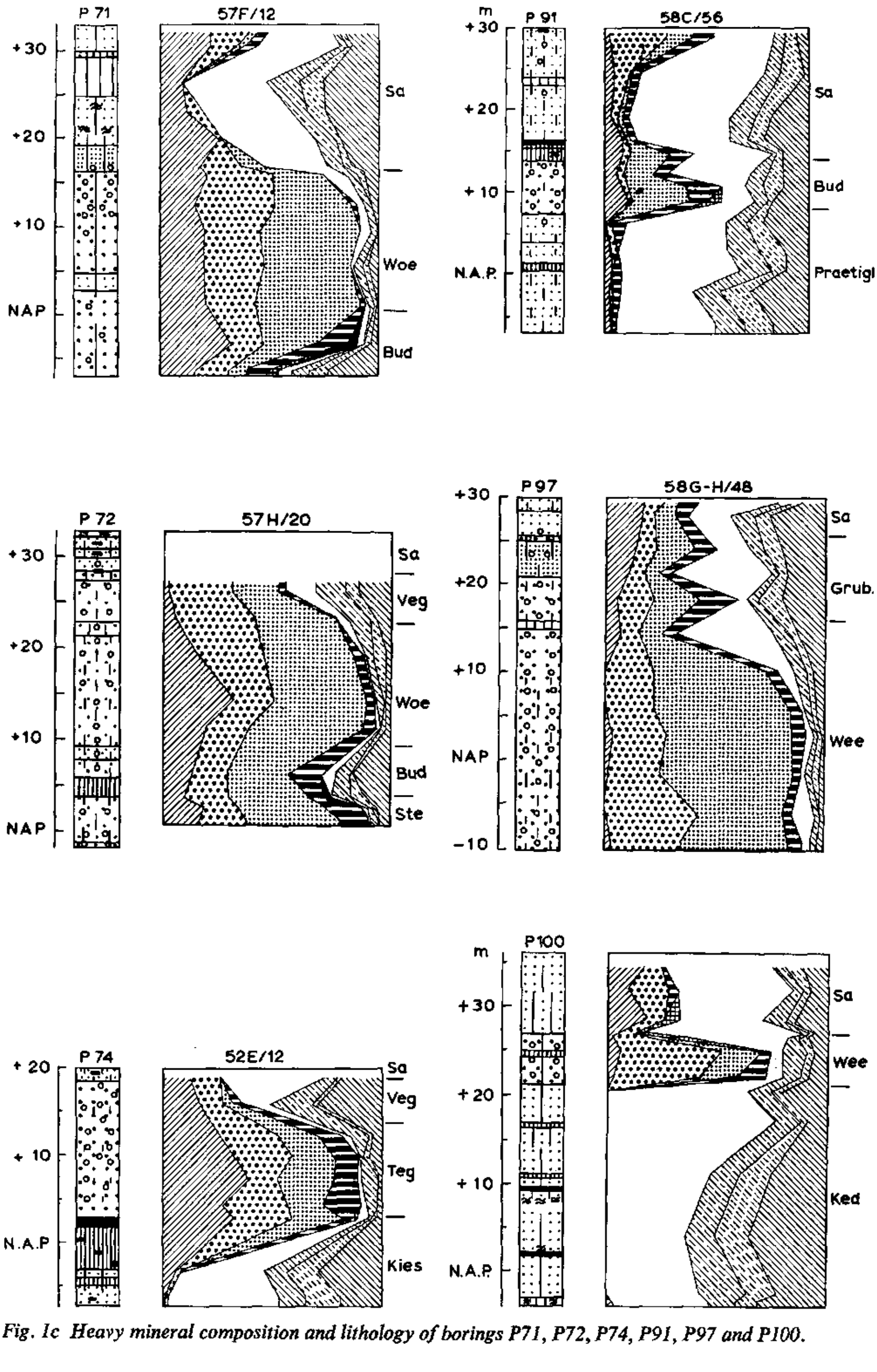

Fig. 1c Heavy mineral composition and lithology of borings P71, P72, P74, P91, P97 and P100.

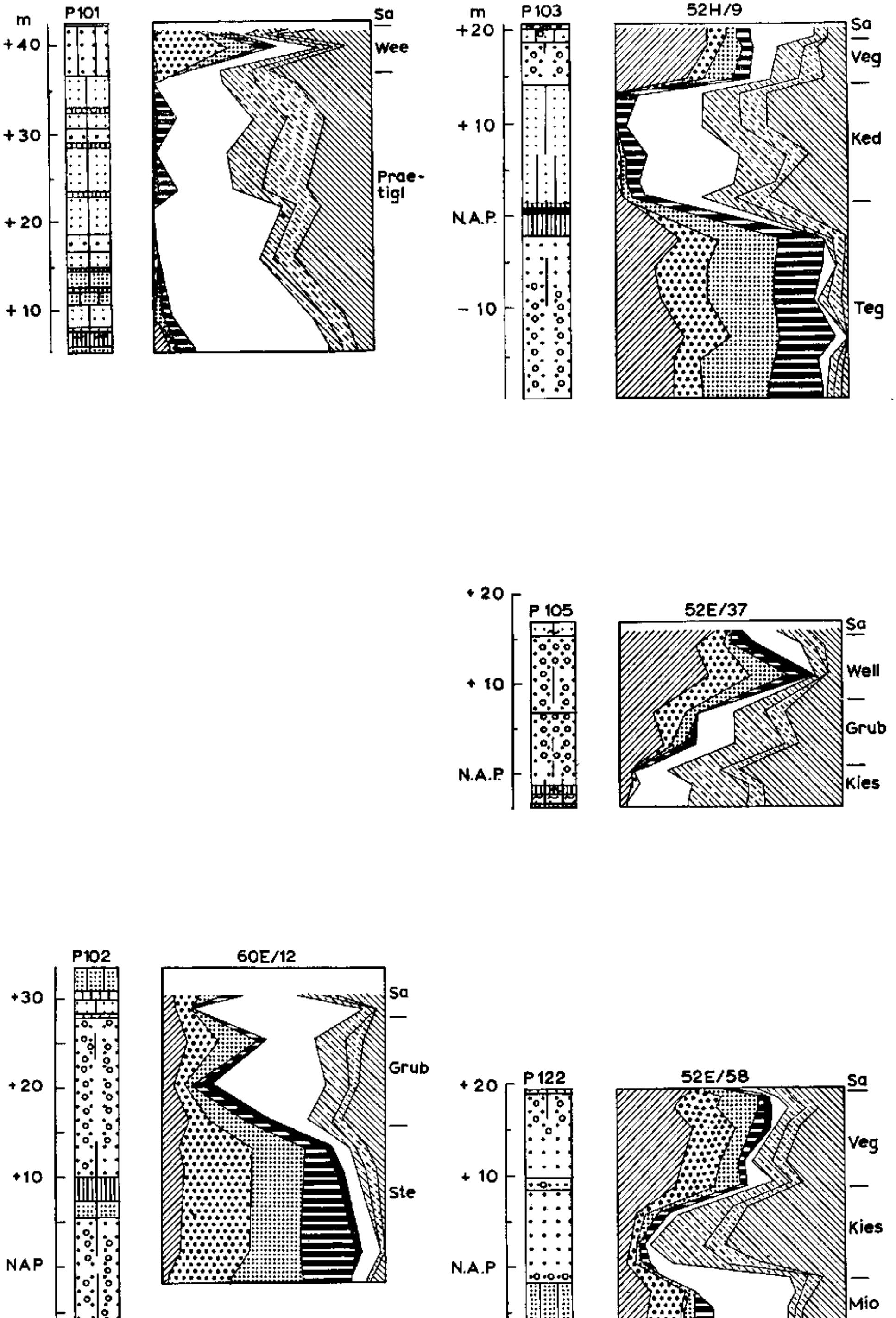

Fig. 1d Heavy mineral composition and lithology of borings P101, P102, P103, P105 and P122.

1.2 Kieseloolite formation

At the end of the Miocene the sea retreated from these regions and henceforward sedimentation was exclusively continental. During the subsequent Pliocene period there was fluviatile aggradation and the Kieseloolite formation came into being (VAN STRAATEN, 1946; ZAGWIJN, 1960; ZONNEVELD, 1947).

This formation consists of light- and dark-grey fine sand, coarse, gravel-bearing sand and humic clay beds. The heavy mineral assemblage chiefly consists of such minerals as tourmaline, metamorphic minerals zircon and rutile (Fig. 1, borings P10, P27, P122, P105, N76 and P74).

ZAGWIJN (1960) was able to distinguish three stages in the Pliocene part of the formation, but these were not indicated in our geological sections due to lack of enough data.

The bulk of the Kieseloolite formation lies at a great depth in the Roervalley graben, where it reaches a considerable thickness. East of the Peel boundary fault these deposits are found at shallow depths and in varying thicknesses. The greatest thickness (60 à 90 m) is reached on the downthrown blocks, e.g. 'Venlo graben'. On the upthrown blocks, however, the deposits are only a few metres thick or at some places even entirely absent.

1.3 Praetiglian

The Praetiglian represents the first Pleistocene Glacial stage in these regions. Paleobotanical investigations have revealed a subarctic parklandscape during that time. Praetiglian follows directly the time of deposition of the Reuver clay which represents the youngest part of the Pliocene (ZAGWIJN, 1960).

Praetiglian deposits are thought to be present in the south-eastern part of the region, near Susteren, Koningsbosch, Stevensweert and Stramproy (sections K-K', L-L', M-M', J-J', and Map 2).

The deposits consist chiefly of fine sand and clays which are rich in humic matter.

Heavy minerals present in these sands include tourmaline, metamorphic minerals, and especially zircon (Fig. 1, borings P91 and P101).

The basis of the Praetiglian lies at 15 m below sea level at maximum; the top at 15 m above sea level, except at the upthrown block of Koningsbosch where the top is found at 36 m above sea level (boring P101, profile M-M').

1.4 Tegelen formation

At the end of the Praetiglian the climate gradually improved, indicating the beginning of the first interglacial of the Pleistocene period, the so-called Tiglian. During this interglacial the Tegelen formation came into being.

It consists of coarse, sometimes gravel-bearing sand and clay, the latter being the well known Tegelen clay. The Tegelen formation is chiefly present in the Venlo-Tegelen area. ZONNEVELD (1947) has pointed out that it is also found at a few places on the Peelhorst.

The heavy minerals of the sands consist of epidote, hornblende, saussurite and particularly high percentages of garnet (Fig. 1, borings N76, P74, and P103). This association, typical of Rhine sediments, is in striking contrast to the heavy-mineral assemblage of the underlying Kieseloolite formation. By means of this kind of investigations its presence could be proved on the Peelhorst near Venray, Horst and Milheeze, places where the formation was hitherto unknown (Map 2).

The Tegelen formation is also found in the Roervalley graben where it lies at about 90 m below sea level (near Veghel and Rosmalen).

1.5 Kedichem formation

ZONNEVELD (1947) drew attention to the fact that on top of the Tegelen formation fine grained deposits occur with a heavy mineral assemblage different from that of his so-called Tegelen-zone. Amongst the minerals which are numerically important this author mentioned tourmaline metamorphic minerals, rutile, zircon. In some cases such minerals as garnet, epidote, hornblende and saussurite are entirely absent, indicating that the sediments have been deposited by the Meuse (Fig. 1, borings P103, P100 and N73). These Meuse deposits are indicated as the Kedichem formation. Paleobotanical investigations enabled ZAGWIJN (1960) to distinguish two glacials, viz. Eburonian and Menapian, separated by an interglacial, the so-called Waalian. Owing to lack of data this subdivision was not extended to the geological sections. However, a number of palynological analyses of clay samples from different places gave the impression that most of the clays belong to the Waalian interglacial.

The Kedichem formation is present in the Roervalley graben where the top dips from 20 m below sea level in the south-east to 60 m below sea level in the northwest. South of the Beegden fault the top lies about at sea level, whereas on some upthrown blocks it is found at 25 to 30 m above sea level. Till now the formation is not found on the Peelhorst, west of the Meuse. East of the Meuse it is present at several places, e.g. near Venlo, Velden, Meinweg, where the top is found at 25 to 35 m above sea level.

1.6 Sterksel formation

The Kedichem formation is covered by sediments of the Sterksel formation which has been dealt with in detail by ZONNEVELD (1947). It consists mainly of coarse, gravel-bearing sands deposited by the Rhine and to a minor part by the Meuse. These sediments are correlated with those of the 'Hauptterrasse' in the Lower Rhine embayment, whereas synchronous Meuse deposits are found on the Pietersberg terrace in South-Limburg (ZONNEVELD, 1958).

Originally four zones, based on differences in heavy mineral composition, were distinguished by ZONNEVELD, namely the zones of Sterksel, Budel, Woensel and Weert. These zones were also found in some of our new borings, e.g. in N83, P69, P70, P71, P72, P97, P100, P102 and N100 (Fig. 1). Later they have been compiled under the name Sterksel formation, as was also done in our geological sections.

The age of these sediments is still partly known. According to DOPPERT and ZONNEVELD (1955), the Sterksel formation is probably of "about Mindel (= Elster) age". This view was corroborated by the discovery of Needian (= Elster – Saale interglacial) deposits on top of the formation at Rosmalen (l.c. 1955). Later investigations showed that at least part of the formation is of Cromerian age (ZAGWIJN and ZONNEVELD, 1956). Part of the formation will date, therefore, from the Elster glacial.

The geological sections show that the formation is only found in the Roervalley graben, and in some areas east of the Meuse and south of the Beegden fault. In these latter areas it lies at the surface or at shallow depth (see also Map 2).

Owing to tectonic movements during deposition the thickness of the formation varies considerably. The bulk of the sediments are found, however, in the Roervalley graben, where the thickness varies from 25 to 60 m. The top of the formation dips here from 15 m above sea level in the southeast to 20 m below sea level in the northwest.

1.7 Rosmalen zone

During the Holsteinian (Elster – Saale Interglacial) the Rhine gradually disappeared from these regions and its function was taken over by the Meuse. In between the Sterksel formation (Rhine sediments) and the overlying Veghel formation (Meuse sediments) a transition layer was found consisting of fine and coarse sands and humic clays. The sands of this layer consist of a mixture of Rhine and Meuse heavy minerals, indicating the contribution of both rivers to the origin of this layer (Fig. 1, borings N73 and N83). Since the clays could be proved to be of Holsteinian age, DE RIDDER and ZAGWIJN (1962) termed this mixture of Rhine and Meuse deposits 'Rosmalen zone'.

Its occurrence is probably mainly confined to a narrow zone in the Roervalley graben along the Peel boundary fault. The thickness of this zone varies from a few meters to more than 10 m.

1.8 Veghel formation

During the Saalian the Rhine took a more easterly course and sedimentation in these regions was exclusively by the Meuse. In a wide valley, reaching from the neighbourhood of Helmond in the west to the German boundary in the east, the Meuse deposited mainly coarse, gravel-bearing sand, known as the Veghel formation (Map 2).

The heavy mineral composition of this formation is characterized by such Meuse-minerals as Vosges hornblende and chloritoid (Fig. 1, borings P10, P122, N76, P74, P72, N83 and N73). On the Peelhorst the formation is found at shallow depth and at some places such as near Meijel, Milheeze, Liesel it lies even at the surface. In the Roervalley graben the formation is covered by 20 to 25 m thick fine sands and loamy sands.

In the area east of the Meuse the occurrence of the formation is chiefly confined to the areas north of Roermond and Venlo. The thickness shows fairly considerably areal variations, but it can generally be stated to be 8 to 10 m.

1.9 Grubbenvorst formation

After deposition of the coarse sandy Veghel formation the Meuse began to degenerate. The river took, however, a more easterly course and still during the Saalian it cut a relatively narrow valley at approximately the place of the present course. Later this valley, which had a depth to about sea level, was filled up by coarse, gravel-bearing sands. These sediments were named by ZONNEVELD (1947) 'Grubbenvorst zone'. Synchronous Rhine sediments were indicated as 'Kreftenheije zone'.

Clay layers found in these zones appeared to vary in age from Eemian to Weichselian (ZONNEVELD, 1956; ZAGWIJN, 1961).

Along the present course these coarse sands are covered by Holocene clay and sand deposits. At a greater distance the covering layer mainly consists of fine sand.

The thickness of the formation varies generally from 5 to 10 m, but in the southern part of the region a thickness of about 20 m was found.

1.10 Well sands

ZONNEVELD (1956) drew attention to the occurrence of augite-bearing sands in the area north of Arcen. These sands would be younger than the Veghel formation and older than the Grubbenvorst formation.

Augite-bearing sands were found in boring P105 (section A-A') where they are lying on top of the Grubbenvorst formation, and thus must be younger than this formation. Near Wanssum, west of the Meuse, ERNST and DE RIDDER (1960) found traces of augite-bearing sands, overlying a peat layer which could be dated by ZAGWIJN (1961) as Amersfoort Interstadial (first interstadial of the Weichselian).

The sands are coarse-grained and gravel-bearing; their areal distribution seems to be limited.

1.11 Sand Diluvium

The entire complex of fine sand, loamy sand, sandy loam, and loam, covering the Veghel and Grubbenvorst formations is designated 'Sand Diluvium'. During the late Saalian most of the Meuse stream channels were filled up with a sequence of sediments grading upward from coarse, gravel-bearing sands into progressively finer deposits of sands, silt and silty loam.

Some peat layers found at a few metres below the surface could be dated as Eemian (Saale-Weichsel Interglacial) BURCK (1956); MENTE (1961). Thus, the greater part of the 'Sand Diluvium' originates from the Saalian.

The upper part of the 'Sand Diluvium' consists of cover sands which were chiefly deposited during the Late Weichselian. These cover sands sometimes dammed the valleys and during the Holocene these topographic depressions or swamps were filled with vegetation, fairly extensive areas of peat being formed.

The thickness of the 'Sand Diluvium' varies from 0 to 25 m. The greatest thickness is found in the Roervalley graben.

2 Grain size

To study the texture of the various sediments grain-size analyses of most of the samples from the new P- and N-wells were made and statistical parameters were derived, recorded and compared.

The specific surface area or U-figure is often used in Holland to indicate the average grain size. The U-figure is defined as the ratio between the total surface area of all particles and the surface area of an equal quantity by weight of particles of the same material having a diameter of 1 cm, it being assumed that the particles are spheroidal.

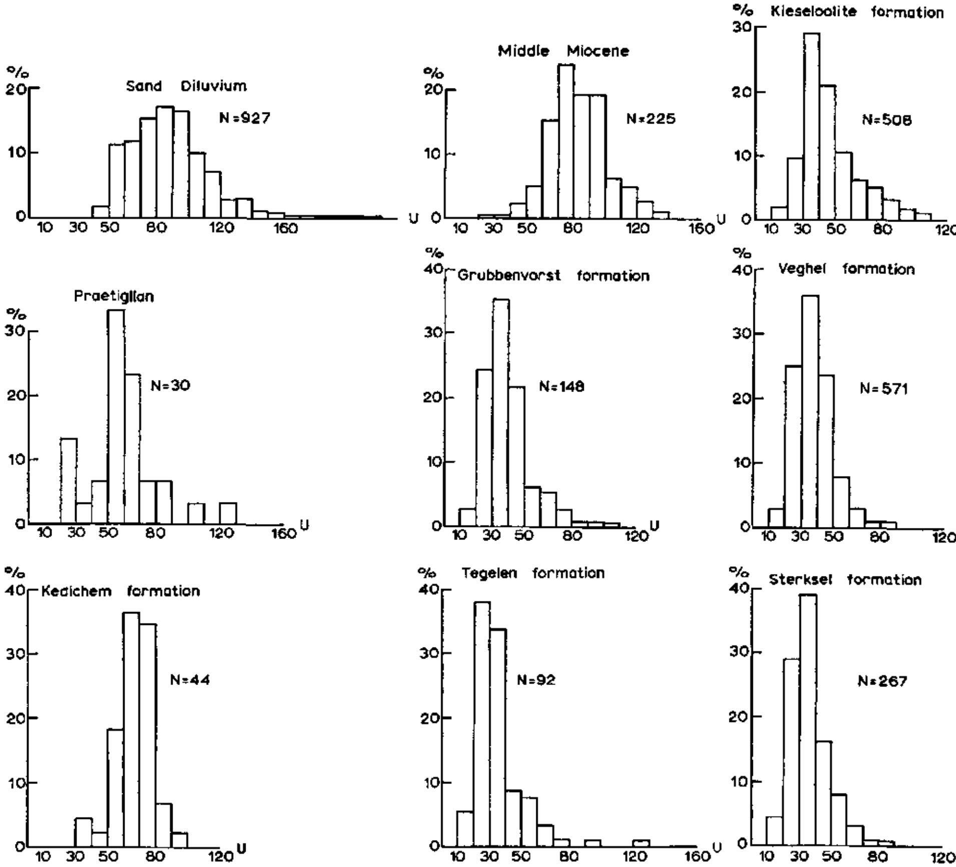

Fig. 2 Frequency distribution of U-figures of the sands from the various geological formations.

Sands with U-figures smaller than 50 are termed coarse, and those with U-figures larger than 50 are termed fine sands. Each group is subdivided, so that the U-figure forms a basis for classification of sandy material (Table 2).

Table 2. Classification of sand according to the U-figure

Name of the sand	U (of the sand fraction)	Specific grain size ($\frac{10}{U}$ mm)
Extremely fine sand	625–160	0.016–0.063
Very fine sand	160–120	0.063–0.083
Middle fine sand	120– 80	0.083–0.125
Moderately fine sand	80– 50	0.125–0.200
Moderately coarse sand	50– 30	0.200–0.333
Middle coarse sand	30– 20	0.333–0.500
Very coarse sand	20– 10	0.500–1.000
Extremely coarse sand	10– 5	1.000–2.000

Fig. 2 shows the histograms of the grain-size frequency (U-)distribution of sands from the main geological formations in the investigated area. From this figure it can be concluded that the Grubbenvorst-, Veghel-, Sterksel-, Tegelen- and Kieseloolite formations consist of predominantly moderately- and middle coarse sands. The Sand Diluvium, Middle Miocene, Kedichem formation and Praetiglian are characterized by moderately- and middle fine sands.

It is interesting to note that some of the Meuse deposits show U-frequency distributions similar to that of some Rhine deposits (Veghel-, Grubbenvorst formations and Sterksel-, Tegelen formations).

For detailed information of the grain-size distribution of the various geological formations the reader may be referred to Appendix II.

3 Structural geology

Since the geologic structure of the region has been dealt with in more detail in two recent papers (DE RIDDER, 1959; DE RIDDER and LENSEN, 1960) this subject will be summarized.

The investigated region forms part of the buried block-faulted landscape of the south-east Netherlands. Three major tectonic elements can be distinguished (Map 2):

1. Roervalley graben
2. Peelhorst
3. Stevensweert-Susteren horst

The Roervalley graben is bounded in the east by the Peel boundary fault and in the west by the Feldbiss.

The Peelhorst is the upthrown block east of the Peel boundary fault; topographically it can be recognized as a broad ridge running through North Limburg in southeast-northwest direction. It is broken by several subsidiary faults of more or less importance, giving rise to several fault blocks which have now different positions. A relatively heavily sunken part is the 'Venlo graben', extending from Venlo in the direction of Venray.

The two other major tectonic elements are also characterized by several subsidiary faults, as is shown on the geologic map 2. The most characteristic feature of the fault system is the phenomenon of bifurcation of the main faults. The branch faults sometimes run parallel to the main fault and join the latter at a certain distance of the point of bifurcation (Meijel fault, Veghel fault (?), Griendtsveen fault).

The fault system probably originated at the end of the Permian and had a period of maximum activity during the Late Cimerian, between the Lower Jurassic and the Cretaceous and another period of activity in the Upper Tertiary (DE SITTER, 1949). The latter can be clearly seen in the geologic sections which show great variations of depth and thickness of the Kieseloolite formation.

But even the Pleistocene period may be described as a period of crustal unrest, since most of the major faults were active during this period. Even the Upper Pleistocene Veghel formation has been displaced from 15 to more than 20 m along the Peel boundary fault and the Veghel fault.

It can be concluded from earthquakes reported in these regions in historical times that even to-day tectonic activity has not altogether ceased (AHORNER and VAN GILS, 1963).

As regards the character of the faults, it is usually stated that normal faulting due to lateral tension is the actual cause of the fracture pattern of the Peel region (DE

SITTER, 1949; 1956). DE RIDDER and LENSEN (1960) preferred the theory of transcurrent faulting as the explanation of this fault system. This theory provides a simpler and possibly truer explanation of many phenomena such as bifurcating and joining faults, accompanied by pitching grabens and horsts, steep pitching wedges, as near Griendtsveen, the south-easterly pitching Miocene abrasion surface in the 'Venlo graben', the steepness of the fault planes in the Tertiary formations, 70° to 80° (ERNST and DE RIDDER, 1960), and many others.

Reversal of movement during the various periods of tectonic activity is well-known in these regions (DE SITTER, 1949; PANNEKOEK, 1956). It is also known that faults changing laterally or vertically from normal to reverse faults probably have a predominantly strike-slip movement. Statistical evidence showing the preference of earthquakes for transcurrent faults has been furnished by SCHEIDEGGER (1959).

Several fault systems in other parts of the world, usually regarded as normal faults, were actually found to be transcurrent faults (HAITES, 1960).

For the adjoining German regions AHORNER (1962) does not stand the above mentioned theory of transcurrent faulting as an explanation for the fault system on German territory. However, horsts and grabens may also be formed by horizontal movements along fault planes, as is shown by LENSEN (1958). RITSEMA (1960) has recently discussed the recognition of fault type from the seismic evidence available. He has concluded: "Pure normal, pure reverse and pure transcurrent fault motions only rarely occur. Mostly there is a smaller or greater transcurrent component in mainly normal or mainly reverse fault motions and also a smaller or greater normal or reverse component in the mainly transcurrent fault motions". The conclusion that only dip-slip movement occurred seems a little prematurely. To verify this conclusion it will be necessary to prove the absence of strike-slip movement.

4 Hydrogeological subdivision

For practical purposes the subsurface geological data should be converted to a hydrogeological scheme. In this connection a survey should be given of the occurrence, distribution and thickness of the water-bearing formations, the covering semi-permeable layers and confined layers and of the depth of the impervious basement

4.1 Depth of the impervious basement

As 'impervious' basement we consider those layers which owing to their lithological composition have a low or very low permeability. Such layers are:

- Middle Miocene
- Kedichem formation

The Middle Miocene is found throughout the entire region, but as impervious basement it is only of importance on the Peelhorst, east of the Peel boundary fault.

Attention has already been drawn on the areal variations in depth of this series, which is due to the tectonic activity in the past. Near Meijel Miocene is found at 30 m above sea level and west of Venlo at 60 m below sea level.

On fault blocks bounded by parallel running faults the depth of the Miocene surface is fairly constant. Where a fault bifurcates or two faults join this Miocene surface dips ('Venlo graben', Sevenum – and Baarlo block).

In the Roervalley graben the top of the Middle Miocene lies at 300 to 400 m below sea level and as the Kedichem formation consists chiefly of fine sand with clay layers on top this formation may here be considered as the impervious basis layer. It is found at various depths, e.g. near Roermond at 20 m below sea level, near Heythuizen and Helmond at 60 m below sea level.

It should be noted that at several places clay horizons were found in the overlying water-bearing formations, e.g. Reuver- and Tegelen clays. For local problems these clay layers cannot be neglected.

4.2 Water-bearing formations

The following formations can be considered as real aquifers:

- Grubbenvorst formation
- Veghel formation

- Sterksel formation
- Tegelen formation
- Kieseloolite formation

Owing to large variations in areal distribution and thickness, these formations are of variable importance as aquifers. Since their areal distribution is limited the Tegelen and Grubbenvorst formations have only local importance. The Kieseloolite formation is an important aquifer on the downthrown blocks of the Peelhorst e.g. in the 'Venlo graben', Sevenum block. However, clay horizons may reduce its importance.

In the Roervalley graben the Sterksel formation is widespread and as its thickness may reach 40 to 55 m it is one of the most promising aquifers.

Although widespread the Veghel formation is of limited importance as an aquifer because its thickness seldom exceeds 10 m.

From the geological sections it can be concluded that the aquifers generally consist of a combination of two or more of the above mentioned formations. In one area these are the Veghel and Kieseloolite formations (Peelhorst), in another area the Veghel and Sterksel formations (Roervalley graben).

The total thickness of the water-bearing formations is shown on Map 3. This map shows the net total thickness of the aquifers. The variations in thickness are closely related to the tectonics of the region. Small thicknesses occur on the Peelhorst. On some downthrown blocks the thickness gradually increases in south-easterly direction ('Venlo graben', Sevenum, Griendtsveen blocks). In the Venlo-Velden area the aquifer reaches even a thickness of 90 to 100 m.

A second important area is the Roervalley graben, where 30 to 80 m water-bearing material is found above the Kedichem formation. Under this formation the Tegelen and Kieseloolite formations are very important water-bearing horizons.

To summarize the above it can be stated that for groundwater exploitation the *Roervalley graben* and the '*Venlo graben*' must be considered as the most promising areas.

Since the aquifer on the Peelhorst is fairly thin this area seems unsuitable for large-scale groundwater exploitation.

4.3 Semi-permeable covering layers

The coarse-sandy, water-bearing formations are covered by 'Sand Diluvium', consisting of fine sand, sandy loam and loam. A knowledge of the thickness of these covering strata is of importance because it shows the depth at which the top of the aquifer can be found, whereas on the other hand an impression can be obtained of the vertical resistance of the covering strata (vertical resistance $c = D_1/k_1$ where D_1 = thickness of the covering stratum and k_1 = vertical hydraulic conductivity).

Map 4 shows an isopach map of the 'Sand Diluvium'. It appears that in the area east of the Meuse and at some places of the Peelhorst the covering stratum is thin or even completely absent. In the IJsselsteijn-Griendtsveen-Horst area the thickness varies from 10 to 15 m.

In the Roervalley graben the 'Sand Diluvium' is 15 to 25 m thick, but in a narrow zone between Meijel and Nederweert 32 m was found. These great thicknesses were caused by tectonic movements during deposition of at least part of the 'Sand Diluvium'.

5 Determination of some geohydrological characteristics

As a part of these investigations special attention was given to the determination of such geohydrological characteristics of the surface and subsurface layers as the transmissibility (kD-value) of the aquifers, vertical resistance ($c = D_1/k_1$) of the semi-pervious layers, specific yield of the covering layers. The present knowledge on these characteristics is based both on data of former studies and on the results of special field and laboratory tests carried out for this investigation. The methods applied are described hereafter and the results obtained are discussed.

5.1 Vertical resistance (c-value)

Quantitative data on the vertical resistance of semi-permeable layers in these regions are scarce. Some data are available from the catchment area of the Lollebeek in North Limburg, where ERNST (1958) found c-values varying from 100 to 600 days, calculated from pumping tests near well P12. In well P14 loam layers are absent; c-values vary from 5 to 10 days. Where in the upper 3 to 4 m loam layers are present c-values may vary from 100 to 300 days for this part of the profile. In a similar area south of Eindhoven ERNST (1956) calculated c-values varying from 50 to 400 days.

As the vertical resistance $c = D_1/k_1$, any changes in the thickness (D_1) or vertical hydraulic conductivity (k_1) of the covering strata will be reflected in the c-value. Both hydraulic conductivity and thickness of the covering strata change from one area to the other (Map 4). For this reason c-values may vary from a few days to over 1000 days throughout the entire region.

5.2 Specific yield

With regard to the specific yield of the covering strata very little is known. ERNST (1958) found values of 0.15 to 0.20 for the catchment area of the Lollebeek in North Limburg, calculated from data on the annual fluctuations of the groundwater table and the precipitation surplus. For the western and eastern part of the catchment area mean values of 0.17 and 0.25 respectively are mentioned.

5.3 Transmissibility

The transmissibility of the aquifers (kD-value, product of horizontal hydraulic conductivity in m/day and thickness of the aquifer in m) was determined according to different methods, viz.:

a. from the grain size distribution of disturbed samples
b. from logs of old borings by estimation
c. from pumping test data

a. It is well known that particle diameter of the sand and hydraulic conductivity are closely related. FAHMY (1961) recently discussed this relationship and showed that at a porosity of 0.40 the proportionality factor between k and $1/U^2$, or in other words, for the product kU^2 varied according to several investigators from 31×10^3 to 71×10^3.
For the present calculations a value of 50×10^3 was used, as this gave results which were in fairly good agreement with those obtained from pumping tests.
For each sample with a low clay content the hydraulic conductivity was calculated, and since clay plus silt, gravel and sorting of the sand fraction influence the hydraulic conductivity in different ways, corrections were made for each of these parameters. Since the thickness of each sampled layer is known, the transmissibility of each layer can be found by multiplying conductivity by thickness. The transmissibility of the aquifer can be determined by summing all values obtained for the whole sequence of coarse layers. Next to each bore hole in the geological sections the transmissibility values, calculated by the above method, are shown for each formation. The transmissibility of the entire aquifer is indicated under each boring. It should be noted that the obtained results are not in all cases very reliable. Sometimes the results were in very good agreement with those of pumping tests, in other cases substantial differences were found. For this reason the figures are given with some reservations; they give only an order of magnitude of the transmissibility.

b. Since no grain size analyses were available of old wells the transmissibility of the aquifer in such wells was estimated from the well logs. It will be clear that these figures are not more than rough estimations, especially when the quality of these old logs was poor. The thickness of the aquifer was in such cases the only reliable datum.

c. The most reliable results are obtained from pumping tests, but since such tests are fairly expensive their number was limited to six. Most of these tests were made in the catchment area of the Lollebeek near the boring P12 (two tests), P14, P35, P11 and P112 (Map 1). In the Hydrogeological Archives at The Hague another ten pumping tests are known, carried out in the past for different purposes. The results of these 16 pumping tests are given in Table 3. In this table kD-values calculated

Table 3. Some formation constants calculated from pumping test data and grain-size distribution

Location	Number of test (archives)	Well number	Transmissibility from pumping test (m^2/day)	Transmissibility from grain size (m^2/day)	Vertical resistance c (days)	$\lambda = \sqrt{kD.c}$ (m)
Vlierden	50		2200			
Grubbenvorst	94		775		116	300
Linne	27		1650 to 5200			
Linne	21		2360 to 3200		12 to 60	150 to 500
Maasbracht	79		4900		18	300
Montfort	101		930			
Born	68		8			25
			840			1430
Weert	118		3400			
Belfeld	115		475			
Linne	113		2900		7	
			2600			
Meerselse Peel		P35	1100	2000		
Venlen		P111	250	470		
Lorbaan		P12^{I}	1000	1200		
Lorbaan		P12^{II}	110			
			2000			
Castenray		P14^{II}	330	1300		
			700			
Wanssum		P112	1050	1750		
			400			

from grain size data are also given. In some cases these values are double those of the pumping tests, others are, however, in fairly good agreement with the results of the field tests.

Based on the results of these 16 pumping tests and on the results of calculations from grain size data at over 130 places a transmissibility map of the entire region was compiled (Map 5). Although we are well aware of the relative value of this map for the above mentioned reasons, it still gives an impression of the order of magnitude of this formation constant.

The following classification of the transmissibility was used:

kD (in m^2/day)	
<250	very low
250– 500	low
500–1000	moderately high
1000–2000	high
>2000	very high

As the transmissibility equals the product of hydraulic conductivity and the thickness of the aquifer, any changes in those properties will be reflected in the transmissibility. Both hydraulic conductivity and thickness of the aquifers vary widely throughout the region, partly due to tectonic reasons (faulting) partly due to the fluvial origin of the aquifers.

A fairly close relationship appears to exist between the geological structure and the transmissibility. The lowest kD-values are found on the Peelhorst where the aquifer is relatively thin. The higher values which occur on this horst have generally also tectonic causes. These higher values are generally found on downthrown blocks, where the aquifer is much thicker than on the upthrown blocks.

High transmissibility values need not always have a tectonic cause, as is shown by the results of two pumping tests on the Peelhorst, near boring P12. The high value (2100 m^2/day) is caused here by the very permeable coarse sands which are encountered at this place.

Generally speaking, however, it can be stated that high and very high transmissibility values are found in the grabens (Roervalley and Venlo grabens), where the thickness of the aquifers are much larger than on the Peelhorst.

The map shows also the kD-values obtained from the 16 pumping tests. As can be seen these figures do not always fit the class indicated on the map. For instance near Grubbenvorst the map shows an area where the transmissibility is higher than 2000 m^2/day, whereas the result of the pumping test was 775 m^2/day. This great difference need not imply a great inaccuracy in the calculation method according to the grain size of the sands. From section E-E' it can be seen that in this area the Pliocene is covered by thick clay beds. The pumping test was carried out in the aquifer overlying this clay bed, so that the figure of 775 m^2/day is related to this upper aquifer and not to both aquifers of which the total kD-value exceeds 2000 m^2/day. The map shows the transmissibilities of the entire water-bearing formation overlying the Miocene or the Kedichem formation. Since the clay layers within the aquifer are generally lenticular in shape, they were not taken into consideration

In the area west of the Peel boundary fault the Kedichem formation is accepted as the impervious basis layer, since at many places clay layers were found in the upper part of this formation. However, is some cases clay layers are completely absent and coarse sand is found to a great depth. Pumping tests at such places will yield higher kD-values than are shown on the map. This is probably the main cause of the high values obtained from pumping tests near Linne and Maasbracht, which are considerably higher than the values indicated on the map, the latter relating exclusively to the waterbearing formations overlying the Kedichem formation.

It should also be noted that little is known about the depth of the Kedichem formation in this area; it was estimated from some distant deep wells. The same can be said of other areas, e.g. the Roervalley graben, where neither the depth of this formation, nor the lithology and permeability of the lower parts of the water-bearing formation are sufficiently known. Owing to this lack of data it will be clear that the transmissibility values for these areas are not more than rough estimations.

Summarizing, it can be said that due to generally low transmissibility values the Peelhorst is less suitable for large-scale groundwater exploitation. In this respect the Roervalley graben and 'Venlo graben', which are sharply bounded by faults, are more suitable.

6 Piezometric surface and direction of groundwater movement

The principal factors that control the shape and slope of the phreatic water table are the topography of the land surface and the underlying bedrock, the transmissibility of the materials through which the groundwater moves, the relative location of areas of recharge and discharge from the groundwater reservoir, and the relative rates of recharge or discharge.

It is not intended to discuss here the configuration of the phreatic surface and the depth to groundwater table since HELLINGS (1958) described these subjects in detail. Hitherto little attention has been given, however, to the piezometric levels in these regions, except the northern part of Limburg for which ERNST (1958) and ERNST and DE RIDDER (1960) published an isopiezometric map.

This map was extended for the entire region and the result is shown in Map 6. To compile this map two-monthly records of P- and N-wells and some other deep wells were used. These data were provided by the Water Table Record Office, T.N.O. at The Hague. The water levels of the Meuse and some small rivers were obtained from the Service for Water Management at The Hague. The map shows the average piezometric surface for 1958.

A groundwater divide extends from Helden and Helenaveen in the direction of IJsselsteijn, with a mound in the Helden-Helenaveen area. This divide coincides approximately with the topographical highest parts of the Peelhorst, one of the major tectonic elements of the region. The low permeable Miocene deposits are found here at relatively shallow depth.

From the Peelhorst the groundwater moves in easterly direction to the Meuse and in westerly to north-westerly direction to east Noord-Brabant. The present flow direction is thus also closely related to the Cenozoic geological structure of the region.

There is much further evidence of the tectonical influence on the configuration of the piezometric surface and on the groundwater movement. From the map it can be seen that the slope of the piezometric surface varies substantially, but generally it amounts to 1:1000 to 1:1200. In some areas the slope is much larger or smaller. A small slope is found on the divide. Steep to very steep slopes of 1:100 to 1:200 also occur, for instance on the left bank of the Meuse, near the village of Neer. From this village in north-westerly direction to Deurne the piezometric surface shows pressure anomalies at rather short distances, e.g. near the villages of Meijel and Deurne. The phenomenon of these anomalous steep slopes has been studied by VISSER (1948) and ERNST and DE RIDDER (1960). It was shown that steep slopes of the groundwater table are found along faults. The anomalies near Neer, Meijel and Deurne are caused by the Peel boundary fault, those near Wanssum by the Velden and Venlo faults. The most probably explanation is that the fault plane is more or less sealed off by clay layers. During tectonical movements of two adjacent fault blocks these clay layers are bent, or even broken and thus plaster the fault plane. Such fault planes act as a subterranean barrier and as the fault planes are usually fairly steep (dips of 70° to 80°) they are extremely resistant to horizontal groundwater flow. At short distance differences in piezometric head up to several metres can be found.

The groundwater flow is not always influenced by faults, as is shown by the Tegelen fault. The slope of the piezometric surface along this fault does not show any anomalies. It should not be excluded, however, that additional investigations along this and other faults will reveal more of these anomalous steep slopes.

In the Neer-Venlo area the Meuse crosses the Peel boundary fault almost perpendicular. The considerable shift in the contour lines near Neer is remarkable. It is difficult to decide whether the steep slopes in the piezometric surface at this place are exclusively caused by tectonic displacements along this fault. At the moment there is no geological evidence for a fault running north-south on the left bank of the river.

Since the greater part of the region is located on a divide and no influx to the groundwater reservoir takes place from adjacent regions, and recharge of the aquifer is thus only by precipitation, the amount of water that can ultimately be produced from the aquifer is limited. As has already been pointed out, the amount of water to be produced on the Peelhorst cannot be increased without the danger of substantially lowering the regional water table.

7 Chemical quality of the groundwater

As part of this investigation the chemical composition of the groundwater from the various water-bearing formations was determined. A total number of 222 analyses were available, 149 of these are water samples from the new P- and N-wells, 73 analyses are from old wells, present in the archives.

To describe the composition of the groundwater and the relationships among the ions in solution, the analyses are expressed as well in milligrams per litre as in milligram equivalents per litre and in percentages of total anions and cations in equivalents per litre, the sum of the equivalents per litre being 100%.

The analyses represented by bar graphs based on per cent of total equivalents per litre are indicated in the geological sections under each well.

For classification of the groundwaters these bar graphs are less suitable and for that reason the Piper-diagram was used (PIPER, 1944), see Fig. 3. In this diagram the overall chemical character of the water as represented by the relationships among the Na+K, Ca+Mg, CO_3+HCO_3 and Cl+SO_4 ions is indicated by a single point plotting. The graph has percentage scales reading in 100 parts (% m. val).

Certain distinct types of water can be quickly discriminated by their plotting in certain subareas of this diagram.

As pointed out previously, the water-bearing formation in these regions is not homogeneous, but is composed of geological formations of different age, origin and mineralogical composition. These formations occur in different combinations throughout the region. Owing to absence of dividing clay horizons of large extent the different aquifers are generally interconnected. For this reason it is not expected at first instance to find such clear-cut relationships between eventual water types and distinguished geological formations.

Table 4. Distribution of water samples over the various geological formations

Formation	Number of analyses
Sand Diluvium	9
Grubbenvorst formation	27
Veghel formation	67
Sterksel formation	47
Tegelen formation	9
Kieseloolite formation	42
Middle Miocene	3

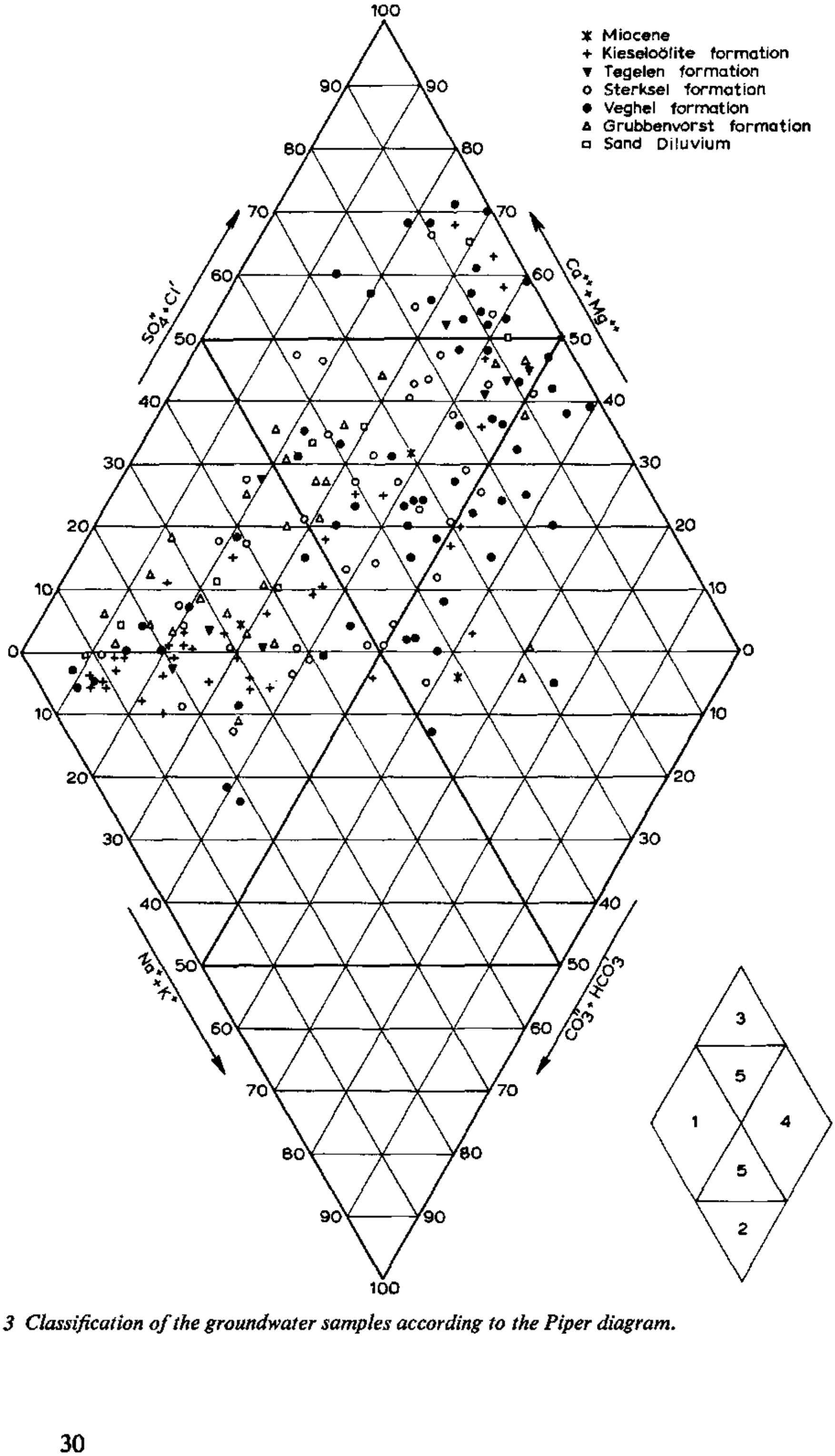

Fig. 3 Classification of the groundwater samples according to the Piper diagram.

The distribution of the analyses over the various formations was determined; samples from the boundary of two formations were omitted. The distribution of the remaining 204 samples is shown is Table 4.

7.1 Evaluation of the results

The Piper diagram is divided in five sub-areas each representing a distinct chemical character.

Area 1: Secondary alkalinity ('carbonate hardness') exceeds 50 per cent, viz. the chemical properties of the water are dominated by alkaline earths and week acids.
Area 2: Primary alkalinity ('carbonate alkali') exceeds 50 per cent, here plot the waters which are inordinately soft in proportion to their content of dissolved solids.
Area 3: Secondary salinity ('non-carbonate hardness') exceeds 50 per cent.
Area 4: Primary salinity ('non-carbonate alkali') exceeds 50 per cent, viz. the chemical properties are dominated by alkalies and strong acids. Ocean water plot in this area.
Area 5: None of the cation-anion pairs exceeds 50 per cent.

From the diagram it can be concluded that four types of groundwater are present in these regions, one type gradually passing into the other.

Type A: This is the calcium bicarbonate type, characterized by temporary or carbonate hardness. A large number of the analyses belongs to this type (Area 1).
Type B: This type is characterized by permanent or non-carbonate hardness. Among the dissolved solids calcium, sulphate and chloride dominate. Compared with type A its occurrence is fairly limited (Area 3).
Type C: This is the non-carbonate alkali type. Among the dissolved solids sodium, sulphate and chloride dominate. Its occurrence is also limited (Area 4).
Type D: This is a transition type. A large number of analyses belong to this type of water (Area 5).

The diagram also shows that no clear relationship exists between chemical character of the groundwater and the geological formations. This is because most of the aquifers are interconnected and mixing of unlike waters render the situation very complex.
In Table 5 the percentage distribution of the analyses of waters from the Kieseloolite-, Veghel -, Sterksel -, and Grubbenvorst formations over the five sub-areas of the Piper diagram are indicated.
From this table it could be concluded that groundwater type A (calcium bicarbonate type) tend to occur chiefly in the Kieseloolite and Grubbenvorst formations. In the

Table 5. Percentage distribution of water analyses over the five sub-areas of the Piper diagram

Formation	Sub – areas					Number of samples
	1	2	3	4	5	
Kieseloolite formation	*64*	0	10	10	16	42
Veghel formation	24	0	21	25	*30*	67
Sterksel formation	32	0	6	15	*47*	47
Grubbenvorst formation	*52*	0	0	14	34	27

Veghel formation all four water types are represented in approximately equal percentages. Water types A and especially D are chiefly found in the Sterksel formation. For a positive statement about such relationships much more analyses should be available.

Since the aquifers consist of fluvial deposits it is difficult to explain why relatively high percentages of water samples show characteristics of primary salinity. The relatively high percentages m. val sodium and chloride, as found in a water sample from the Middle Miocene are understandable because this series is of marine origin, whereas the sluggish circulation of water in these clay-bearing fine sands is probably the reason why these salts were not completely removed by flushing.

Some of the water samples from the Kieseloolite formation show the same characteristics. These samples are all collected in the north of the region, where the Pliocene coast line has been traced. The primary salinity of the samples can therefore be due to the nearshore facies of the formation in this part of the region.

It is also noteworthy that a fairly high percentage of water samples from the Veghel- and Sterksel formations are characterized by relatively high concentrations of calcium, sulphate and chloride, thus showing permanent (non-carbonate) hardness. The origin of this water in these formations (Rhine- and Meuse deposits) is difficult to explain.

Generally speaking it can be stated that the groundwater in the investigated region is soft, having a total hardness of less than 8 °D. Moderately hard groundwater (8-16 ° D) is found near Posterholt, Roggel, Horn, near Grubbenvorst, north-west of Meijel, and south-west of Gemert. Only two wells (739/33 and 751/17) yield very hard water >16 °D).

8 Groundwater quality in relation to agricultural use

The quantity of water used for sprinkler irrigation is very large. For an average supply of 100 mm the quantity of water needed amounts to 1000 m^3 per hectare.

Water to be used for sprinkler irrigation is subject to quality limitations. On the other hand the water, which is chiefly pumped from deep wells, may contain distinct elements which are essential to proper plant nutrition. For that reason the available analyses will be evaluated with regard to the toxic and nutritious constituents of the groundwater.

8.1 Toxic constituents

Among the toxic constituents in the waters iron (Fe) and chloride (Cl) are of much interest.

In horticulture in particular considerable damage can be caused if the crops are irrigated with water containing more than 3 mg Fe per litre. In agriculture concentrations even up to 15 or 20 mg Fe per litre did not seem to cause any damage to the crops. During the dry summer of 1959, however, the crops showed brown colouring. Experience has learned that aluminium and galvanized steel pipes were corroded sooner if water with high iron concentrations was used.

Little is known about the damaging effect of chloride. ROORDA VAN EYSINGA (1961) pointed to the damage at horticultural crops caused by chloride. Other investigations have shown that serious damage may be caused if water is used, having a pH less than 4.5 and a chlorid concentration of 50 to 80 mg per litre (NOTA no. 12, Instituut voor Cultuurtechniek en Waterhuishouding). The average chlorid concentration in 274 samples amounts to 32.2 mg per litre, 21.5 per cent of the analyses have chlorid contents of 50 mg per litre or higher.

8.2 Fe-content of the groundwater

The total number of Fe-analyses available is 262, of which 143 are waters from the new P- and N-wells, whereas the remaining 119 were taken from the records.

To study the areal distribution of the Fe-concentrations and to find out whether or not any relationship exists between Fe-content of the water and the geological formations, the analyses are arranged according to the various formations. Taking into

Table 6. Iron concentrations of waters from various geological formations

Formation	Fe-classes (mg/1)					Number of analyses
	<3	3-6	6-15	15-30	>30	
Sand Diluvium	1	2	3	0	1	7
Grubbenvorst formation	12	9	13	2	1	37
Veghel formation	16	15	34	24	7	96
Sterksel formation	12	9	23	6	1	51
Kedichem formation	0	2	3	0	0	5
Tegelen formation	0	3	5	4	0	12
Kieseloolite formation	10	11	22	5	1	49
Middle Miocene	1	1	0	2	1	5
	52	52	103	43	12	262

account of the significant limit of 3 mg per litre, as used in horticulture, the Fe-concentrations are subdivided in five classes (Table 6).

This table shows that the groundwater is generally rich in iron. Only 52 of 262 samples have concentrations less than 3 mg Fe per litre. Groundwater from the Veghel formation shows variable concentrations of iron, but seems to be more rich in iron than that from the Sterksel and Kieseloolite formations, which have more or less similar percentage concentrations. Low to medium Fe-concentrations tend to occur in the groundwater from the Young Pleistocene Grubbenvorst formation.

8.3 Areal distribution of Fe-concentrations

The areal distribution of Fe-concentrations is shown in Fig. 4. At first sight the map shows a fairly arbitrary distribution of Fe-concentrations, although certain areas are characterized by high concentrations, e.g. North Limburg. On the other hand extreme high and low concentrations are found sometimes at short distances.

A closer inspection of the areal distribution of Fe-concentrations in groundwater from the Veghel formation reveals a clear relationship with the geological structure of the region, which, as has been pointed out previously, consists of three tectonic elements (Roervalley graben, Peelhorst, 'Venlo graben', the latter being a part of the Peelhorst).

When we consider the three main Fe-classes <3, 3–15 and >15 mg Fe per litre, then the analyses are arranged as shown in Table 7.

This table shows clearly that medium to high Fe-concentrations are chiefly found on the Peelhorst, whereas low to medium concentrations dominate in the Venlo- and Roervalley graben.

The most credible source of the higher concentrations of iron on the Peelhorst is the underlying marine Miocene series. The Veghel formation lies directly on this series

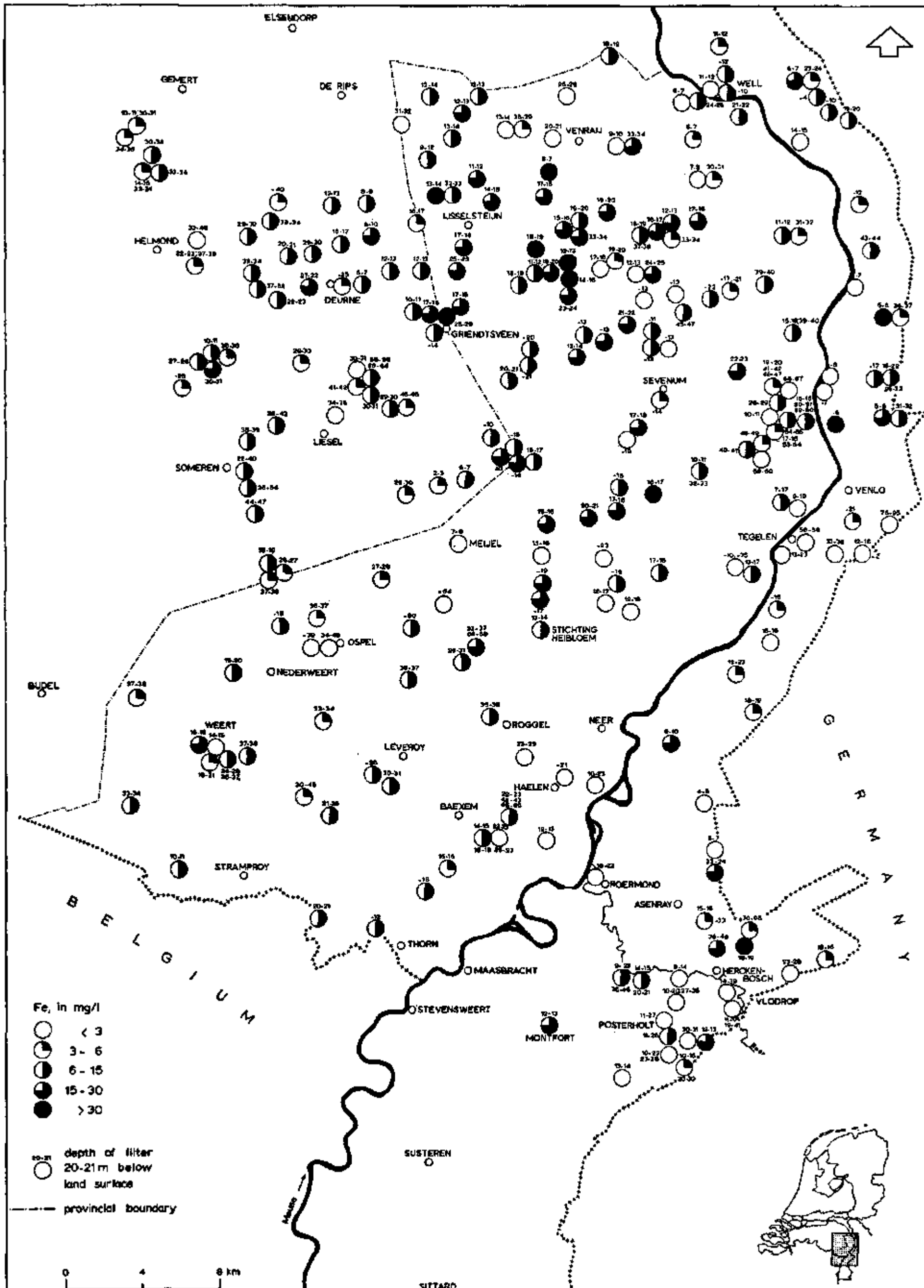

Fig. 4 Areal distribution of Fe-concentrations in the groundwater.

Table 7. Percentage distribution of analyses from the Veghel formation over the three main Fe-classes

Tectonic element	Fe-classes (mg/l)			Total number of analyses
	<3	3-15	>15	
Roervalley graben	10	86	4	22
Peelhorst	15	43	42	56
'Venlo graben'	44	31	25	18

or is separated from it by a thin layer of Pliocene. The Miocene sediments are very rich in glauconite ($K_2O \cdot 2\,MgO \cdot 3\,(Fe,\ Al)_2O_3 \cdot 12\,SiO_2 \cdot 6H_2O$) which owing to its chemical composition may be one of the main sources of iron. Iron is an important constituent in glauconite, as can be seen in Table 8, showing the weight percentages of FeO and Fe_2O_3 in this mineral (see also BENTOR and KASTNER, 1965).

The most probable source of the high concentration of iron in the Veghel waters on the Peelhorst is therefore, this underlying glauconite-bearing Miocene.

In the Roervalley and Venlo grabens the Miocene is deep to very deep and between this series and the Veghel formation thick layers of Pliocene and Pleistocene age are intercalated. This explains the relatively low Fe-concentrations of the Veghel water in these graben areas.

With regard to the water from the *Sterksel formation* chiefly present in the Roervalley graben, it can be stated that medium high Fe-concentrations dominate. High concentrations are found near Herkenbosch, Asenray and Stichting Heibloem, low concentrations are present near Posterholt, Vlodrop, Haelen, Weert, Ospel, Liesel and Helmond. At Weert Fe-concentrations in this formation were found to increase downward over a distance of 20 m from less than 3 to 15 mg per litre.

The *Kieseloolite formation* is characterized by medium to high Fe-concentrations. Low concentrations are found in the neighbourhood of Venlo and Tegelen and at some places in north Limburg e.g. near Venray. Where high concentrations occur these may partly be due to a direct contact of this formation with the underlying iron-bearing Miocene.

The groundwater from the *Grubbenvorst formation* seems generally to be less rich

Table 8. Percentages of FeO and Fe_2O_3 in glauconite

Analyses	Fe_2O_3	FeO	Origin
1	28.12	0.94	Israel
2	24.34	1.65	Israel
3	18.80	3.98	U.S.A.
4	18.00	3.10	U.S.A.
5	6.17	3.87	Germany

in iron; low to medium concentrations dominate. The areal distribution of the Fe-concentrations is fairly arbitrary.

8.4 Nutritious constituents

Among the nutritious constituents in groundwater Ca, Mg, P, N and K are of interest, and in certain cases also Mn can be added to this range.

The mean concentrations of these constituents for a number of 215 groundwater samples were calculated and the results are shown in Table 9.

Table 9. The mean concentrations of the most important salts in the deep groundwater in mg/l

CaO	MgO	P_2O_5	N	K_2O*	Na_2O*
39.3	8.6	0.4	1.6	39.9	26.3

* Calculated as 100% K_2O and 100% Na_2O respectively from the analysed alkali-concentration

The concentrations in milligrams per litre correspond to the number of kilograms per 100 mm of irrigation water per hectare. To get an impression of the fertilizing effect of sprinkler irrigation from groundwater, some data relating to the mean annual consumption of the main nutrients by crops are shown in Table 10. The lowest figure refers to rye, the highest to sugar beet. The figures in parentheses refer to the mean consumption as can be expected with the crop rotation generally applied in the investigated region.

Table 10. The mean yearly consumption of some nutrients by agricultural crops in kg per ha

CaO	MgO	P_2O_5	N	K_2O
9-104	8-77	25-82	50-226	52-350
(30)	(17)	(39)	(83)	(137)

It is clear that only the quantities of CaO, MgO and K_2O are of any importance. In only 8 cases a N-concentration was found of about 10 mg per litre in which the nitrogen is present as nitrate. In nearly all other analyses nitrogen is present as ammonia.

The real quantity of K_2O in the groundwater is in most cases of less importance than could be concluded from Table 9, because in general the alkali ions are composed of sodium, unless a certain quantity of nitrate is present. This was only found in 29 out of 263 samples. On the other hand K_2O can be partly substituted by Na_2O for such crops as sugar beets.

The concentration of CaO in 100 mm irrigation water should correspond to approximately the yearly consumption. However, the annual supply may be increased tenfold in order to raise the pH, especially on sandy soils.

The natural precipitation can also supply a small amount of nutrients in the soil (Table 11).

Only CaO and MgO are of some importance. The quantity of nitrogen equals approximately the quantity leached down every year. Nitrogen is chiefly present in the form of ammonia.

The variation in the salt concentration can be very large in the neighbourhood of the sea or chemical industries.

Table 11. The concentration of salts in the mean annual precipitation of 700 mm in kg per ha

CaO	MgO	N	Cl
16.8-24.5	9.1-19.7	5-6.5	22.4-113.4

8.5 Ca-content of the groundwater

The total number of Ca-analyses available is 206, of which 146 refer to the new P- and N-wells, the remaining 60 being taken from the records.

The analyses were arranged according to the various geological formations, and the Ca-concentrations are subdivided in five classes.

As can be seen in table 12, there seems to be no clear-cut relationship between the Ca-concentrations and the distinguished geological formations. The groundwater from the Grubbenvorst formation seems to be more rich in calcium than the waters from the Veghel formation. The remaining analyses generally belong to the middle classes.

Table 12. CaO-concentrations of waters from various geological formations

Formation	CaO-classes (mg/l)					Number of analyses
	<10	10-20	20-50	50-100	>100	
Sand Diluvium	0	1	0	3	1	5
Grubbenvorst formation	1	4	8	11	4	28
Veghel formation	17	20	28	9	2	76
Sterksel formation	3	11	20	8	2	44
Kedichem formation	0	0	0	2	0	2
Tegelen formation	0	1	6	0	0	7
Kieseloolite formation	4	8	19	11	0	42
Middle Miocene	0	2	0	0	0	2
	25	47	81	44	9	206

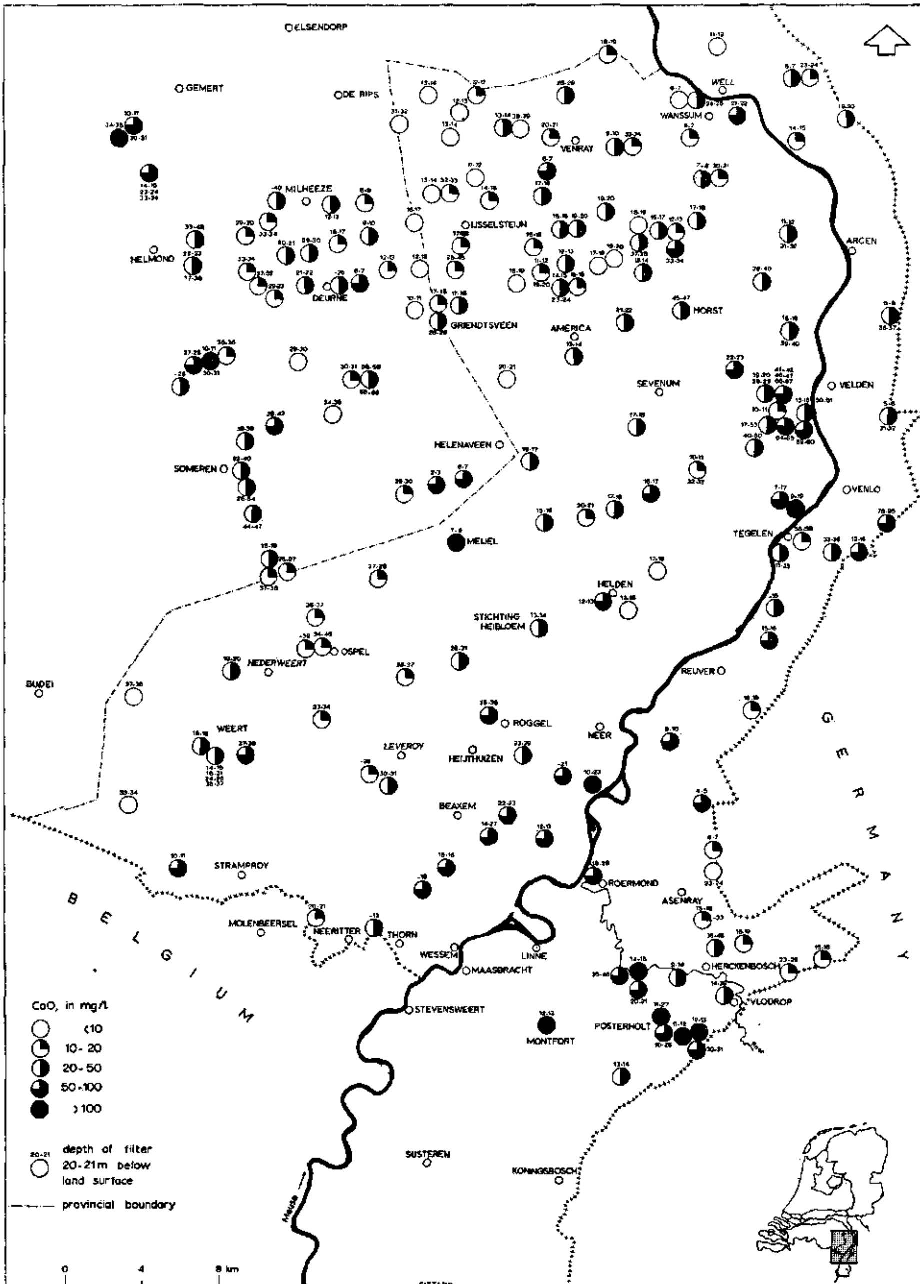

Fig. 5 Areal distribution of CaO-concentrations in the groundwater.

8.6 Areal distribution of CaO-concentrations

The areal distribution of CaO-concentrations is shown in Fig. 5. Although at first sight the distribution seems to be fairly arbitrary there still is a certain relationship with the geological structure of the region. Medium high to high CaO-concentrations are found in the Roervalley graben and the 'Venlo graben'. Low to very low values occur locally on the Peelhorst, running NW-SE, via IJsselsteijn, Helden, Reuver to Herkenbosch. Low values are also found to the west of Weert and remarkably in a narrow zone in the Roervalley graben near the villages of Gemert, Ospel and Neerritter.

8.7 Mg-concentration of the groundwater

The total number of Mg-analyses available is 206, of which 146 refer to the new P- and N-wells, the remaining 60 being taken from the records.

In this case also the analyses were arranged according to the various geological formations, and the Mg-concentrations are subdivided in five classes (Table 13).

Table 13. MgO-concentrations of waters from various geological formations

Formation	MgO-classes (mg/1)					Number of analyses
	<2	2-5	5-10	10-20	>20	
Sand Diluvium	0	2	1	1	1	5
Grubbenvorst formation	2	7	12	6	1	28
Veghel formation	2	15	32	20	7	76
Sterksel formation	2	16	14	12	0	44
Kedichem formation	0	1	1	0	0	2
Tegelen formation	0	0	5	1	1	7
Kieseloolite formation	1	20	10	8	3	42
Middle Miocene	0	1	1	0	0	2
	7	62	76	48	13	206

As can be seen in this table, the distribution of the samples over the different classes does not show much variation for the various geological formations. The middle classes usually predominate. The Kieseloolite waters tend to be less rich in magnesium than the Veghel and Sterksel waters.

8.8 Areal distribution of Mg-concentrations

The areal distribution of Mg-concentrations indicated in Fig. 6 shows to a certain degree a similar picture as that of the Ca-concentrations. In general it can be stated

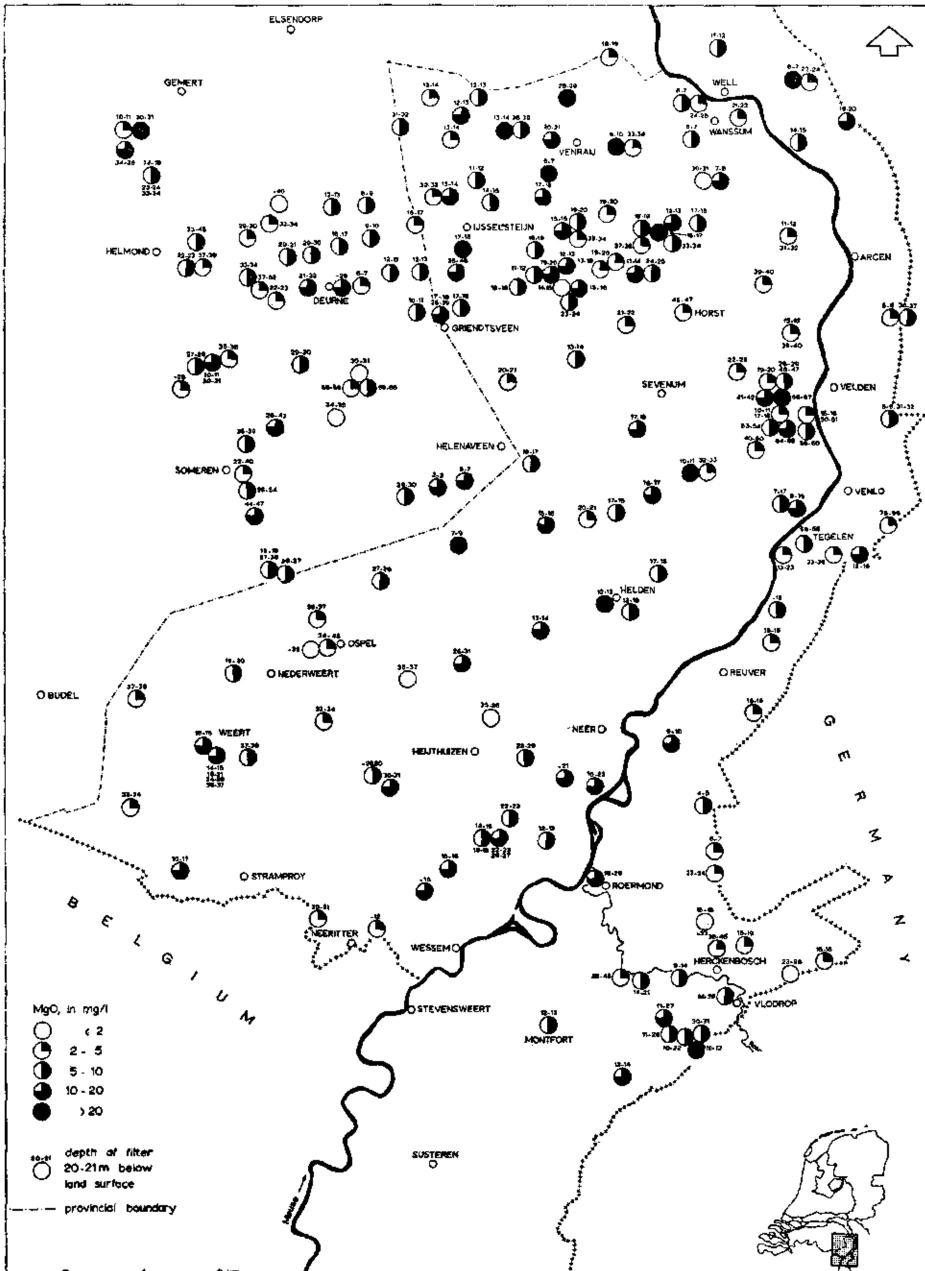

Fig. 6 Areal distribution of MgO-concentrations in the groundwater.

that the Roervalley graben and the 'Venlo graben' are characterized by medium high to high MgO-concentrations. The groundwater from the Peelhorst is, however, also fairly rich in Mg, except near the villages of Reuver and Herkenbosch. Low to very low concentrations are found west of Weert, and in a narrow strip of the Roervalley graben near Elsendorp, Ospel, Neerritter and locally in the 'Venlo graben' (Horst, Wanssum, Arcen, Velden area).

8.9 Alkali content of the groundwater

The total number of alkali analyses available is 209, of which 146 refer to the new P- and N- wells, the remaining 63 being taken from the records.

Table 14 shows the alkali concentrations of the groundwater from the various geological formations subdivided in five classes. Since sodium and potassium have not been determined separately the Na_2O- and K_2O- concentrations were calculated from the alkali content. Hence two different scales were used in Table 14 and Fig. 7.

Table 14. Alkali concentrations in groundwater from various geological formations

Formation	K_2O Na_2O	<20 <13	20-30 13-20	30-40 20-26	40-50 26-33	>50 >33	Number of analyses
Sand Diluvium		1	1	10	0	2	4
Grubbenvorst formation		6	8	2	5	5	26
Veghel formation		8	21	16	13	18	76
Sterksel formation		6	12	13	5	10	46
Kedichem formation		1	2	1	0	0	4
Tegelen formation		0	3	0	3	1	7
Kieseloolite formation		9	20	9	1	5	44
Middle Miocene		1	1	0	0	0	2
		32	68	41	27	41	209

A comparison of the distribution of the samples over the different classes with those of in the foregoing tables shows that the alkali concentrations are fairly regularly distributed. The water from the Kieseloolite formation is characterized by low alkali concentrations. Medium-high and high concentrations predominate in the Veghel and Sterksel waters, whereas the water from the Grubbenvorst formation also shows low and high concentrations.

The areal distribution of the alkali concentrations is shown in Fig. 7. From this map it can be concluded that medium-high and high concentrations are found at many places on the Peelhorst and in the northern part of the 'Venlo graben' in the Venray-Wanssum area, where the marine Miocene lies at relatively shallow depths. In the southern part of this graben, in the Horst-Arcen-Venlo area where Miocene is found at greater depths, the alkali concentrations are generally low. But certain parts of the

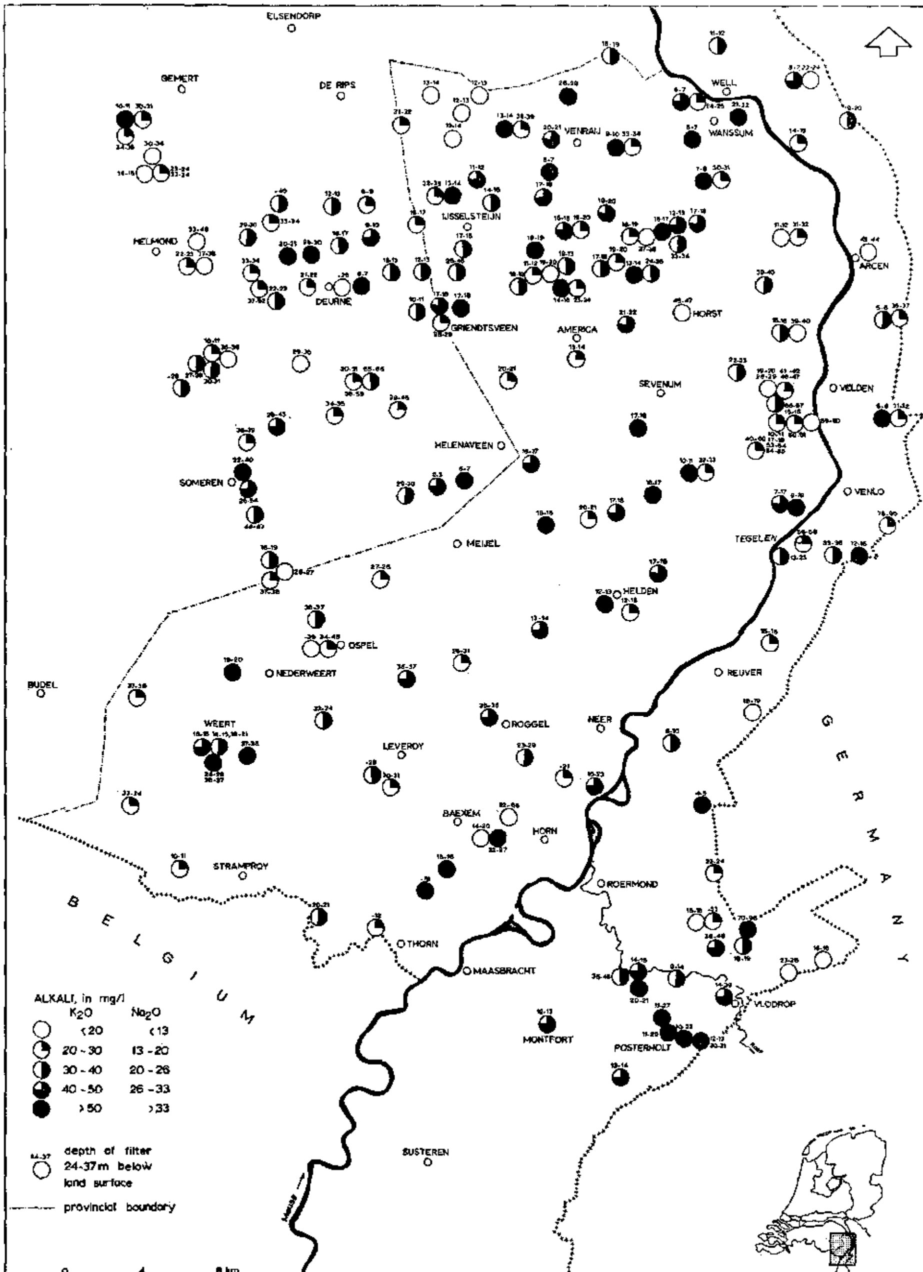

Fig. 7 Areal distribution of alkali (K_2O and Na_2O) concentrations in the groundwater.

Peelhorst also show low values, e.g. near De Rips, America, Helden, Reuver and east of Vlodrop.

Low alkali concentrations also occur in the Roervalley graben, except near Posterholt, Baxem, Weert and Someren, where high and very high concentrations predominate.

Summary

In the Peel region of the S.E. Netherlands the principal water-bearing formations are the Pliocene and Pleistocene sand and gravel deposits of the Rhine and the Meuse. Owing to differences in heavy mineral composition these river deposits could be clearly distinguished. Marine deposits of Middle Miocene age underlie the greater part of the region. Numerous drillings and statigraphic investigations revealed a fairly complicated fault pattern. The Neogene, and even the Pleistocene formations are broken, giving rise to a buried block-faulted landscape. Owing to this block-faulting the impervious basement (Middle Miocene) is found at various depths, whereas the thickness of the water-bearing formations varies considerably throughout the region. On the Peelhorst the thickness is at some places not more than 10 m, but on some downthrown blocks it increases to 100 m ('Venlo graben'). The greatest thickness is found in the Roervalley graben, which must be considered as the most promising area for groundwater exploitation. The transmissibility of the aquifers is closely related to the geological structure of the region. The lowest values generally are found on the upthrown blocks where the aquifer is thin. The highest values occur in the graben areas and downthrown blocks where the aquifers reach a considerable thickness.

The general movement of the groundwater is from the topographically highest parts of the Peelhorst eastward towards the river Meuse and westward towards the lower lying province of Noord-Brabant. Some of the faults act as groundwater barriers causing abnormally steep gradients in the piezometric surface.

Generally, the groundwater is of the calcium bicarbonate type, although some waters have appreciable amounts of sulphate. The groundwater is usually rich in iron, whereas the chloride contents are low. Since the aquifers are interconnected no clear relationship between the chemical character of the groundwater and the geological formations could be demonstrated. The groundwater on the upthrown blocks of the Peelhorst tend to be more rich in iron than on the downthrown blocks and grabens. This is probably due to the underlying marine Miocene, which is rich in glauconite.

References

AHORNER, L. 1962 Untersuchungen zur quartären Bruchtektonik der Niederrheinischen Bucht. *Eiszeitalter und Gegenwart, 13:* 24–105.

AHORNER, L. and J. M. VAN GILS 1963 Das Erdbeben vom 25 Juni 1960 im belgisch-niederländischen Grenzgebiet. Sonderveröffentlichungen des Geol. Inst. Univ. Köln 9: 1–28.

BENTOR, Y. K. and M. KASTNER 1965 Notes on the mineralogy and origin of glauconite. *J. Sedimentary Petrology, 35, 1*: 155–166.

BURCK, H. D. M. 1956 Het Jong-Kwartair op de Peelhorst en in de westelijk van de horst gelegen Grote Slenk. Meded. Geol. Stichting, N.S. 10: 44–51.

DOPPERT, J. W. C. and J. I. S. ZONNEVELD 1955 Over de stratigrafie van het fluviatiele Pleistoceen in West-Nederland en Noord-Brabant. Meded. Geol. Stichting, N.S. 8: 13–30.

ERNST, L. F. 1956 Infiltratie in het Boven-Dommelgebied. Rapport Landbouwproefst. en Bodemk. Inst. Groningen, 42 p.

ERNST, L. F. 1958 Onderzoek van grondwaterstromingen in het Lollebeekgebied. Meded. 4, I. C. W. Wageningen: 16–39.

ERNST, L. F. and N. A. DE RIDDER 1960 High resistance to horizontal groundwater flow in coarse sediments due to faulting. *Geol. en Mijnbouw, N.S. 22*: 66–85.

FAHMY, M. I. 1961 The influence of clay particles on the hydraulic conductivity of sandy soils. Diss. Wageningen, 89 p.

HAITES, T. B. 1960 Transcurrent faults in Western Canada. *J. Alberta Soc. Petroleum Geol. 8,2*: 33–78.

HELLINGS, A. J. 1958 De landbouwwaterhuishouding in de provincie Limburg. Rapport 12, Comm. Landbouwwaterhuishouding Nederland, T.N.O. 's-Gravenhage.

HEM, J. D. 1959 Study and interpretation of the chemical characteristics of natural water. Geol. Survey Water-supply paper 1473, Washington, 269 p.

LENSEN, G. J. 1958 A method of horst and graben formation. *J. of Geol. 66,5*: 579–587.

MENTE, A. 1961 Het resultaat van een palynologisch onderzoek van een Eemien afzetting bij Liesel (N.Br.). *Geol. en Mijnb. 40,2*: 75–78.

NOTA No. 12 1959 Instituut voor Cultuurtechniek en Waterhuishouding, Wageningen.

PANNEKOEK, A. J. 1956 Geologische geschiedenis van Nederland. 's-Gravenhage, 154 p.

PIPER, A. M. 1944 A graphic procedure in the geochemical interpretation of water analyses. *Amer. Geoph. Union, Trans. 25:* 914–923.

ROORDA VAN EIJSINGA, J. P. N. L. 1961 Problemen met ijzerhoudend sproeiwater in de groenteteelt onder glas. *Med. Dir. Tuinb. 24:* 641–644.

RIDDER, N. A. DE 1959 De kwartaire en jongtertiaire tektoniek van Midden Limburg en zuidoostelijk Noord-Brabant. *Geol. en Mijnb., N.S. 21*: 1–24.

RIDDER, N. A. DE and G. J. LENSEN, 1960 Indirect evidence for transcurrent faulting and some examples from New Zealand and the Netherlands, Techn. Bull. 15, I.C.W., Wageningen, 13 p.

RIDDER, N. A. DE and W. H. ZAGWIJN, 1962 A mixed Rhine-Meuse deposit of Holsteinian age from the southeastern part of the Netherlands. *Geol. en Mijnb. 41, 3*: 125–130.

RITSEMA, A. R. 1960 Focal mechanism of some earthquakes of the year 1950. *Geophys. Journal of Roy. Astron. Soc. 3,3*: 307–313.

SCHEIDEGGER, A. E. 1959 Statistical analysis of recent fault-plane solutions of earthquakes, Bull. Seismol. Soc. Amer. 49, 4: 337–347.

SITTER, L. U. DE 1949 Eindverslag van het geofysische onderzoek in zuidoost Nederland. Meded. Geol. Stichting, serie C, I, 3, 1.

SITTER, L. U. DE 1956 Structural geology. McGraw Hill, New York.

STRAATEN, L. M. J. U. VAN 1946 Grindonderzoek in Zuid-Limburg. Meded. Geol. Stichting, Serie C, VII, 2.

VISSER, W. C. 1948 Het probleem van de wijstgronden. *Tijdschr. Kon. Ned. Aardr. Gen. 2, LXV*: 798–823.

VOORTHUYSEN, J. H. VAN 1962 Die obermiozäne Transgression im Nordseebecken und die Tertiär-Quartärgrenze. Mem. Soc. belge de Géol., de Paléontol. et d'Hydrol. 8, no. 6: 64–82.

ZAGWIJN, W. H. 1957 Vegetation, climate and time-correlations in the Early Pleistocene of Europe. *Geol. en Mijnb. N.S. 19*: 233–244.

ZAGWIJN, W. H. 1960 Aspects of the Pliocene and Early Pleistocene vegetation in the Netherlands. Diss. Leiden, 78 p.

ZAGWIJN, W. H. 1961 Vegetation, climate and radiocarbon datings in the Late Pleistocene of the Netherlands. Meded. Geol. Stichting N.S. 14: 15–45.

ZAGWIJN, W. H. and J. I. S. ZONNEVELD 1956 The interglacial of Westerhoven. *Geol. en Mijnb. N.S. 18*: 37–46.

ZONNEVELD, J. I. S. 1947 Het Kwartair van het Peelgebied en de naaste omgeving. Meded. Geol. Stichting, Serie C, XI, 3. 223 p.

ZONNEVELD, J. I. S. 1956 Das Quartär der südöstlichen Niederlande. *Geol. en Mijnb. N.S. 18*: 379–385.

ZONNEVELD, J. I. S. 1958 Litho-stratigrafische eenheden in het Nederlandse Pleistoceen. Meded. Geol. Stichting N.S. 12: 31–64.

Appendix II
Mass and particle properties of various geological formations in borings
P6-P13, P14^{II}-P49, P56-P112 and N70-N99

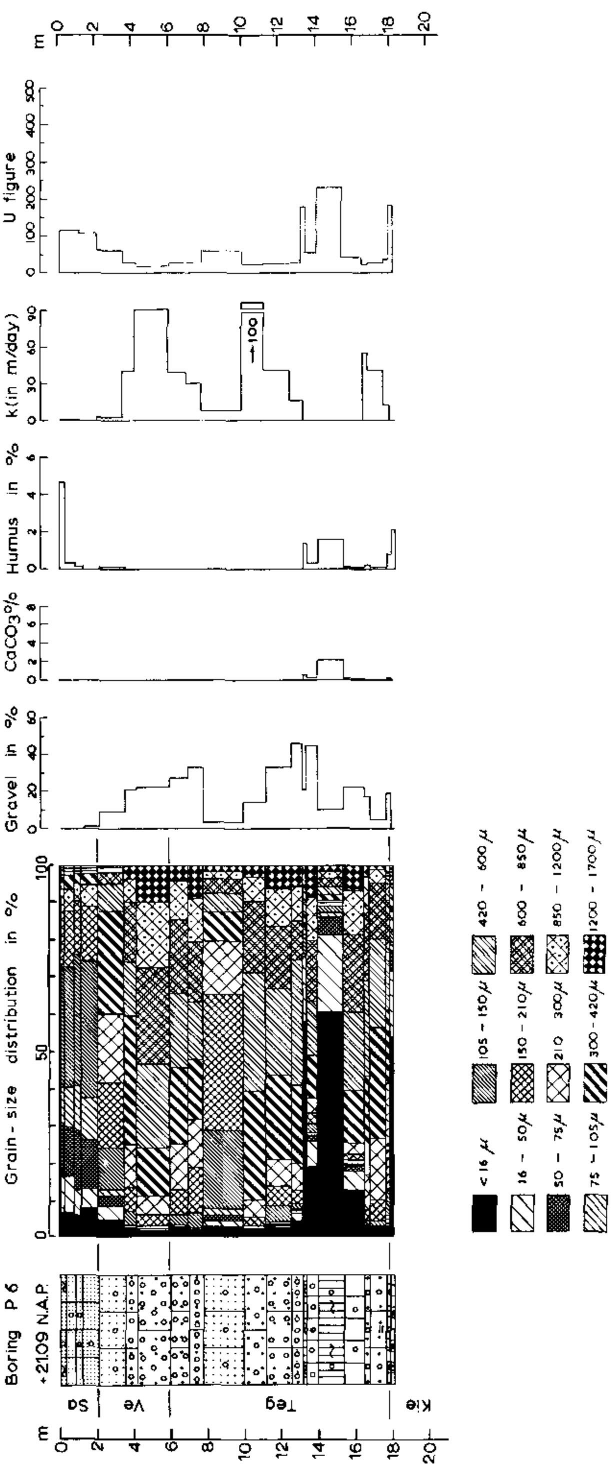

Boring P 6
+21.09 N.A.P.
Sa
Ve
Teg
Kie
m
Grain - size distribution in %
Gravel in %
CaCO3 %
Humus in %
k (in m/day)
U figure
→100
< 16 μ
16 - 50 μ
50 - 75 μ
75 - 105 μ
105 - 150 μ
150 - 210 μ
210 - 300 μ
300 - 420 μ
420 - 600 μ
600 - 850 μ
850 - 1200 μ
1200 - 1700 μ

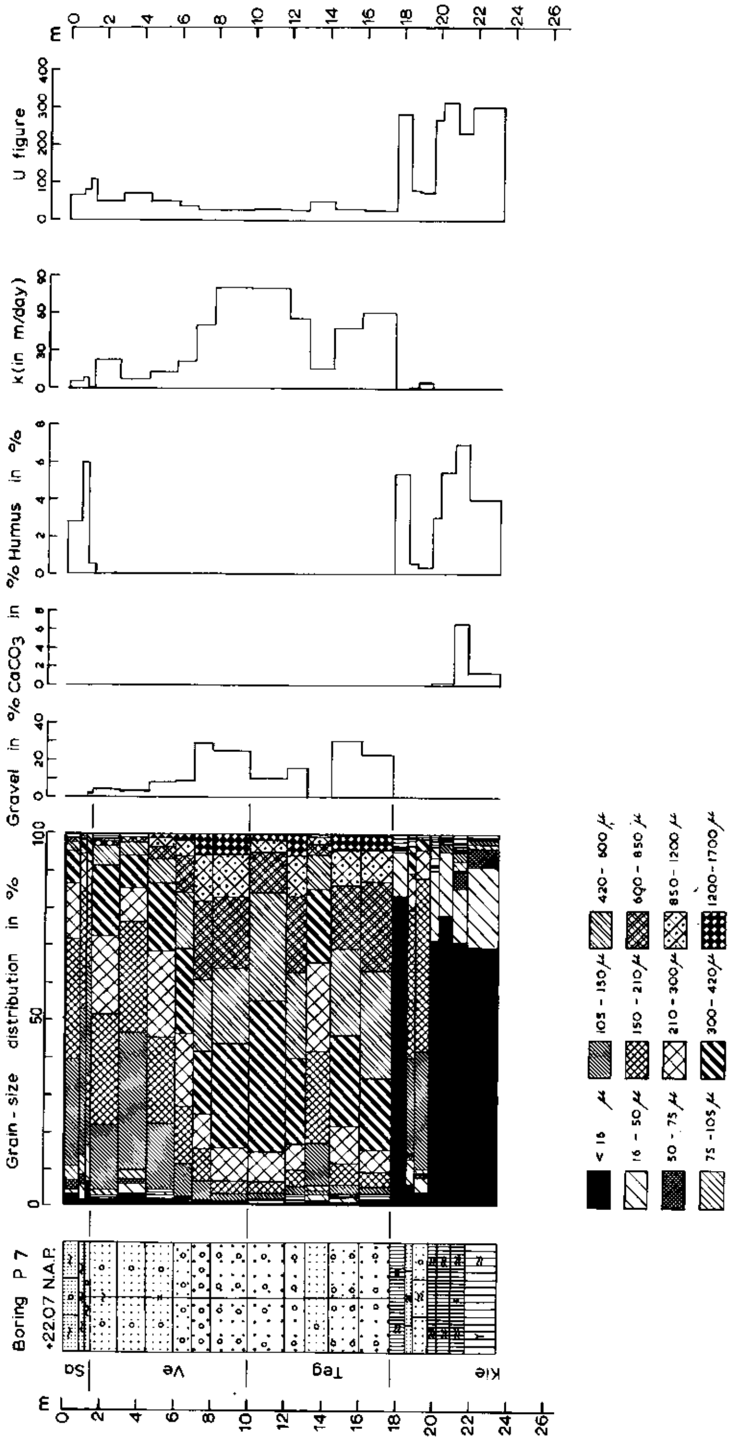
Boring P 7
+22.07 N.A.P.
Sa
Ve
Teg
Kie
m
Grain - size distribution in %
Gravel in %
% CaCO3 in %
% Humus in %
k (in m/day)
U figure
< 16 μ
16 - 50 μ
50 - 75 μ
75 - 105 μ
105 - 150 μ
150 - 210 μ
210 - 300 μ
300 - 420 μ
420 - 600 μ
600 - 850 μ
850 - 1200 μ
1200 - 1700 μ

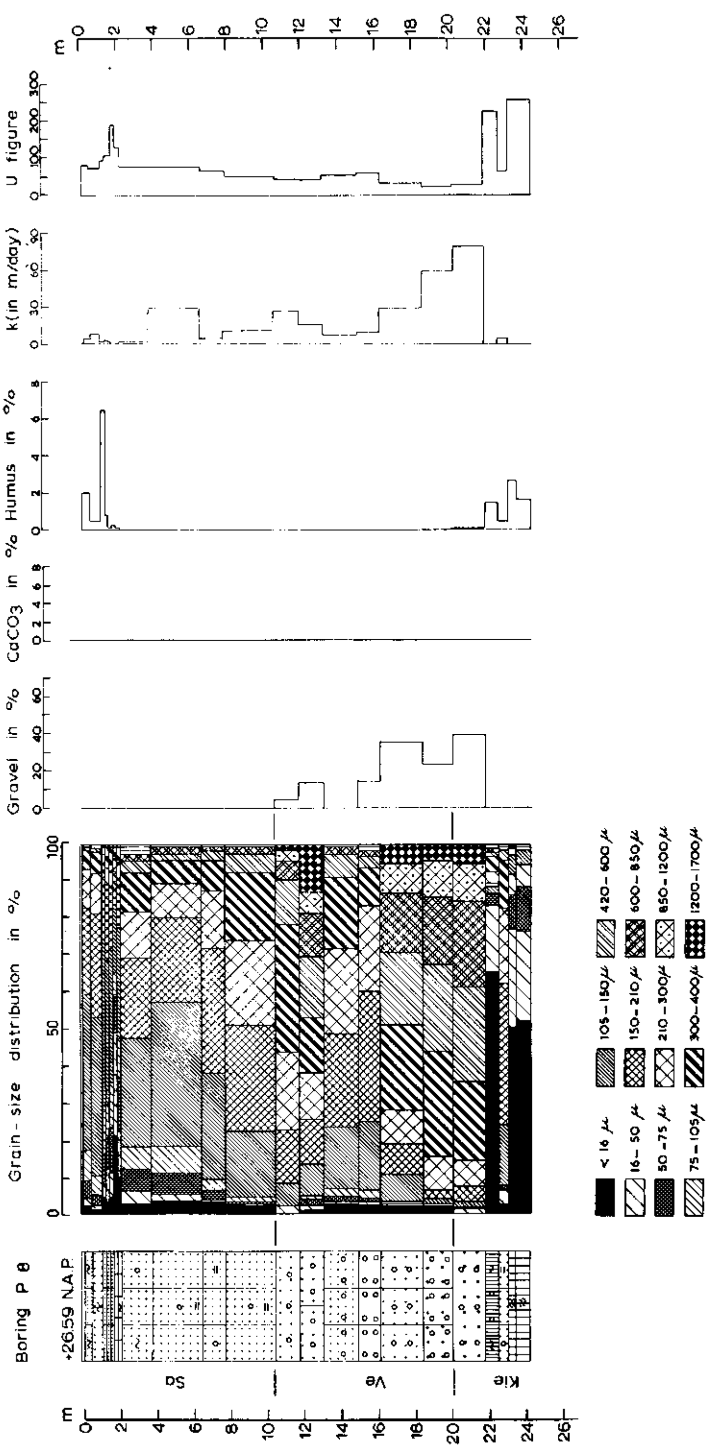
Boring P 8
+26.59 N.A.P.
m
Sa
Ve
Kie
Grain - size distribution in %
Gravel in %
CaCO3 in %
Humus in %
k (in m/day)
U figure
< 16 μ
16 - 50 μ
50 - 75 μ
75 - 105 μ
105 - 150 μ
150 - 210 μ
210 - 300 μ
300 - 400 μ
420 - 600 μ
600 - 850 μ
850 - 1200 μ
1200 - 1700 μ

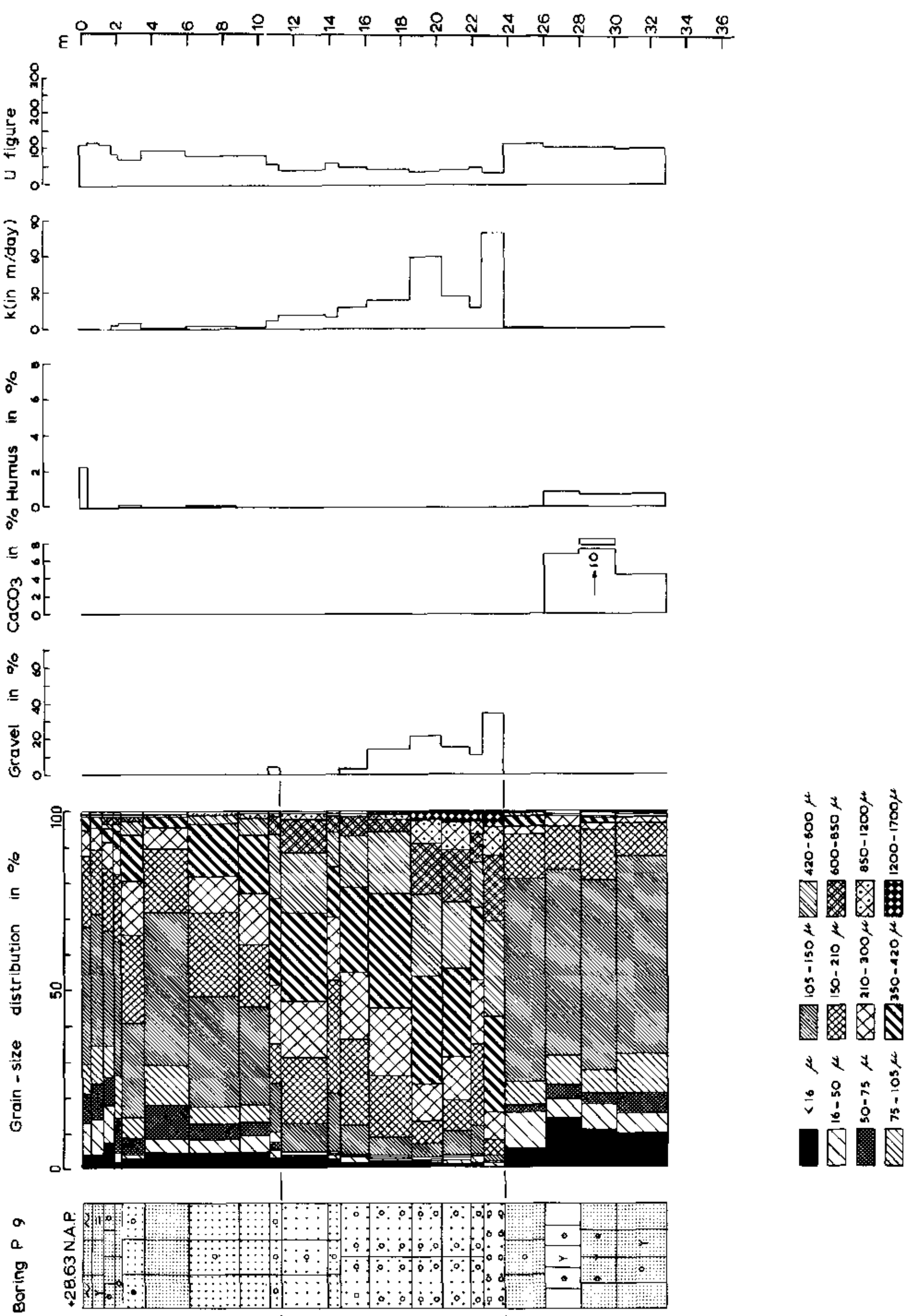
Boring P 9
+28.63 N.A.P.
Grain - size distribution in %
Gravel in %
CaCO3 in
% Humus in %
k(in m/day)
U figure
So
Ve
Mio
m
< 16 μ
16 - 50 μ
50 - 75 μ
75 - 105 μ
105 - 150 μ
150 - 210 μ
210 - 300 μ
350 - 420 μ
420 - 600 μ
600 - 850 μ
850 - 1200 μ
1200 - 1700 μ

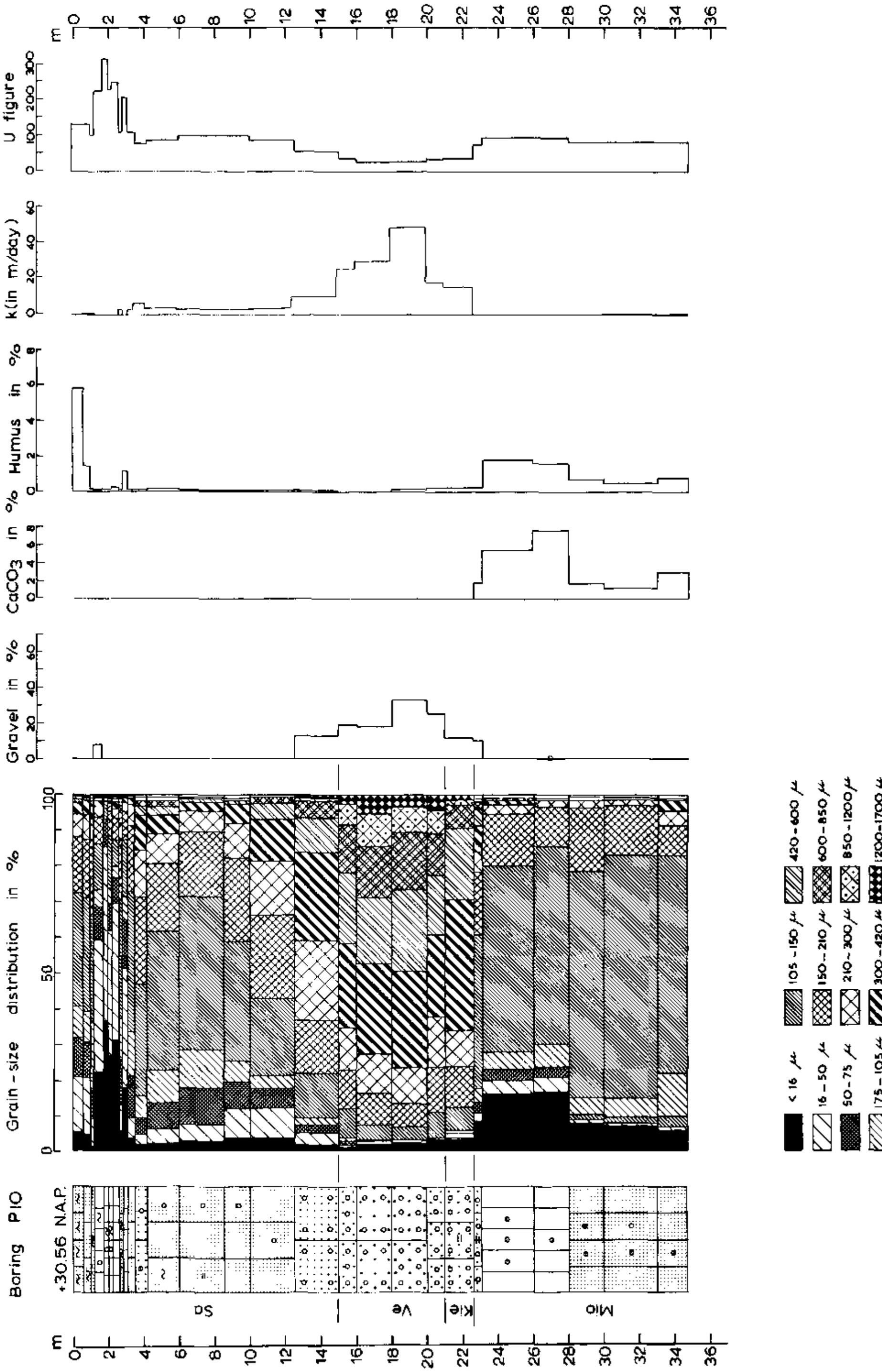

m
U figure
k (in m/day)
Humus in %
$CaCO_3$ in %
Gravel in %
Grain-size distribution in %
Boring PIO
+30.56 N.A.P.
Sa
Ve
Kie
Mio
< 16 µ
16 - 50 µ
50 - 75 µ
75 - 105 µ
105 - 150 µ
150 - 210 µ
210 - 300 µ
300 - 420 µ
420 - 600 µ
600 - 850 µ
850 - 1200 µ
1200 - 1700 µ

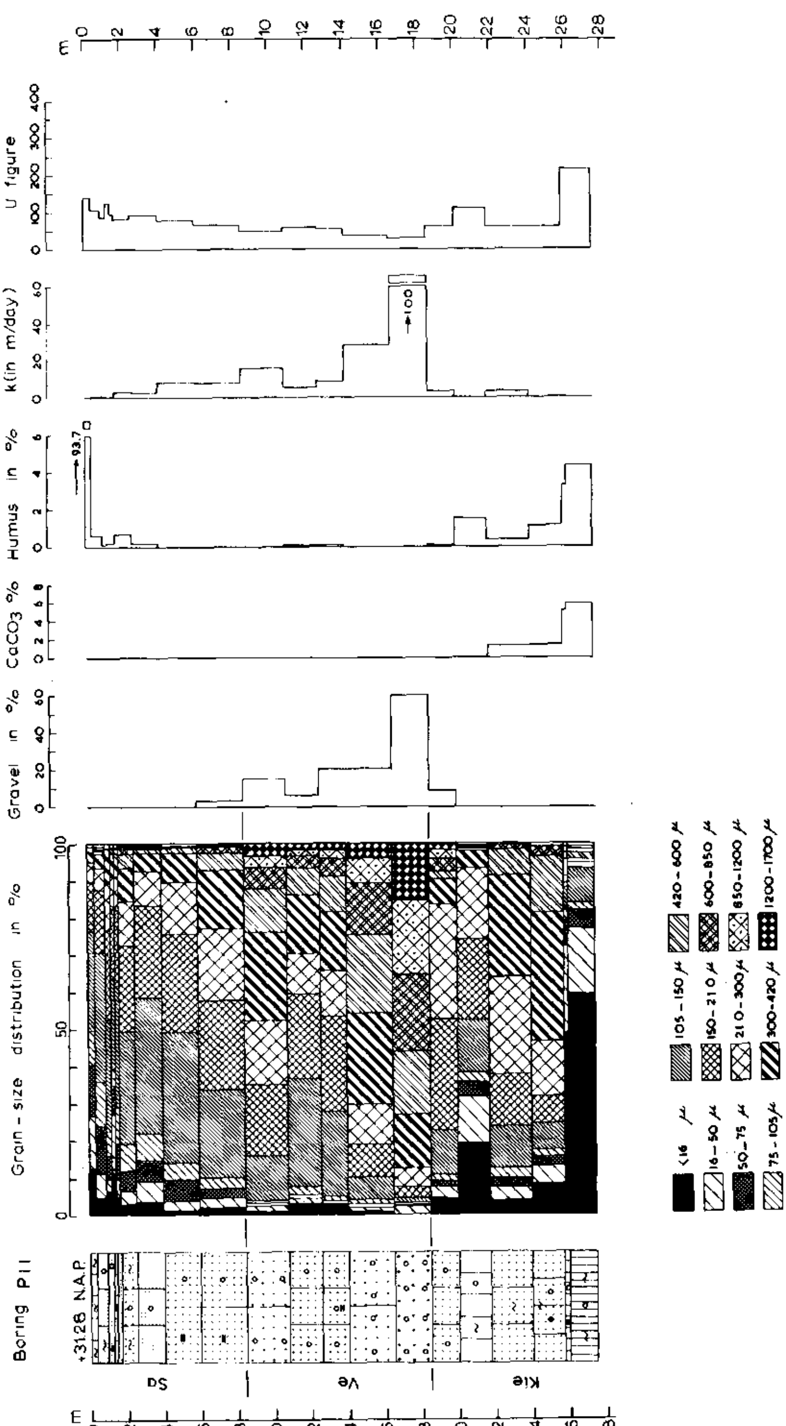
Boring P11
+3128 N.A.P.
Grain - size distribution in %
Gravel in %
$CaCO_3$ %
Humus in %
k (in m/day)
U figure
Sa
Ve
Kie
m
→93.7
→100
<16 μ
16–50 μ
50–75 μ
75–105 μ
105–150 μ
150–210 μ
210–300 μ
300–420 μ
420–600 μ
600–850 μ
850–1200 μ
1200–1700 μ

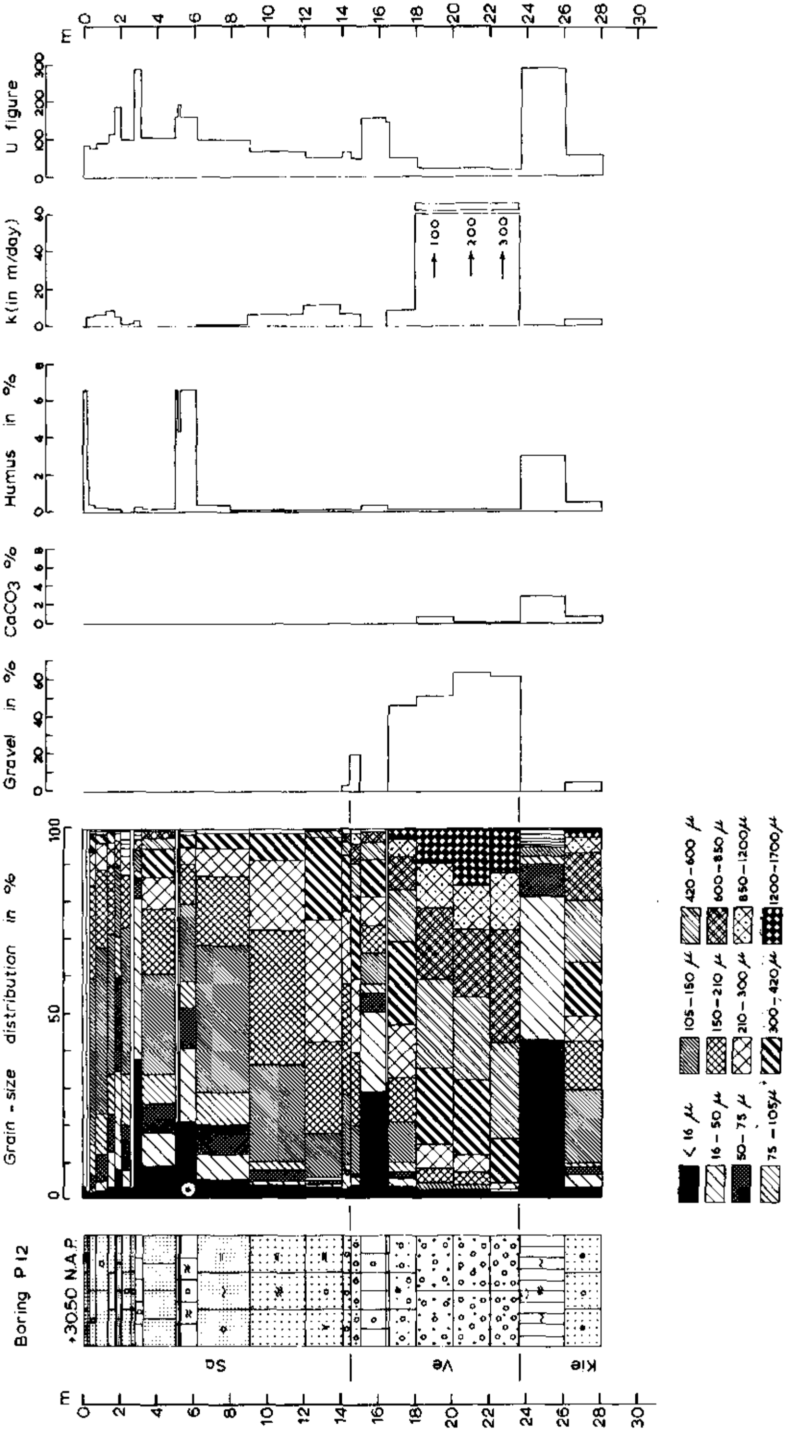
Boring P 12
+30.50 N.A.P.
Grain - size distribution in %
Gravel in %
CaCO3 %
Humus in %
k (in m/day)
U figure
m
Sa
Ve
Kie
100
200
300
< 16 μ
16 – 50 μ
50 – 75 μ
75 – 105 μ
105 – 150 μ
150 – 210 μ
210 – 300 μ
300 – 420 μ
420 – 600 μ
600 – 850 μ
850 – 1200 μ
1200 – 1700 μ

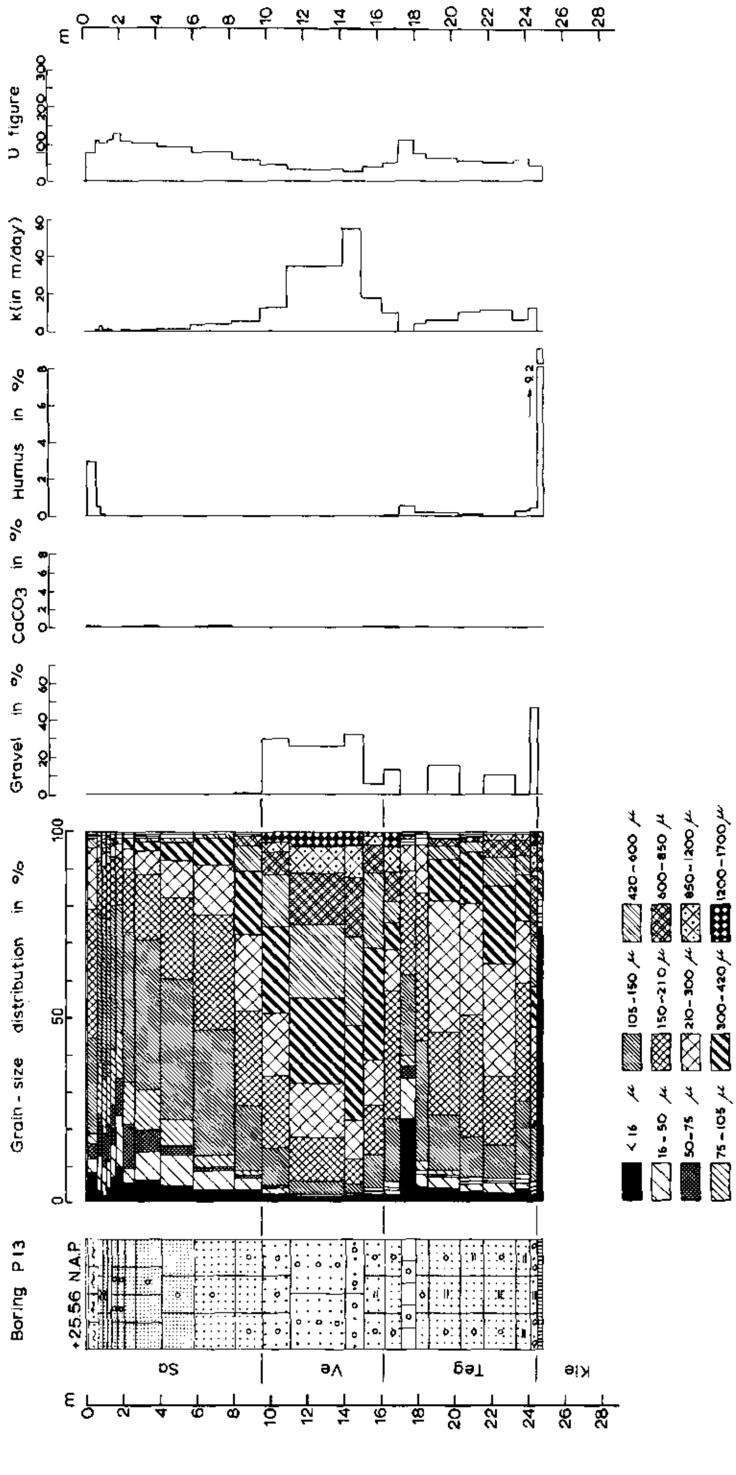
Boring P 13
+25.56 N.A.P.
Grain-size distribution in %
Gravel in %
CaCO3 in %
Humus in %
k(in m/day)
U figure
m
Sa
Ve
Teg
Kie
< 16 μ
16-50 μ
50-75 μ
75-105 μ
105-150 μ
150-210 μ
210-300 μ
300-420 μ
420-600 μ
600-850 μ
850-1200 μ
1200-1700 μ

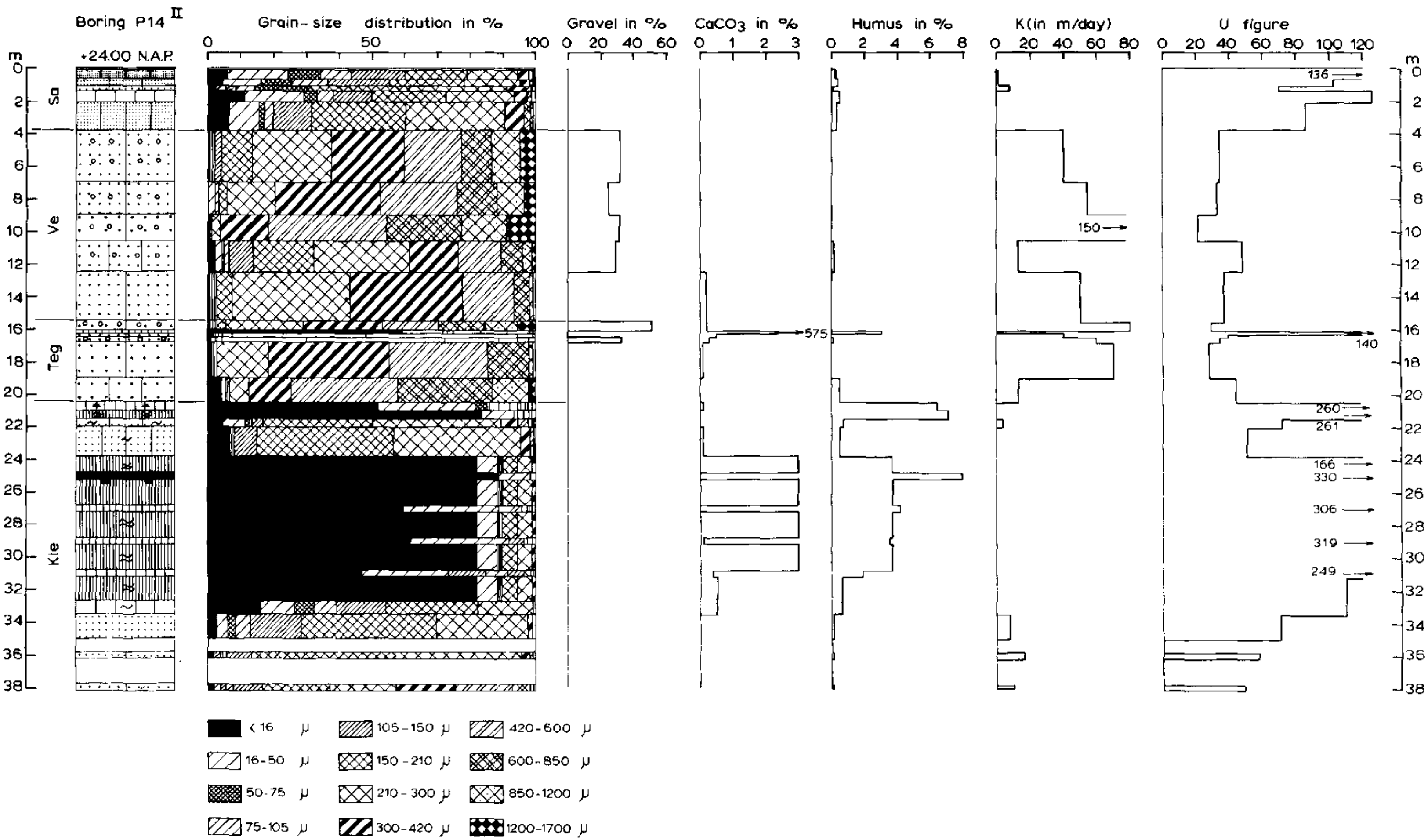

Boring P14 II
+24.00 N.A.P.
Sa
Ve
Teg
Kie
Grain-size distribution in %
Gravel in %
$CaCO_3$ in %
Humus in %
K (in m/day)
U figure
m
575
150
136
140
260
261
166
330
306
319
249
< 16 μ
16-50 μ
50-75 μ
75-105 μ
105-150 μ
150-210 μ
210-300 μ
300-420 μ
420-600 μ
600-850 μ
850-1200 μ
1200-1700 μ

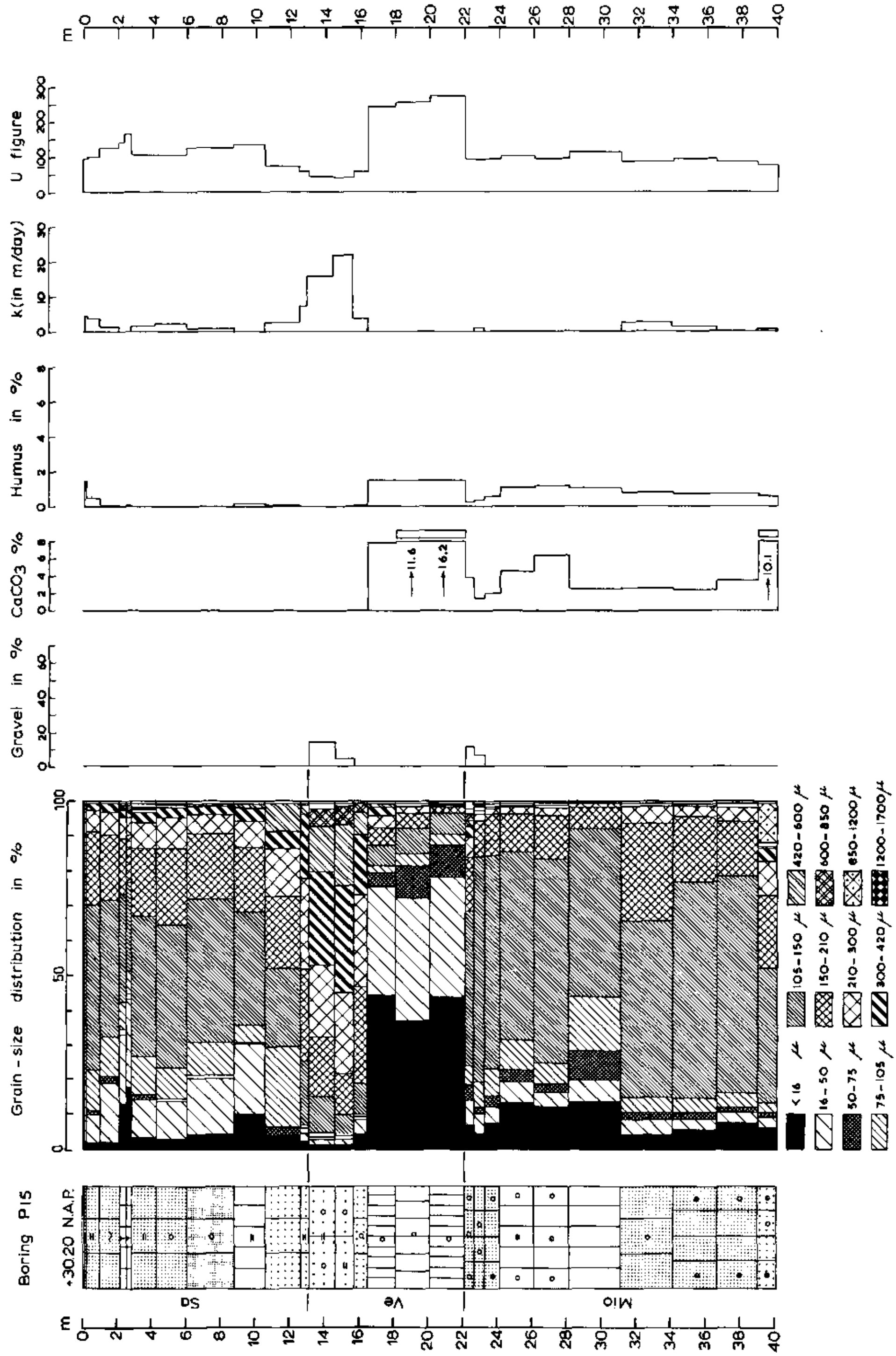

Boring P15
+30.20 N.A.P.
Grain - size distribution in %
Gravel in %
CaCO3 %
Humus in %
k (in m/day)
U figure
Sa
Ve
Mio
11.6
16.2
10.1
< 16 μ
16 - 50 μ
50 - 75 μ
75 - 105 μ
105 - 150 μ
150 - 210 μ
210 - 300 μ
300 - 420 μ
420 - 600 μ
600 - 850 μ
850 - 1200 μ
1200 - 1700 μ

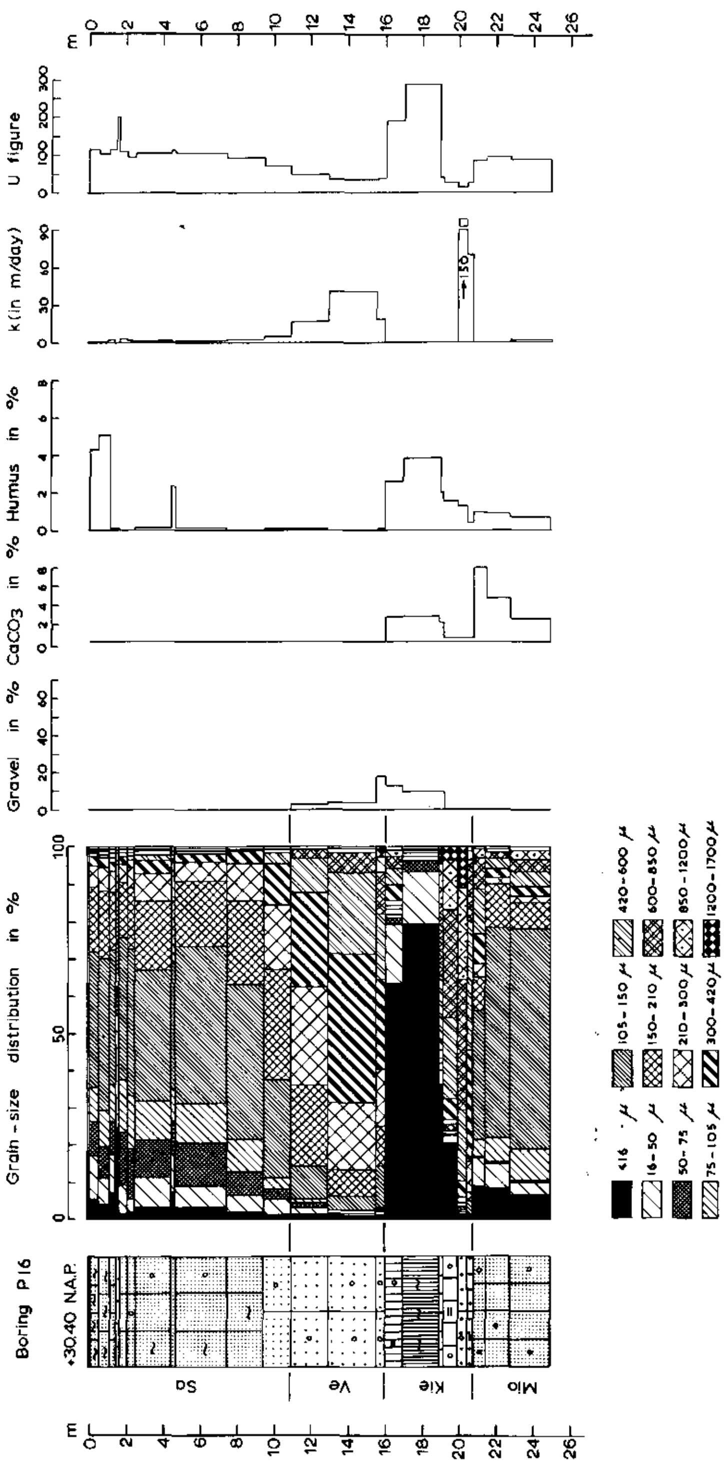

Boring P16
+30.40 N.A.P.
Sa
Ve
Kie
Mio
Grain - size distribution in %
Gravel in %
CaCO3 in %
Humus in %
k (in m/day)
U figure
m
<16 μ
16-50 μ
50-75 μ
75-105 μ
105-150 μ
150-210 μ
210-300 μ
300-420 μ
420-600 μ
600-850 μ
850-1200 μ
1200-1700 μ

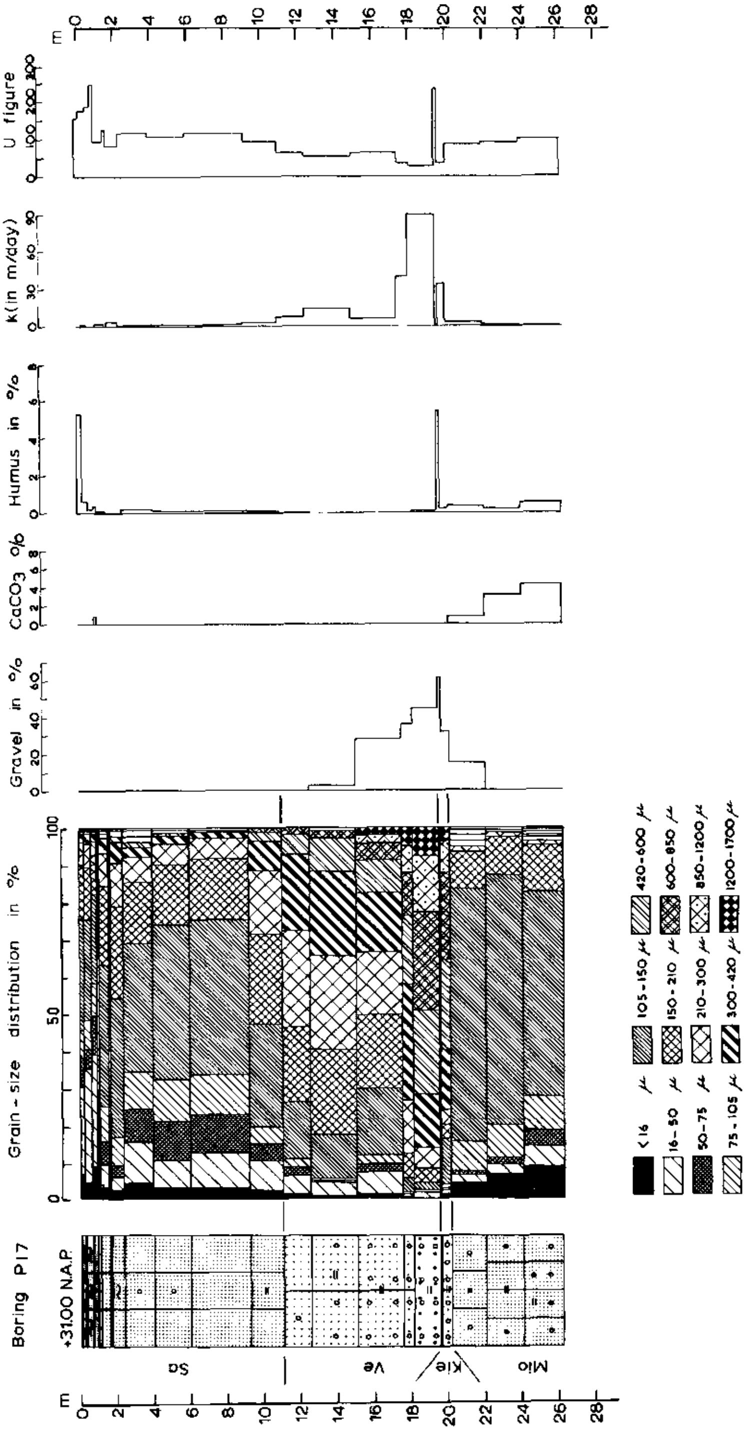

Boring P17
+31.00 N.A.P.
Sa
Ve
Kie
Mio
Grain - size distribution in %
Gravel in %
CaCO3 %
Humus in %
k (in m/day)
U figure
m
< 16 μ
16 - 50 μ
50 - 75 μ
75 - 105 μ
105 - 150 μ
150 - 210 μ
210 - 300 μ
300 - 420 μ
420 - 600 μ
600 - 850 μ
850 - 1200 μ
1200 - 1700 μ

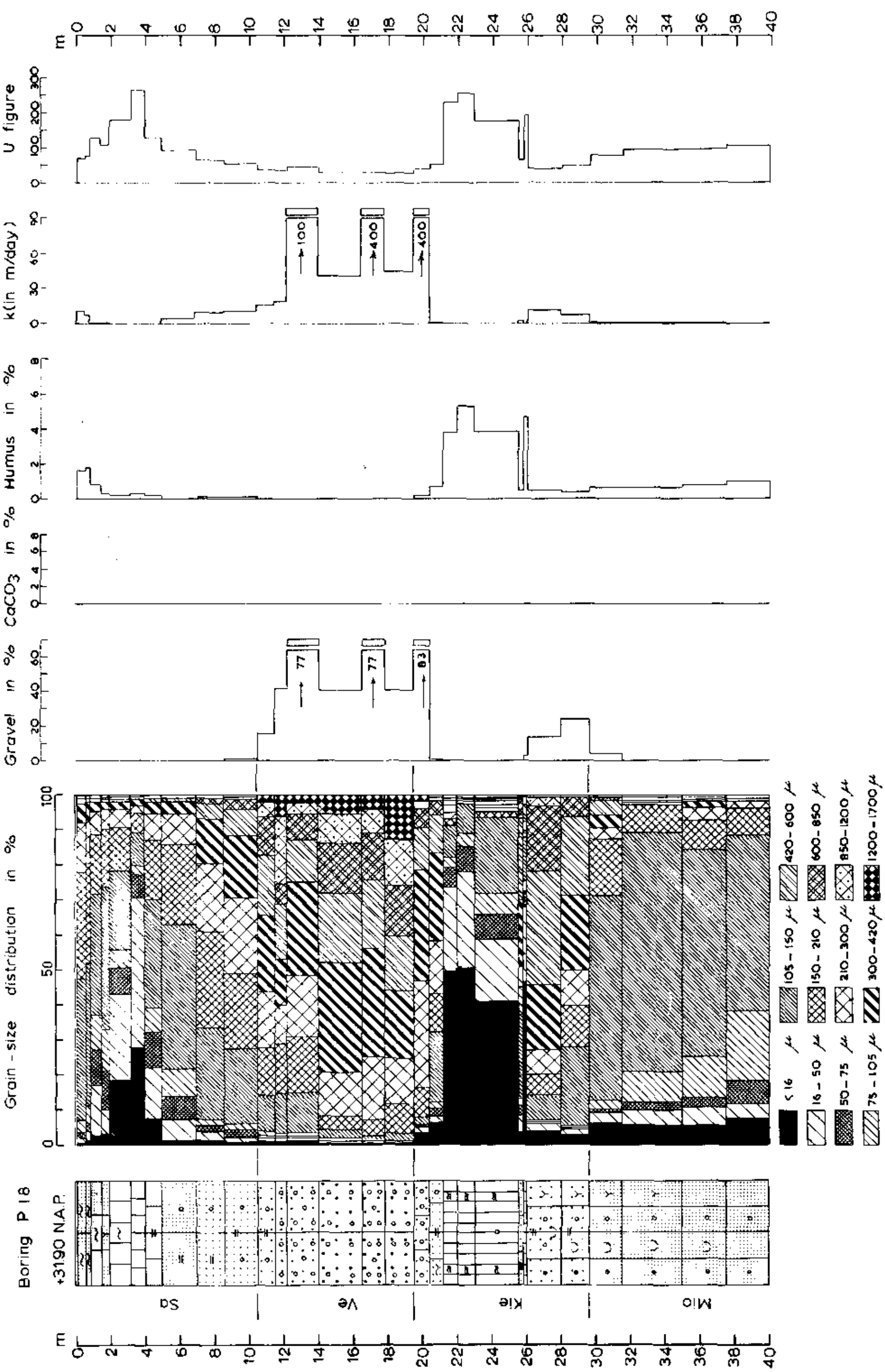
Boring P 18
+31.90 N.A.P.
Grain - size distribution in %
Gravel in %
$CaCO_3$ in %
Humus in %
k (in m/day)
U figure
Sa
Ve
Kie
Mio
< 16 μ
16 - 50 μ
50 - 75 μ
75 - 105 μ
105 - 150 μ
150 - 210 μ
210 - 300 μ
300 - 420 μ
420 - 600 μ
600 - 850 μ
850 - 1200 μ
1200 - 1700 μ

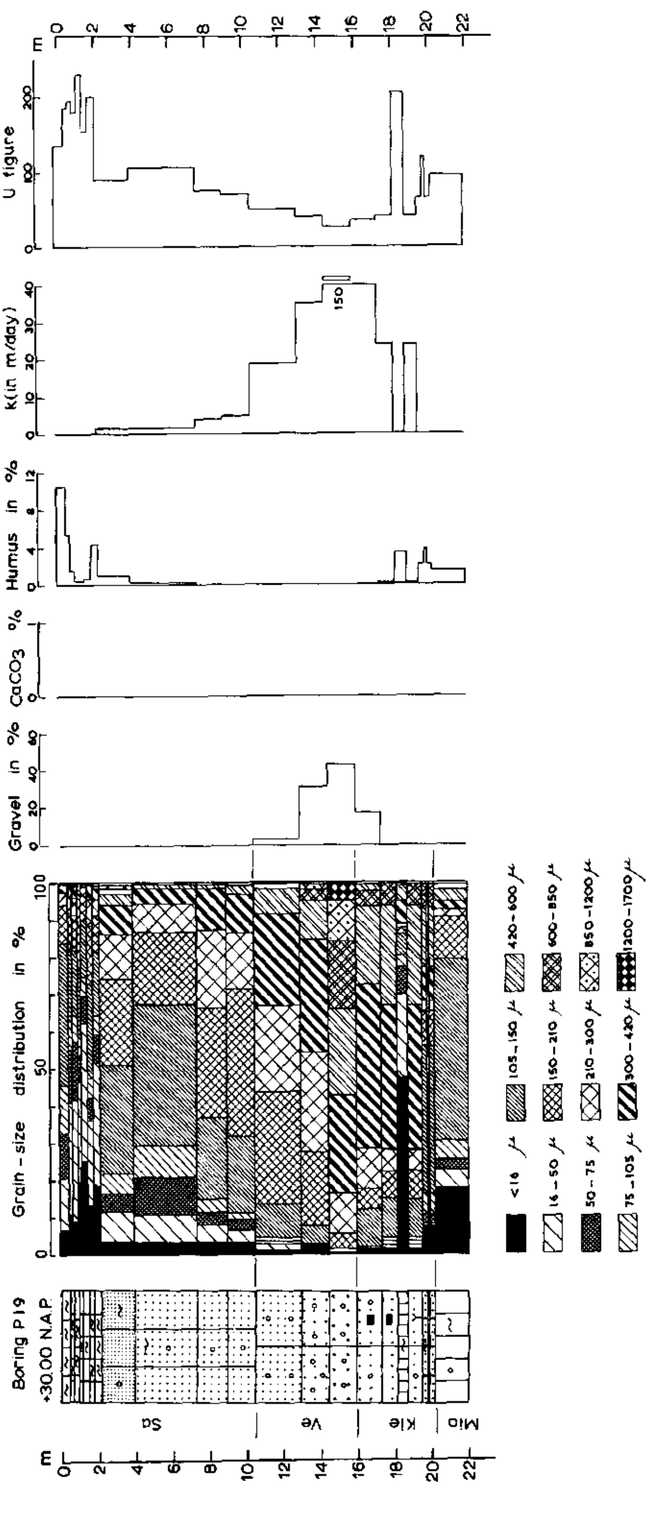
Boring P19
+30.00 N.A.P.
Sa
Ve
Kle
Mio
m
Grain - size distribution in %
Gravel in %
CaCO3 %
Humus in %
k (in m/day)
150
U figure
<16 μ
16-50 μ
50-75 μ
75-105 μ
105-150 μ
150-210 μ
210-300 μ
300-420 μ
420-600 μ
600-850 μ
850-1200 μ
1200-1700 μ

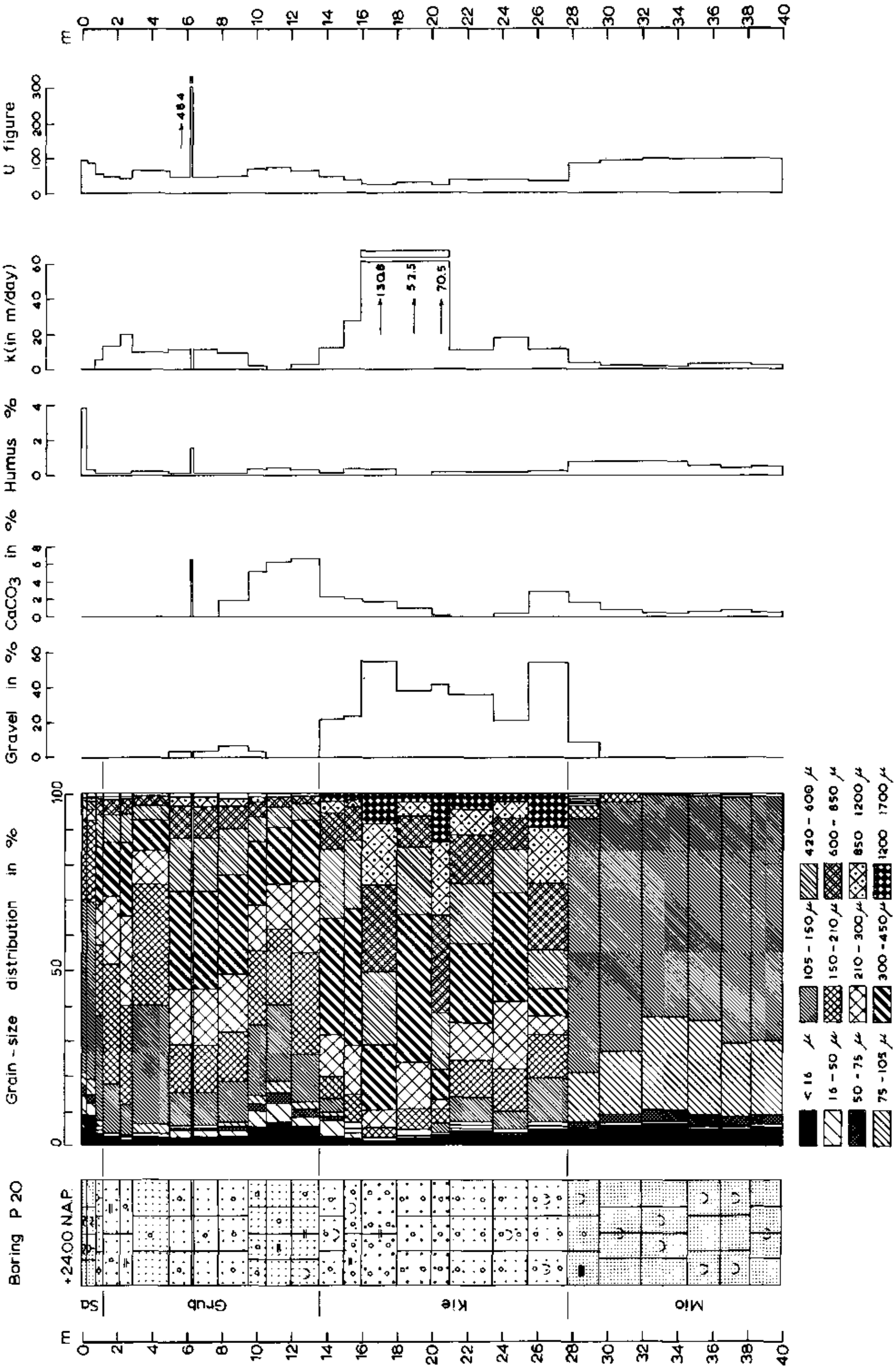
Boring P 20
+24.00 N.A.P.
Grain - size distribution in %
Gravel in %
CaCO3 in %
Humus %
k(in m/day)
U figure
m
Sa
Grub
Kie
Mio
484
130.8
53.5
70.5
< 16 μ
16 - 50 μ
50 - 75 μ
75 - 105 μ
105 - 150 μ
150 - 210 μ
210 - 300 μ
300 - 450 μ
420 - 600 μ
600 - 850 μ
850 1200 μ
1200 1700 μ

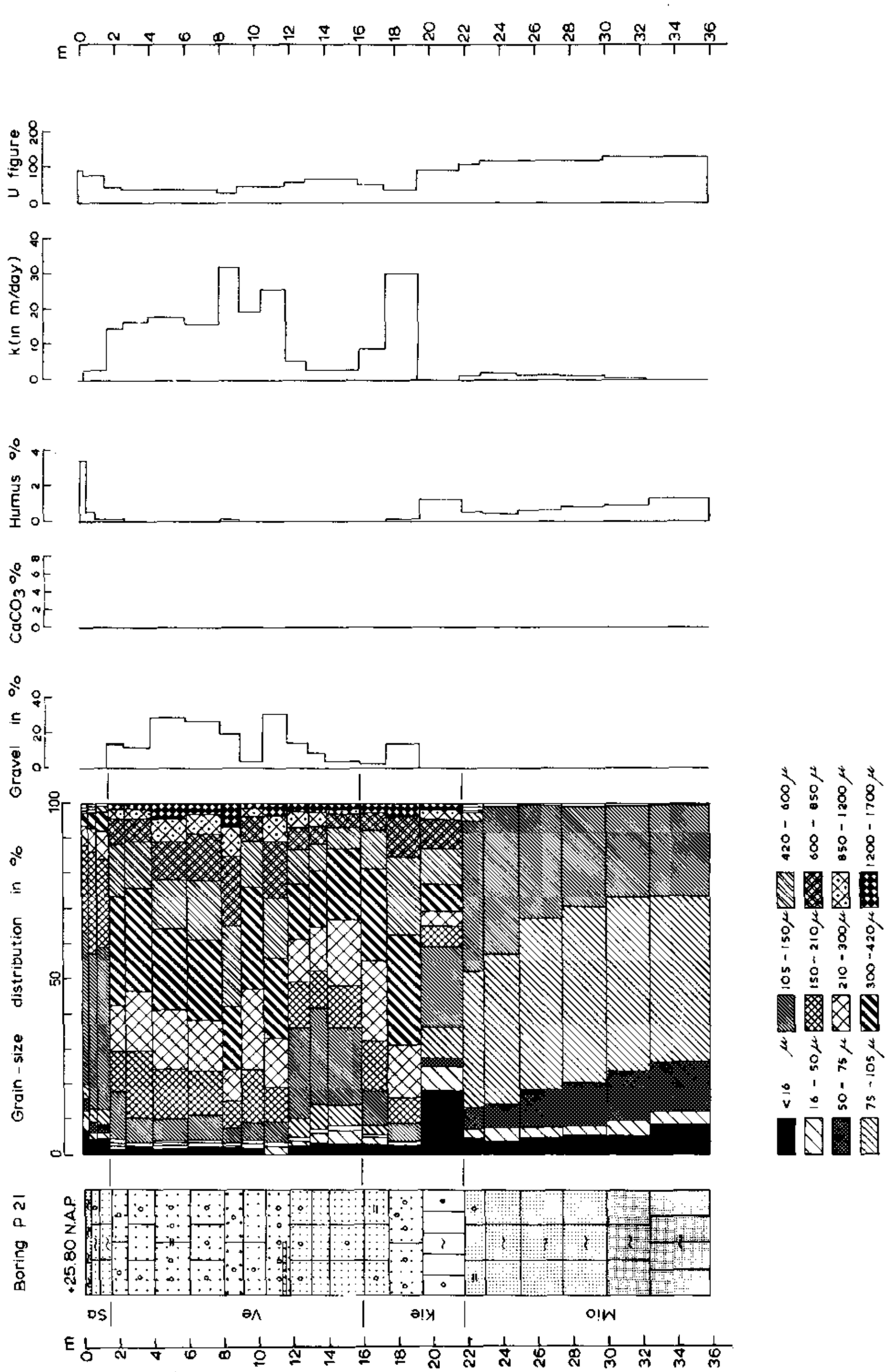
Boring P 21
+25.80 N.A.P.
Sa
Ve
Kie
Mio
Grain - size distribution in %
Gravel in %
CaCO3 %
Humus %
k (in m/day)
U figure
m
< 16 μ
16 - 50 μ
50 - 75 μ
75 - 105 μ
105 - 150 μ
150 - 210 μ
210 - 300 μ
300 - 420 μ
420 - 600 μ
600 - 850 μ
850 - 1200 μ
1200 - 1700 μ

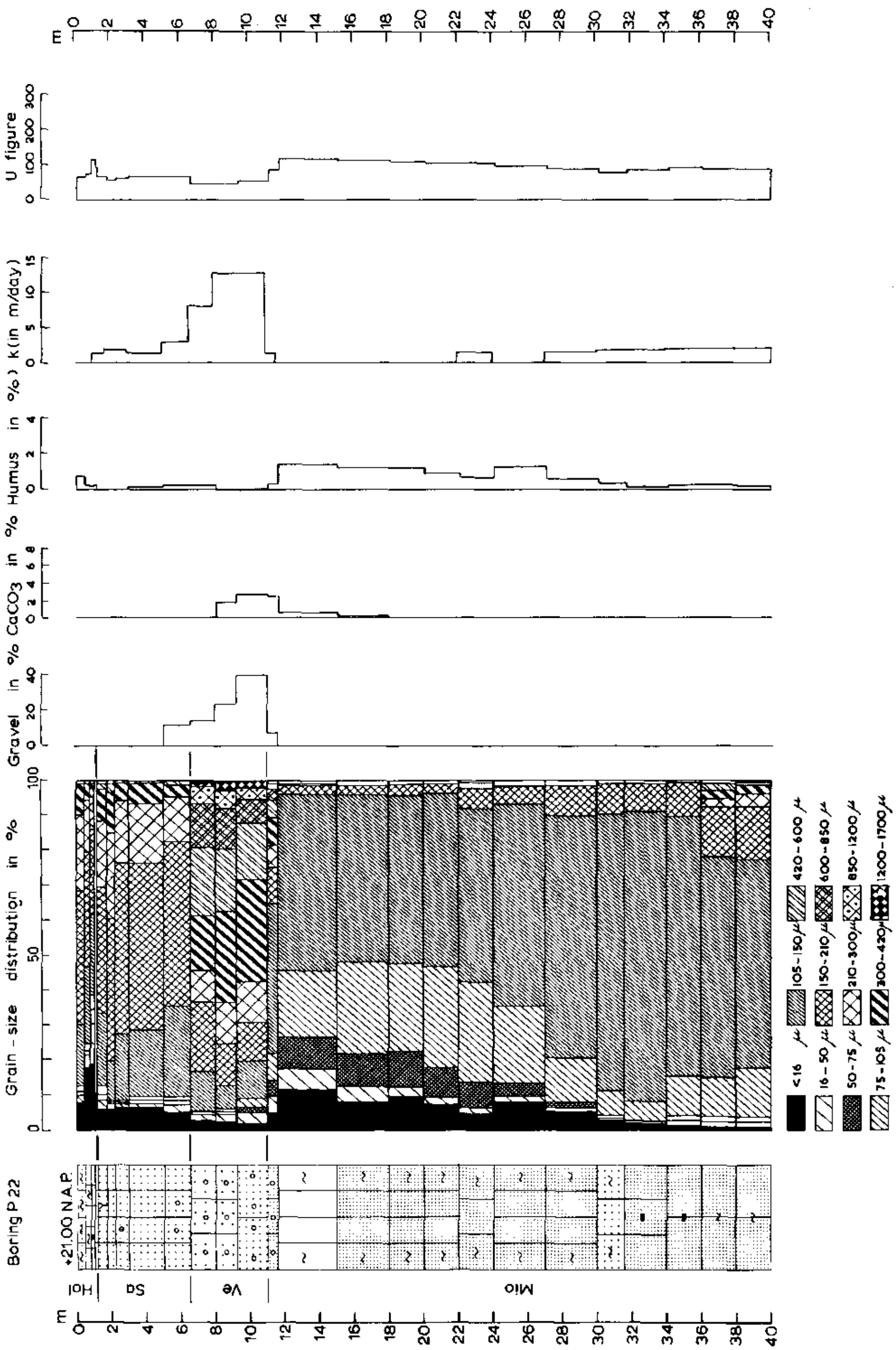

Boring P 22
+21.00 N.A.P.
Hol
Sa
Ve
Mio
m
Grain - size distribution in %
Gravel in %
CaCO3 in %
Humus in %
k (in m/day)
U figure
< 16 μ
16 - 50 μ
50 - 75 μ
75 - 105 μ
105 - 150 μ
150 - 210 μ
210 - 300 μ
300 - 420 μ
420 - 600 μ
600 - 850 μ
850 - 1200 μ
1200 - 1700 μ

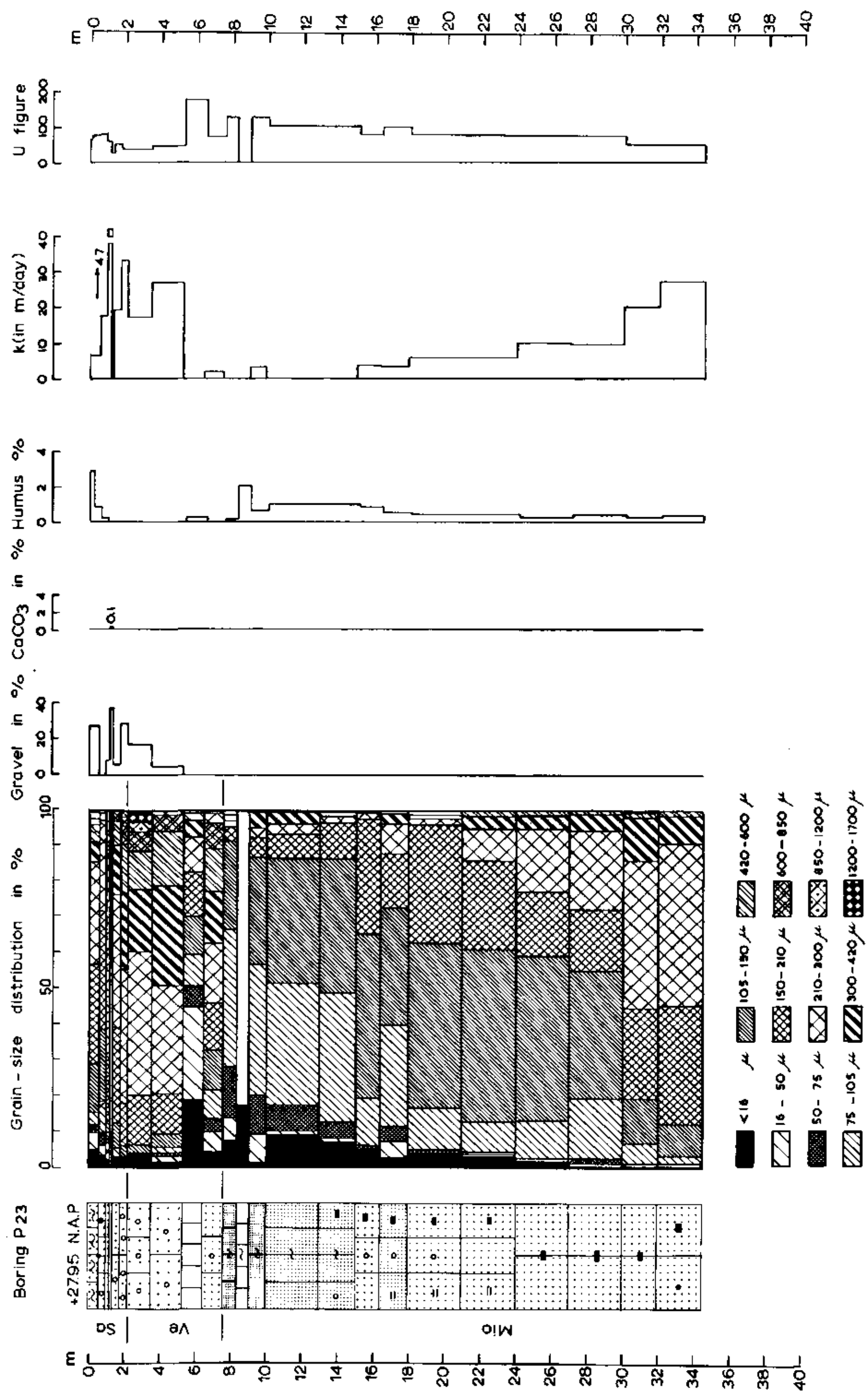
Boring P 23
+2795 N.A.P
Sa
Ve
Mio
m
Grain - size distribution in %
Gravel in %
$CaCO_3$ in %
Humus %
k (in m/day)
U figure
0.1
47
<16 μ
16 - 50 μ
50 - 75 μ
75 - 105 μ
105 - 150 μ
150 - 210 μ
210 - 300 μ
300 - 420 μ
420 - 600 μ
600 - 850 μ
850 - 1200 μ
1200 - 1700 μ

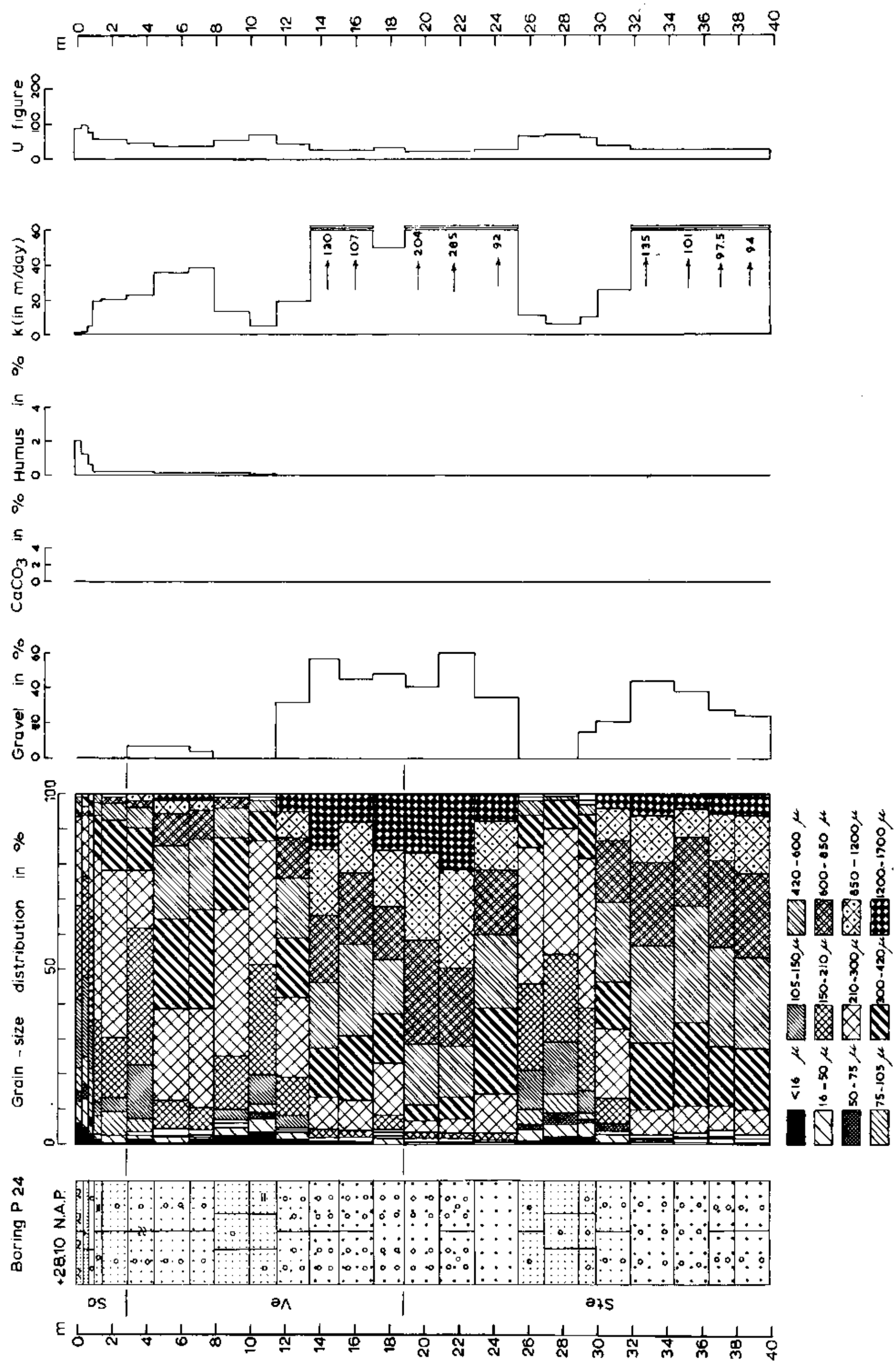

Boring P 24
+28,10 N.A.P.
Sd
Ve
Ste
Grain - size distribution in %
Gravel in %
CaCO3 in %
Humus in %
k (in m/day)
U figure
m
130
107
204
285
92
135
101
97.5
94
<16 μ
16 - 50 μ
50 - 75 μ
75 - 105 μ
105 - 150 μ
150 - 210 μ
210 - 300 μ
300 - 420 μ
420 - 600 μ
600 - 850 μ
850 - 1200 μ
1200 - 1700 μ

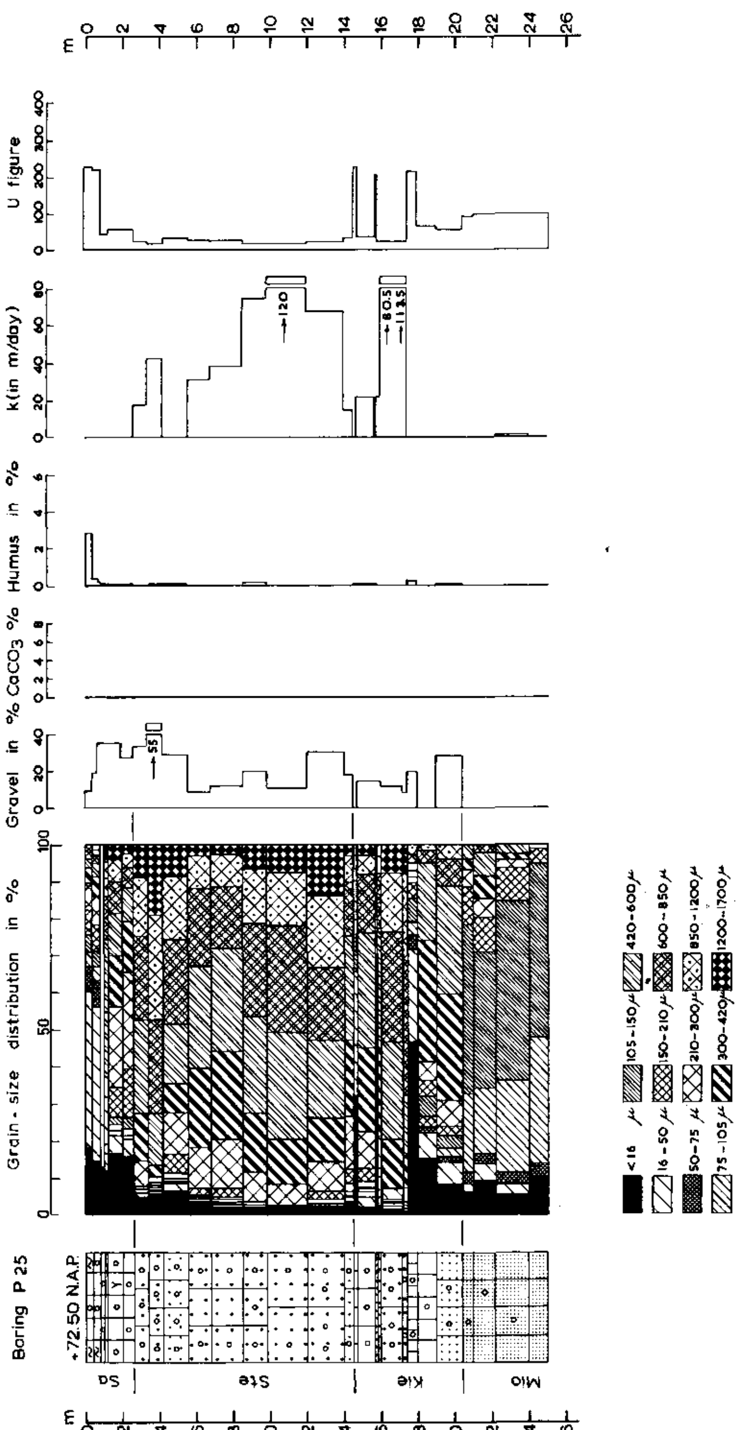
Boring P 25
+72.50 N.A.P.
Sa
Ste
Kie
Mio
Grain - size distribution in %
Gravel in %
% CaCO$_3$ %
Humus in %
k (in m/day)
U figure
120
80.5
113.5
55
< 16 μ
16 - 50 μ
50 - 75 μ
75 - 105 μ
105 - 150 μ
150 - 210 μ
210 - 300 μ
300 - 420 μ
420 - 600 μ
600 - 850 μ
850 - 1200 μ
1200 - 1700 μ
m

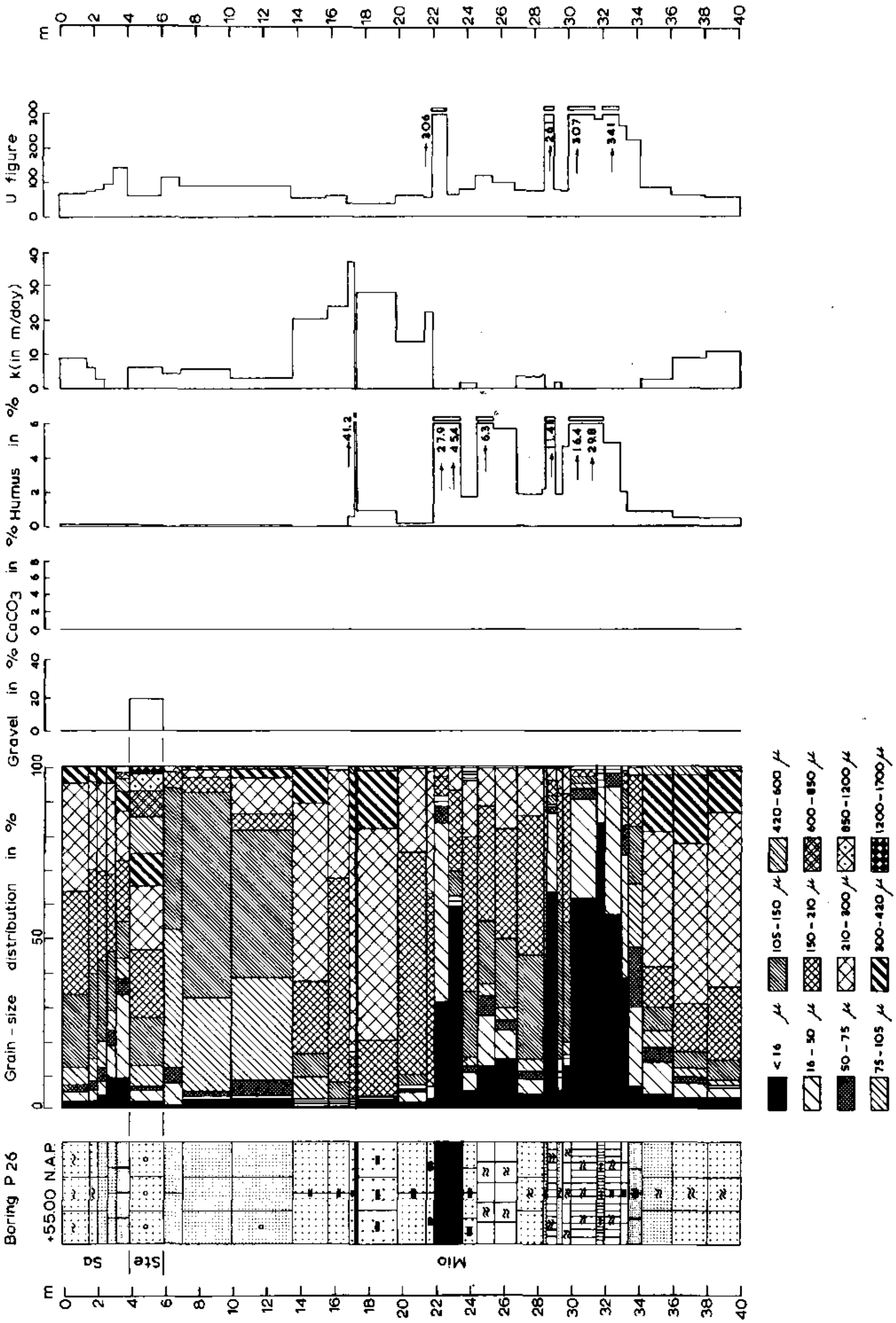
Boring P 26
+55.00 N.A.P.
Sa
Ste
Mio
Grain - size distribution in %
Gravel in %
% CaCO3 in
% Humus in %
k (in m/day)
U figure
m
< 16 μ
16 - 50 μ
50 - 75 μ
75 - 105 μ
105 - 150 μ
150 - 210 μ
210 - 300 μ
300 - 420 μ
420 - 600 μ
600 - 850 μ
850 - 1200 μ
1200 - 1700 μ
41.2
27.9
45.4
6.3
14.8
16.4
29.8
306
261
307
341

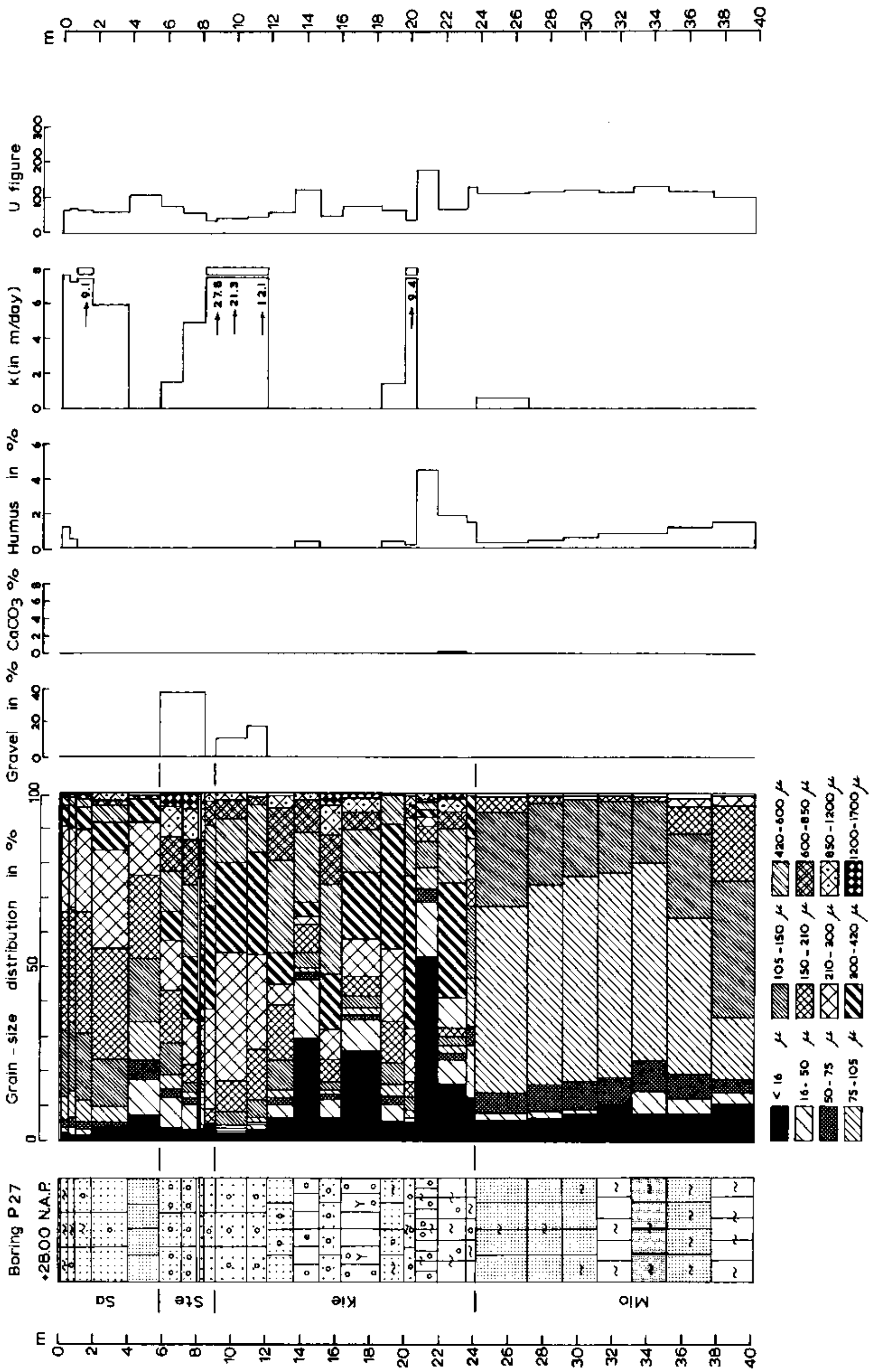
Boring P27
+28.00 N.A.P.
Sa
Ste
Kie
Mio
Grain - size distribution in %
Gravel in %
CaCO3 %
Humus in %
k (in m/day)
U figure
m
9.1
27.8
21.3
12.1
9.4
< 16 μ
16 - 50 μ
50 - 75 μ
75 - 105 μ
105 - 150 μ
150 - 210 μ
210 - 300 μ
300 - 420 μ
420 - 600 μ
600 - 850 μ
850 - 1200 μ
1200 - 1700 μ

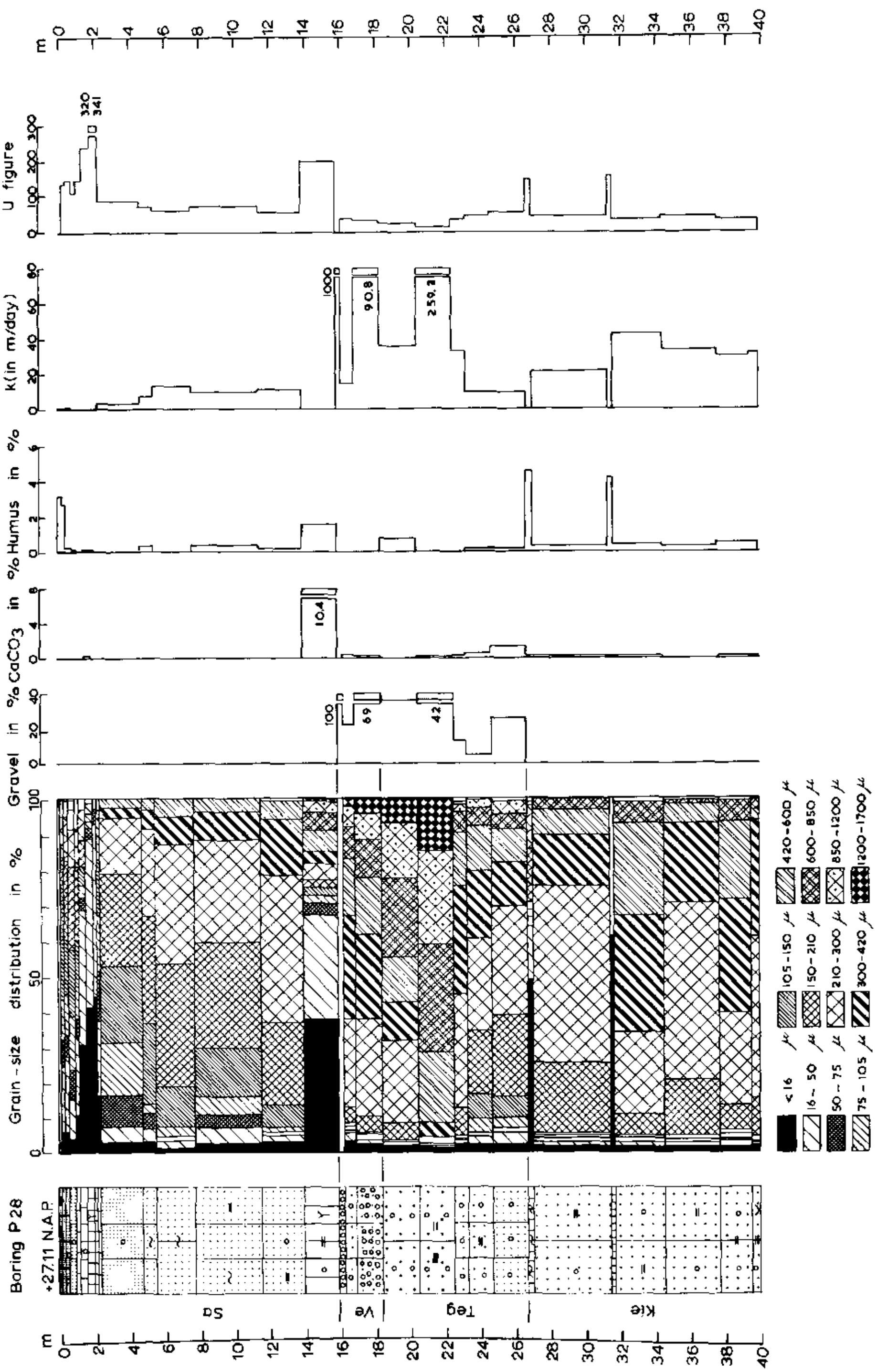

Boring P 28
+27.11 N.A.P.
m
Sa
Ve
Teg
Kie
Grain - size distribution in %
Gravel in %
CaCO3 in %
% Humus in %
k (in m/day)
U figure
100
69
42
10.4
1000
90.8
259.2
320
341
<16 μ
16 - 50 μ
50 - 75 μ
75 - 105 μ
105 - 150 μ
150 - 210 μ
210 - 300 μ
300 - 420 μ
420 - 600 μ
600 - 850 μ
850 - 1200 μ
1200 - 1700 μ

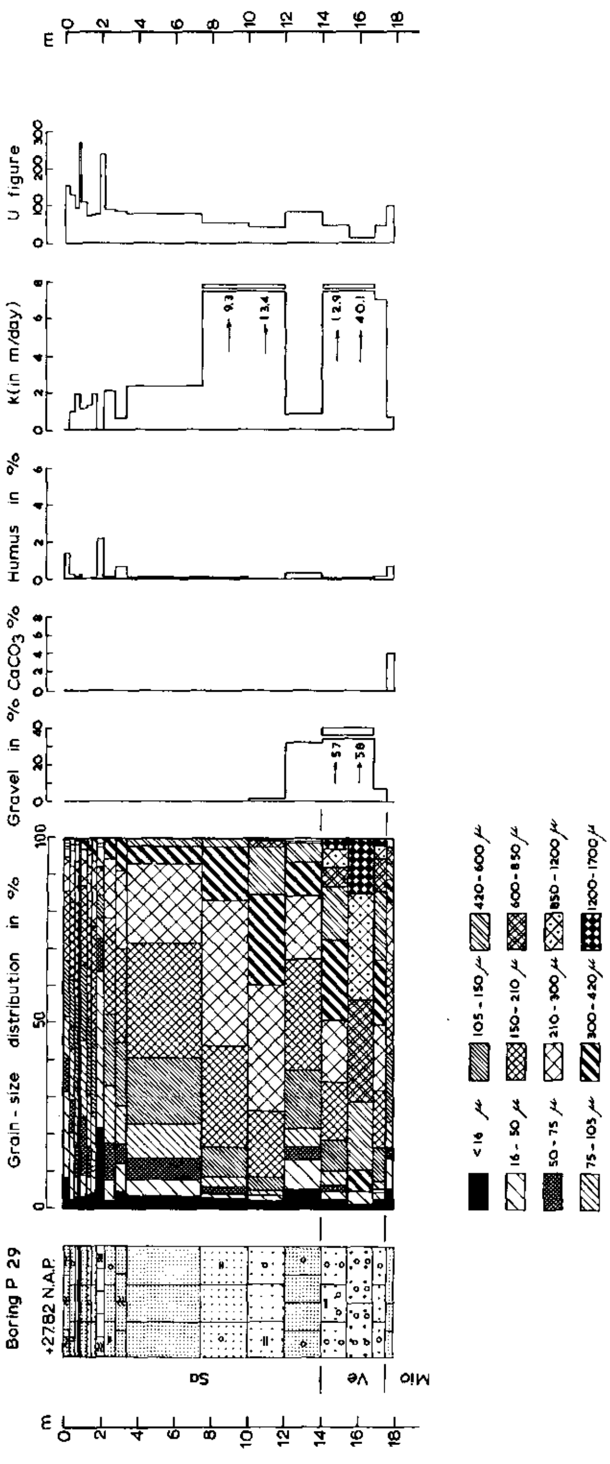
Boring P 29
+27.82 N.A.P.
Sa
Ve
Mio
m
Grain - size distribution in %
Gravel in %
$CaCO_3$ %
Humus in %
K (in m/day)
U figure
< 16 μ
16 - 50 μ
50 - 75 μ
75 - 105 μ
105 - 150 μ
150 - 210 μ
210 - 300 μ
300 - 420 μ
420 - 600 μ
600 - 850 μ
850 - 1200 μ
1200 - 1700 μ

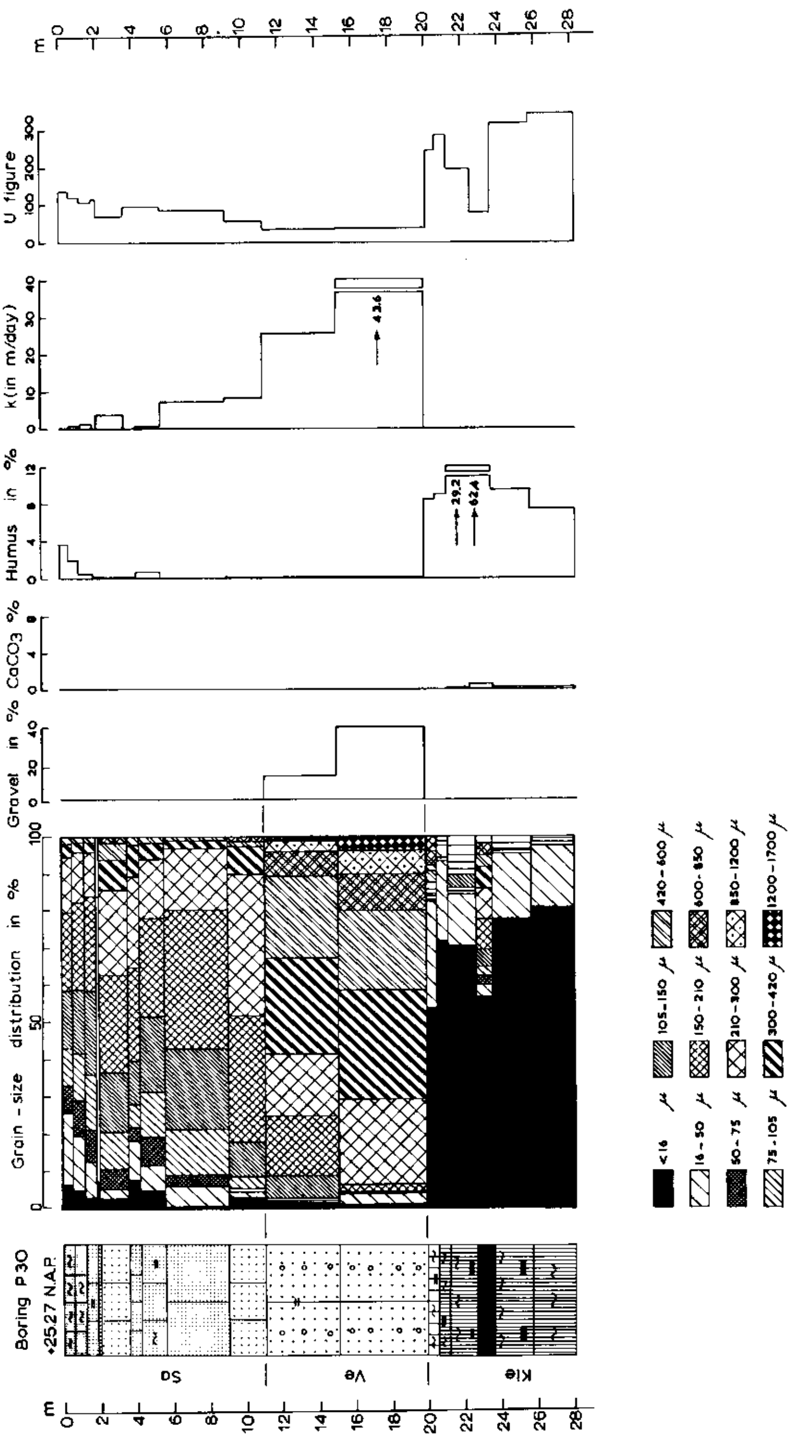

Boring P30
+25.27 N.A.P.
Sa
Ve
Kle
m
Grain - size distribution in %
Gravel in %
CaCO3 %
Humus in %
k (in m/day)
U figure
43.6
29.2
62.4
<16 μ
16 - 50 μ
50 - 75 μ
75 - 105 μ
105 - 150 μ
150 - 210 μ
210 - 300 μ
300 - 420 μ
420 - 600 μ
600 - 850 μ
850 - 1200 μ
1200 - 1700 μ

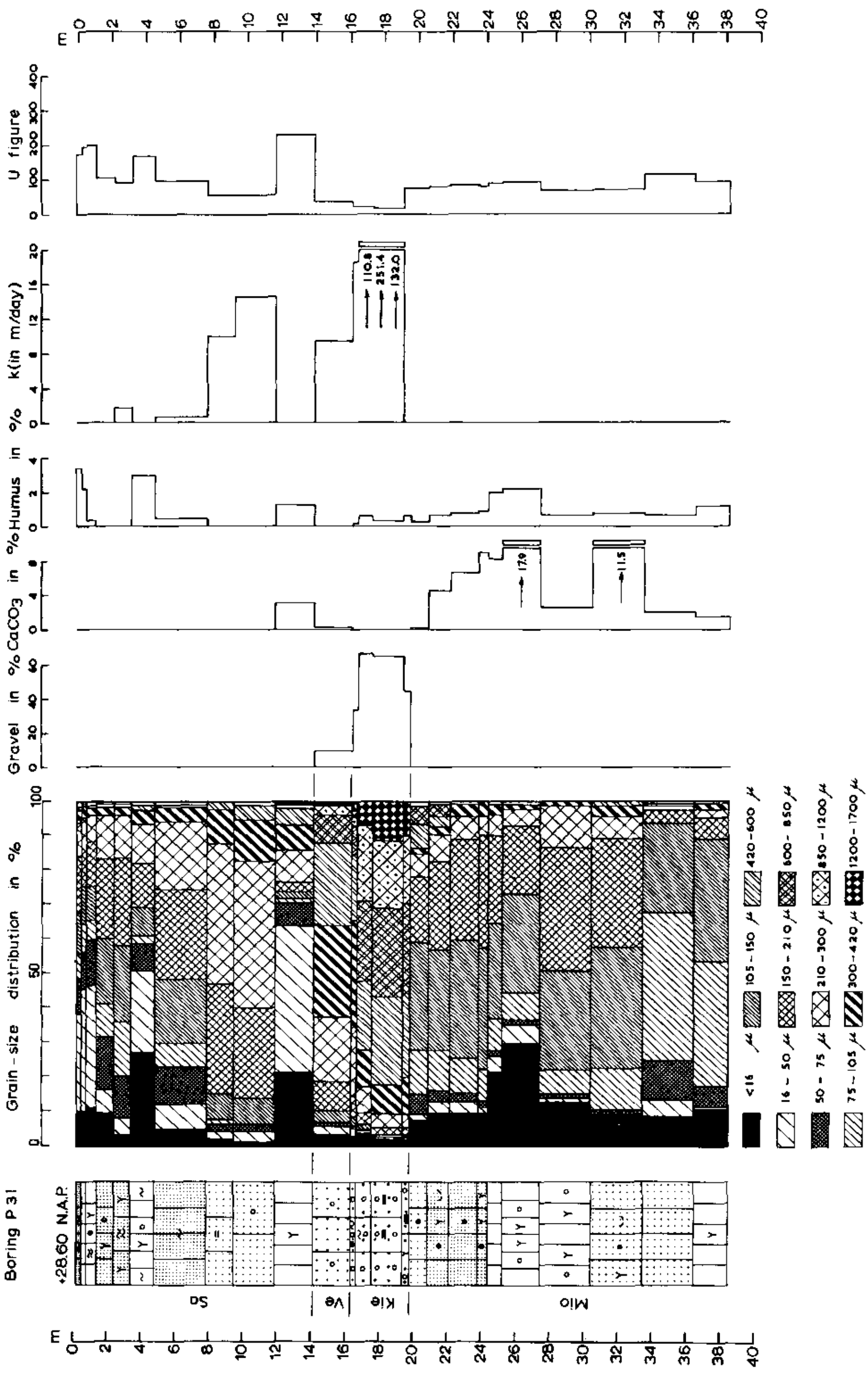

Boring P 31
+28.60 N.A.P.
Sa
Ve
Kie
Mio
Grain - size distribution in %
Gravel in %
% CaCO3 in %
% Humus in %
% k(in m/day)
U figure
m
110.8
251.4
132.0
17.9
11.5
<16 μ
16 - 50 μ
50 - 75 μ
75 - 105 μ
105 - 150 μ
150 - 210 μ
210 - 300 μ
300 - 420 μ
420 - 600 μ
600 - 850 μ
850 - 1200 μ
1200 - 1700 μ

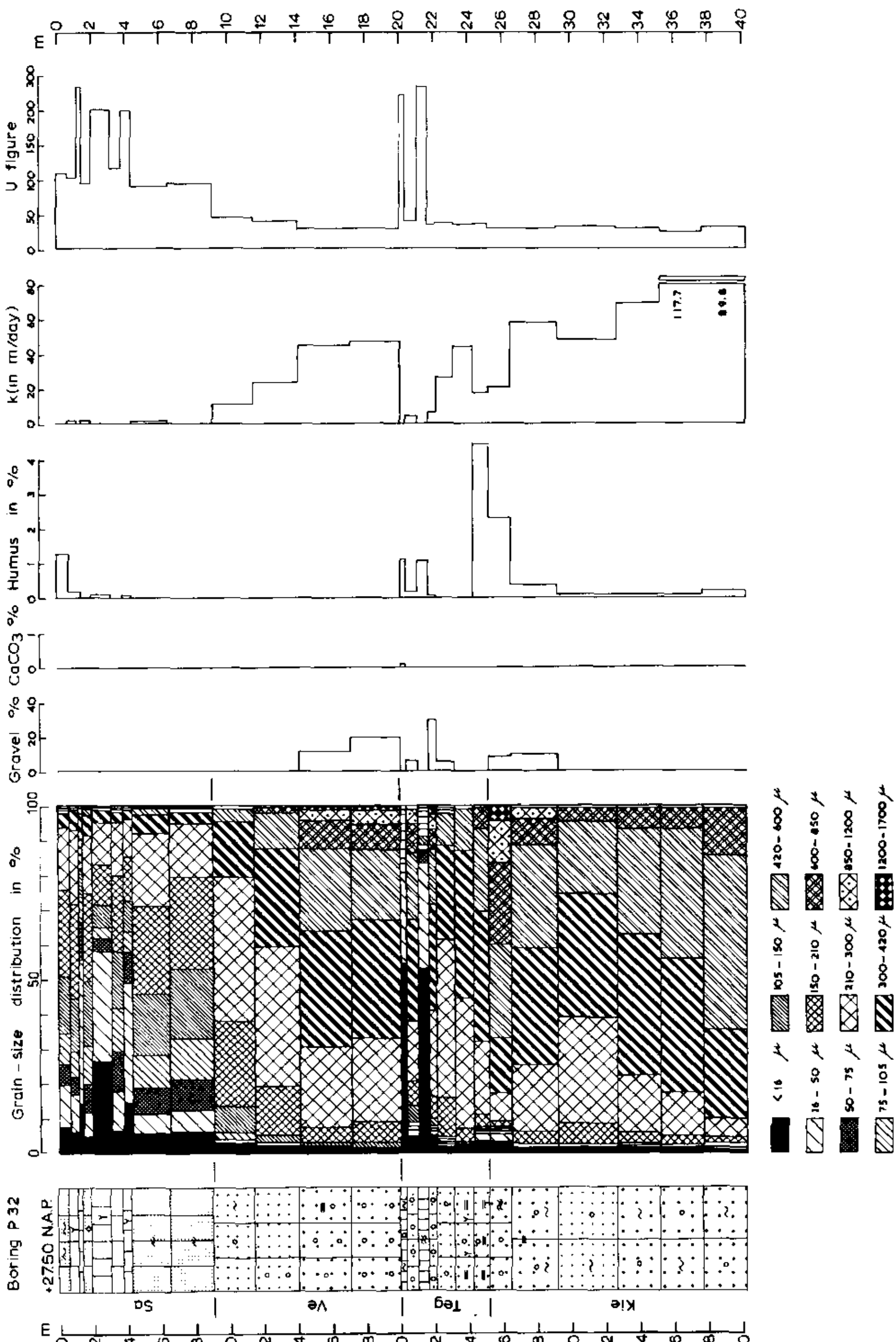
Boring P 32
+27.50 N.A.P.
m
Sa
Ve
Teg
Kie
Grain - size distribution in %
Gravel %
CaCO3 %
Humus in %
k (in m/day)
U figure
< 16 μ
16 - 50 μ
50 - 75 μ
75 - 105 μ
105 - 150 μ
150 - 210 μ
210 - 300 μ
300 - 420 μ
420 - 600 μ
600 - 850 μ
850 - 1200 μ
1200 - 1700 μ

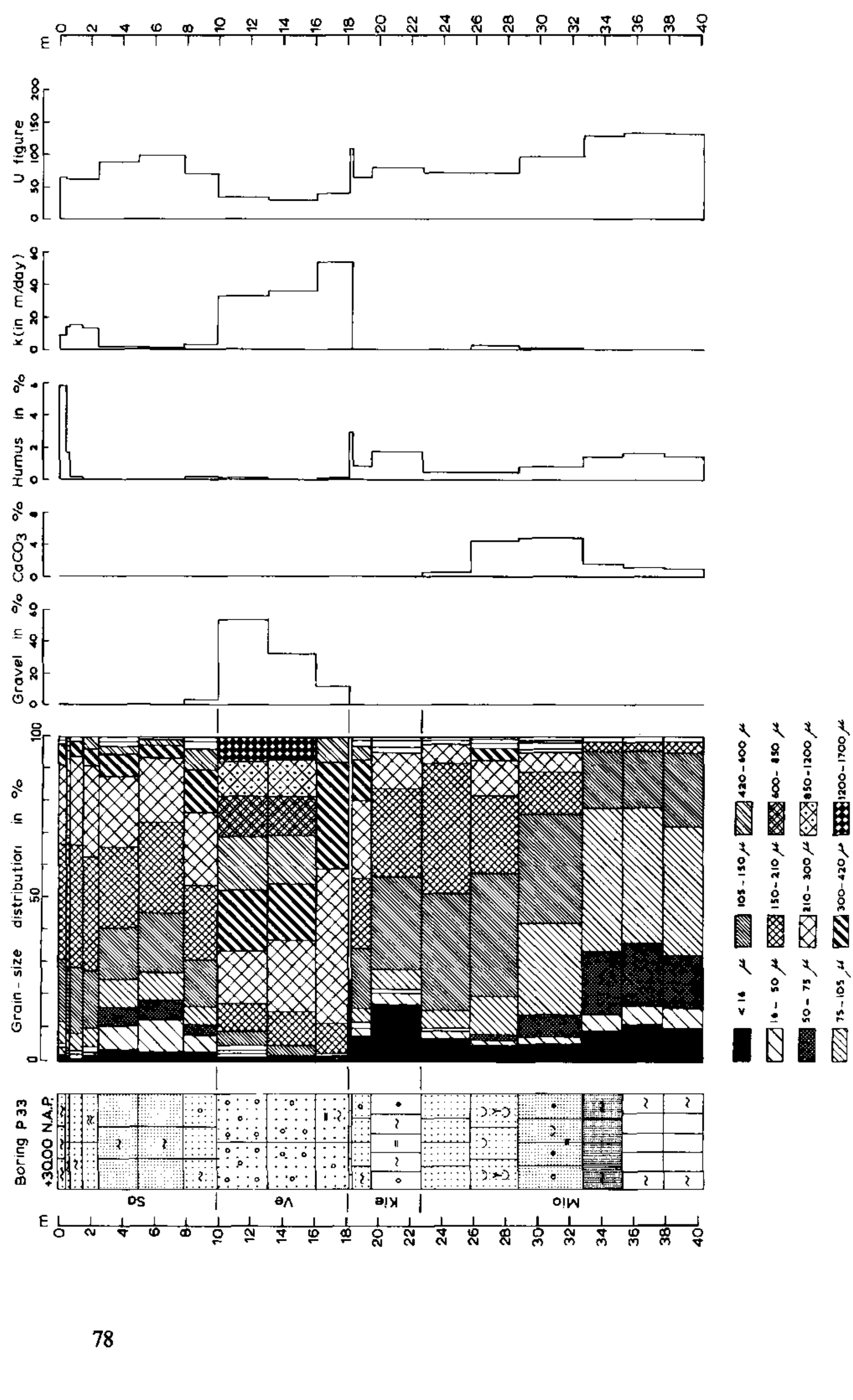
Boring P 33
+30.00 N.A.P.
m
Sa
Ve
Kie
Mio
Grain - size distribution in %
Gravel in %
$CaCO_3$ %
Humus in %
k (in m/day)
U figure
< 16 μ
16 - 50 μ
50 - 75 μ
75 - 105 μ
105 - 150 μ
150 - 210 μ
210 - 300 μ
300 - 420 μ
420 - 600 μ
600 - 850 μ
850 - 1200 μ
1200 - 1700 μ

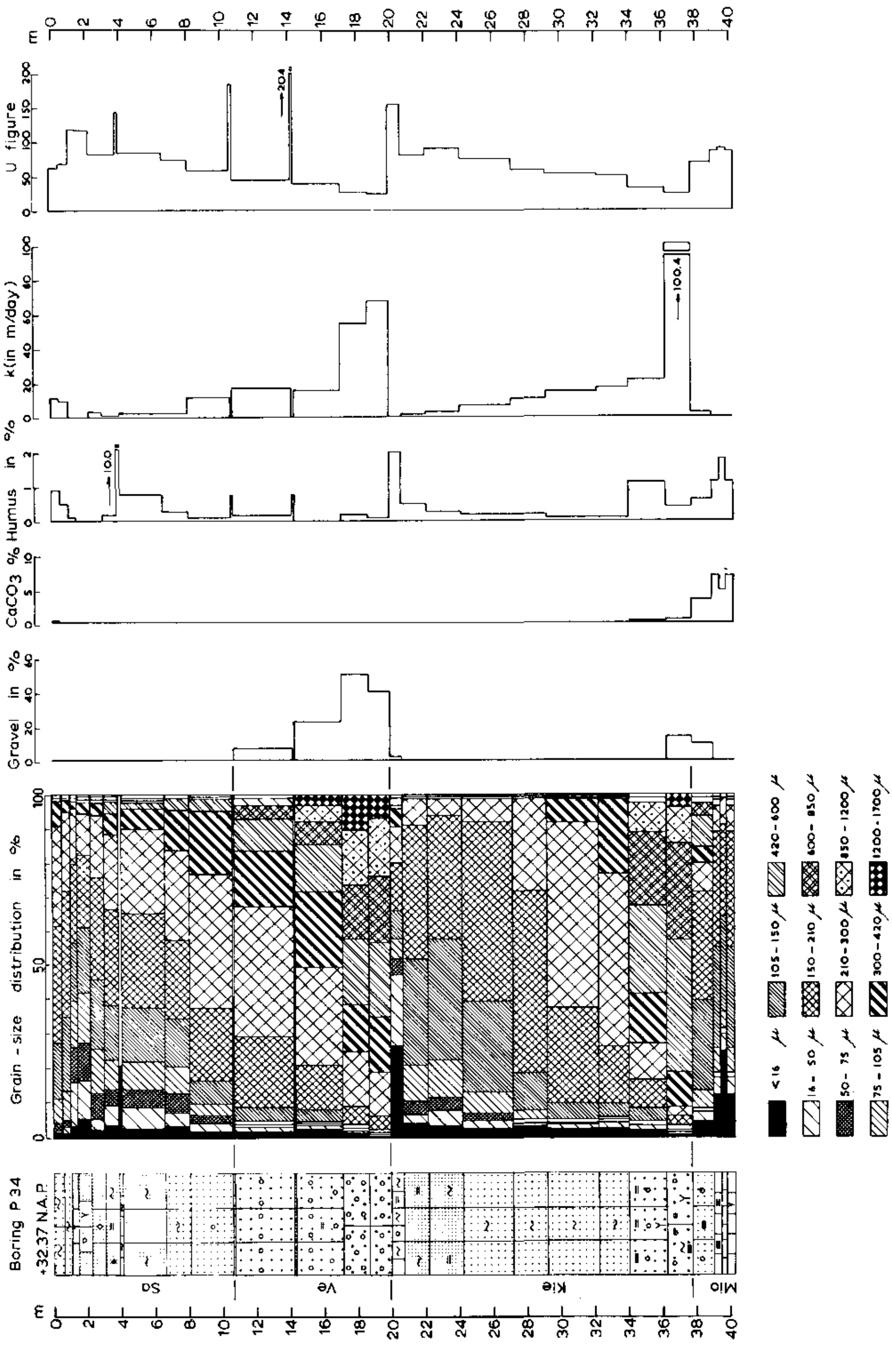

Boring P 34
+32.37 N.A.P.
Sa
Ve
Kie
Mio
m
Grain - size distribution in %
Gravel in %
CaCO3 %
Humus in %
k(in m/day)
U figure
204
100.4
10.0
< 16 μ
16 - 50 μ
50 - 75 μ
75 - 105 μ
105 - 150 μ
150 - 210 μ
210 - 300 μ
300 - 420 μ
420 - 600 μ
600 - 850 μ
850 - 1200 μ
1200 - 1700 μ

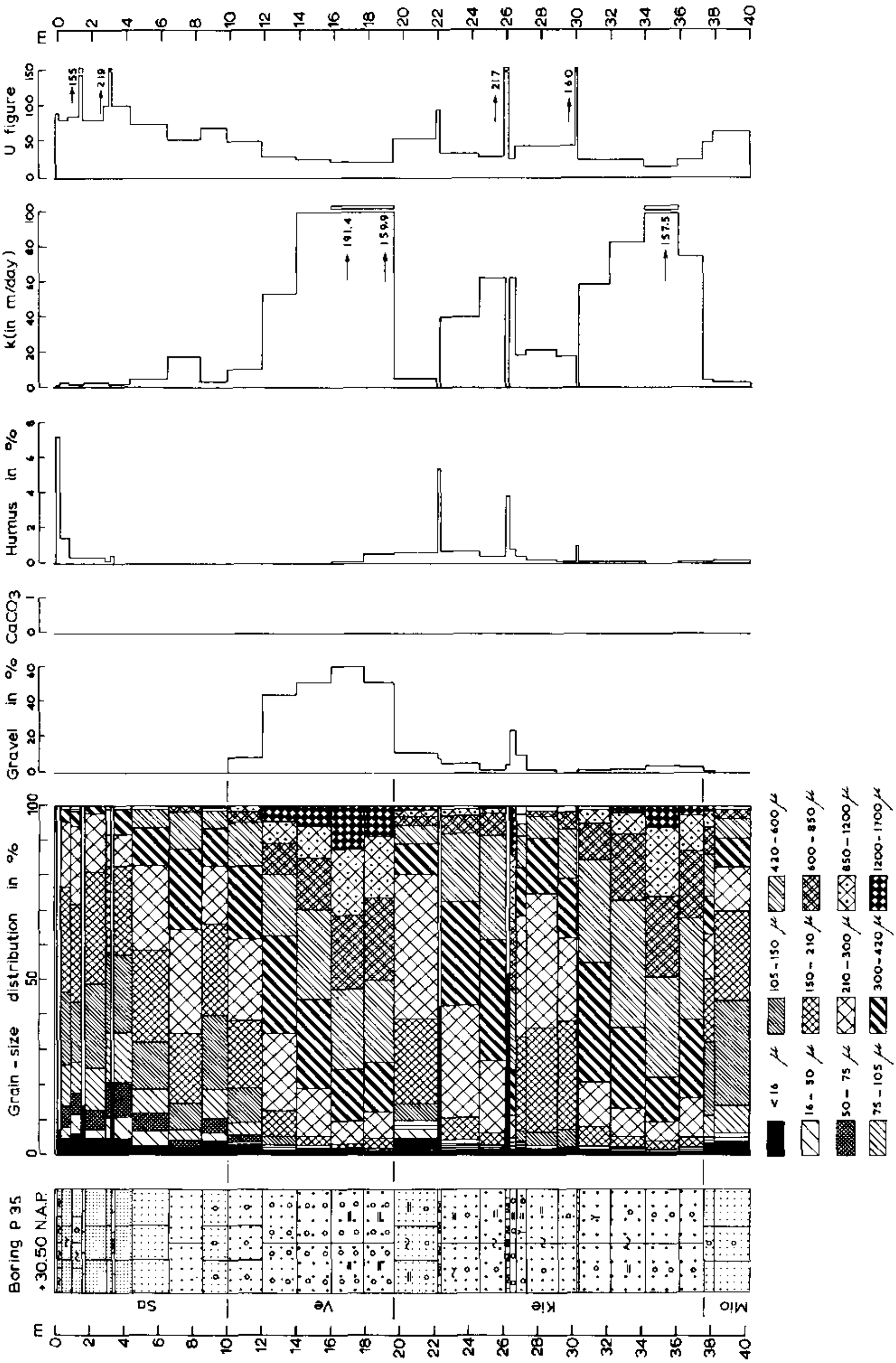
Boring P 35
+30.50 N.A.P.
Grain - size distribution in %
Gravel in %
CaCO3
Humus in %
k (in m/day)
U figure
m
Sa
Ve
Kie
Mio
<16 μ
16 - 50 μ
50 - 75 μ
75 - 105 μ
105 - 150 μ
150 - 210 μ
210 - 300 μ
300 - 420 μ
420 - 600 μ
600 - 850 μ
850 - 1200 μ
1200 - 1700 μ
191.4
159.9
157.5
155
219
217
160

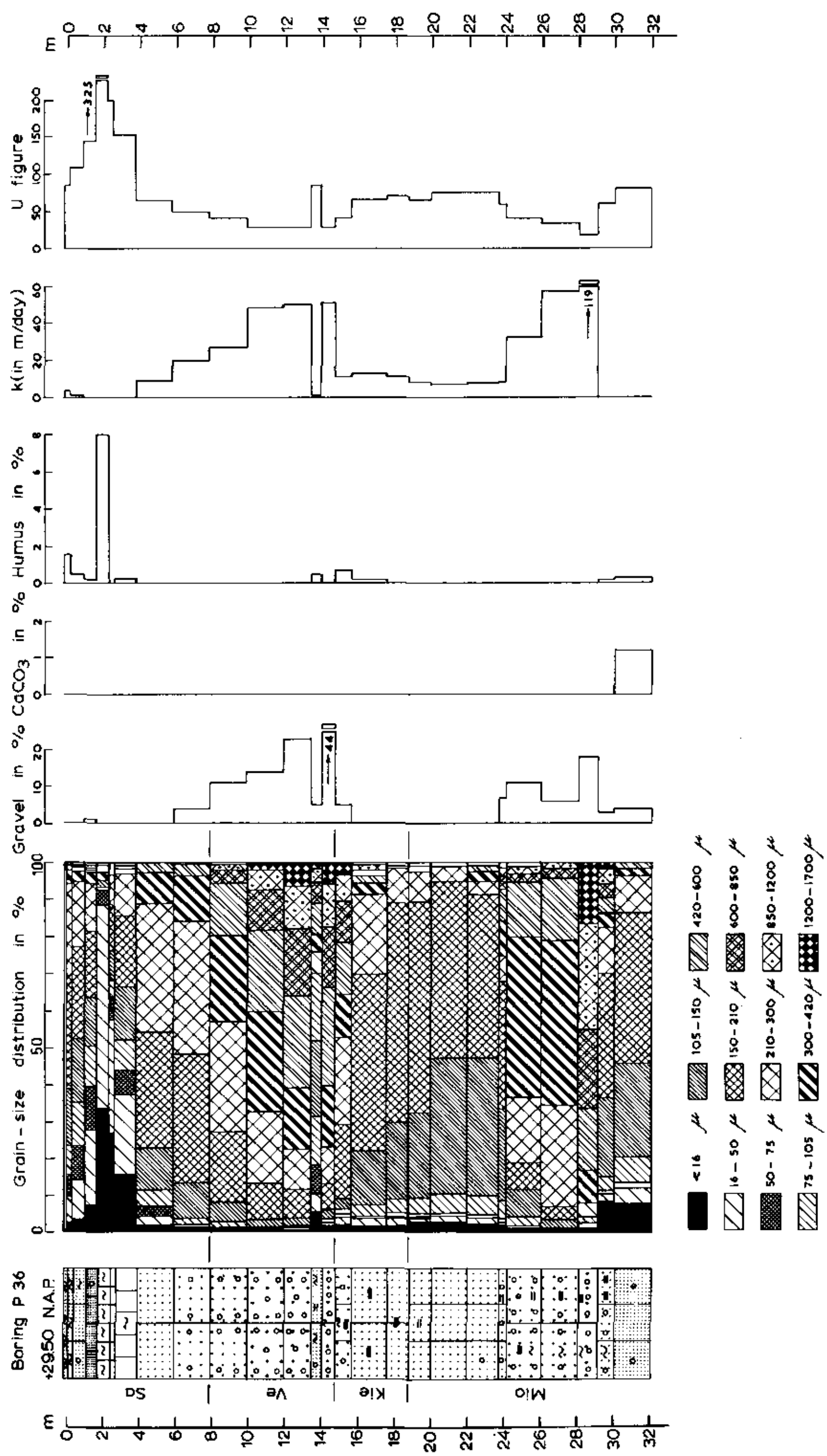

Boring P 36
+29.50 N.A.P.
Sa
Ve
Kie
Mio
m
0 2 4 6 8 10 12 14 16 18 20 22 24 26 28 30 32
Grain - size distribution in %
Gravel in %
CaCO3 in %
Humus in %
k (in m/day)
U figure
325
119
44
< 16 μ
16 – 50 μ
50 – 75 μ
75 – 105 μ
105 – 150 μ
150 – 210 μ
210 – 300 μ
300 – 420 μ
420 – 600 μ
600 – 850 μ
850 – 1200 μ
1200 – 1700 μ

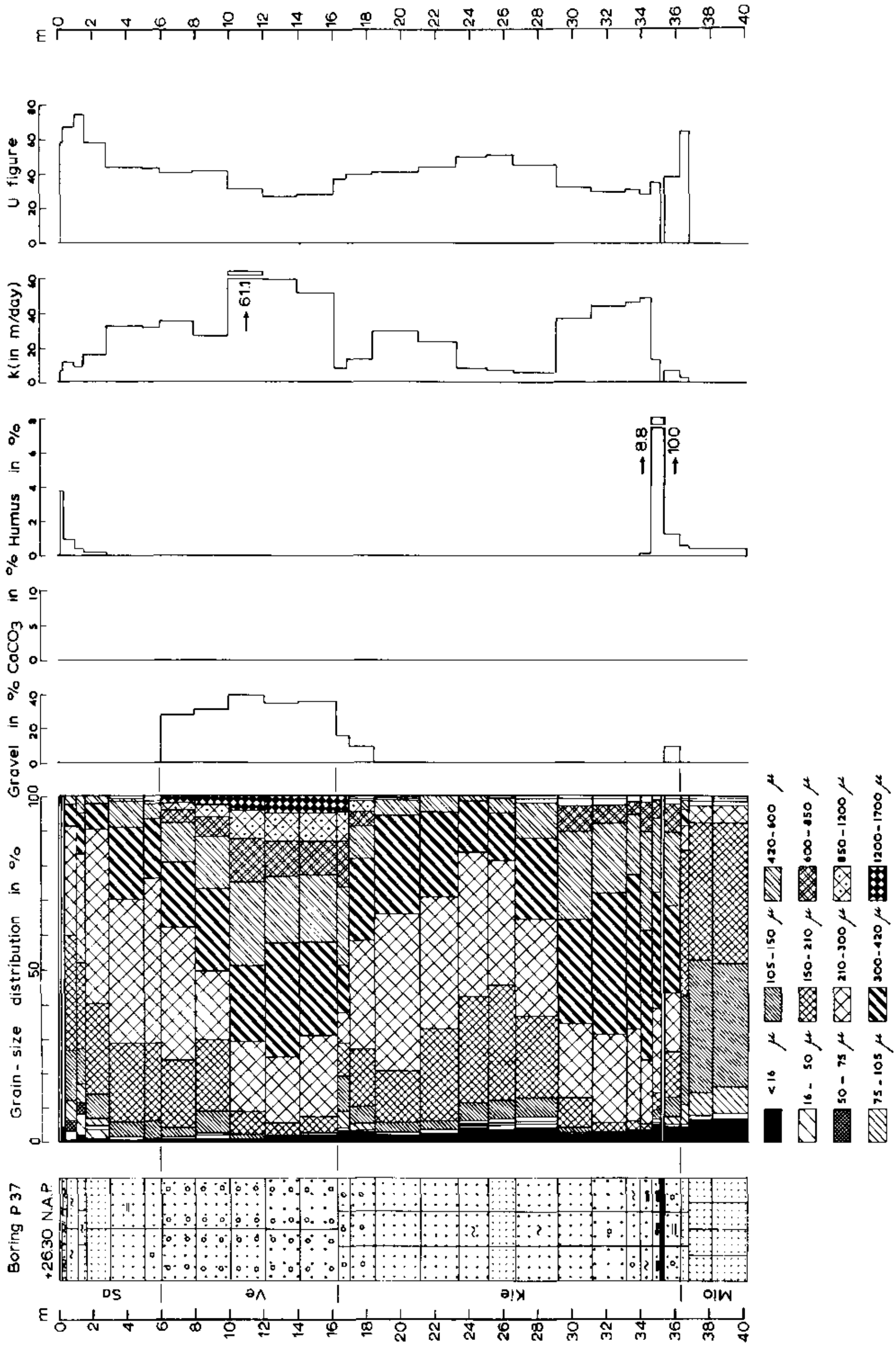
Boring P 37
+26.30 N.A.P.
Sa
Ve
Kie
Mio
m
Grain - size distribution in %
Gravel in %
$CaCO_3$ in %
% Humus in %
8.8
100
k (in m/day)
61.1
U figure
< 16 μ
16 - 50 μ
50 - 75 μ
75 - 105 μ
105 - 150 μ
150 - 210 μ
210 - 300 μ
300 - 420 μ
420 - 600 μ
600 - 850 μ
850 - 1200 μ
1200 - 1700 μ

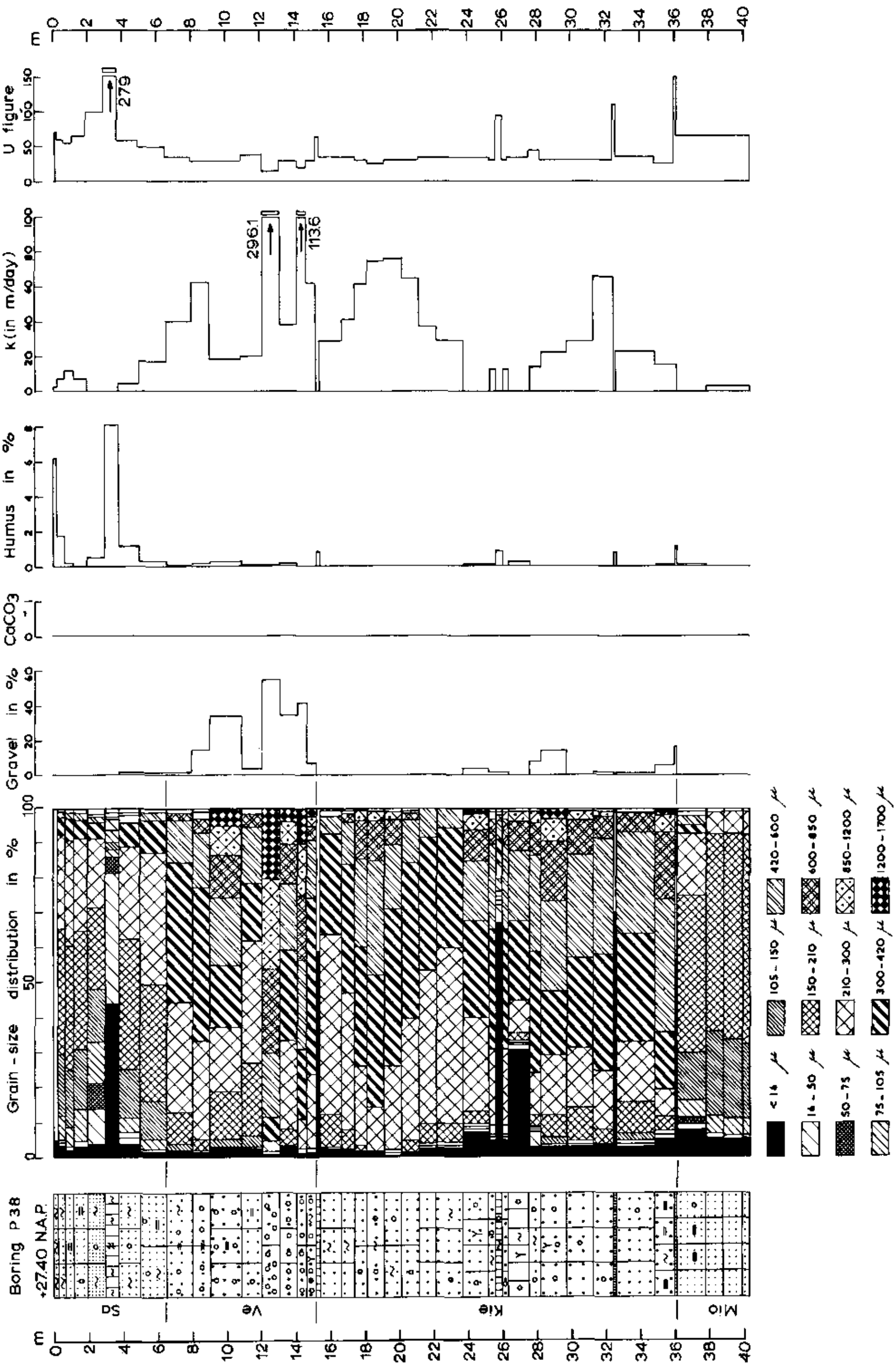

Boring P 38
+27.40 N.A.P.
Grain - size distribution in %
Gravel in %
CaCO3
Humus in %
k (in m/day)
U figure
m
2961
1136
279
Sa
Ve
Kie
Mio
< 16 μ
16 - 50 μ
50 - 75 μ
75 - 105 μ
105 - 150 μ
150 - 210 μ
210 - 300 μ
300 - 420 μ
420 - 600 μ
600 - 850 μ
850 - 1200 μ
1200 - 1700 μ

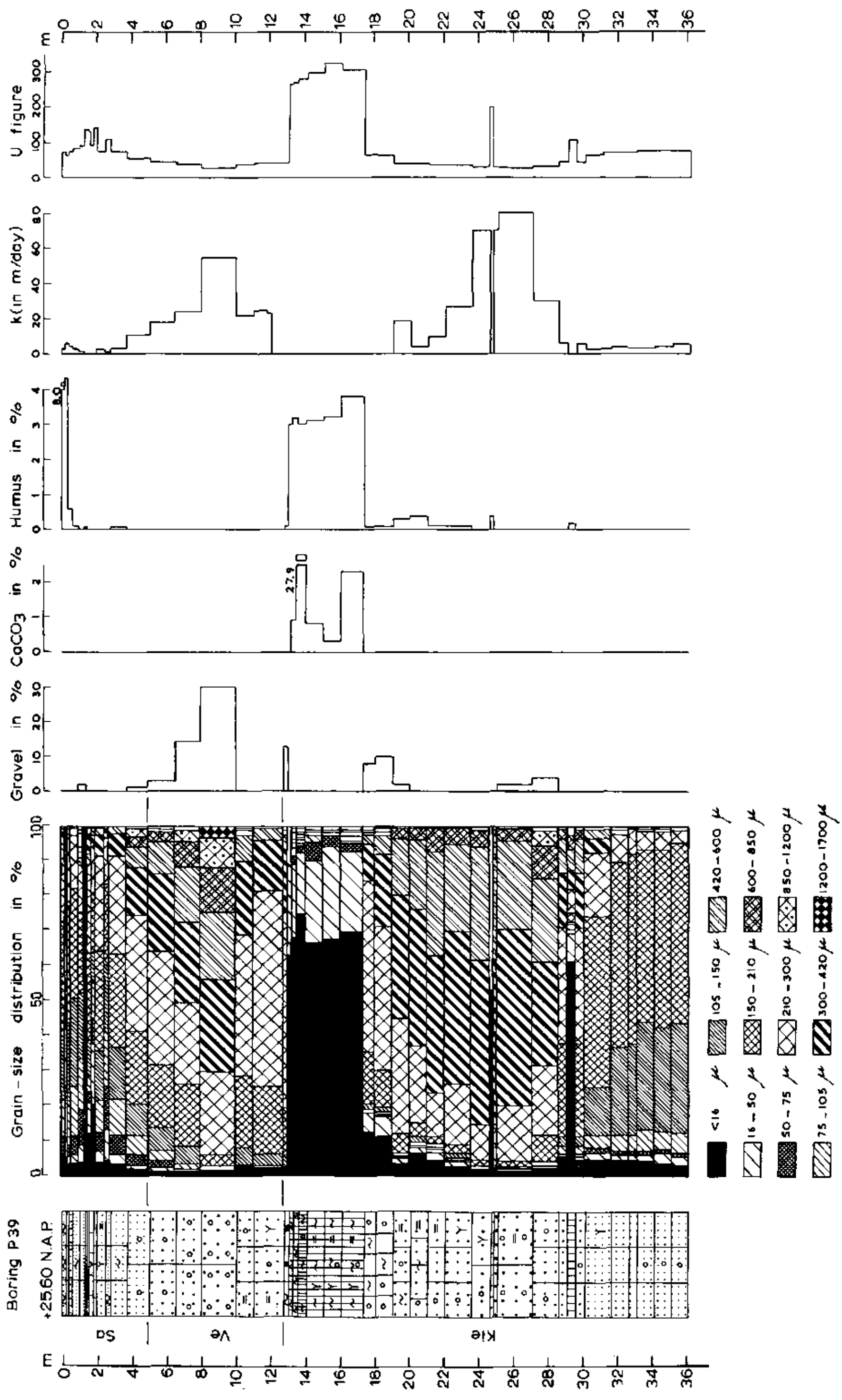
Boring P39
+25.60 N.A.P.
Sa
Ve
Kie
m
Grain - size distribution in %
Gravel in %
CaCO3 in %
27.9
Humus in %
8.0
k (in m/day)
U figure
<16 μ
16 – 50 μ
50 – 75 μ
75 – 105 μ
105 – 150 μ
150 – 210 μ
210 – 300 μ
300 – 420 μ
420 – 600 μ
600 – 850 μ
850 – 1200 μ
1200 – 1700 μ

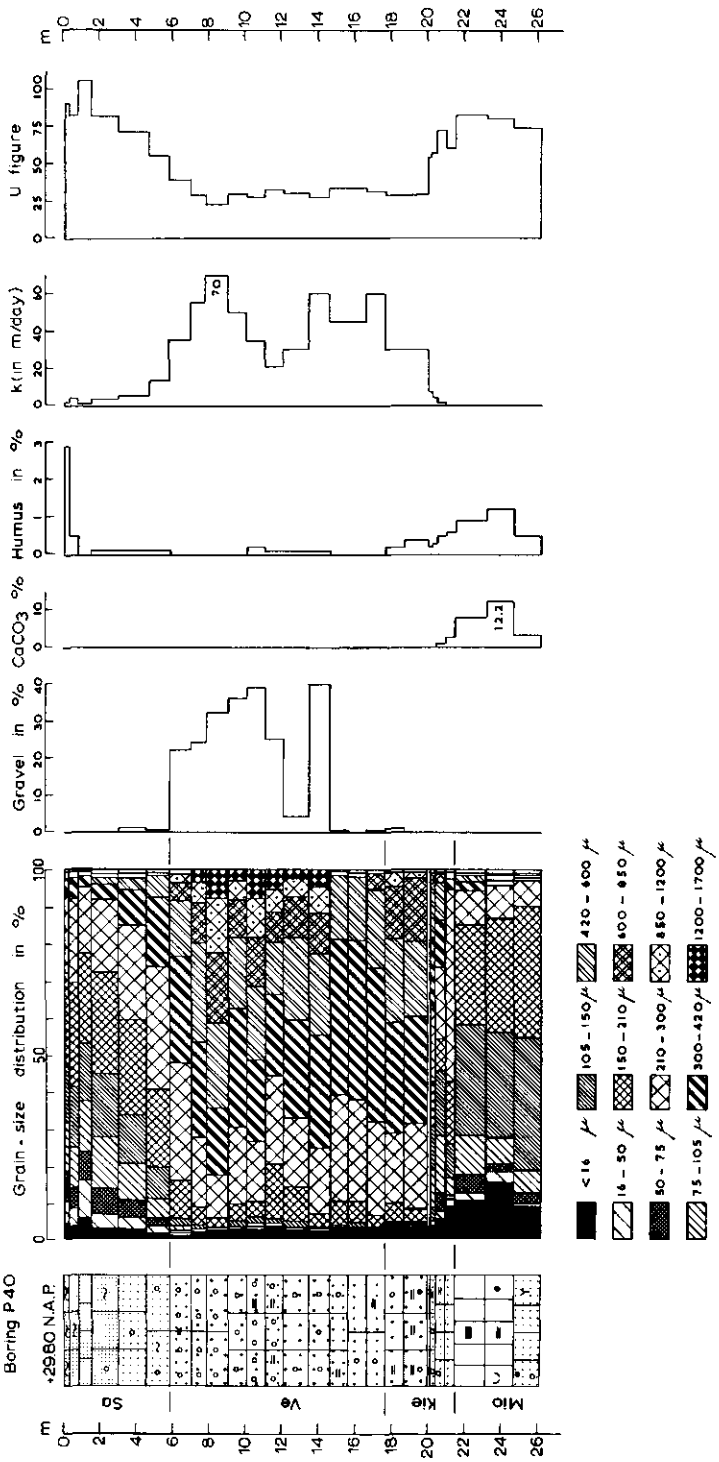

Boring P40
+29.80 N.A.P.
So
Ve
Kie
Mio
m
Grain - size distribution in %
Gravel in %
CaCO3 %
Humus in %
k (in m/day)
70
U figure
12.2
<16 μ
16 - 50 μ
50 - 75 μ
75 - 105 μ
105 - 150 μ
150 - 210 μ
210 - 300 μ
300 - 420 μ
420 - 600 μ
600 - 850 μ
850 - 1200 μ
1200 - 1700 μ

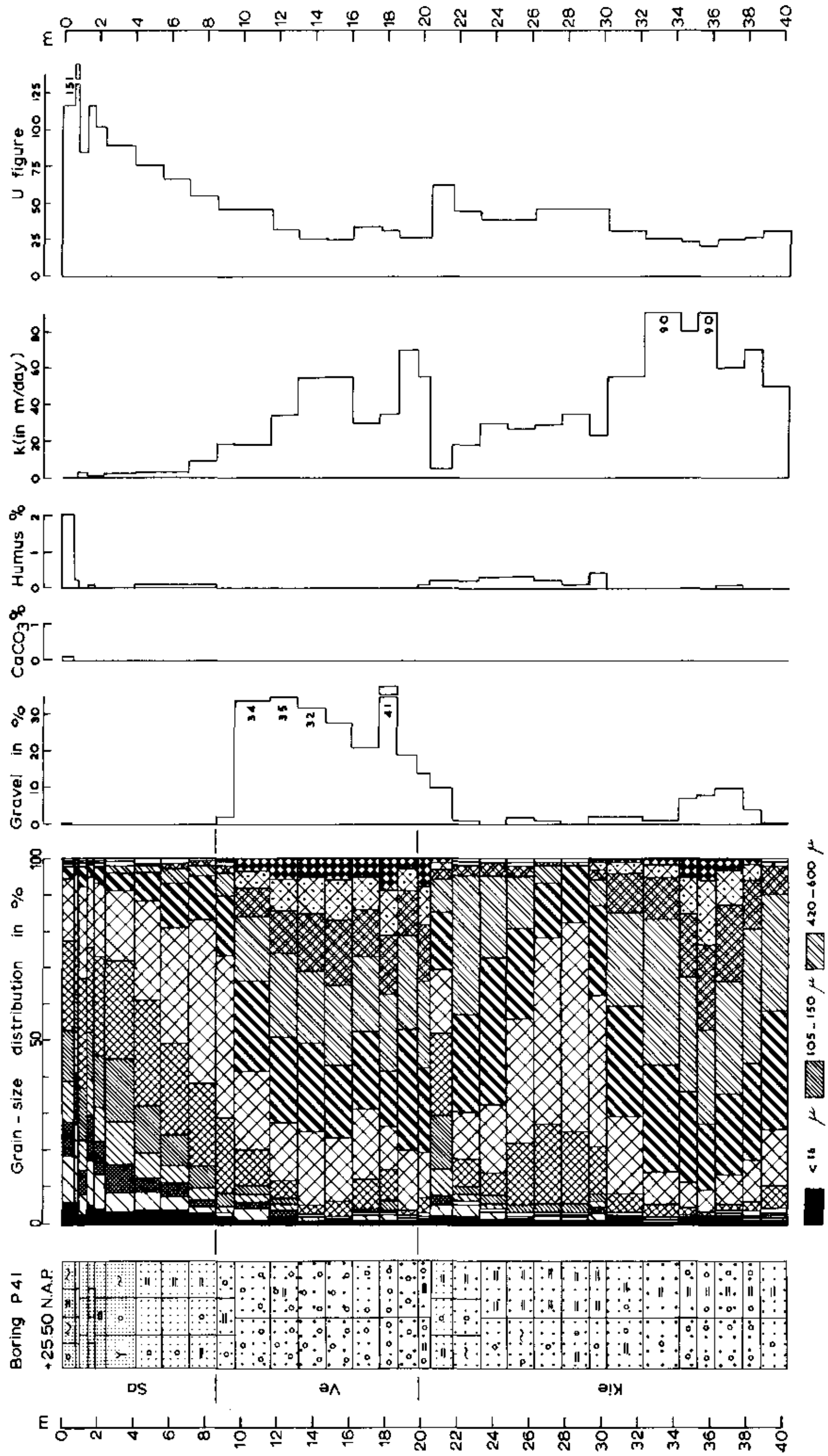

Boring P41 +25.50 N.A.P.
Grain - size distribution in %
Gravel in %
CaCO3 %
Humus %
k (in m/day)
U figure
Sa
Ve
Kie
m
< 16 μ
16 - 50 μ
50 - 75 μ
75 - 105 μ
105 - 150 μ
150 - 210 μ
210 - 300 μ
300 - 420 μ
420 - 600 μ
600 - 850 μ
850 - 1200 μ
1200 - 1700 μ

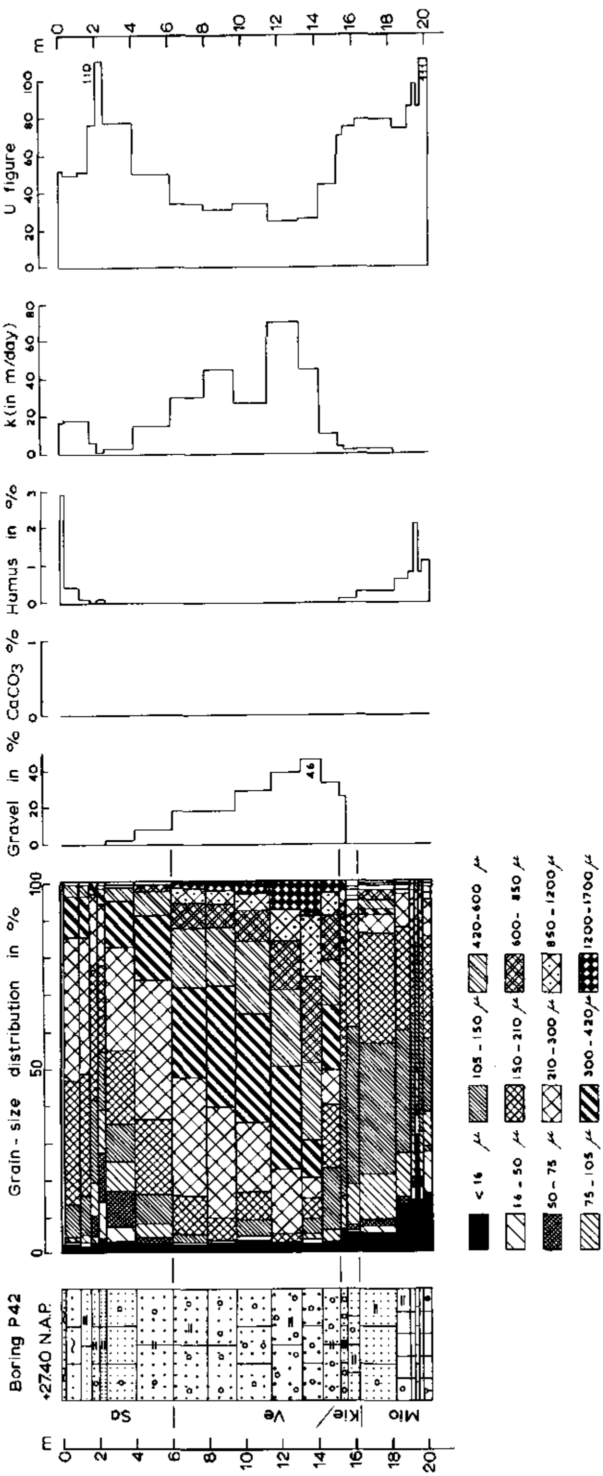

Boring P42
+27.40 N.A.P.
Sa
Ve
Kie
Mio
m
Grain - size distribution in %
Gravel in %
CaCO3 %
Humus in %
k (in m/day)
U figure
< 16 μ
16 - 50 μ
50 - 75 μ
75 - 105 μ
105 - 150 μ
150 - 210 μ
210 - 300 μ
300 - 420 μ
420 - 600 μ
600 - 850 μ
850 - 1200 μ
1200 - 1700 μ

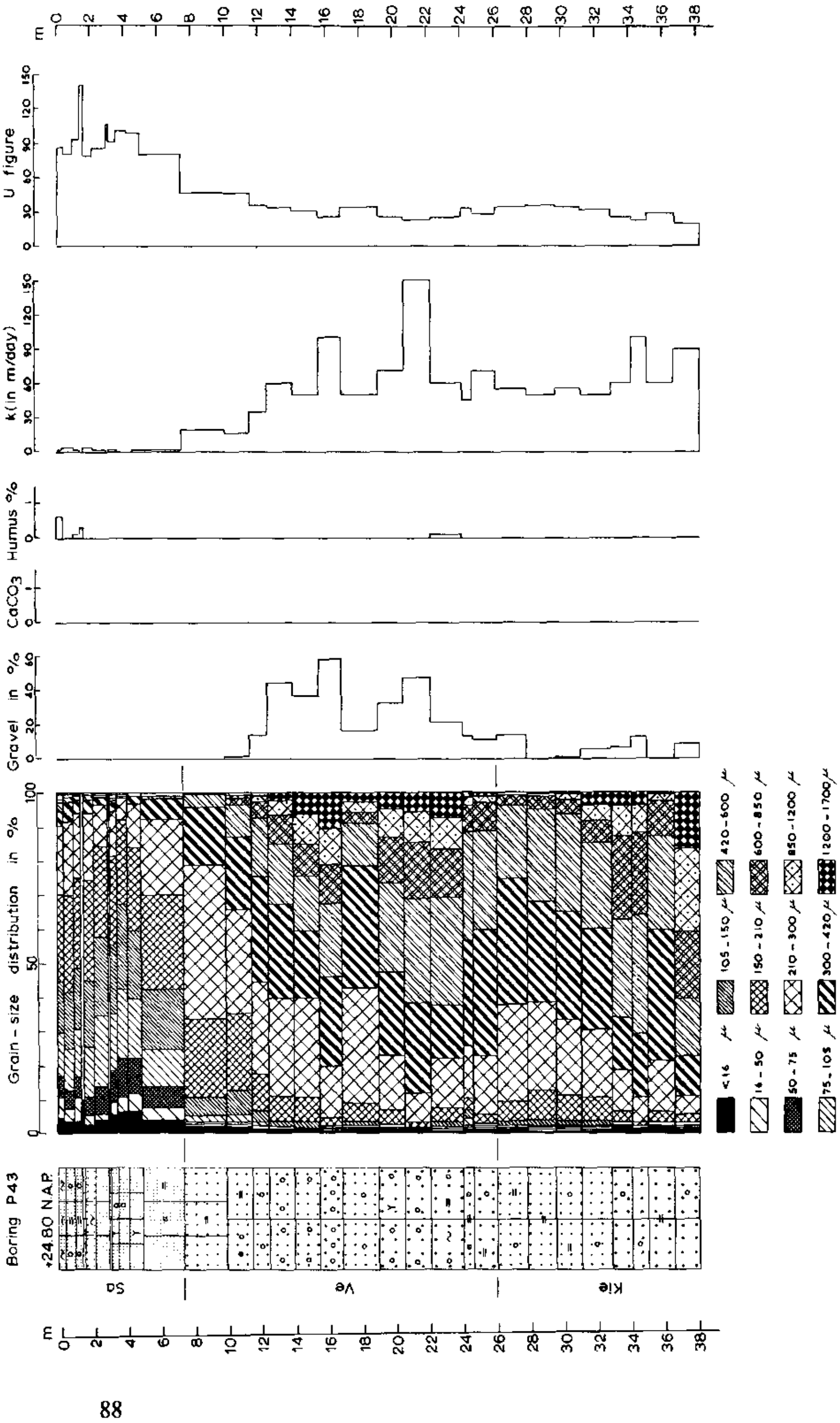

Boring P43
+24.80 N.A.P.
Sa
Ve
Kie
m
Grain - size distribution in %
Gravel in %
CaCO3
Humus %
k (in m/day)
U figure
<16 μ
16 - 50 μ
50 - 75 μ
75 - 105 μ
105 - 150 μ
150 - 210 μ
210 - 300 μ
300 - 420 μ
420 - 600 μ
600 - 850 μ
850 - 1200 μ
1200 - 1700 μ

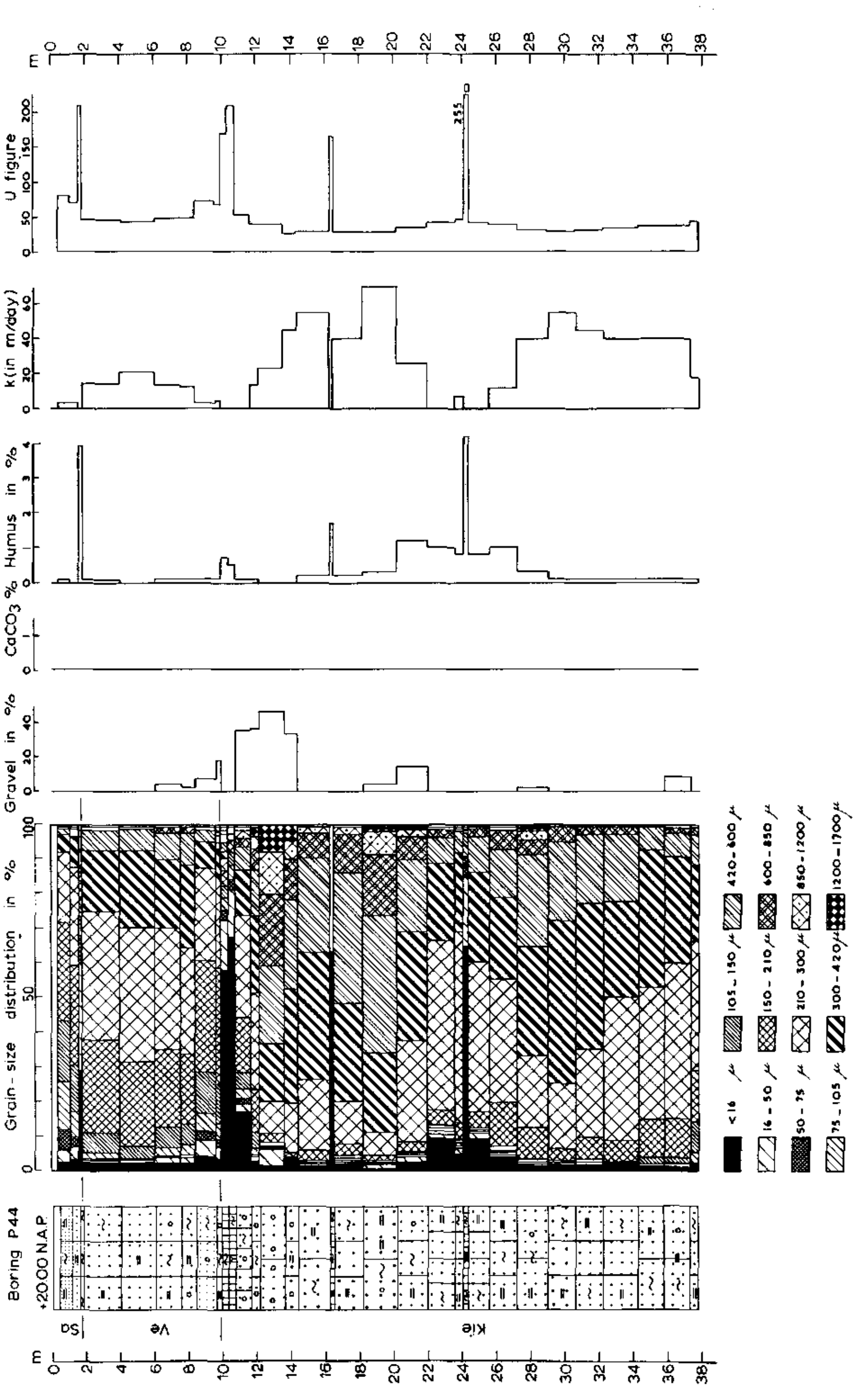

m
U figure
255
k (in m/day)
Humus in %
$CaCO_3$ %
Gravel in %
Grain-size distribution in %
Boring P44
+20.00 N.A.P.
Sa
Ve
Kie
<16 μ
16 - 50 μ
50 - 75 μ
75 - 105 μ
105 - 150 μ
150 - 210 μ
210 - 300 μ
300 - 420 μ
420 - 600 μ
600 - 850 μ
850 - 1200 μ
1200 - 1700 μ

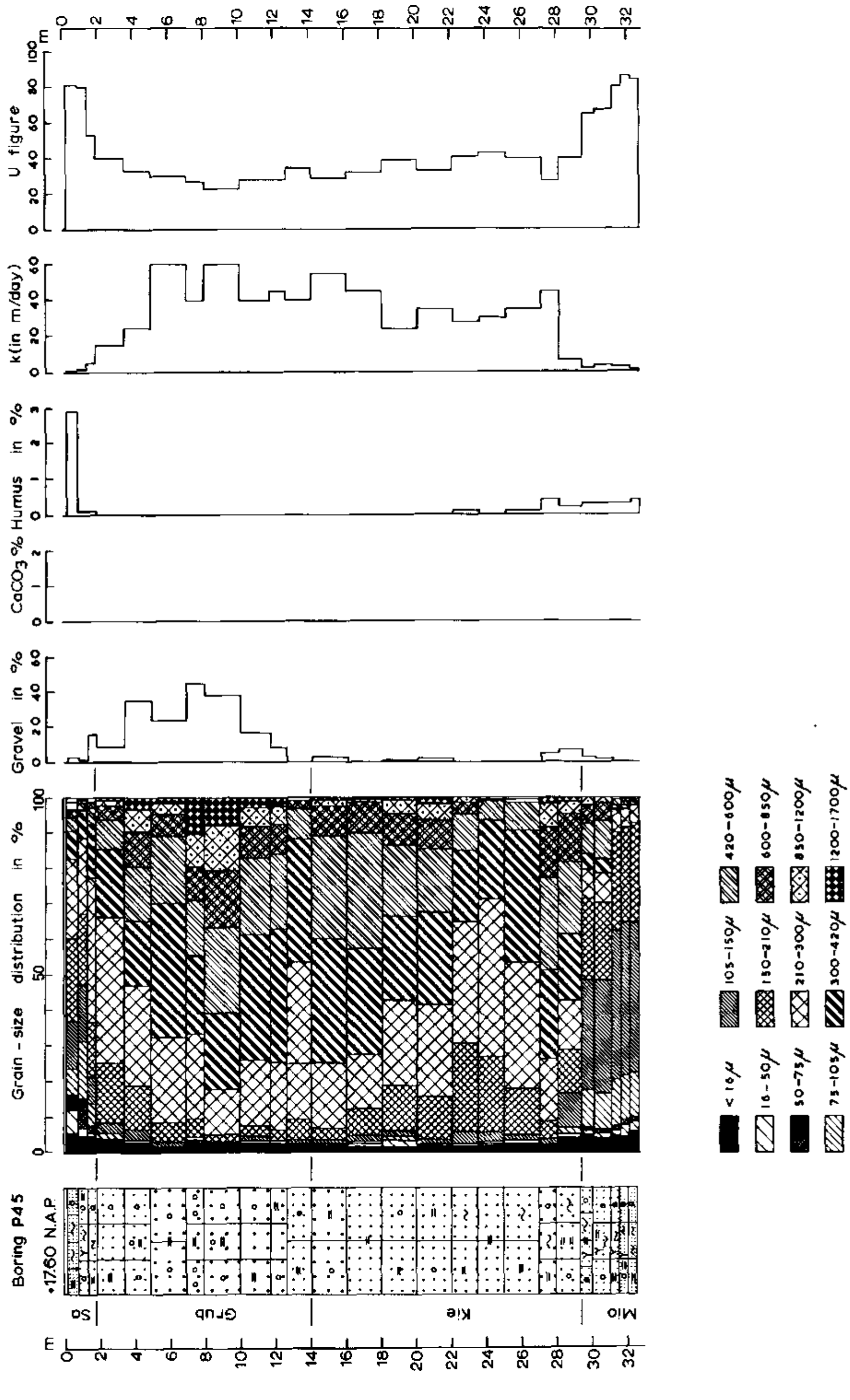

Boring P45
+17.60 N.A.P.
Sa
Grub
Kie
Mio
Grain - size distribution in %
Gravel in %
CaCO3 %
Humus in %
k (in m/day)
U figure
m
< 16µ
16-50µ
50-75µ
75-105µ
105-150µ
150-210µ
210-300µ
300-420µ
420-600µ
600-850µ
850-1200µ
1200-1700µ

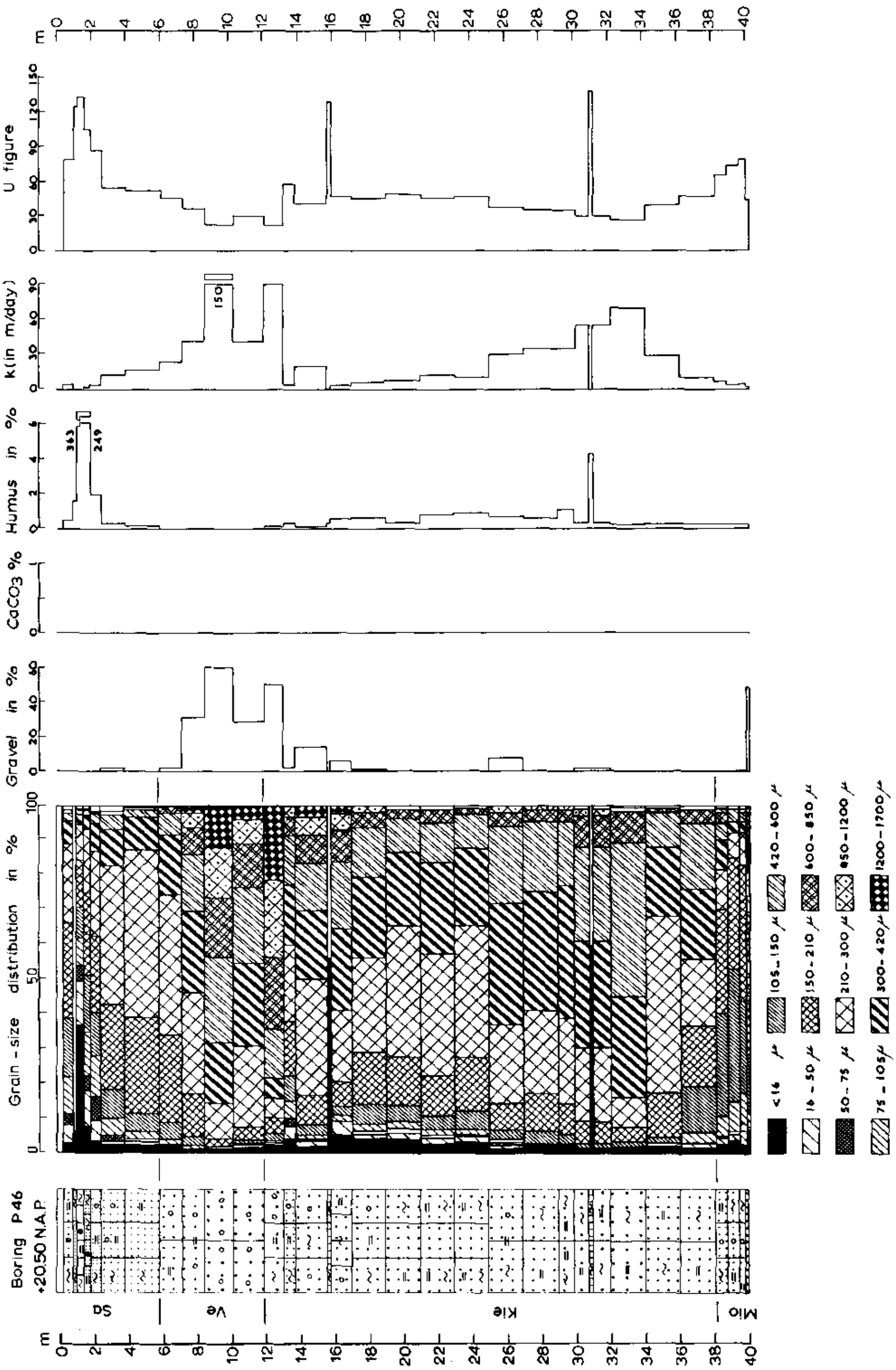
Boring P46
+20.50 N.A.P.
Grain-size distribution in %
Gravel in %
CaCO3 %
Humus in %
k (in m/day)
U figure
m
Sa
Ve
Kie
Mio
363
249
150
< 16 μ
16 - 50 μ
50 - 75 μ
75 - 105 μ
105 - 150 μ
150 - 210 μ
210 - 300 μ
300 - 420 μ
420 - 600 μ
600 - 850 μ
850 - 1200 μ
1200 - 1700 μ

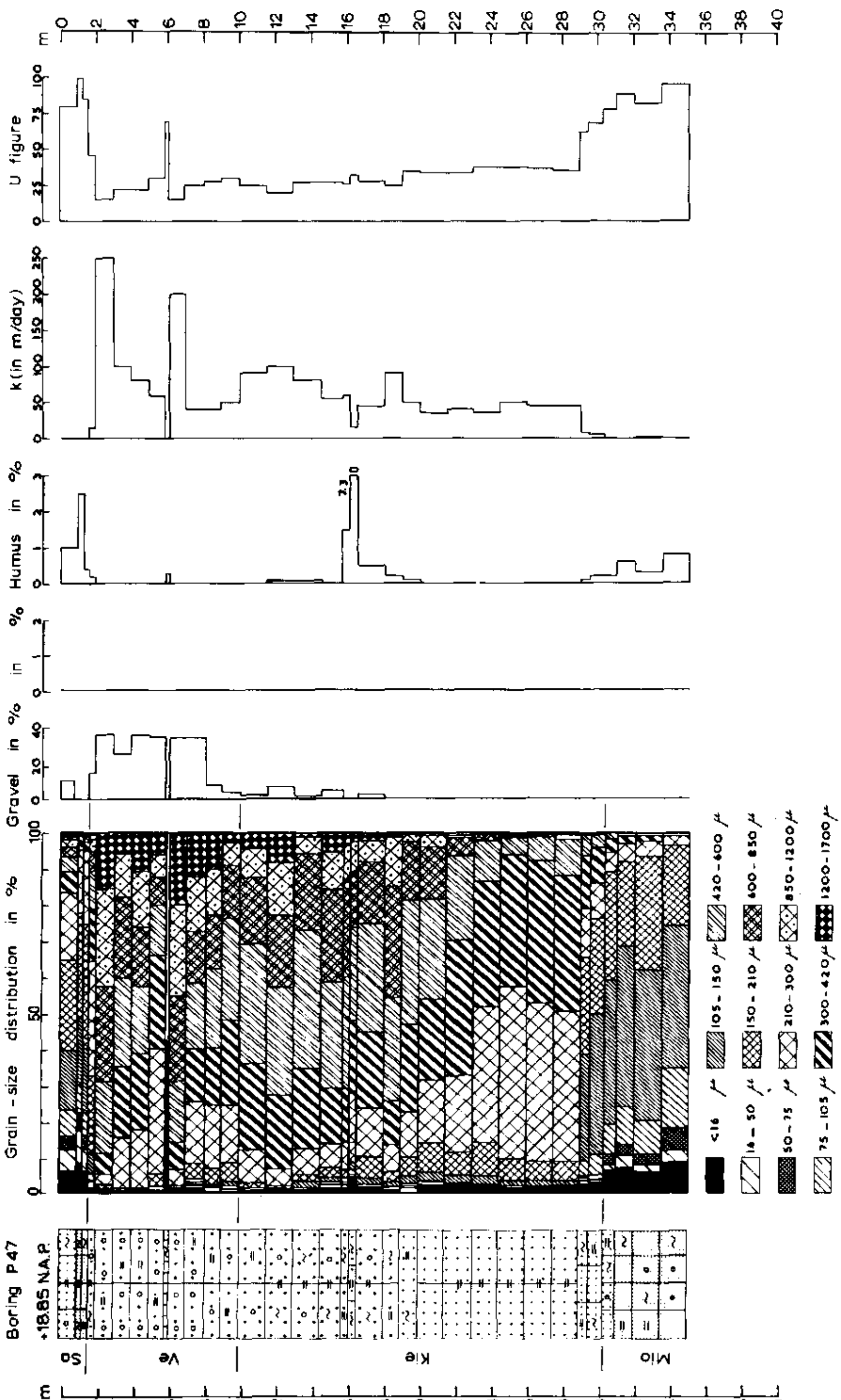
Boring P47
+18.65 N.A.P.
Sa
Ve
Kie
Mio
Grain - size distribution in %
Gravel in %
in %
Humus in %
k (in m/day)
U figure
m
<16 μ
16 – 50 μ
50 – 75 μ
75 – 105 μ
105 – 150 μ
150 – 210 μ
210 – 300 μ
300 – 420 μ
420 – 600 μ
600 – 850 μ
850 – 1200 μ
1200 – 1700 μ

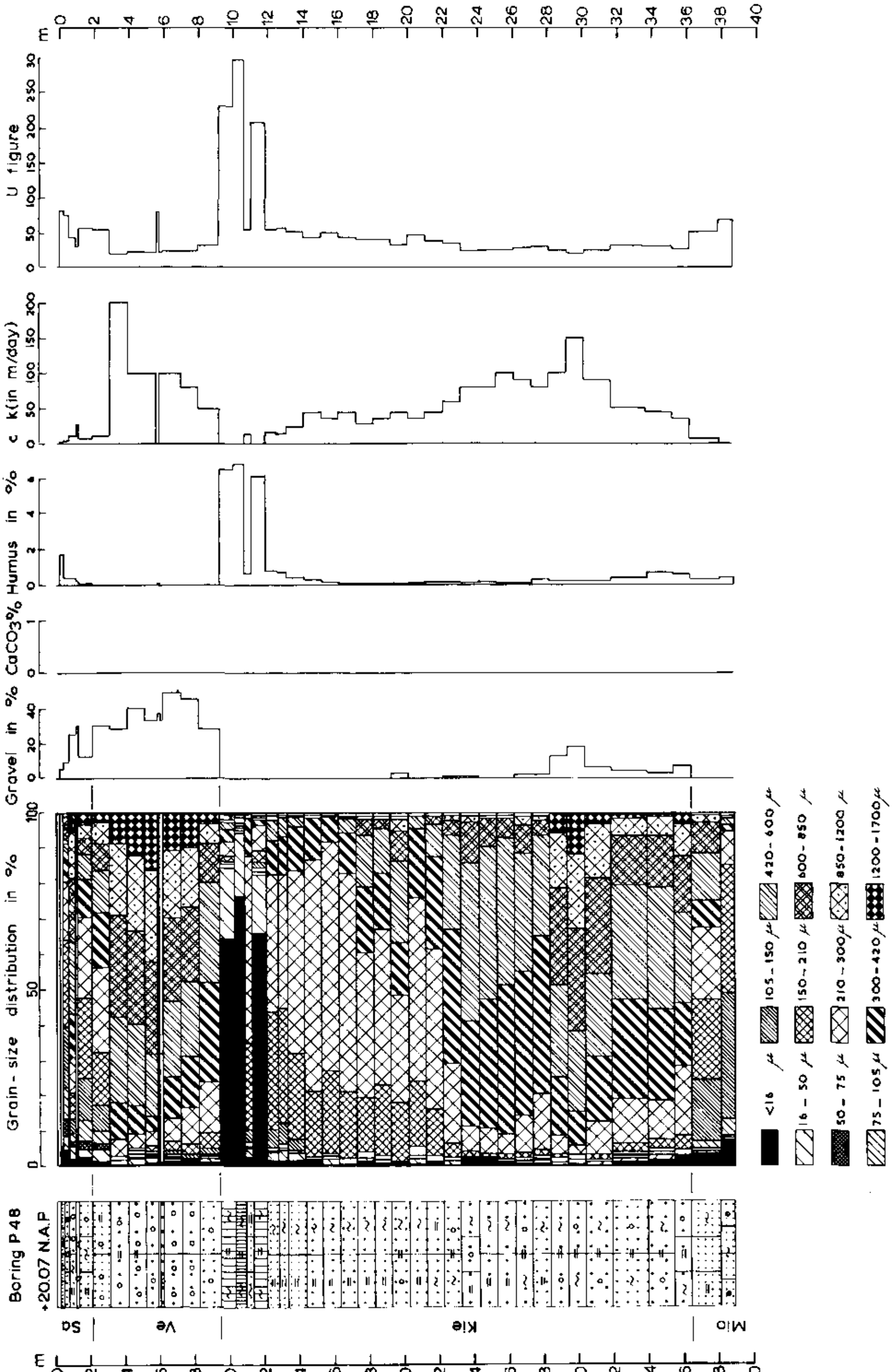

Boring P 48
+20.07 N.A.P
Sa
Ve
Kie
Mio
Grain - size distribution in %
Gravel in %
CaCO3 %
Humus in %
c k (in m/day)
U figure
m
<16 μ
16 - 50 μ
50 - 75 μ
75 - 105 μ
105 - 150 μ
150 - 210 μ
210 - 300 μ
300 - 420 μ
420 - 600 μ
600 - 850 μ
850 - 1200 μ
1200 - 1700 μ

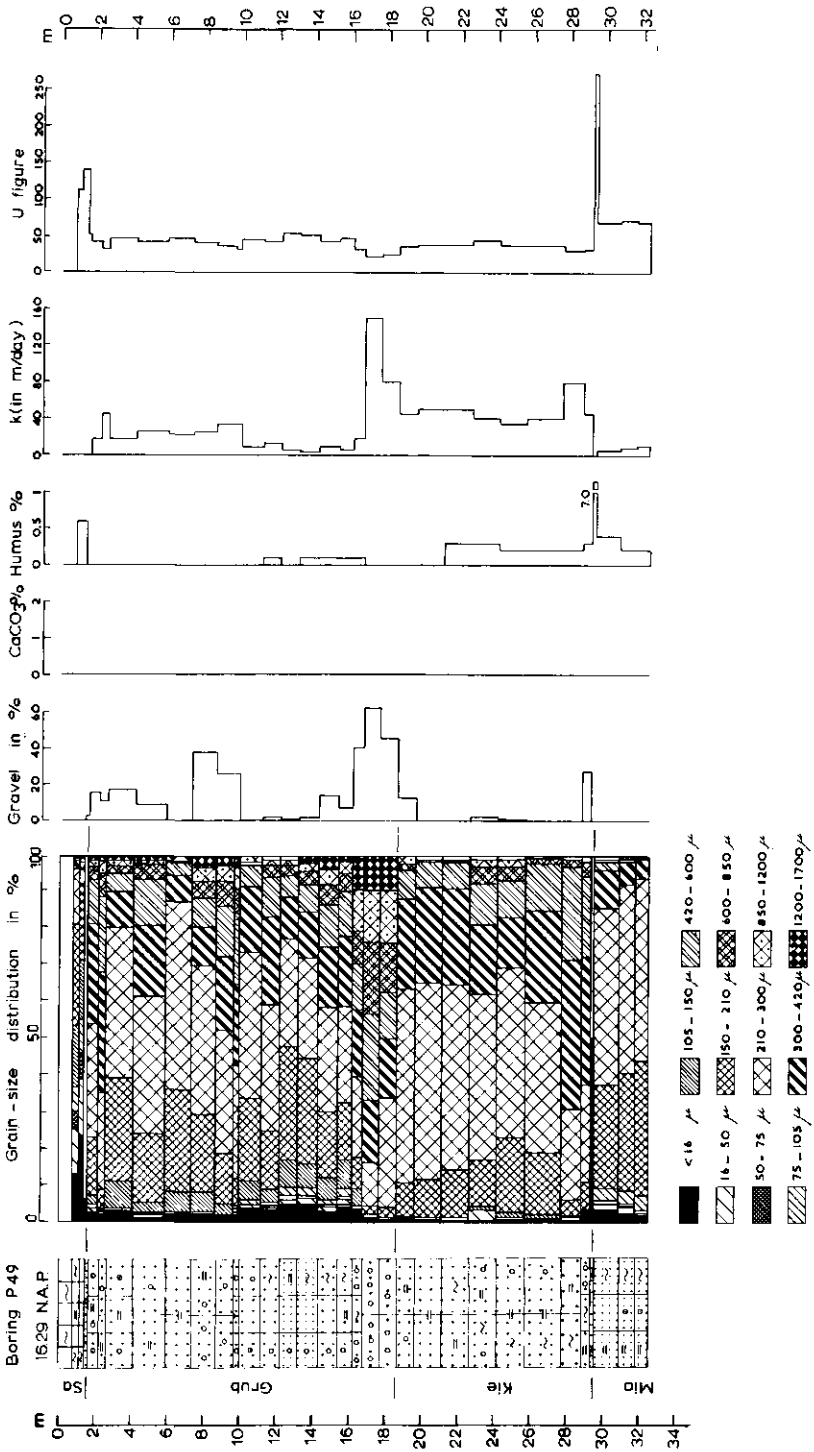

Boring P49
16.29 N.A.P.
Grain - size distribution in %
Gravel in %
CaCO3 %
Humus %
k (in m/day)
U figure
m
Sa
Grub
Kie
Mio
7.0
< 16 μ
16 - 50 μ
50 - 75 μ
75 - 105 μ
105 - 150 μ
150 - 210 μ
210 - 300 μ
300 - 420 μ
420 - 600 μ
600 - 850 μ
850 - 1200 μ
1200 - 1700 μ

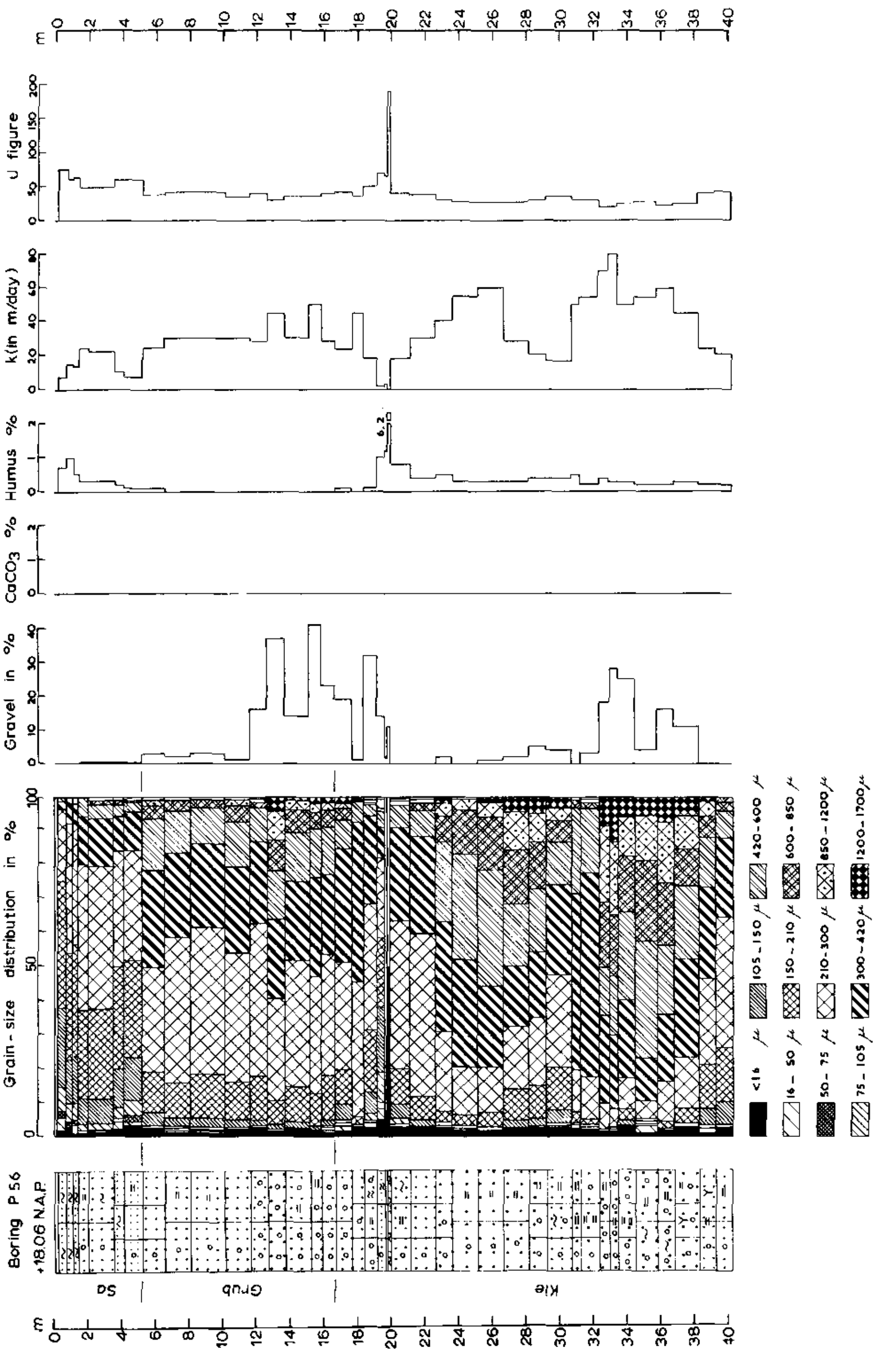
m
U figure
k (in m/day)
Humus %
6.2
CaCO3 %
Gravel in %
Grain-size distribution in %
Boring P 56
+18.06 N.A.P.
Sa
Grub
Kle
<16 μ
16 - 50 μ
50 - 75 μ
75 - 105 μ
105 - 150 μ
150 - 210 μ
210 - 300 μ
300 - 420 μ
420 - 600 μ
600 - 850 μ
850 - 1200 μ
1200 - 1700 μ

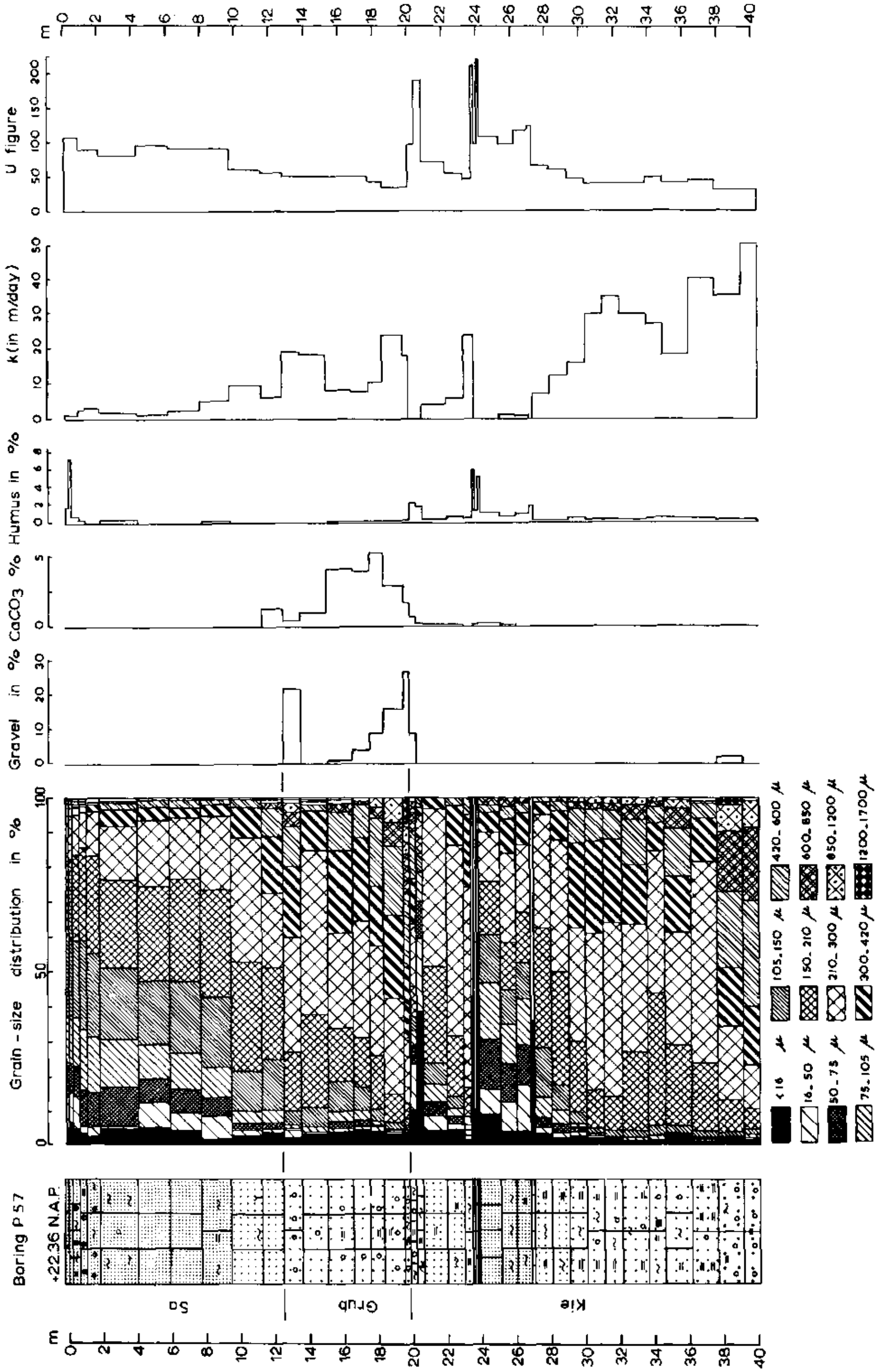

Boring P 57
+22.36 N.A.P.
Sa
Grub
Kie
Grain - size distribution in %
Gravel in %
CaCO3 %
Humus in %
k (in m/day)
U figure
m
<16 μ
16-50 μ
50-75 μ
75-105 μ
105-150 μ
150-210 μ
210-300 μ
300-420 μ
420-600 μ
600-850 μ
850-1200 μ
1200-1700 μ

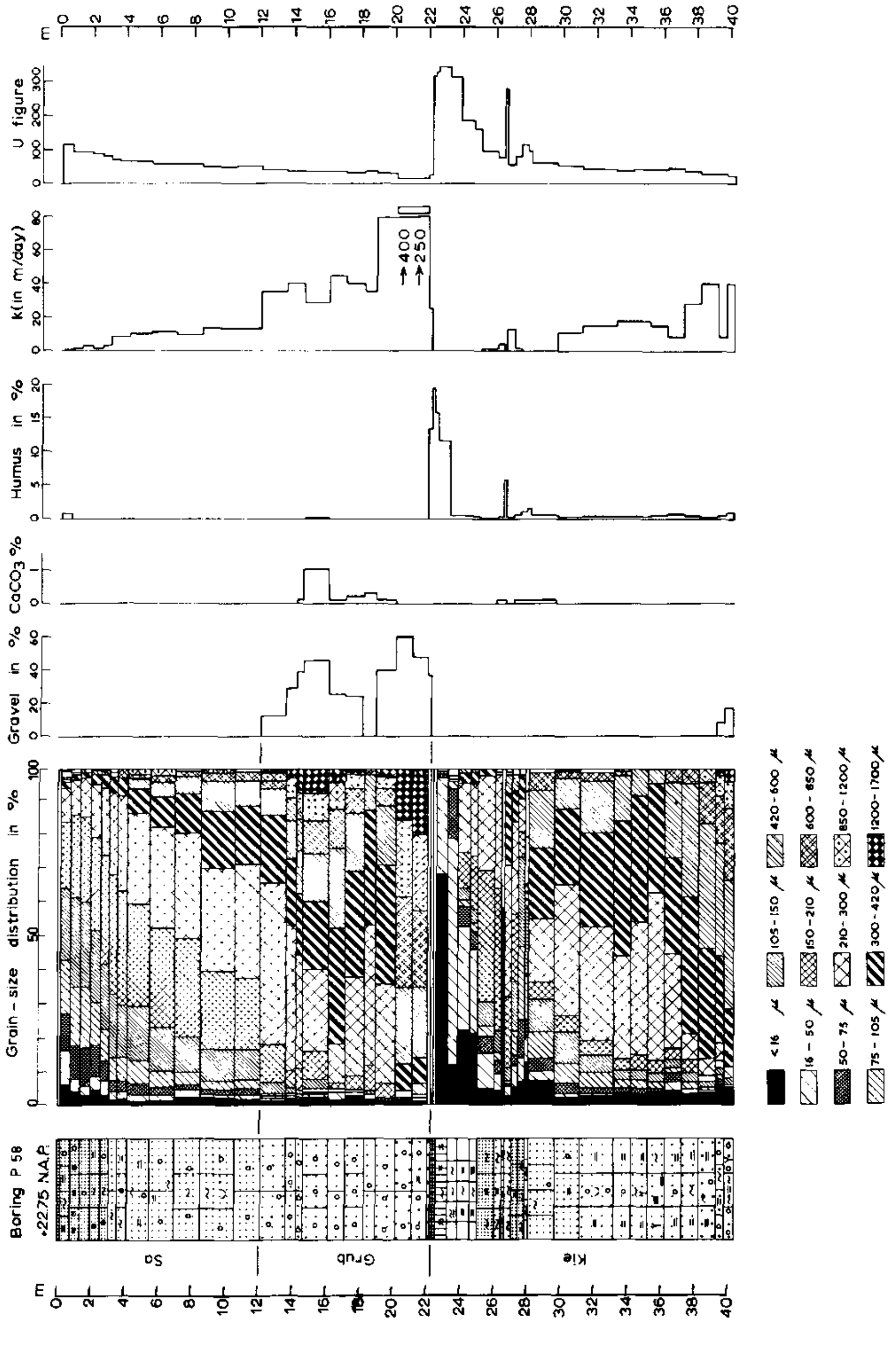

Boring P 58
+2275 N.A.P.
Sa
Grub
Kie
m
Grain - size distribution in %
Gravel in %
CaCO3 %
Humus in %
k(in m/day)
→400
→250
U figure
< 16 μ
16 - 50 μ
50 - 75 μ
75 - 105 μ
105 - 150 μ
150 - 210 μ
210 - 300 μ
300 - 420 μ
420 - 600 μ
600 - 850 μ
850 - 1200 μ
1200 - 1700 μ

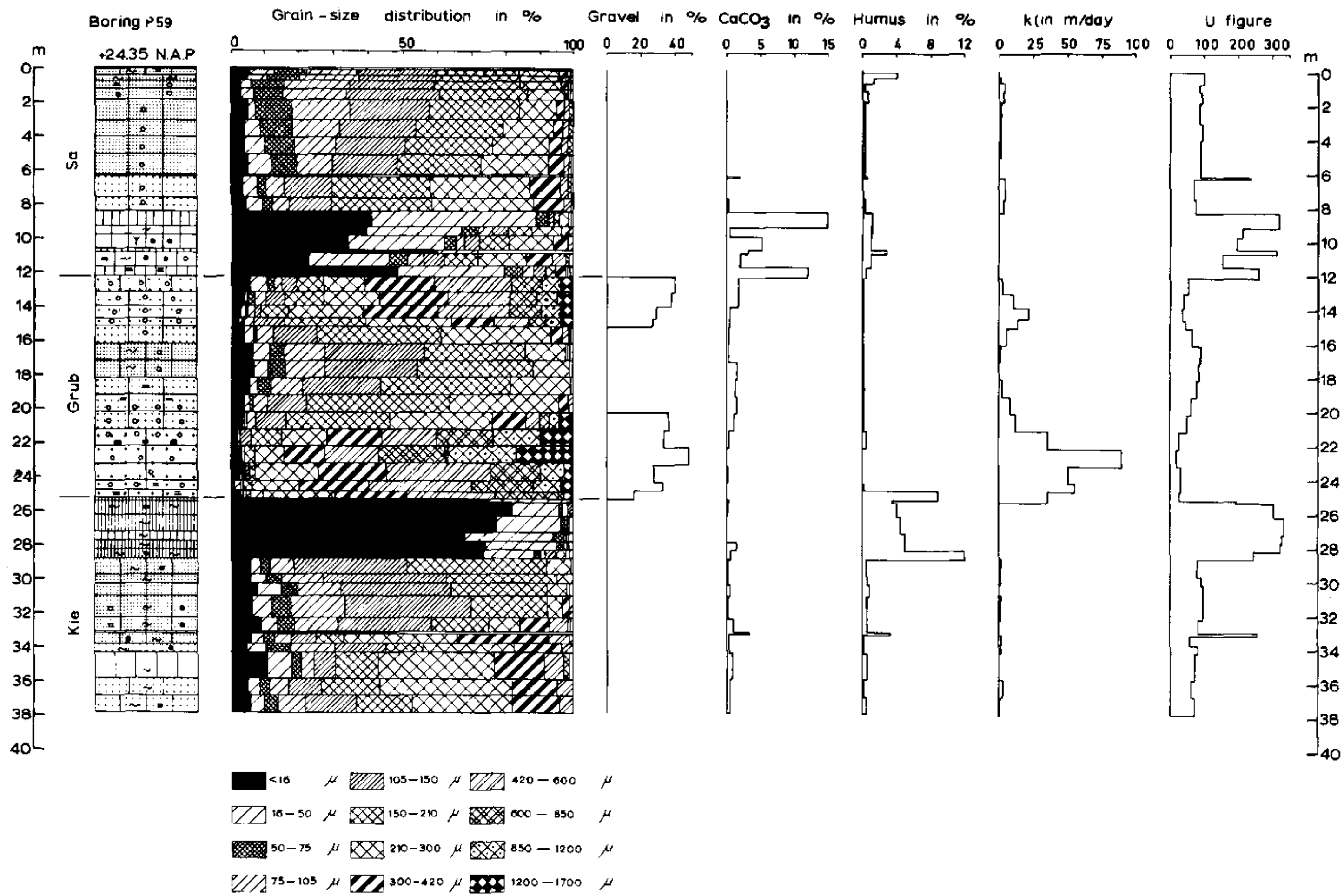
Boring P59
+24.35 N.A.P
m
Sa
Grub
Kie
Grain - size distribution in %
Gravel in %
$CaCO_3$ in %
Humus in %
k (in m/day
U figure
<16 μ
16 – 50 μ
50 – 75 μ
75 – 105 μ
105 – 150 μ
150 – 210 μ
210 – 300 μ
300 – 420 μ
420 — 600 μ
600 — 850 μ
850 — 1200 μ
1200 — 1700 μ

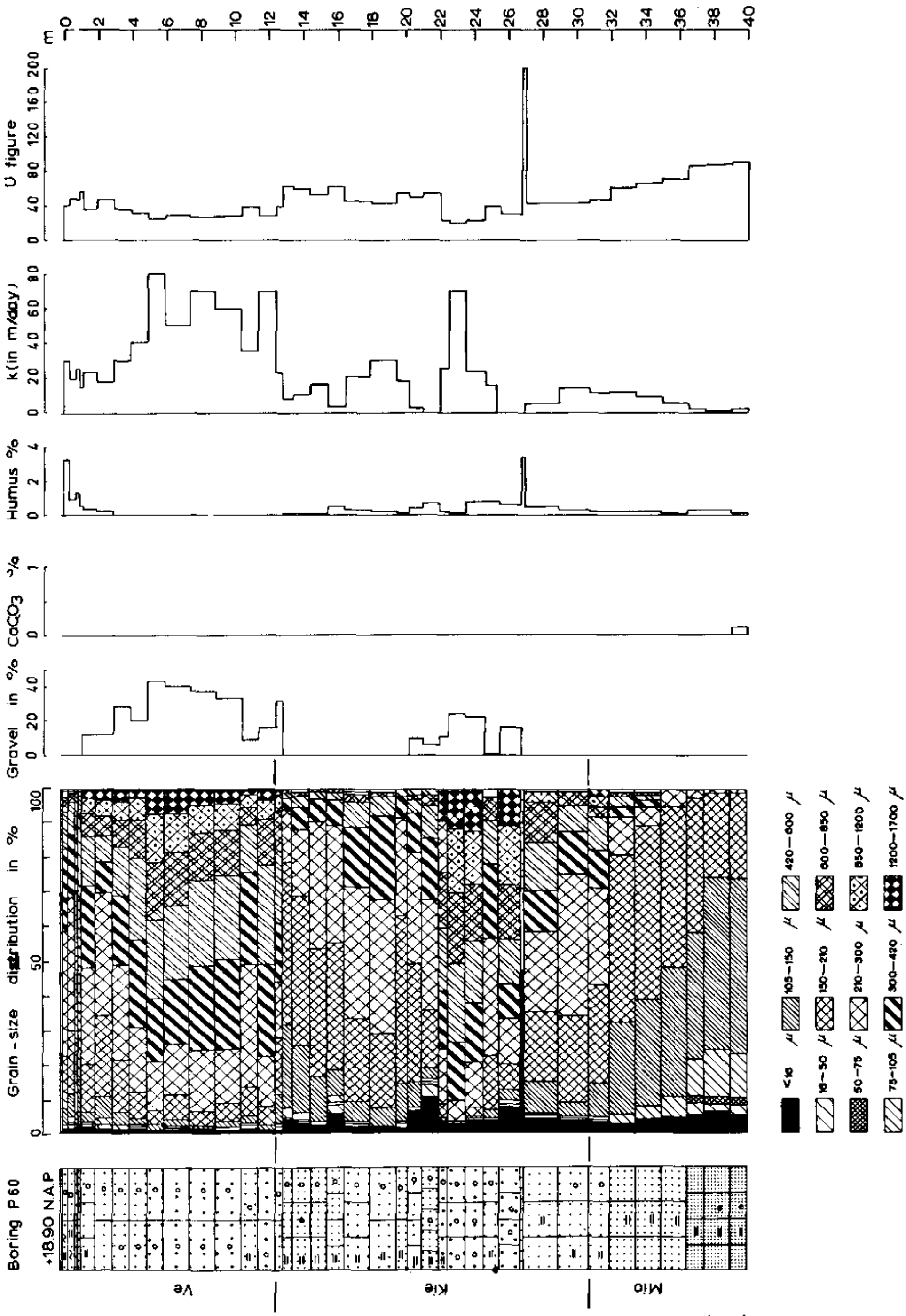

m
U figure
k (in m/day)
Humus %
CaCO3 %
Gravel in %
Grain-size distribution in %
Boring P60 +18.90 NAP
Ve
Kie
Mio
<16 μ
16–50 μ
50–75 μ
75–105 μ
105–150 μ
150–210 μ
210–300 μ
300–420 μ
420–600 μ
600–850 μ
850–1200 μ
1200–1700 μ

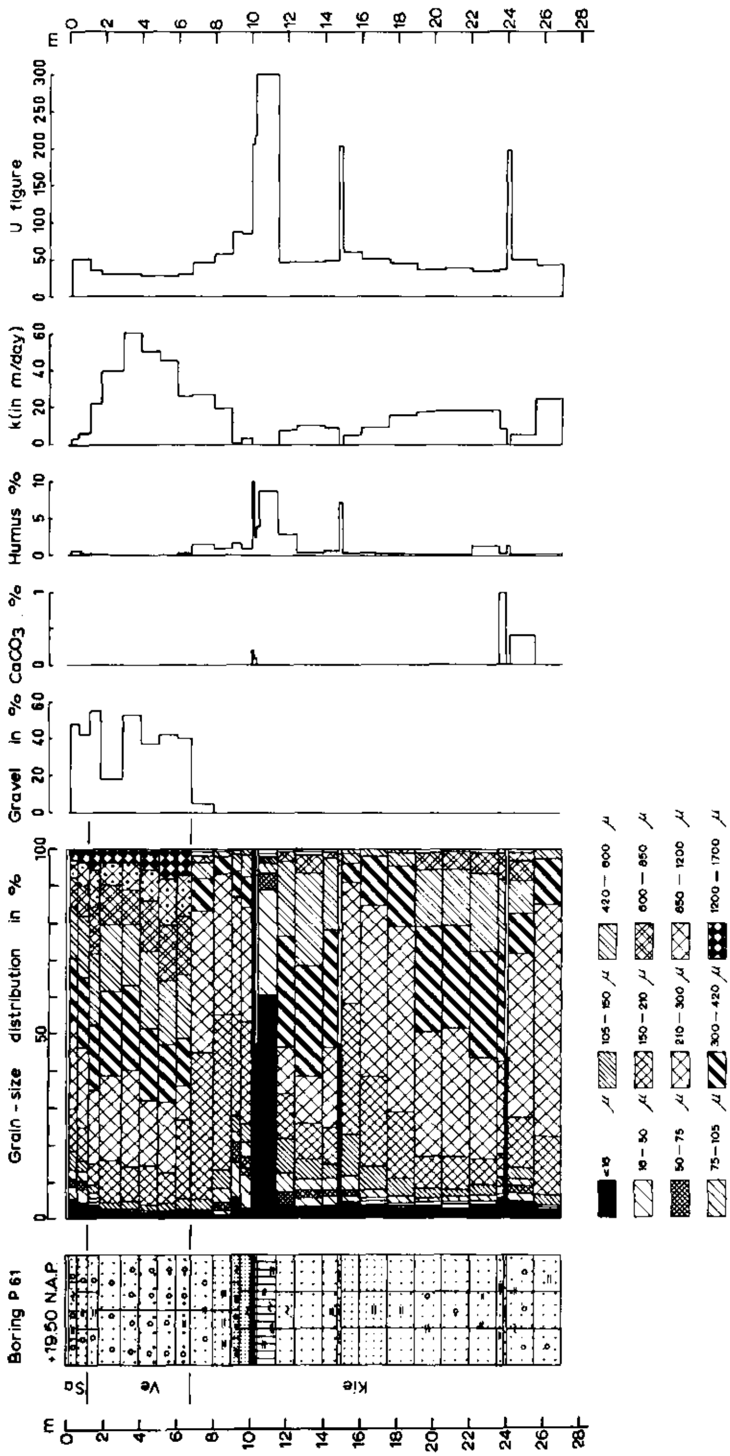
Boring P 61
+19.50 N.A.P.
Grain - size distribution in %
Gravel in %
CaCO3 %
Humus %
k(in m/day)
U figure
Sa
Ve
Kie
m
<16
16 - 50 μ
50 - 75 μ
75 - 105 μ
105 - 150 μ
150 - 210 μ
210 - 300 μ
300 - 420 μ
420 - 600 μ
600 - 850 μ
850 - 1200 μ
1200 - 1700 μ

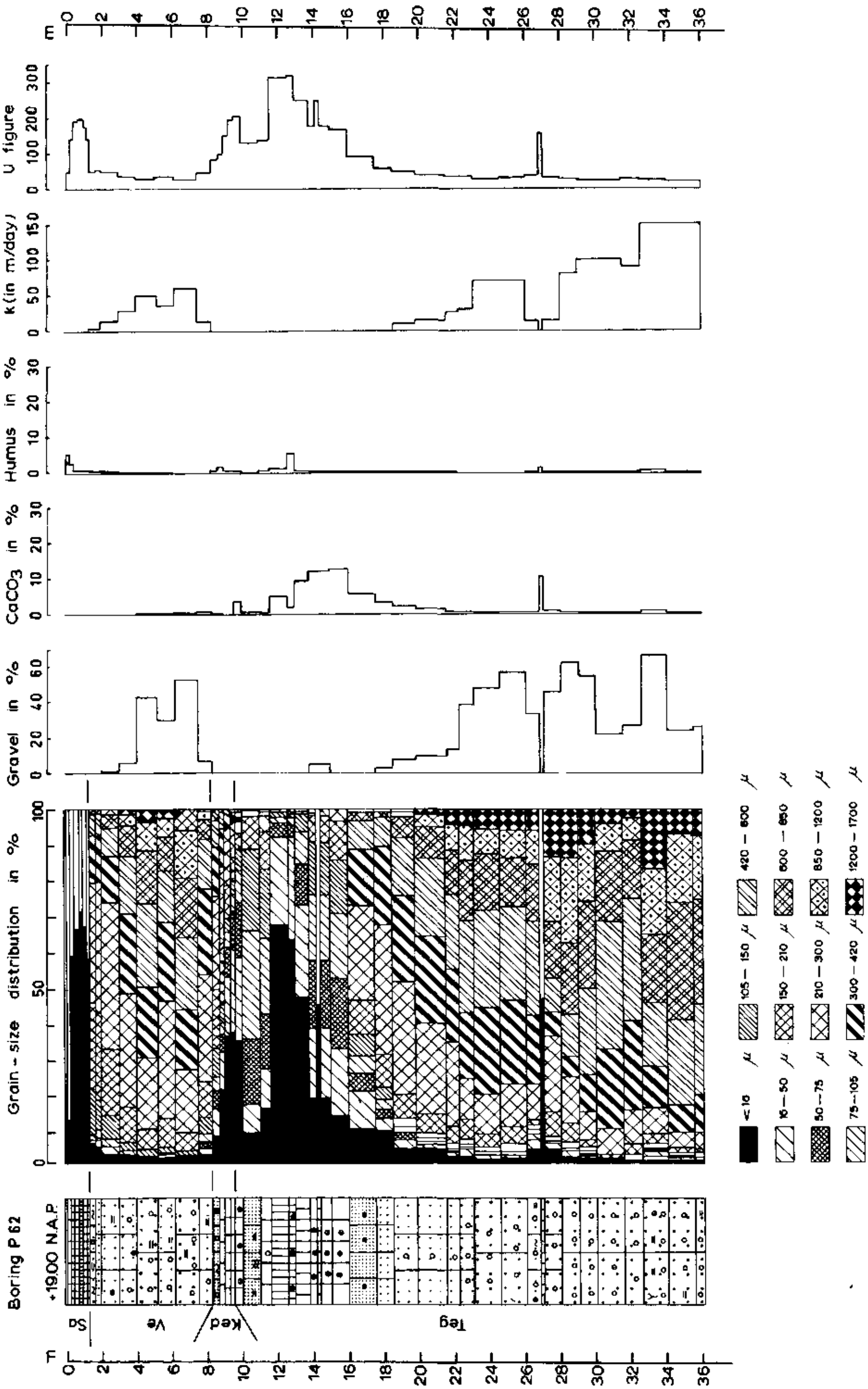

m
U figure
k (in m/day)
Humus in %
CaCO3 in %
Gravel in %
Grain - size distribution in %
Boring P 62
+19.00 N.A.P.
Sa
Ve
Ked
Teg
< 16 μ
16 — 50 μ
50 — 75 μ
75 — 105 μ
105 — 150 μ
150 — 210 μ
210 — 300 μ
300 — 420 μ
420 — 600 μ
600 — 850 μ
850 — 1200 μ
1200 — 1700 μ

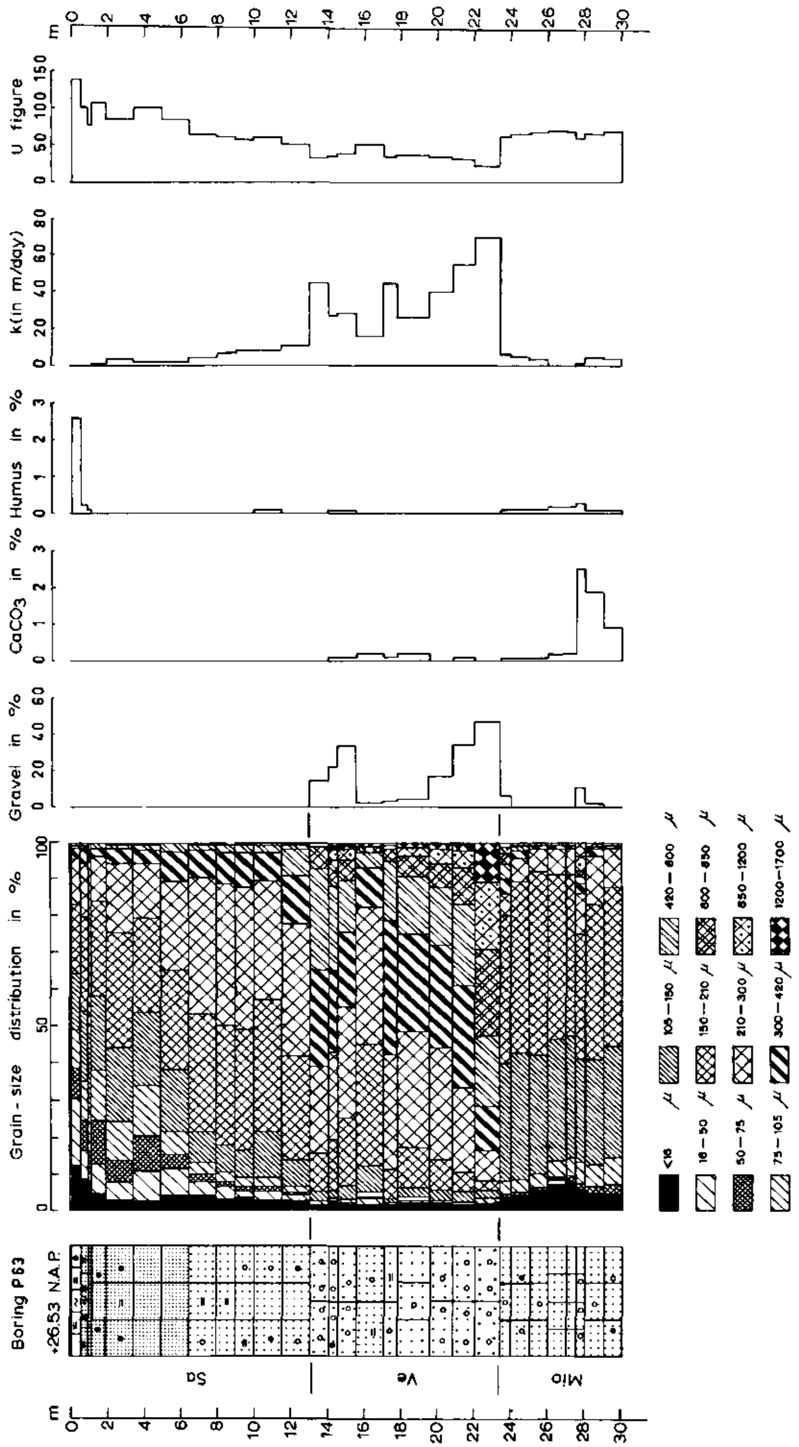

Boring P 63
+26.53 N.A.P.
Sa
Ve
Mio
Grain-size distribution in %
Gravel in %
$CaCO_3$ in %
Humus in %
k (in m/day)
U figure
m
<16 μ
16–50 μ
50–75 μ
75–105 μ
105–150 μ
150–210 μ
210–300 μ
300–420 μ
420–600 μ
600–850 μ
850–1200 μ
1200–1700 μ

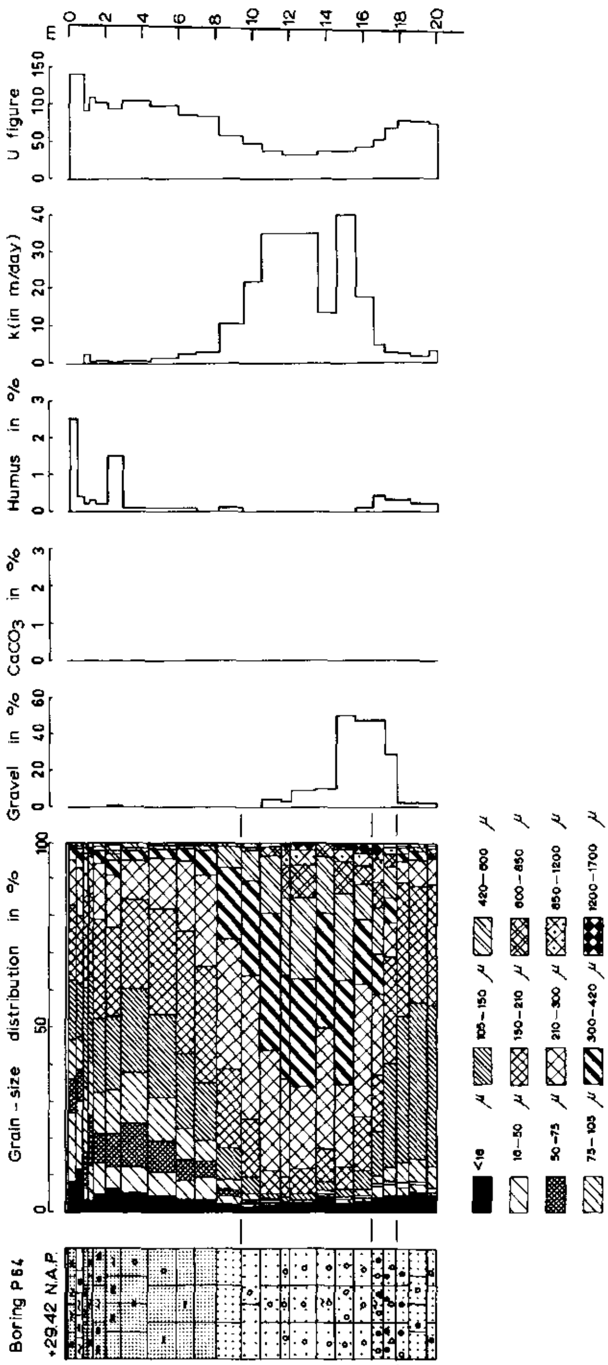
Boring P 64
+29.42 N.A.P.
Sa
Ve
Kie
Mio
Grain - size distribution in %
Gravel in %
CaCO3 in %
Humus in %
k (in m/day)
U figure
m
<16 μ
16–50 μ
50–75 μ
75–105 μ
105–150 μ
150–210 μ
210–300 μ
300–420 μ
420–600 μ
600–850 μ
850–1200 μ
1200–1700 μ

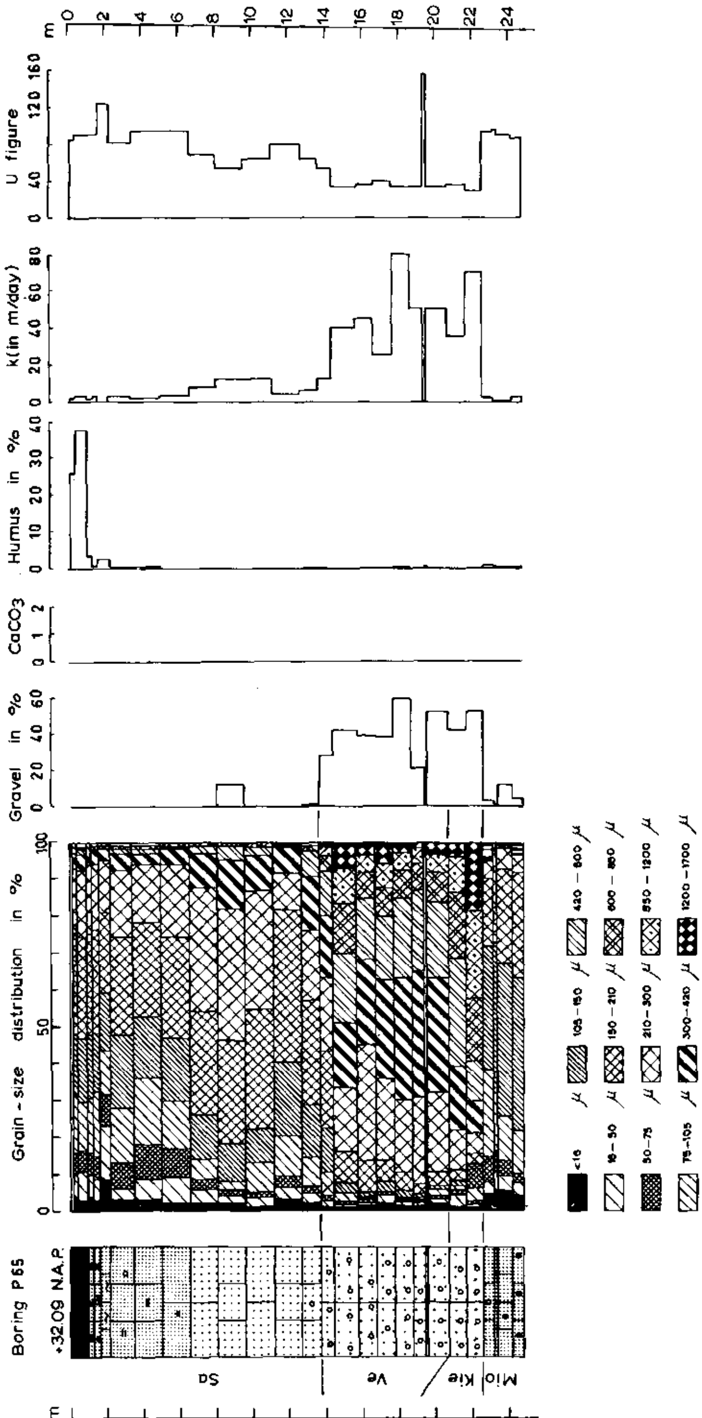
Boring P65
+32.09 N.A.P.
Grain - size distribution in %
Gravel in %
CaCO3
Humus in %
k(in m/day)
U figure
m
Sa
Ve
Kie
Mio
<16 μ
16 – 50 μ
50 – 75 μ
75 – 105 μ
105 – 150 μ
150 – 210 μ
210 – 300 μ
300 – 420 μ
420 – 600 μ
600 – 850 μ
850 – 1200 μ
1200 – 1700 μ

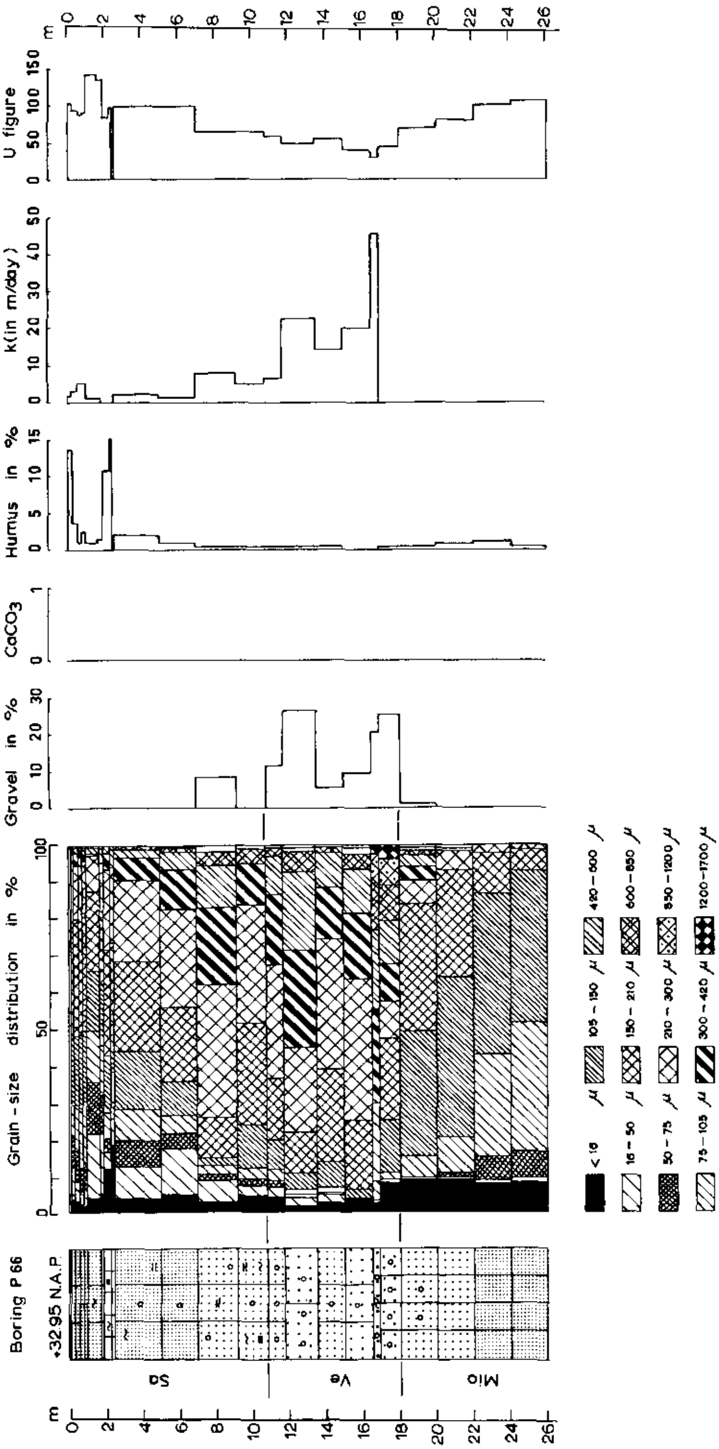

Boring P 66
+32.95 N.A.P.
Sa
Ve
Mio
Grain - size distribution in %
Gravel in %
CaCO3
Humus in %
k(in m/day)
U figure
m
< 16 μ
16 – 50 μ
50 – 75 μ
75 – 105 μ
105 – 150 μ
150 – 210 μ
210 – 300 μ
300 – 420 μ
420 – 600 μ
600 – 850 μ
850 – 1200 μ
1200 – 1700 μ

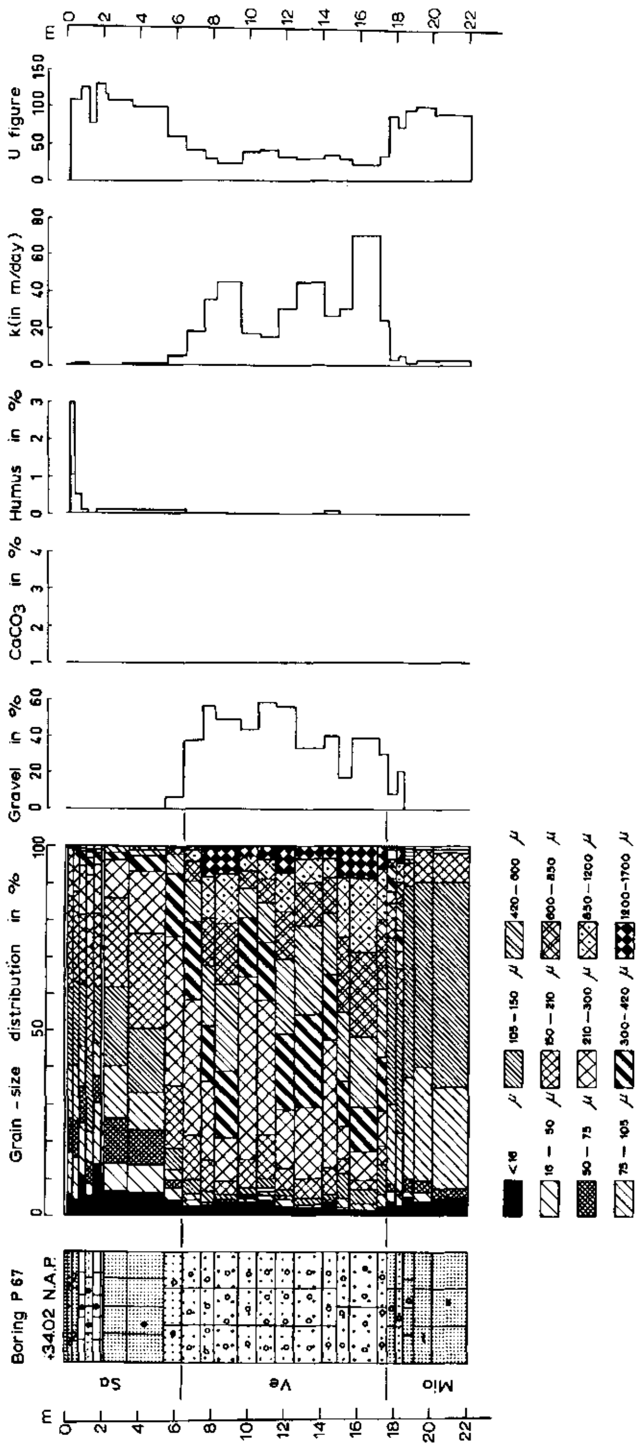
Boring P 67
+34.02 N.A.P.
Sa
Ve
Mio
Grain - size distribution in %
Gravel in %
CaCO3 in %
Humus in %
k(in m/day)
U figure
m
<16 μ
16 — 50 μ
50 — 75 μ
75 — 105 μ
105 — 150 μ
150 — 210 μ
210 — 300 μ
300 — 420 μ
420 — 600 μ
600 — 850 μ
850 — 1200 μ
1200 — 1700 μ

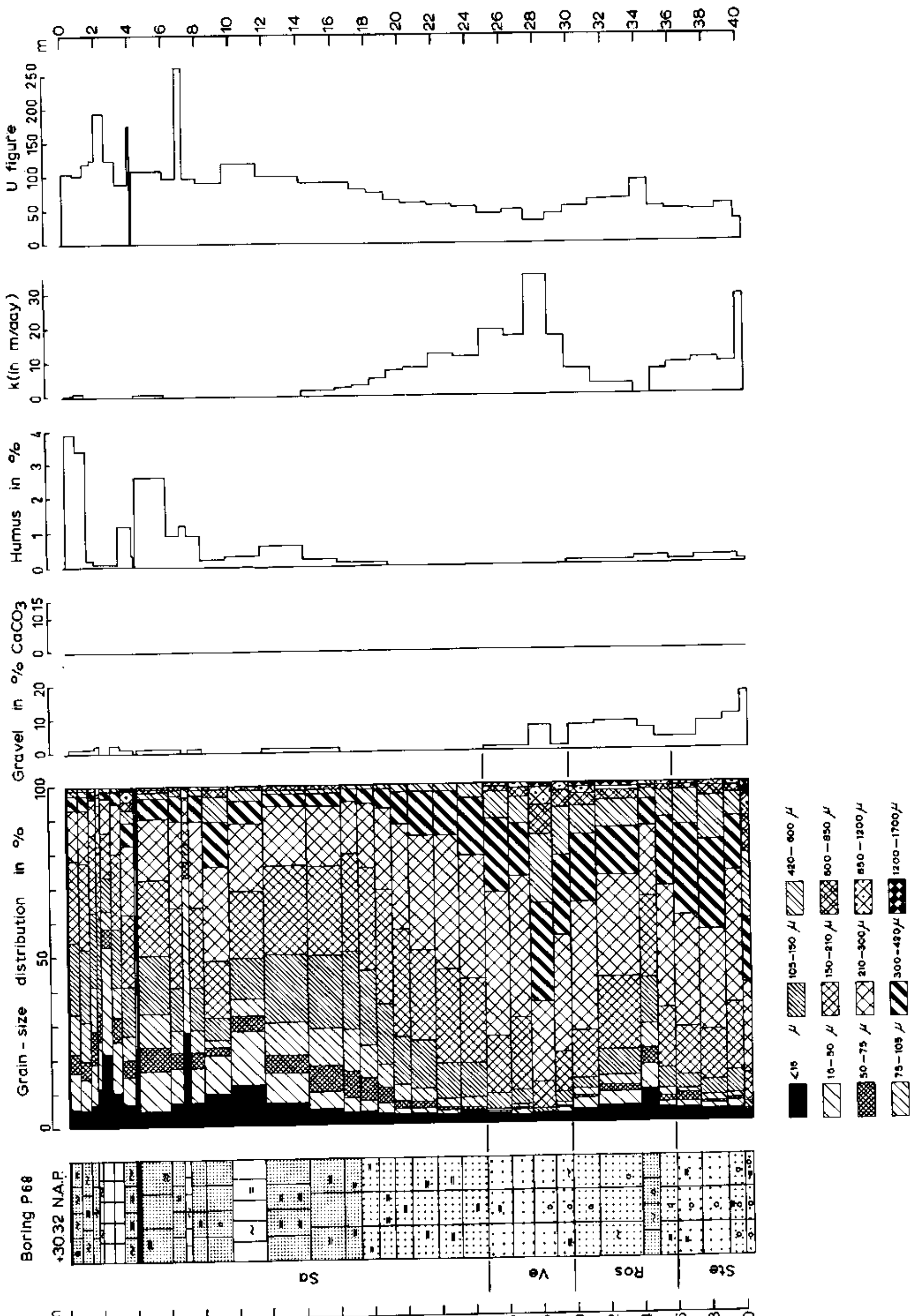

m
U figure
k (in m/day)
Humus in %
% CaCO3
Gravel in %
Grain - size distribution in %
Boring P68
+30.32 N.A.P.
Sa
Ve
Ros
Ste
<16 μ
16–50 μ
50–75 μ
75–105 μ
105–150 μ
150–210 μ
210–300 μ
300–420 μ
420–600 μ
600–850 μ
850–1200 μ
1200–1700 μ

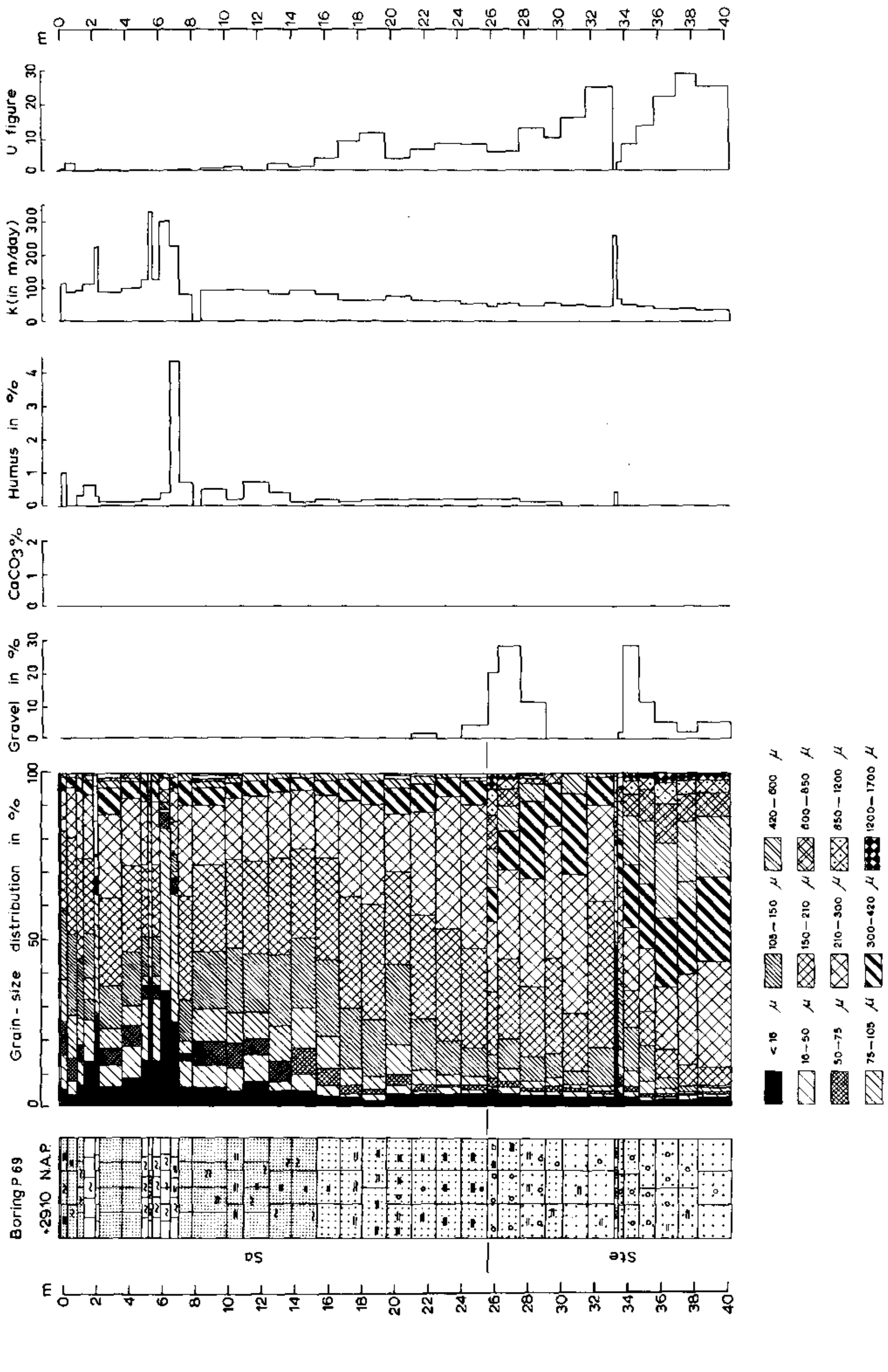
m
U figure
K (in m/day)
Humus in %
CaCO3 %
Gravel in %
Grain - size distribution in %
Boring P 69
+29.10 N.A.P.
Sa
Ste
< 16 μ
16—50 μ
50—75 μ
75—105 μ
105—150 μ
150—210 μ
210—300 μ
300—420 μ
420—600 μ
600—850 μ
850—1200 μ
1200—1700 μ

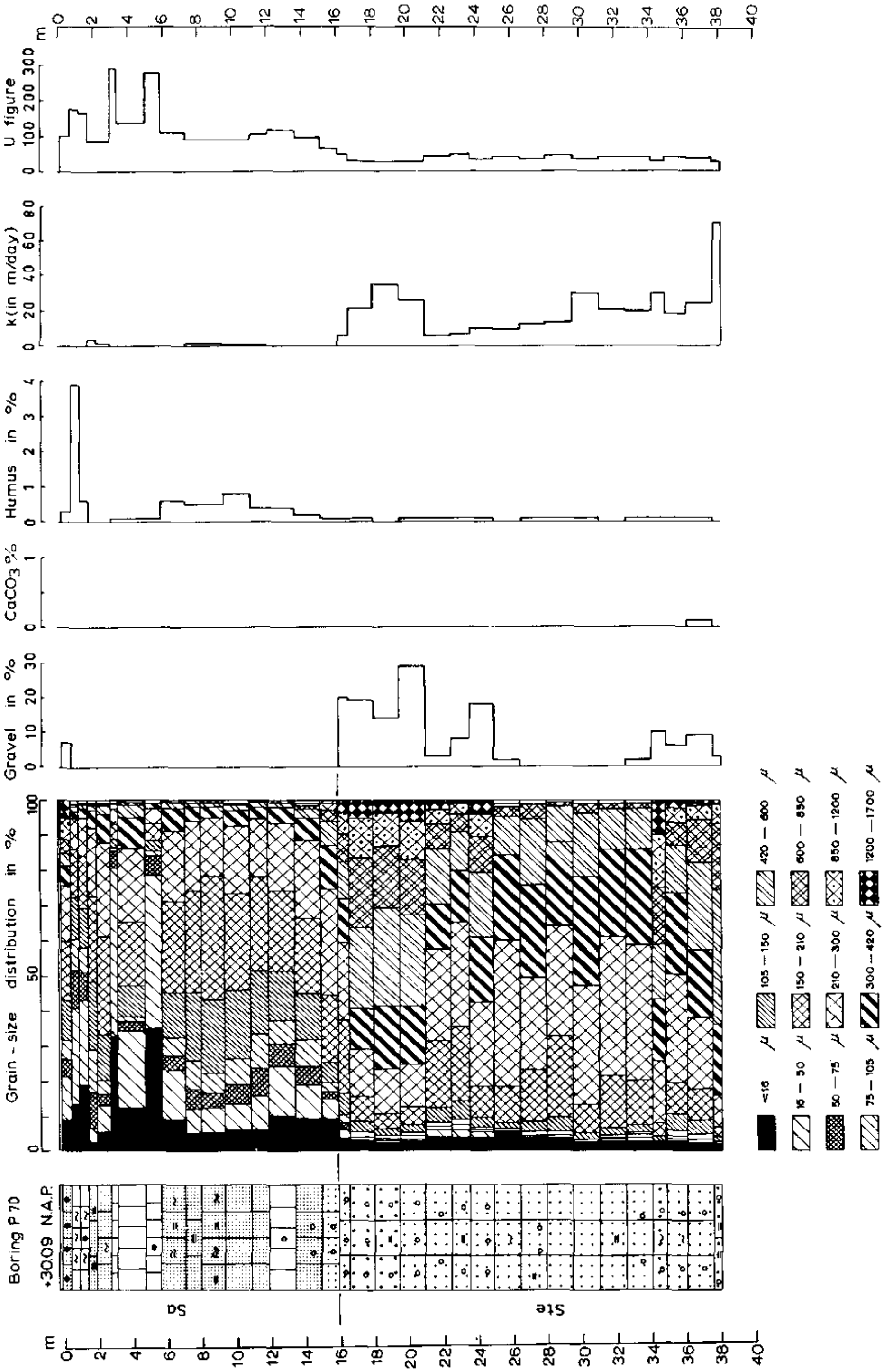

Boring P 70
+30.09 N.A.P.
Grain - size distribution in %
Gravel in %
CaCO3 %
Humus in %
k (in m/day)
U figure
m
Sa
Ste
<16 μ
16 — 50 μ
50 — 75 μ
75 — 105 μ
105 — 150 μ
150 — 210 μ
210 — 300 μ
300 — 420 μ
420 — 600 μ
600 — 850 μ
850 — 1200 μ
1200 — 1700 μ

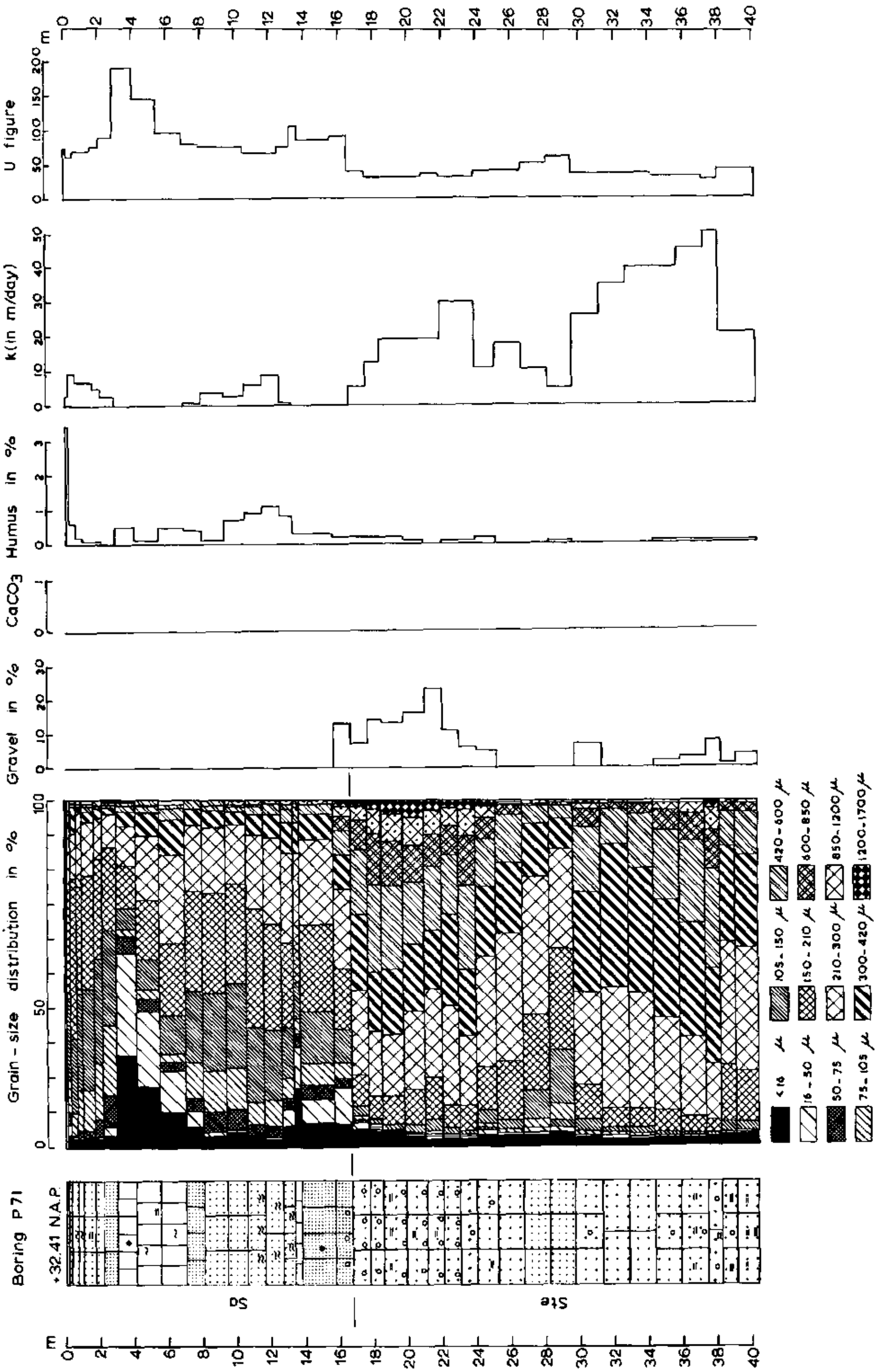

U figure
k (in m/day)
Humus in %
CaCO3
Gravel in %
Grain - size distribution in %
Boring P71
+32.41 N.A.P.
Sa
Ste
m
< 16 μ
16 - 50 μ
50 - 75 μ
75 - 105 μ
105 - 150 μ
150 - 210 μ
210 - 300 μ
300 - 420 μ
420 - 600 μ
600 - 850 μ
850 - 1200 μ
1200 - 1700 μ

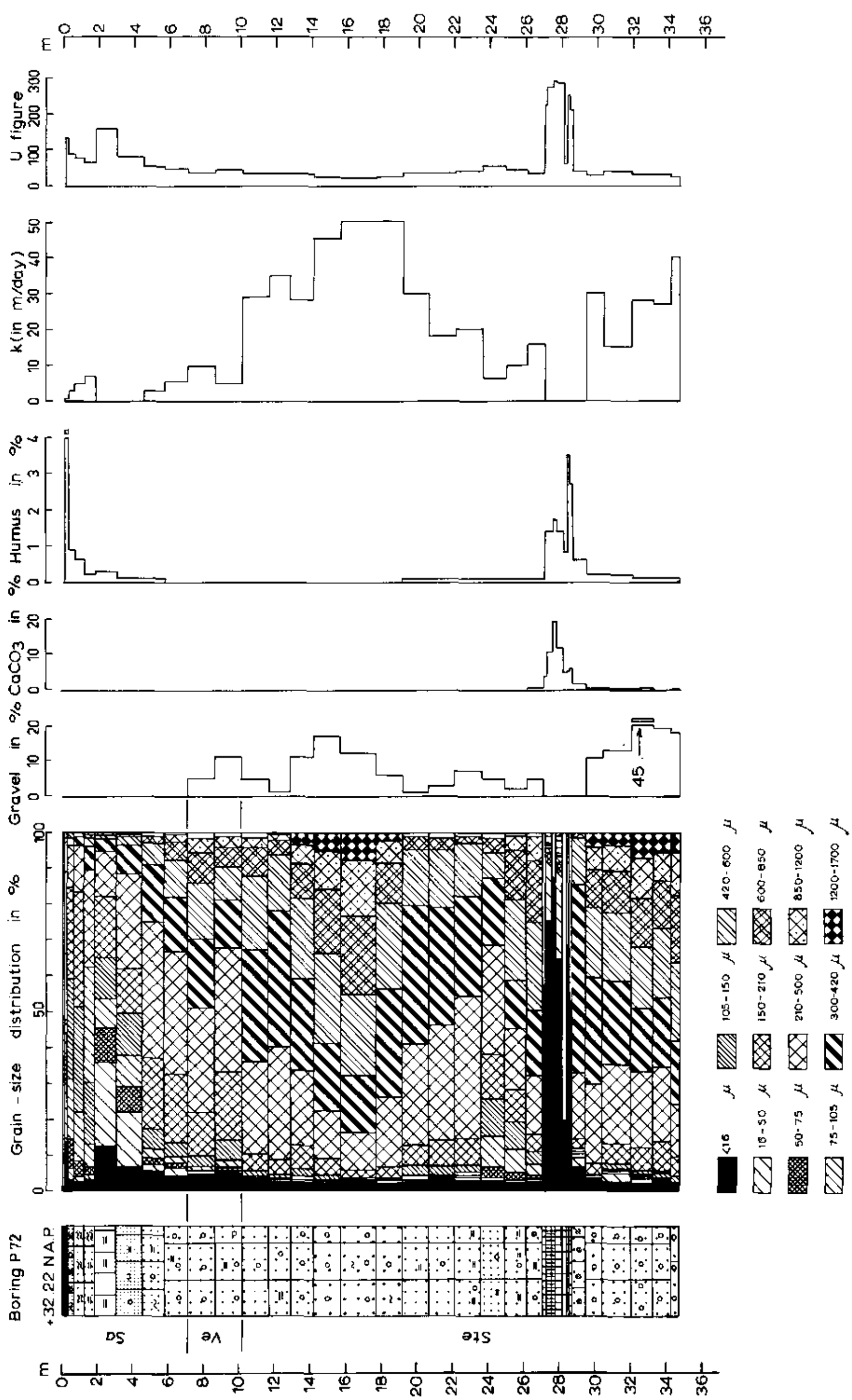

Boring P 72
+32.22 N.A.P.
Grain - size distribution in %
Gravel in %
CaCO$_3$ in %
% Humus in %
k (in m/day)
U figure
m
Sa
Ve
Ste
45
<16 μ
16-50 μ
50-75 μ
75-105 μ
105-150 μ
150-210 μ
210-300 μ
300-420 μ
420-600 μ
600-850 μ
850-1200 μ
1200-1700 μ

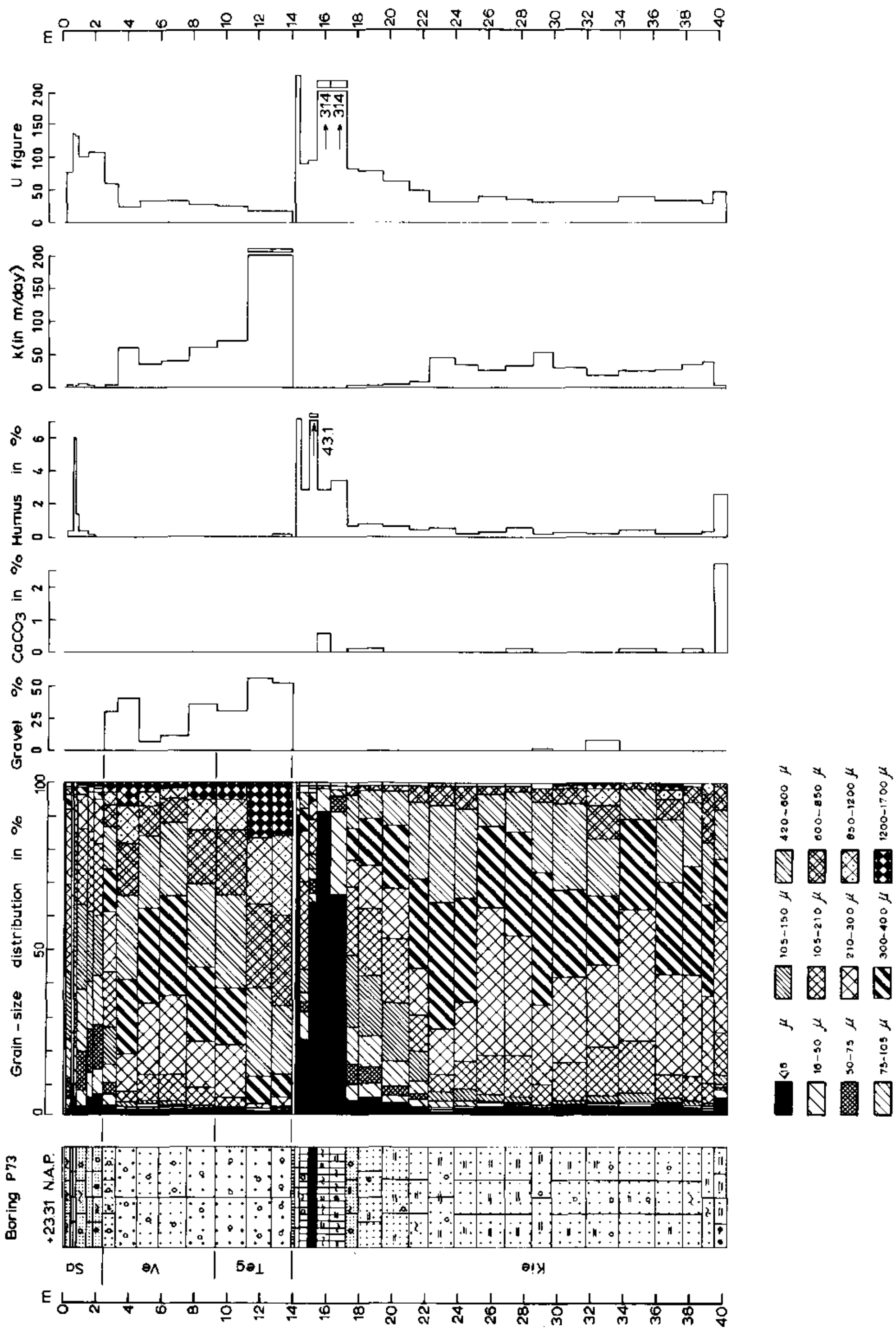

Boring P73
+23.31 N.A.P.
Sa
Ve
Teg
Kie
Grain - size distribution in %
Gravel %
CaCO3 in %
Humus in %
k(in m/day)
U figure
431
314
314
m
<16 μ
16-50 μ
50-75 μ
75-105 μ
105-150 μ
105-210 μ
210-300 μ
300-400 μ
420-600 μ
600-850 μ
850-1200 μ
1200-1700 μ

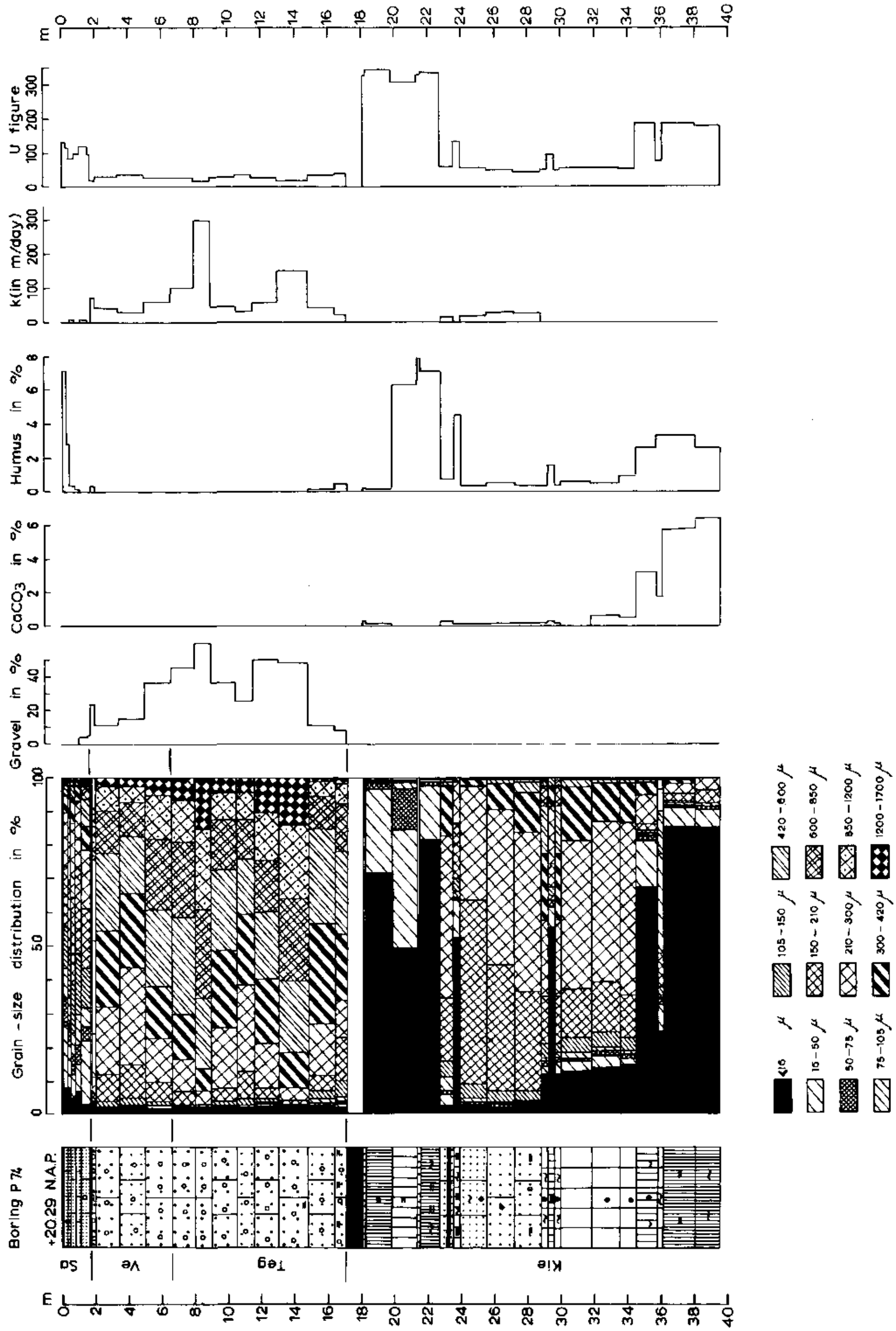
Boring P 74
+20.29 N.A.P.
Grain - size distribution in %
Gravel in %
$CaCO_3$ in %
Humus in %
k(in m/day)
U figure
m
Sa
Ve
Teg
Kie
<16 μ
16 - 50 μ
50 - 75 μ
75 - 105 μ
105 - 150 μ
150 - 210 μ
210 - 300 μ
300 - 420 μ
420 - 600 μ
600 - 850 μ
850 - 1200 μ
1200 - 1700 μ

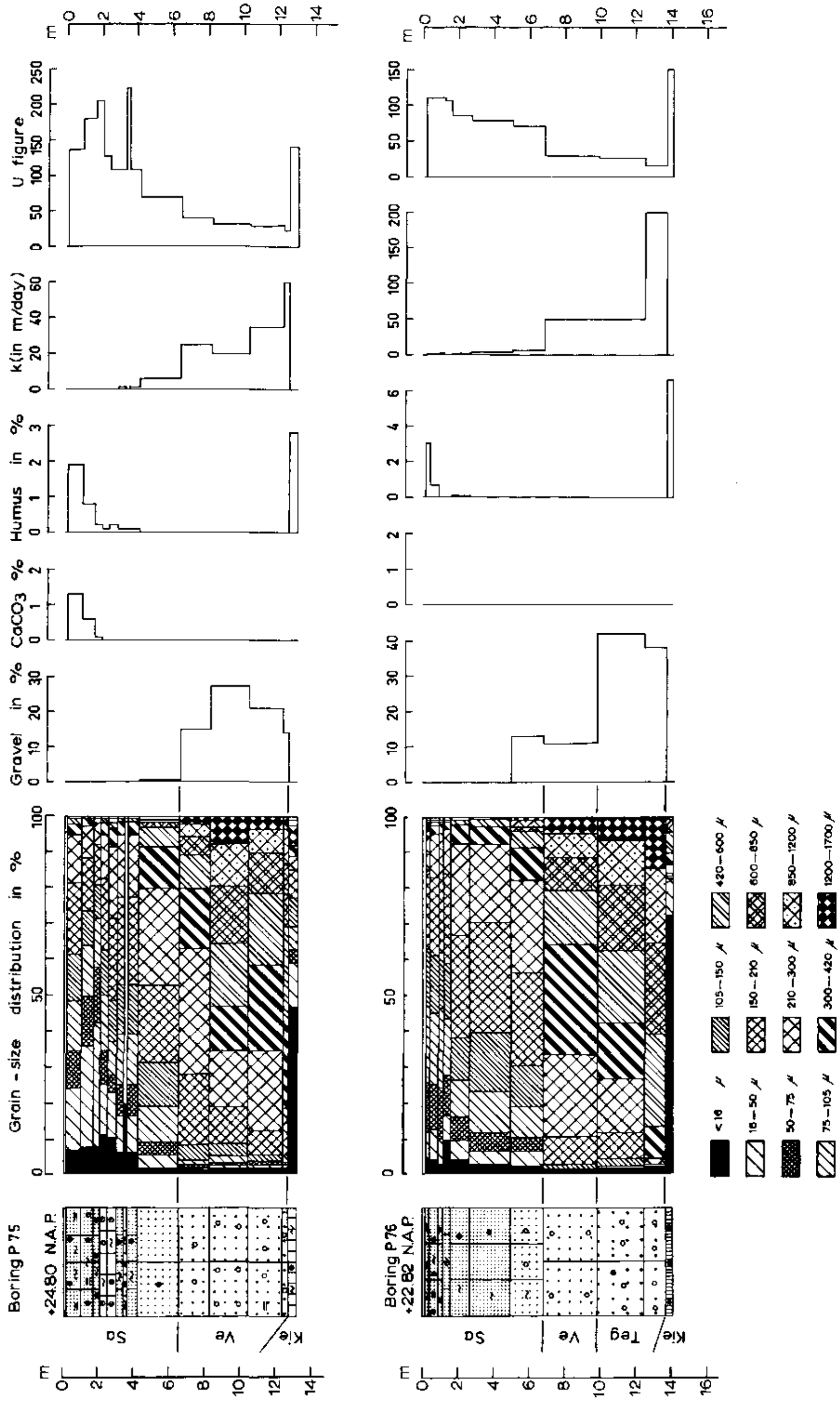

Boring P 75
+24.80 N.A.P
Boring P76
+22.82 N.A.P
Sa
Ve
Teg
Kie
m
Grain - size distribution in %
Gravel in %
CaCO3 %
Humus in %
k (in m/day)
U figure
< 16 μ
16–50 μ
50–75 μ
75–105 μ
105–150 μ
150–210 μ
210–300 μ
300–420 μ
420–600 μ
600–850 μ
850–1200 μ
1200–1700 μ

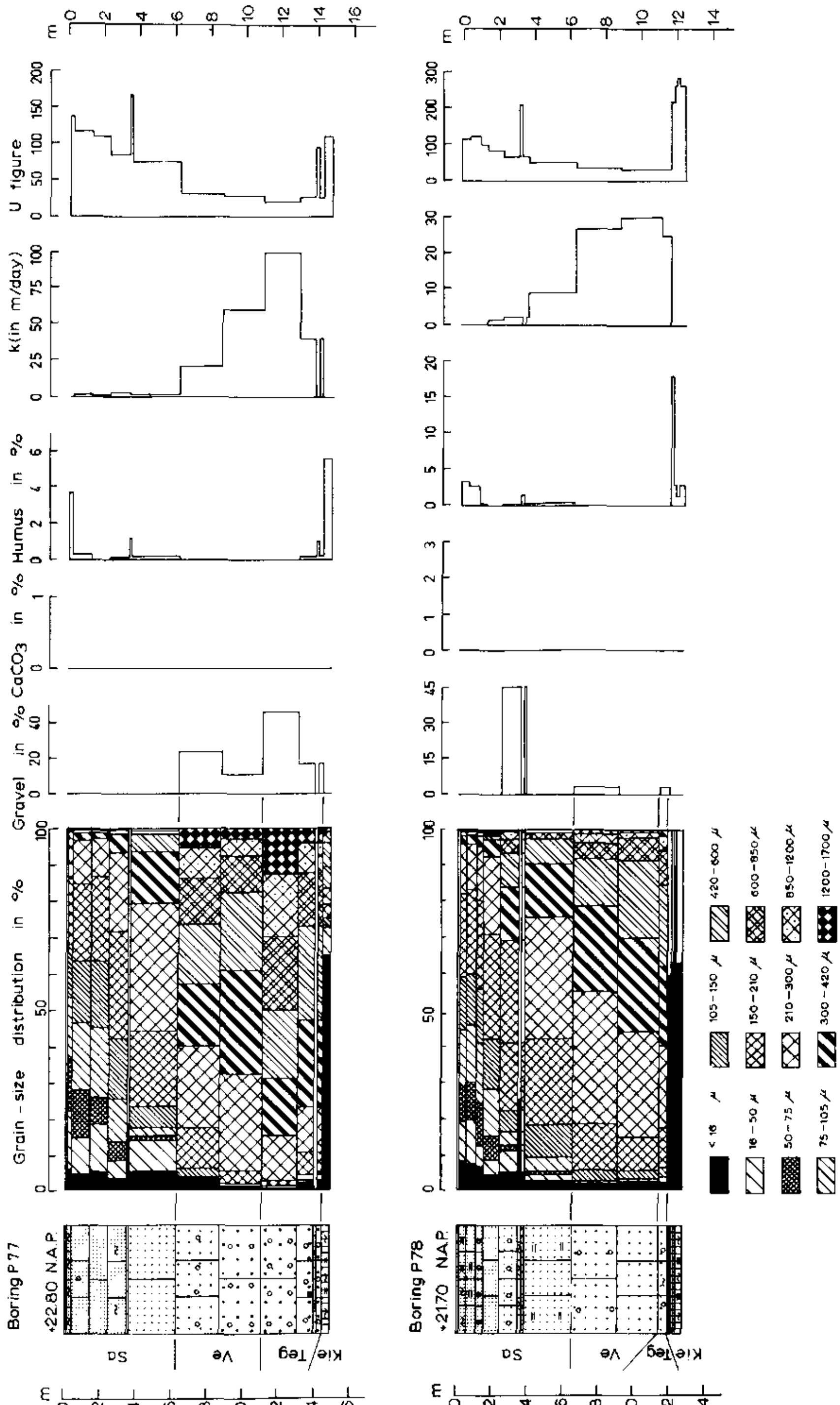

Boring P77
+22.80 NAP
Boring P78
+21.70 NAP
Sa
Ve
Teg
Kie
m
Grain - size distribution in %
Gravel in %
CaCO3 in %
Humus in %
k(in m/day)
U figure
< 16 μ
16 – 50 μ
50 – 75 μ
75 – 105 μ
105 – 150 μ
150 – 210 μ
210 – 300 μ
300 – 420 μ
420 – 600 μ
600 – 850 μ
850 – 1200 μ
1200 – 1700 μ

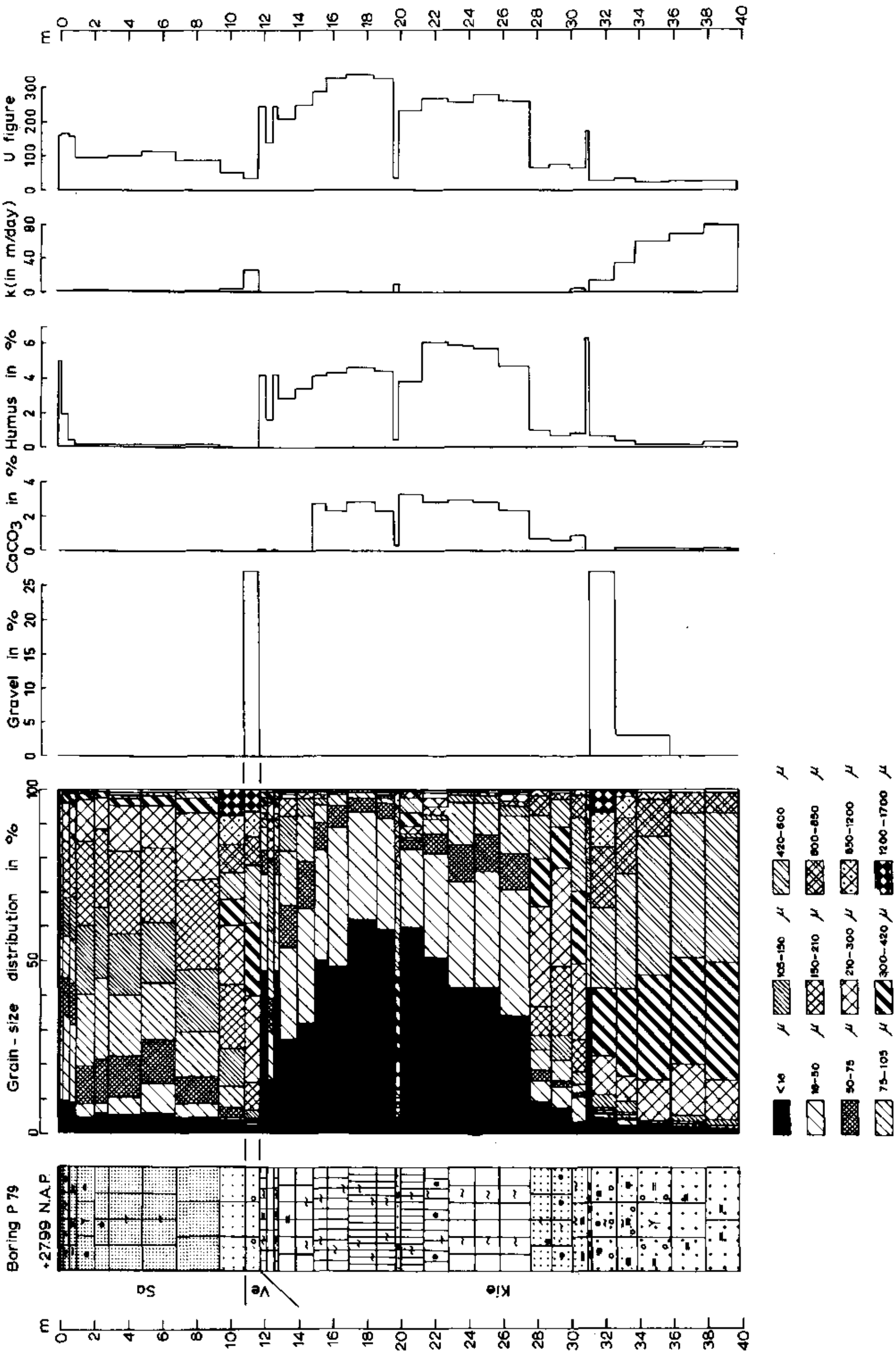

Boring P 79
+27.99 N.A.P.
Sa
Ve
Kle
m
Grain - size distribution in %
Gravel in %
CaCO3 in %
Humus in %
k (in m/day)
U figure
< 16 μ
16–50 μ
50–75 μ
75–105 μ
105–150 μ
150–210 μ
210–300 μ
300–420 μ
420–600 μ
600–850 μ
850–1200 μ
1200–1700 μ

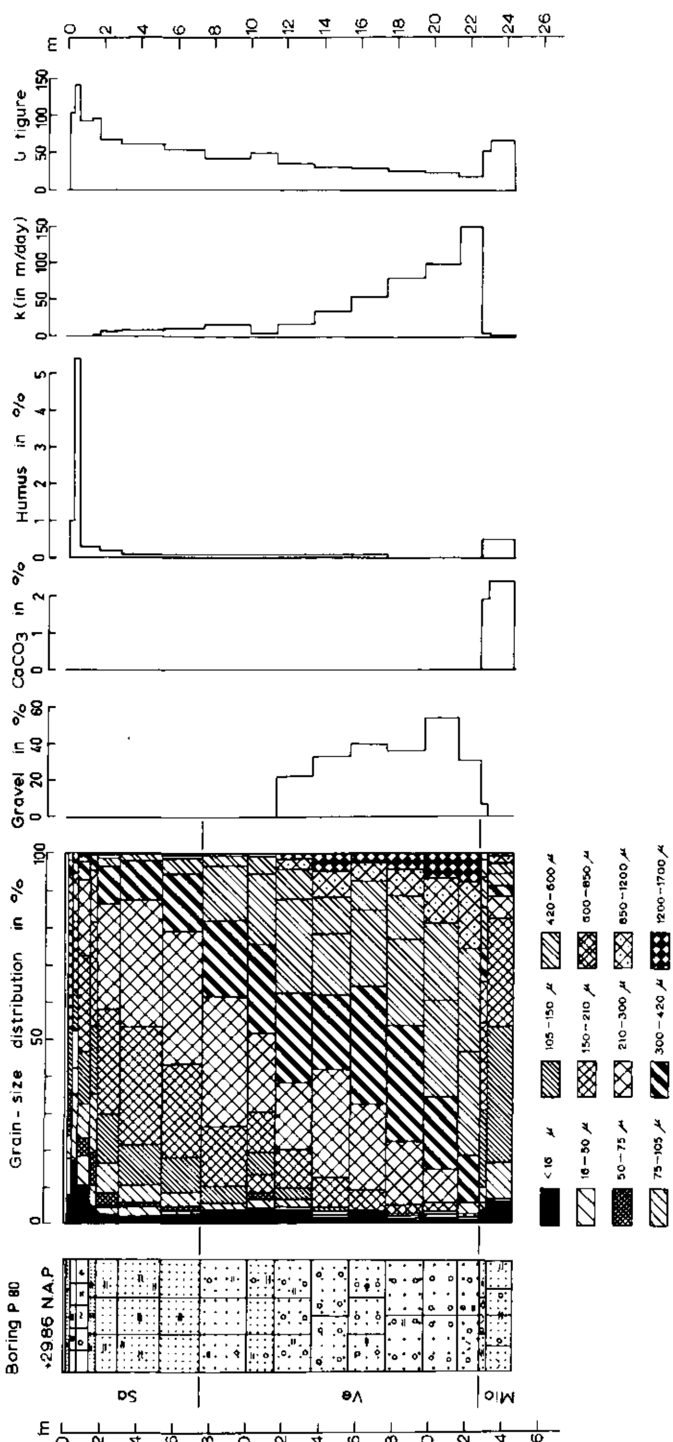

Boring P 80
+29.86 N.A.P
Sa
Ve
Mio
Grain - size distribution in %
< 16 μ
16 – 50 μ
50 – 75 μ
75 – 105 μ
105 – 150 μ
150 – 210 μ
210 – 300 μ
300 – 420 μ
420 – 600 μ
600 – 850 μ
850 – 1200 μ
1200 – 1700 μ
Gravel in %
$CaCO_3$ in %
Humus in %
k (in m/day)
U figure
m

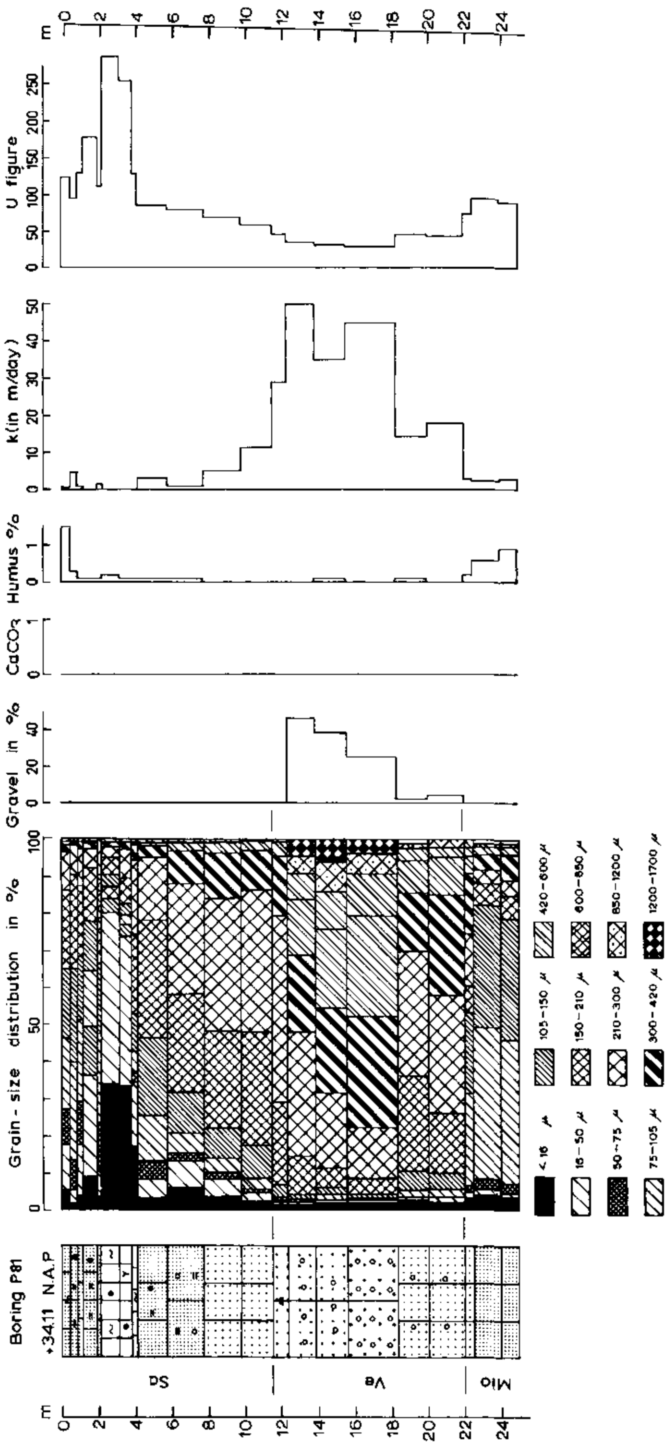

Boring P81
+34.11 N.A.P
Grain - size distribution in %
Gravel in %
CaCO3
Humus %
k (in m/day)
U figure
m
Sd
Ve
Mio
< 16 μ
16 - 50 μ
50 - 75 μ
75 - 105 μ
105 - 150 μ
150 - 210 μ
210 - 300 μ
300 - 420 μ
420 - 600 μ
600 - 850 μ
850 - 1200 μ
1200 - 1700 μ

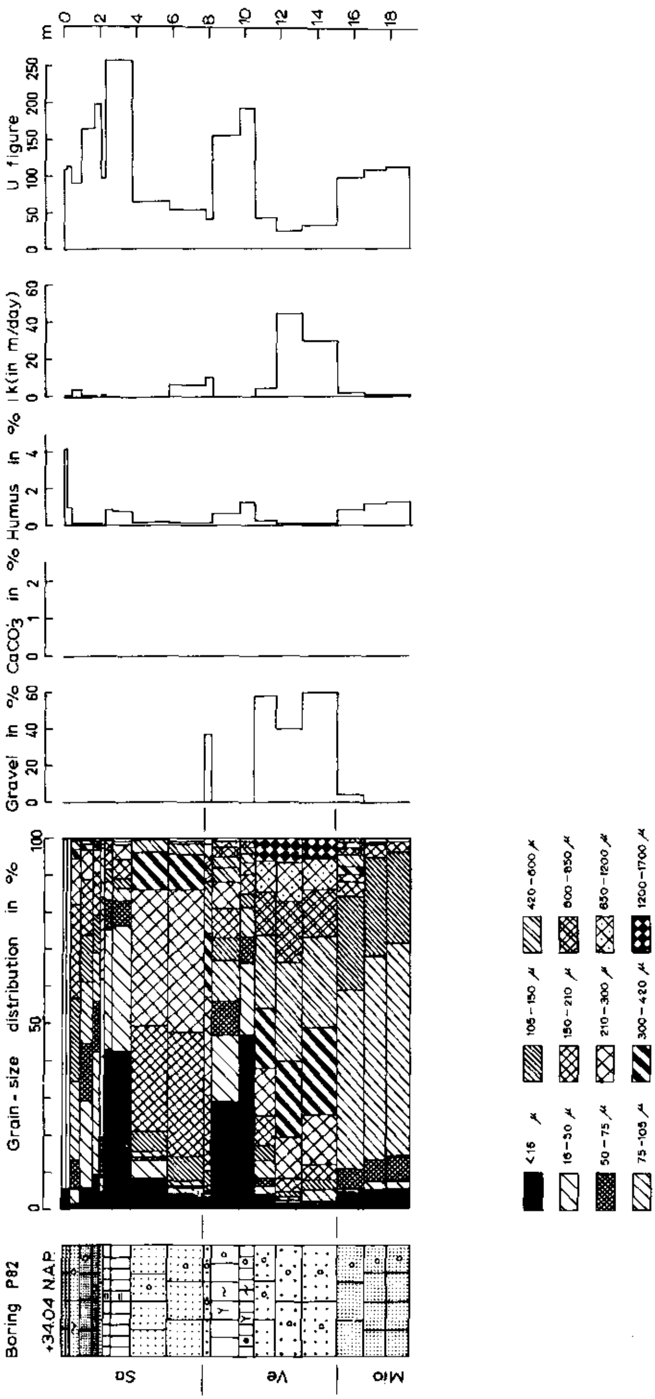
Boring P82
+34.04 N.A.P.
Sa
Ve
Mio
m
Grain - size distribution in %
Gravel in %
CaCO3 in %
Humus in %
k (in m/day)
U figure
<16 μ
16-50 μ
50-75 μ
75-105 μ
105-150 μ
150-210 μ
210-300 μ
300-420 μ
420-600 μ
600-850 μ
850-1200 μ
1200-1700 μ

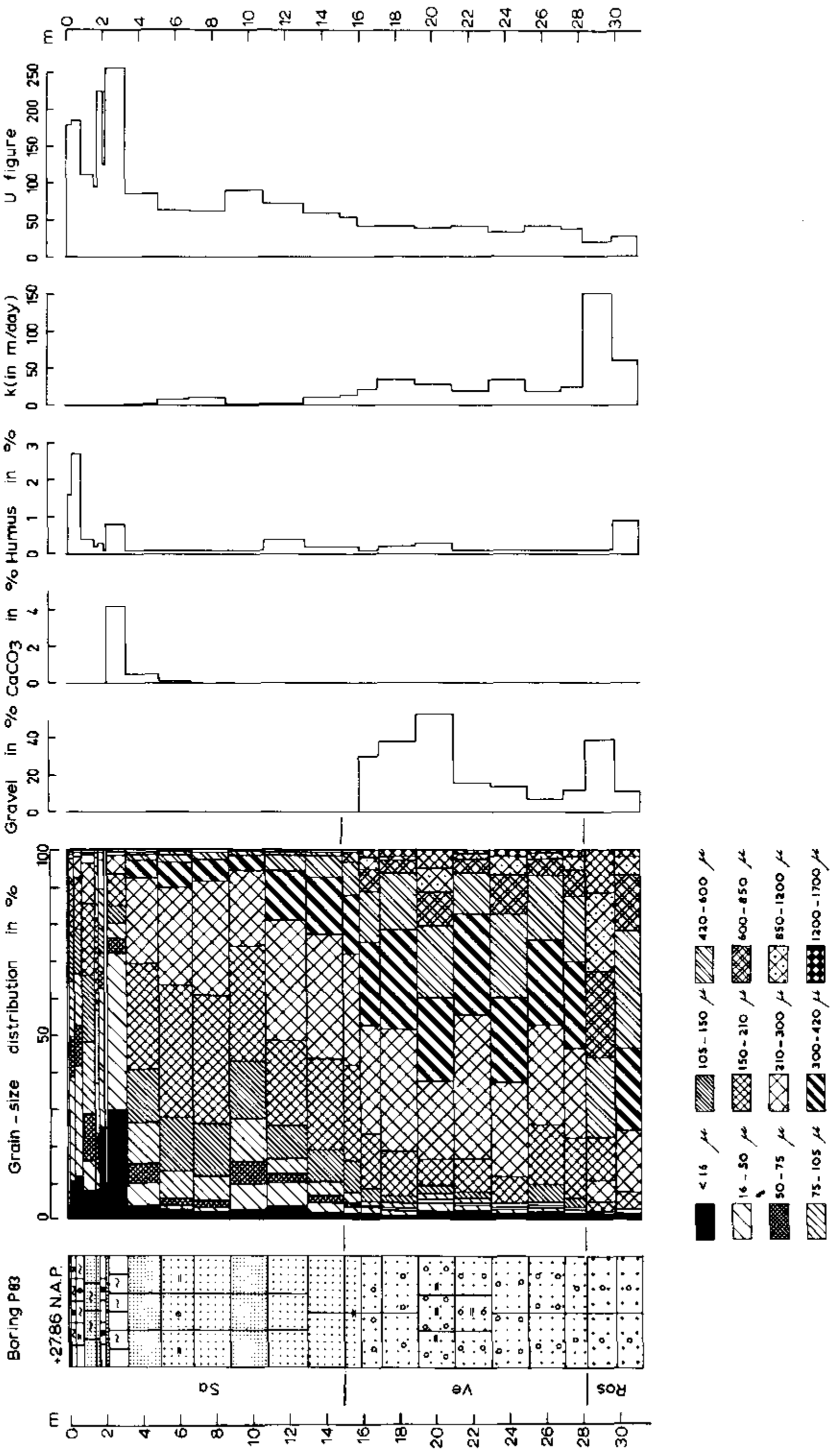
Boring P83
+27.86 N.A.P.
Sa
Ve
Ros
m
Grain - size distribution in %
Gravel in %
CaCO3 in %
Humus in %
k(in m/day)
U figure
< 16 μ
16 - 50 μ
50 - 75 μ
75 - 105 μ
105 - 150 μ
150 - 210 μ
210 - 300 μ
300 - 420 μ
420 - 600 μ
600 - 850 μ
850 - 1200 μ
1200 - 1700 μ

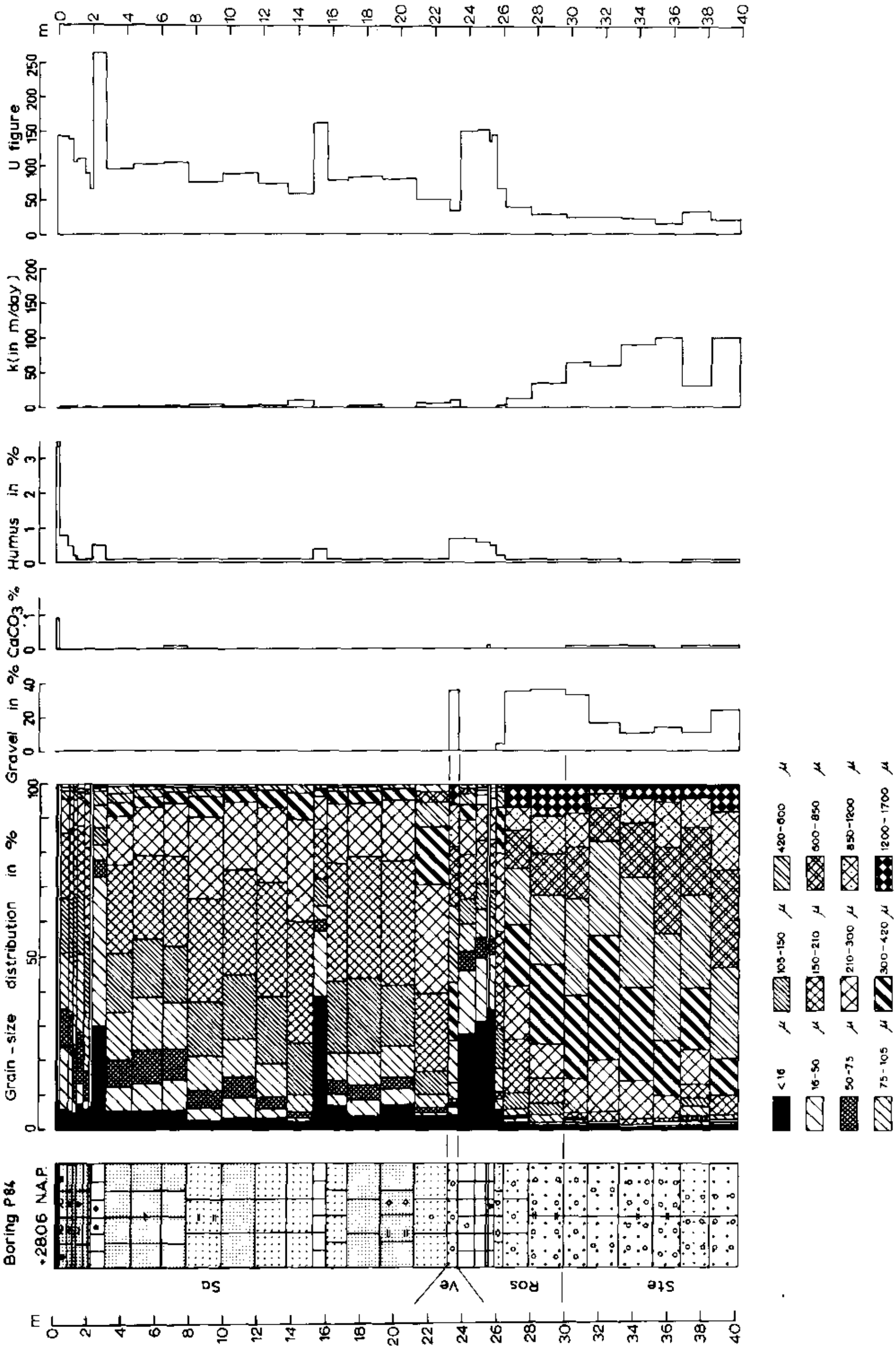
Boring P84
+2806 N.A.P.
Grain - size distribution in %
Gravel in %
CaCO3 %
Humus in %
k(in m/day)
U figure
m
Sa
Ve
Ros
Ste
< 16 μ
16-50 μ
50-75 μ
75-105 μ
105-150 μ
150-210 μ
210-300 μ
300-420 μ
420-600 μ
600-850 μ
850-1200 μ
1200-1700 μ

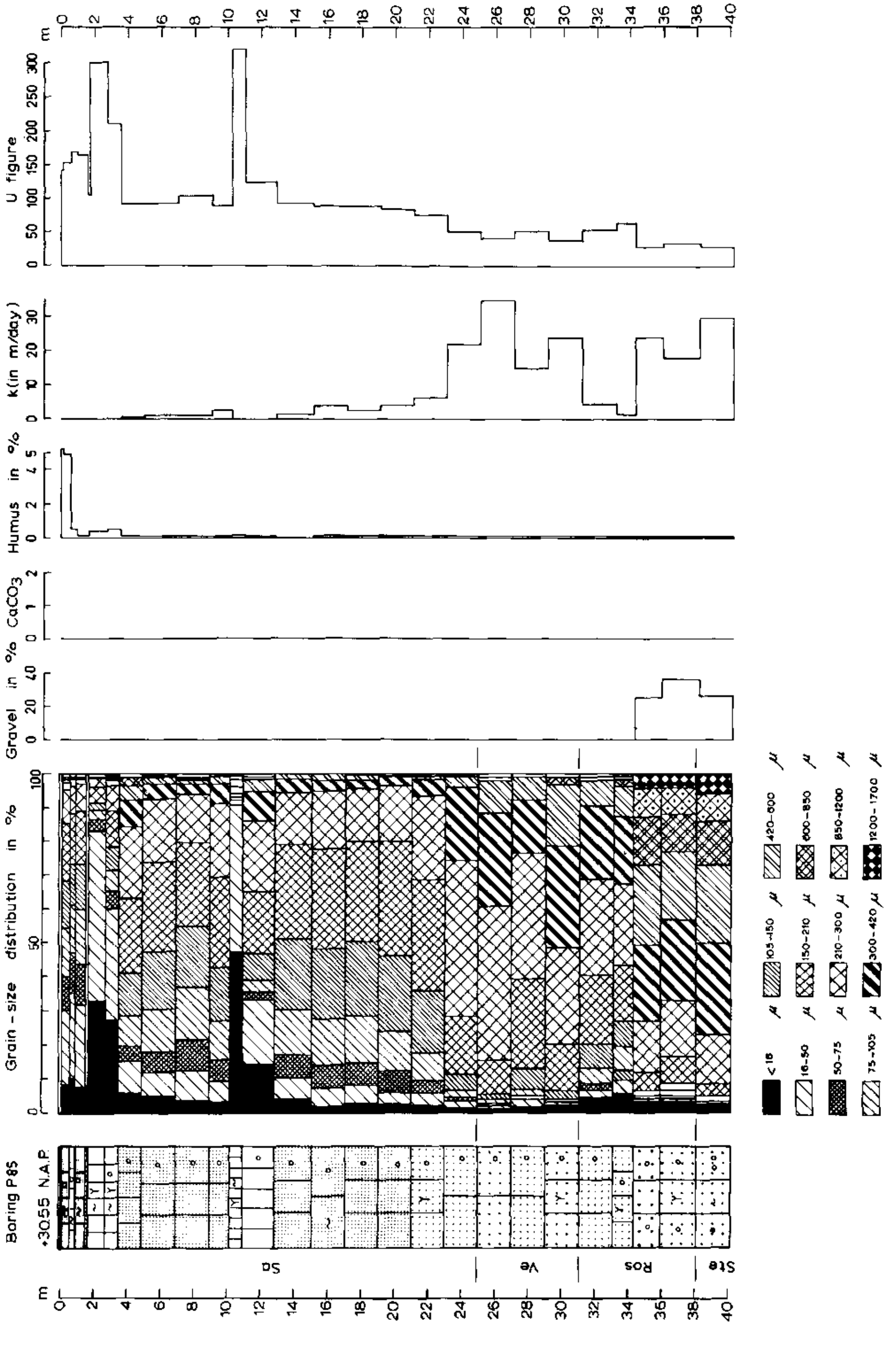
U figure
k(in m/day)
Humus in %
CaCO3
Gravel in %
Grain - size distribution in %
Boring P85
+30.55 N.A.P.
m
Sa
Ve
Ros
Ste
<16 μ
16-50 μ
50-75 μ
75-105 μ
105-150 μ
150-210 μ
210-300 μ
300-420 μ
420-600 μ
600-850 μ
850-1200 μ
1200-1700 μ

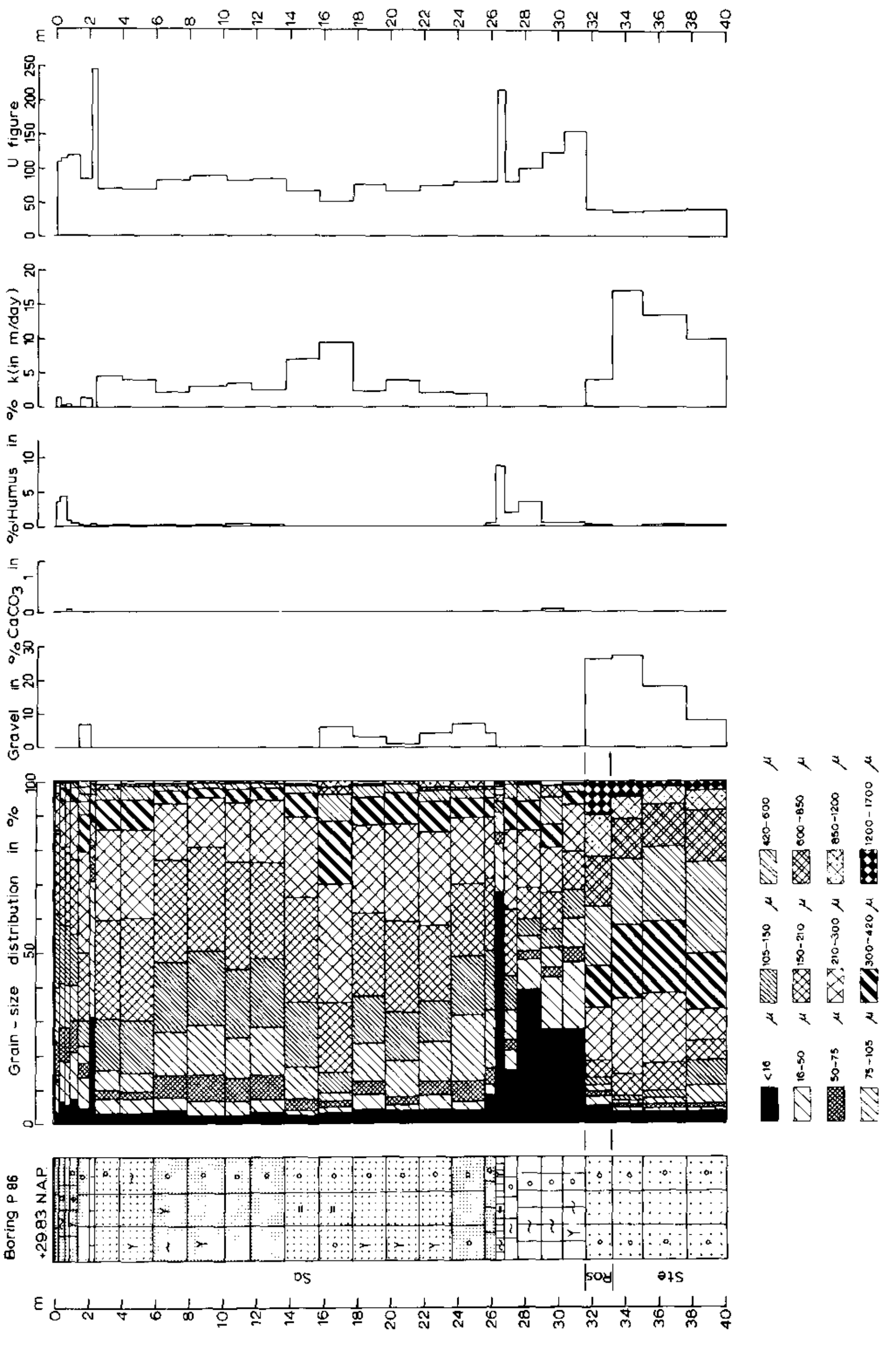

Boring P 86
+29.83 N.A.P.
Grain - size distribution in %
Gravel in %
% CaCO3 in
% Humus in
% k (in m/day)
U figure
m
So
Ros
Ste
<16 μ
16-50 μ
50-75 μ
75-105 μ
105-150 μ
150-210 μ
210-300 μ
300-420 μ
420-600 μ
600-850 μ
850-1200 μ
1200-1700 μ

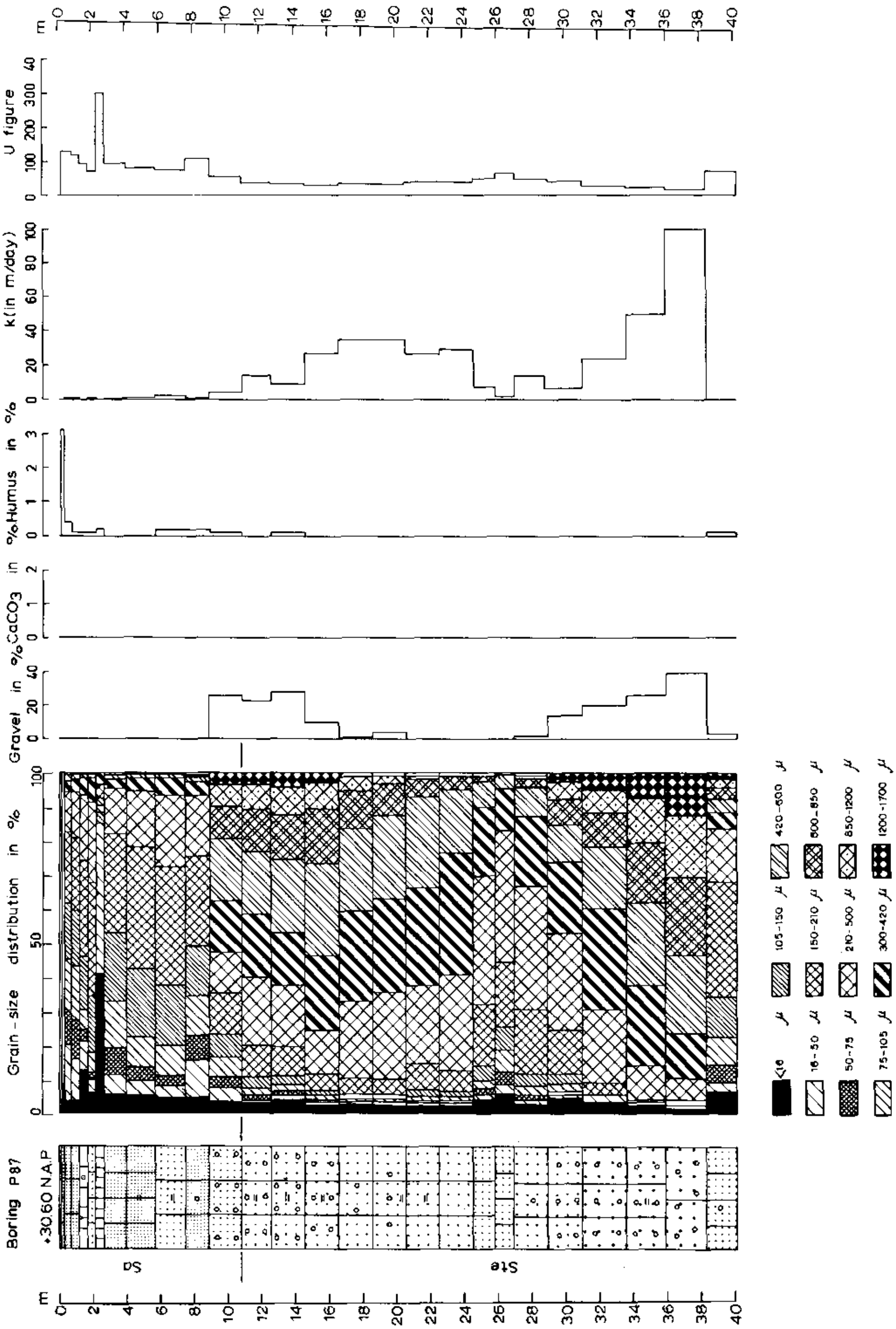
Boring P87
+30.60 N.A.P.
Sa
Ste
Grain - size distribution in %
Gravel in %
%CaCO3 in %
%Humus in %
k (in m/day)
U figure
m
<16 μ
16-50 μ
50-75 μ
75-105 μ
105-150 μ
150-210 μ
210-300 μ
300-420 μ
420-600 μ
600-850 μ
850-1200 μ
1200-1700 μ

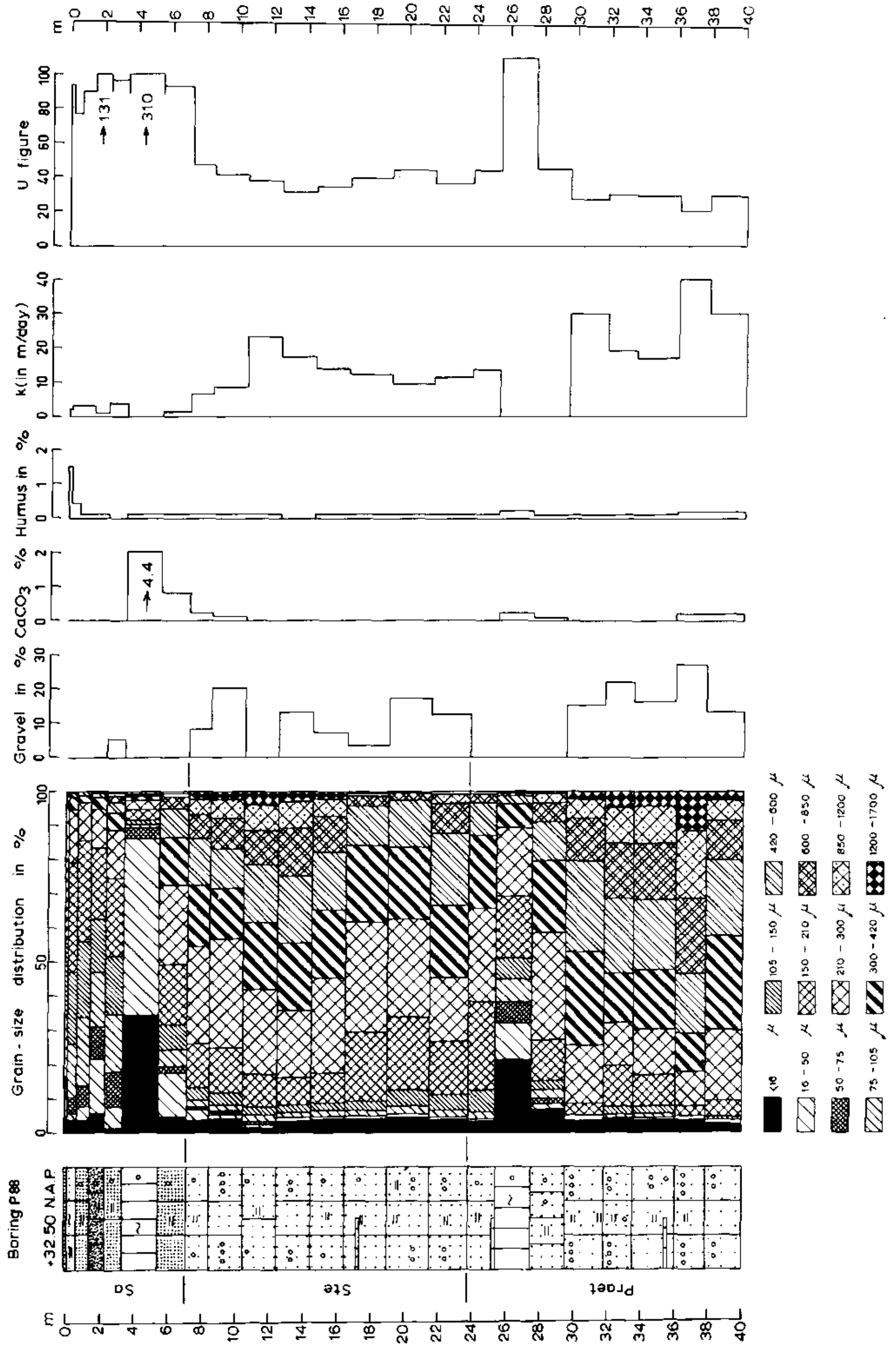

U figure
k (in m/day)
Humus in %
$CaCO_3$ %
Gravel in %
Grain - size distribution in %
Boring P 88
+32.50 N.A.P.
Sa
Ste
Praet
m
→131
→310
→4.4
<16 μ
16 - 50 μ
50 - 75 μ
75 - 105 μ
105 - 150 μ
150 - 210 μ
210 - 300 μ
300 - 420 μ
420 - 600 μ
600 - 850 μ
850 - 1200 μ
1200 - 1700 μ

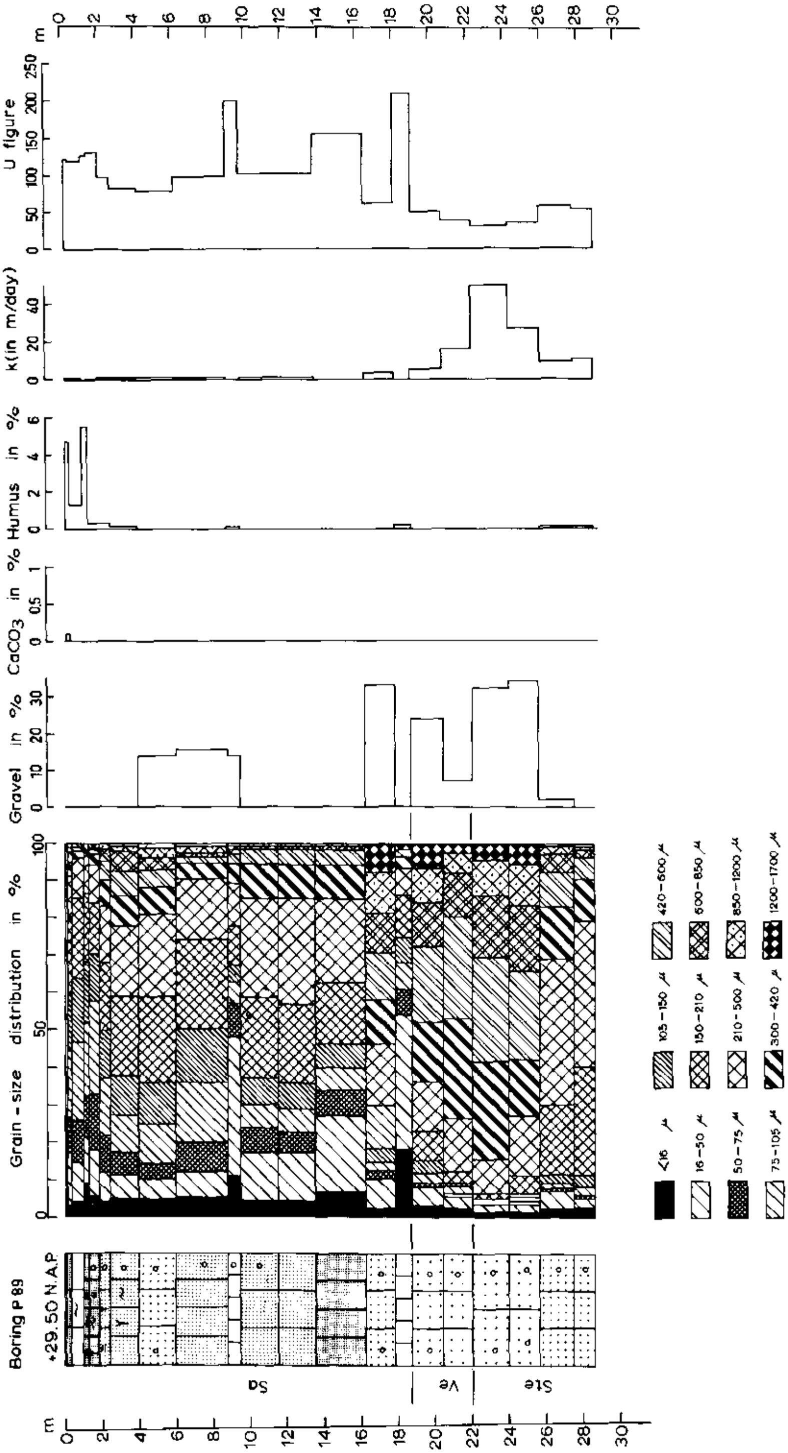
Boring P 89
+29.50 N.A.P.
Sa
Ve
Ste
Grain - size distribution in %
Gravel in %
$CaCO_3$ in %
Humus in %
k (in m/day)
U figure
m
<16 μ
16-50 μ
50-75 μ
75-105 μ
105-150 μ
150-210 μ
210-300 μ
300-420 μ
420-600 μ
600-850 μ
850-1200 μ
1200-1700 μ

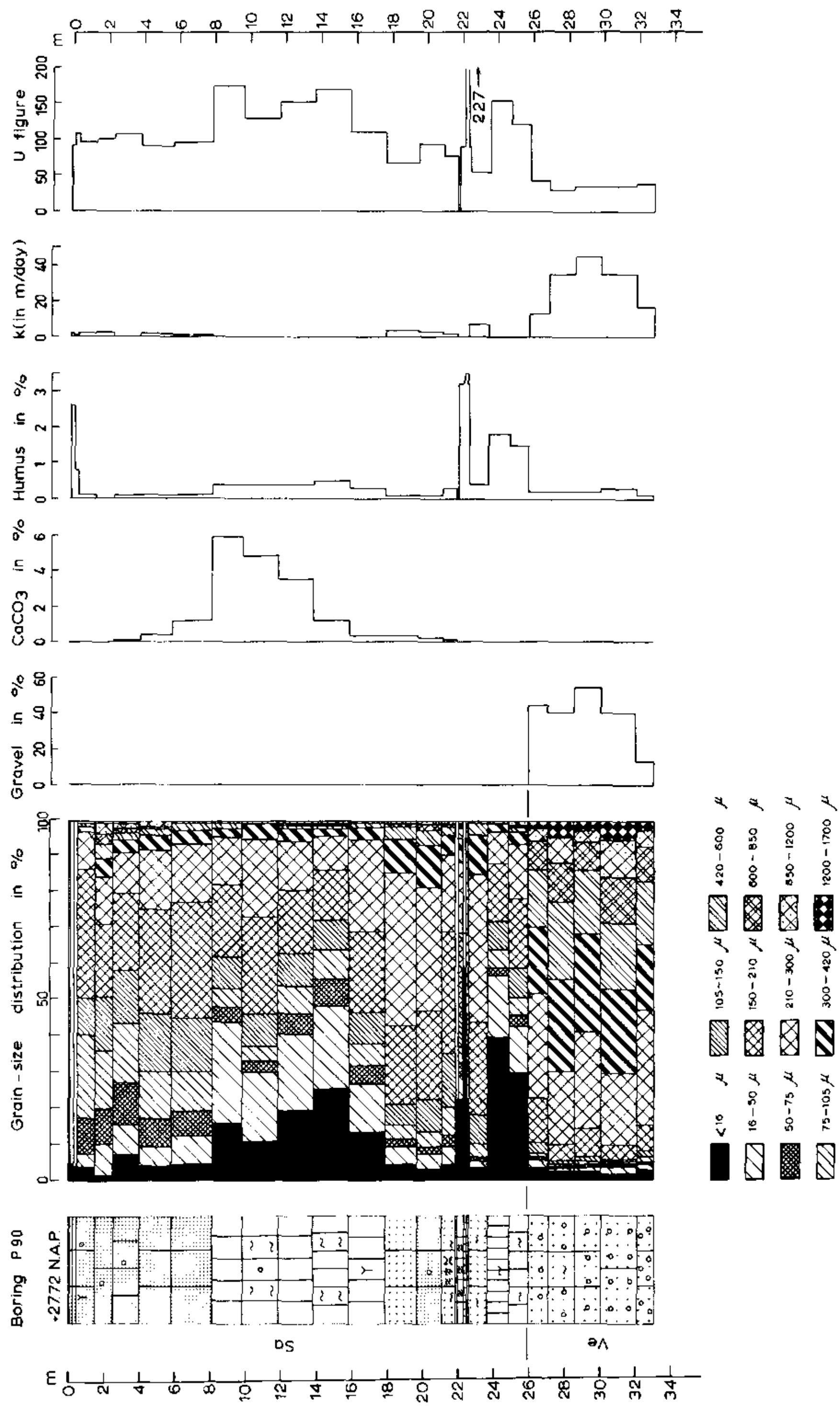
Boring P 90
-27.72 N.A.P.
Grain-size distribution in %
Gravel in %
CaCO3 in %
Humus in %
k (in m/day)
U figure
227
Sa
Ve
m
< 16 μ
16 – 50 μ
50 – 75 μ
75 – 105 μ
105 – 150 μ
150 – 210 μ
210 – 300 μ
300 – 420 μ
420 – 600 μ
600 – 850 μ
850 – 1200 μ
1200 – 1700 μ

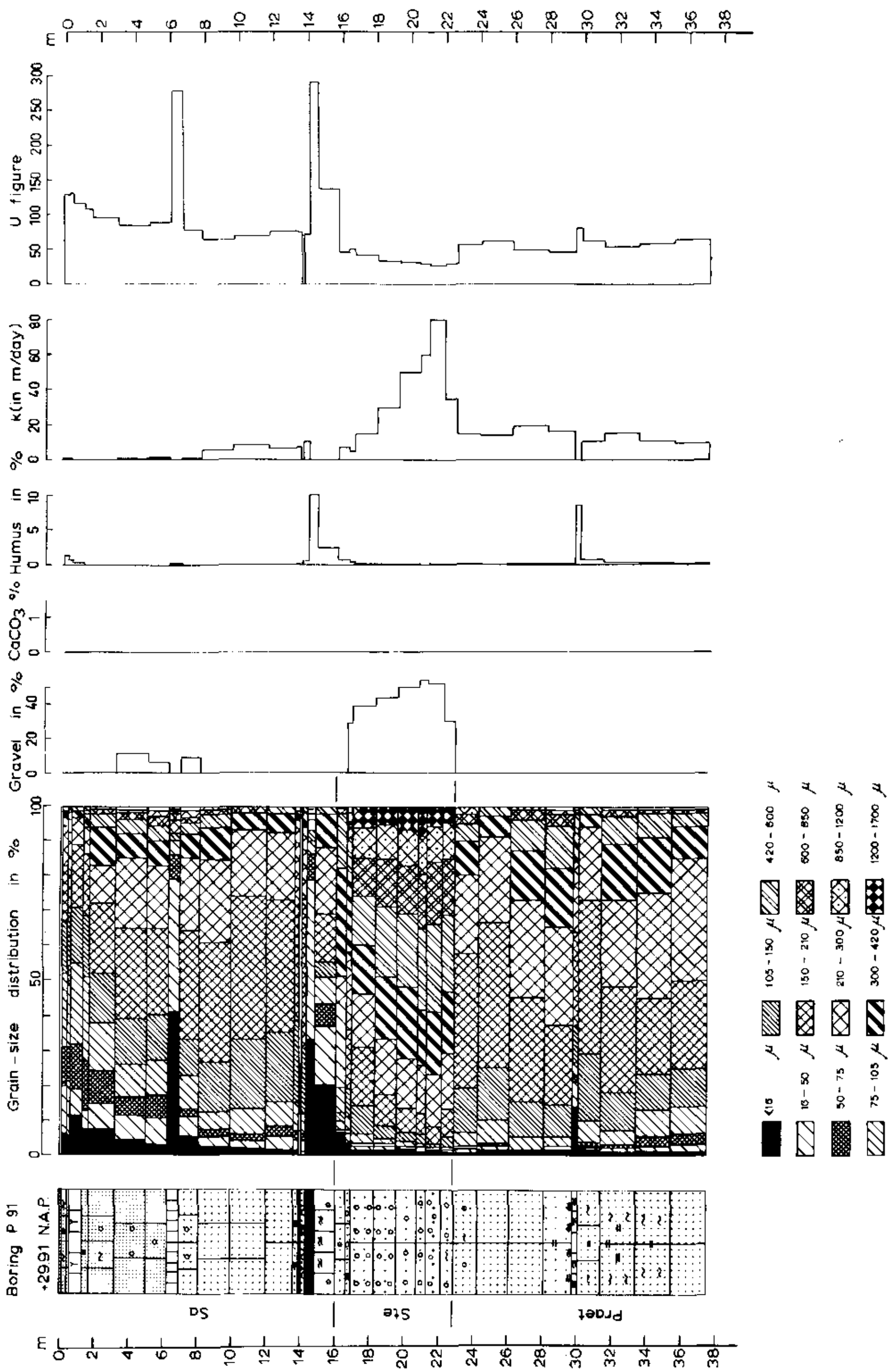
Boring P 91 +29.91 N.A.P.
Grain - size distribution in %
Gravel in %
CaCO3 %
Humus in %
% k (in m/day)
U figure
m
Sa
Ste
Praet
<16 μ
16 - 50 μ
50 - 75 μ
75 - 105 μ
105 - 150 μ
150 - 210 μ
210 - 300 μ
300 - 420 μ
420 - 600 μ
600 - 850 μ
850 - 1200 μ
1200 - 1700 μ

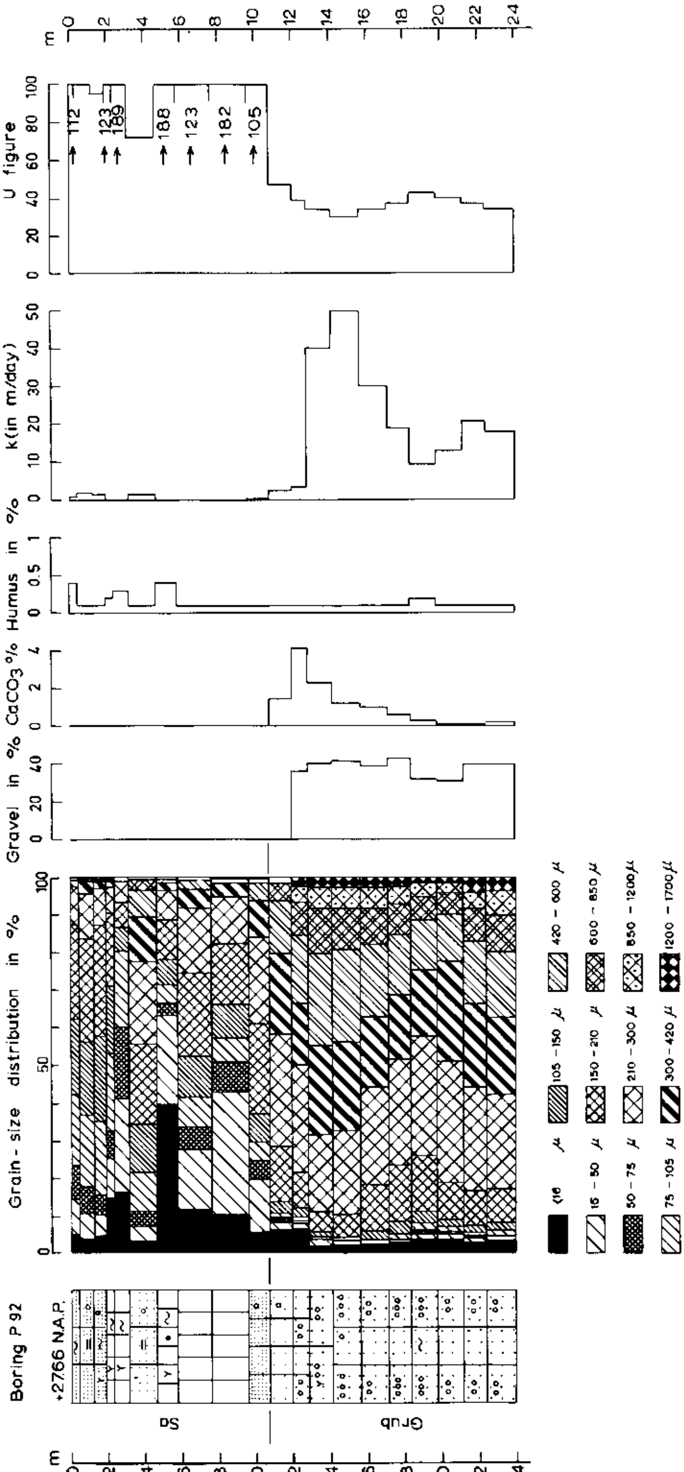
Boring P 92
+2766 N.A.P.
Sa
Grub
Grain - size distribution in %
Gravel in %
$CaCO_3$ %
Humus in %
k(in m/day)
U figure
112
123
189
188
123
182
105
<16 μ
16 - 50 μ
50 - 75 μ
75 - 105 μ
105 - 150 μ
150 - 210 μ
210 - 300 μ
300 - 420 μ
420 - 600 μ
600 - 850 μ
850 - 1200 μ
1200 - 1700 μ
m

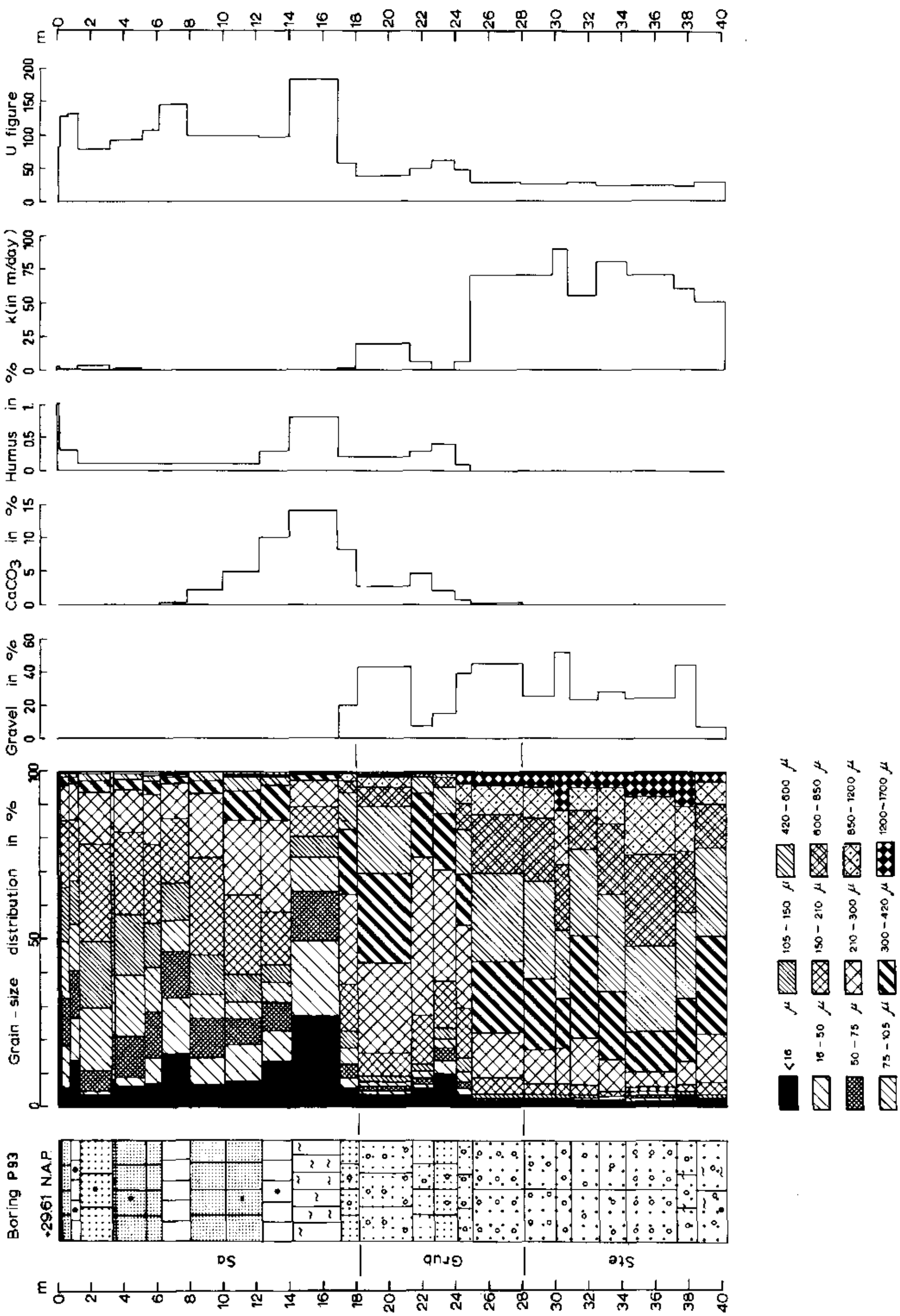

m
0
2
4
6
8
10
12
14
16
18
20
22
24
26
28
30
32
34
36
38
40
U figure
0
50
100
150
200
% k (in m/day)
0
25
50
75
100
Humus in
0
0.5
1
CaCO3 in %
0
5
10
15
Gravel in %
0
20
40
60
Grain - size distribution in %
0
50
100
Boring P93
+29.61 N.A.P.
Sa
Grub
Ste
<16
16 - 50 μ
50 - 75 μ
75 - 105 μ
105 - 150 μ
150 - 210 μ
210 - 300 μ
300 - 420 μ
420 - 600 μ
600 - 850 μ
850 - 1200 μ
1200 - 1700 μ

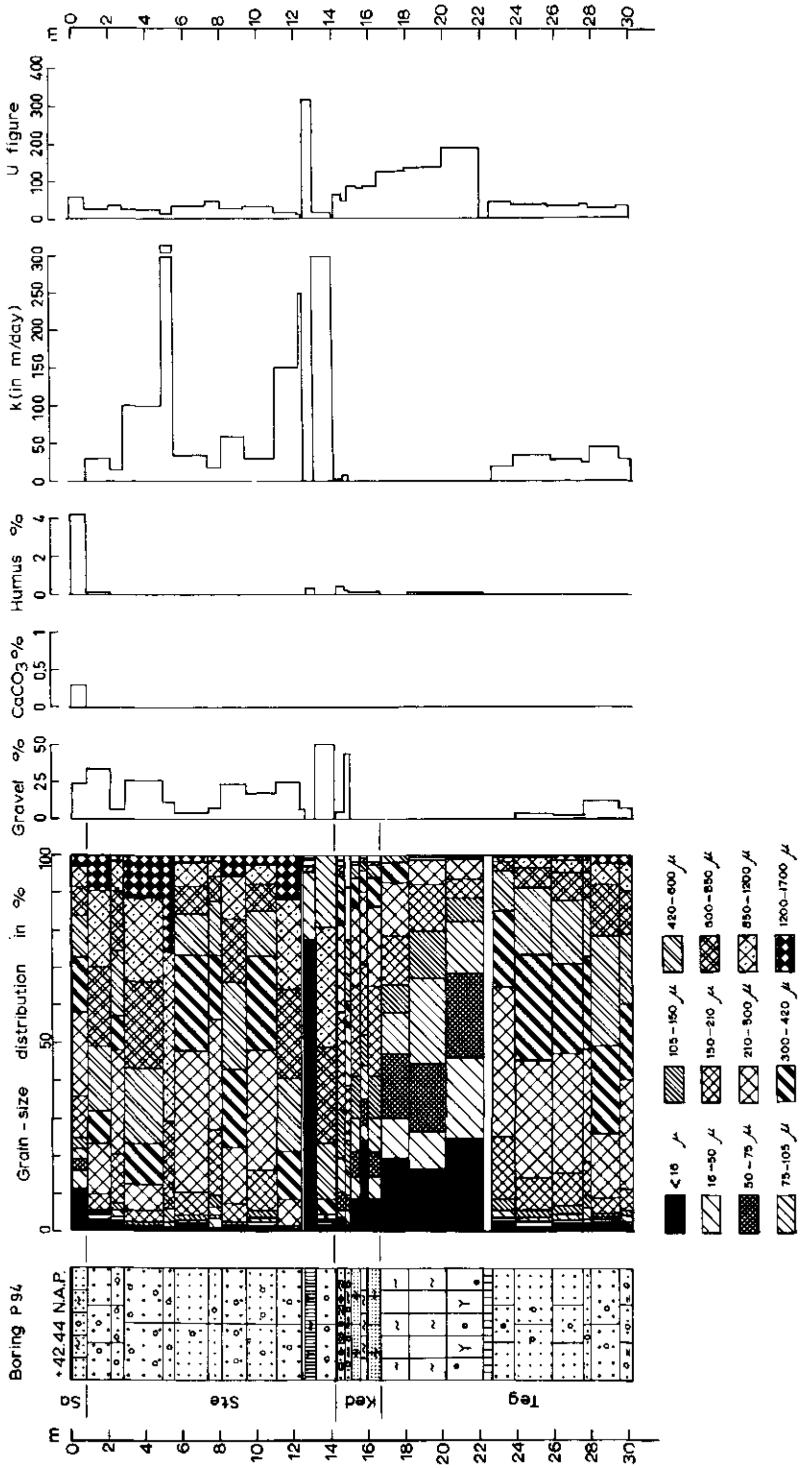

m
Sa
Ste
Ked
Teg
Boring P 94
+42.44 N.A.P.
Grain - size distribution in %
Gravel %
CaCO3 %
Humus %
k (in m/day)
U figure
< 16 μ
16 - 50 μ
50 - 75 μ
75 - 105 μ
105 - 150 μ
150 - 210 μ
210 - 300 μ
300 - 420 μ
420 - 600 μ
600 - 850 μ
850 - 1200 μ
1200 - 1700 μ

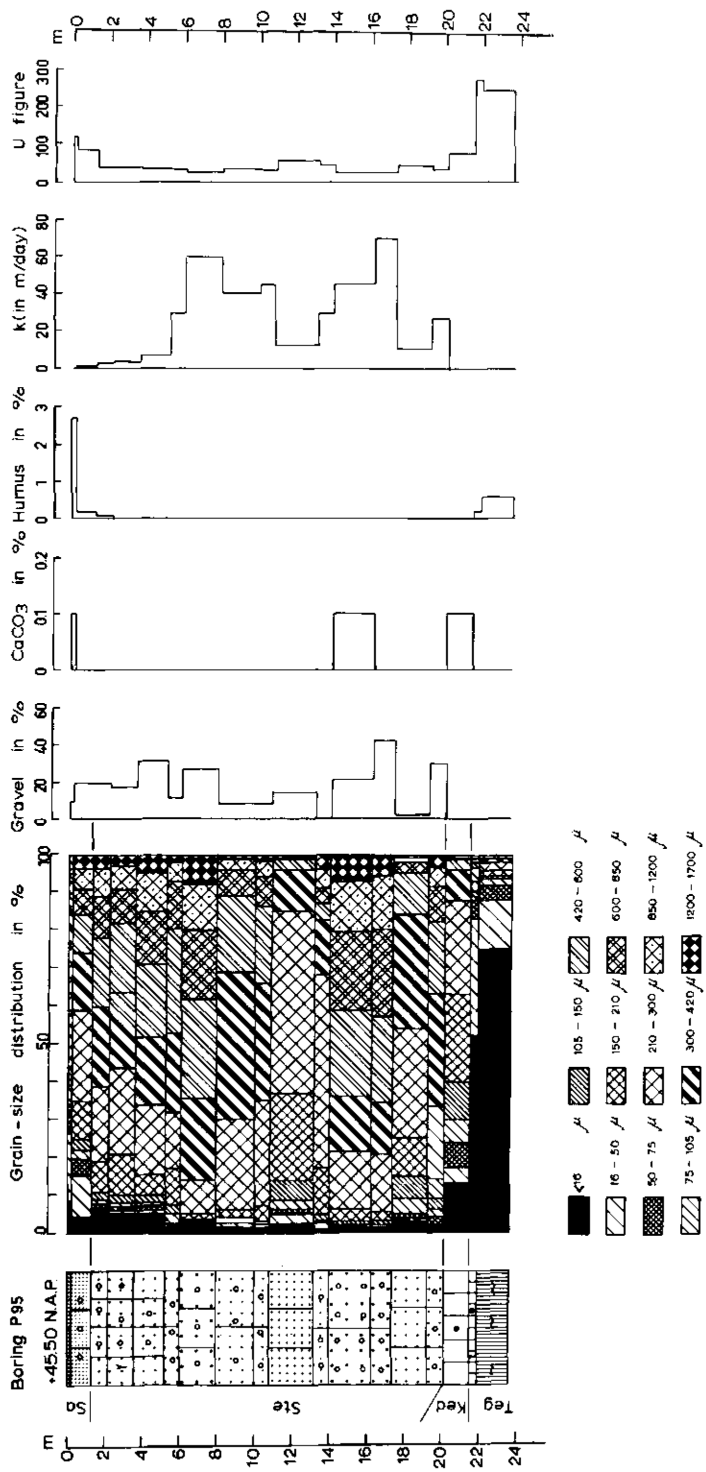
Boring P95
+45.50 N.A.P.
Sa
Ste
Ked
Teg
m
Grain - size distribution in %
Gravel in %
CaCO3 in %
Humus in %
k (in m/day)
U figure
<16 μ
16 - 50 μ
50 - 75 μ
75 - 105 μ
105 - 150 μ
150 - 210 μ
210 - 300 μ
300 - 420 μ
420 - 600 μ
600 - 850 μ
850 - 1200 μ
1200 - 1700 μ

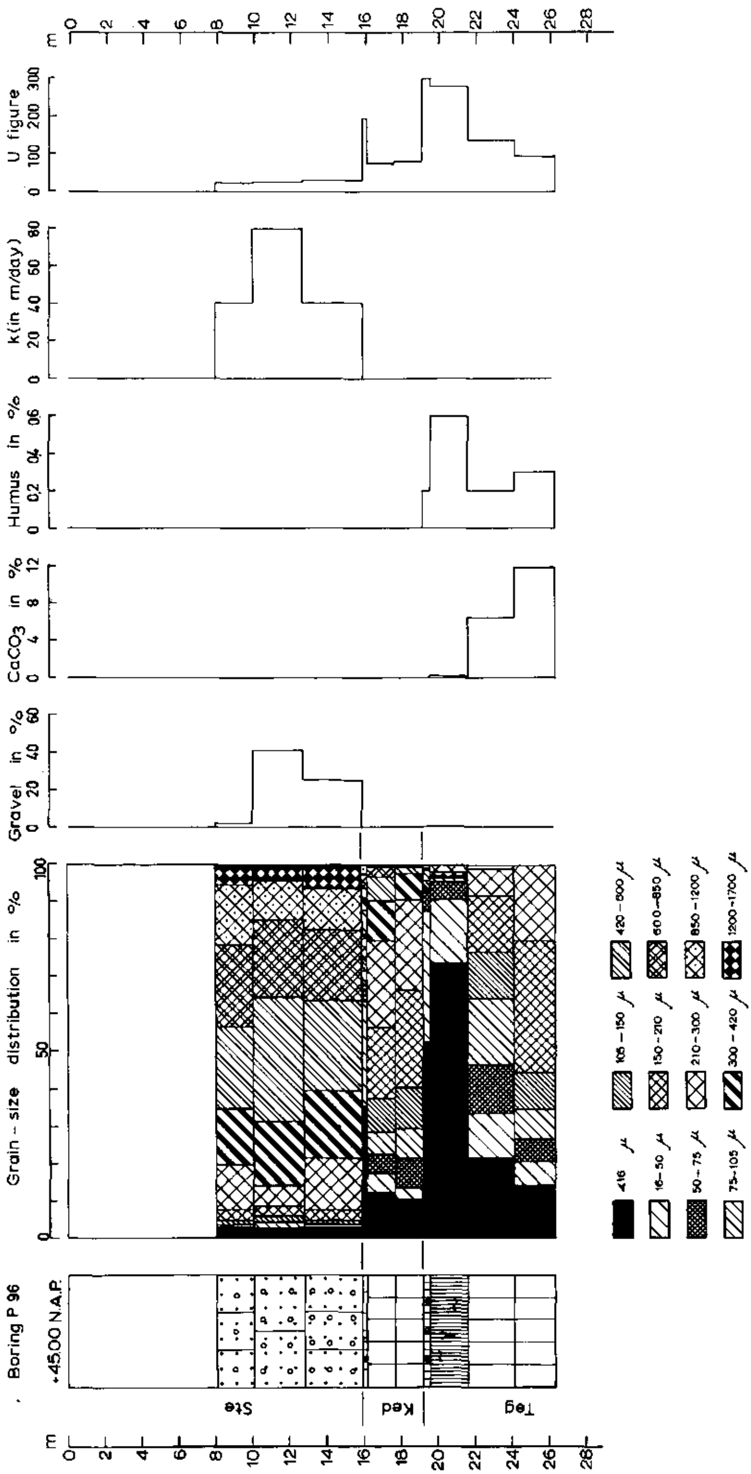
Boring P 96
+45.00 N.A.P.
Grain - size distribution in %
Gravel in %
$CaCO_3$ in %
Humus in %
k (in m/day)
U figure
m
Ste
Ked
Teg
<16 μ
16-50 μ
50-75 μ
75-105 μ
105-150 μ
150-210 μ
210-300 μ
300-420 μ
420-600 μ
600-850 μ
850-1200 μ
1200-1700 μ

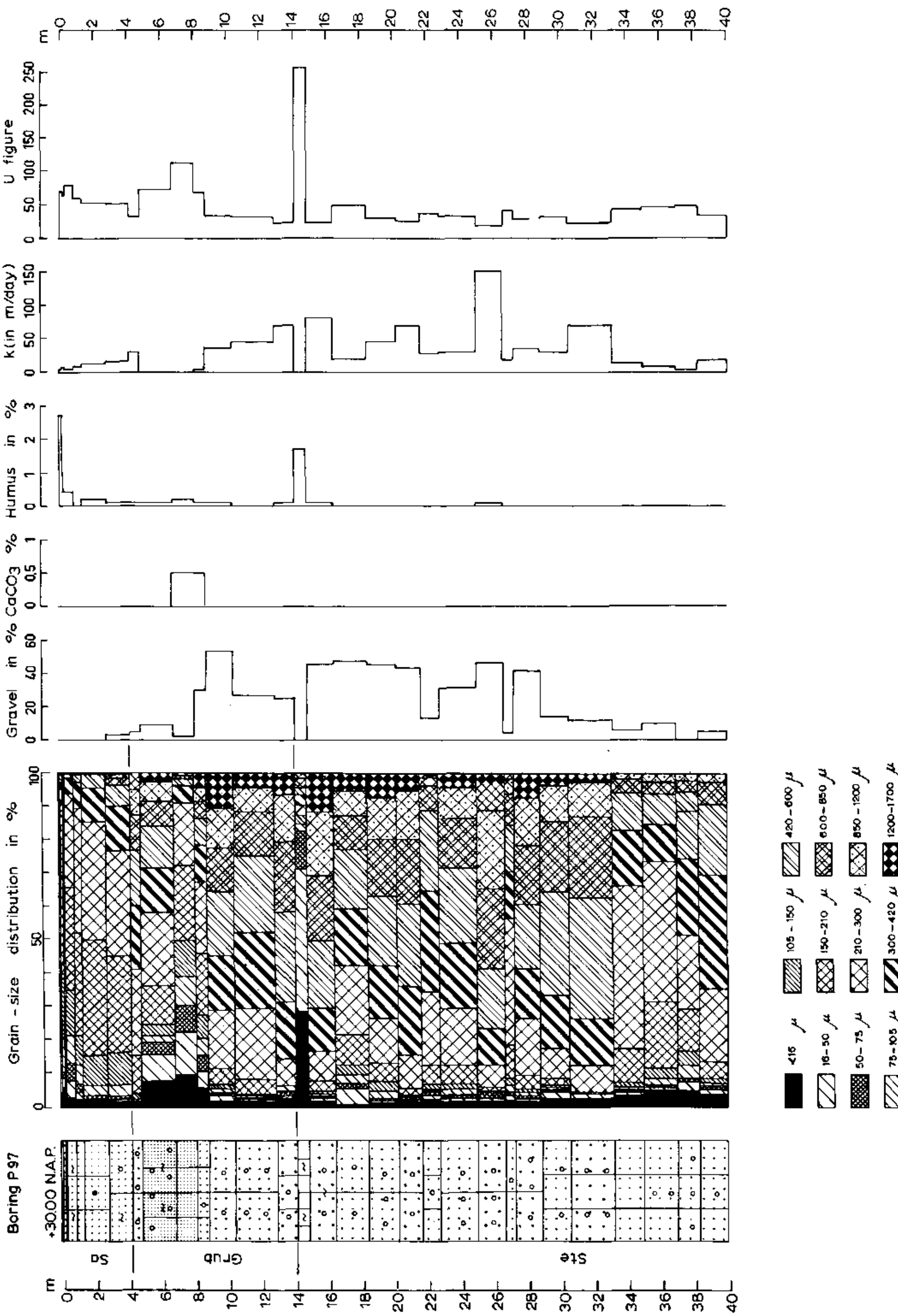

U figure
k (in m/day)
Humus in %
CaCO3 %
Gravel in %
Grain - size distribution in %
Boring P97
+30.00 N.A.P.
Sa
Grub
Ste
m
<16 μ
16-50 μ
50-75 μ
75-105 μ
105-150 μ
150-210 μ
210-300 μ
300-420 μ
420-600 μ
600-850 μ
850-1200 μ
1200-1700 μ

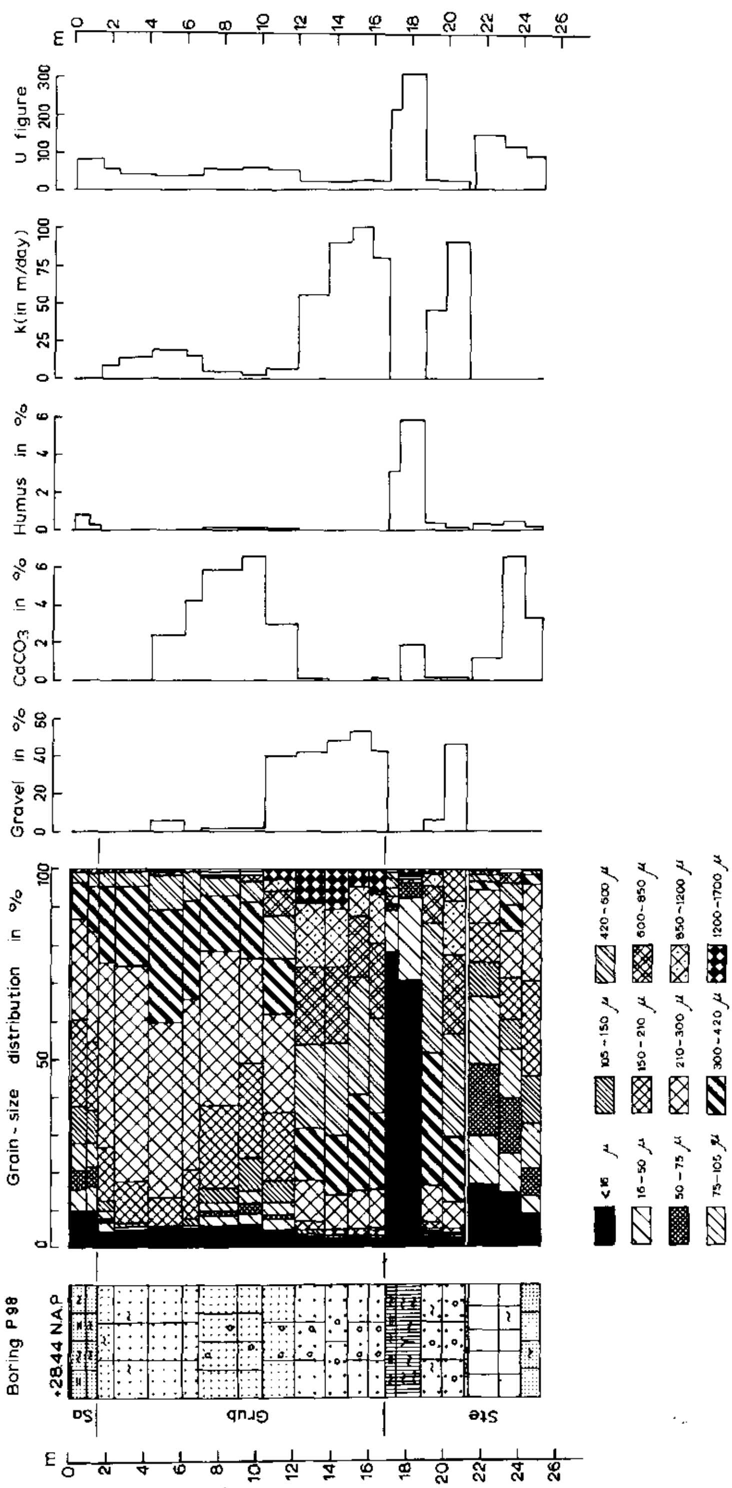

Boring P 98
+28.44 N.A.P.
Sa
Grub
Ste
Grain-size distribution in %
Gravel in %
CaCO3 in %
Humus in %
k (in m/day)
U figure
m
< 16 μ
16 - 50 μ
50 - 75 μ
75 - 105 μ
105 - 150 μ
150 - 210 μ
210 - 300 μ
300 - 420 μ
420 - 600 μ
600 - 850 μ
850 - 1200 μ
1200 - 1700 μ

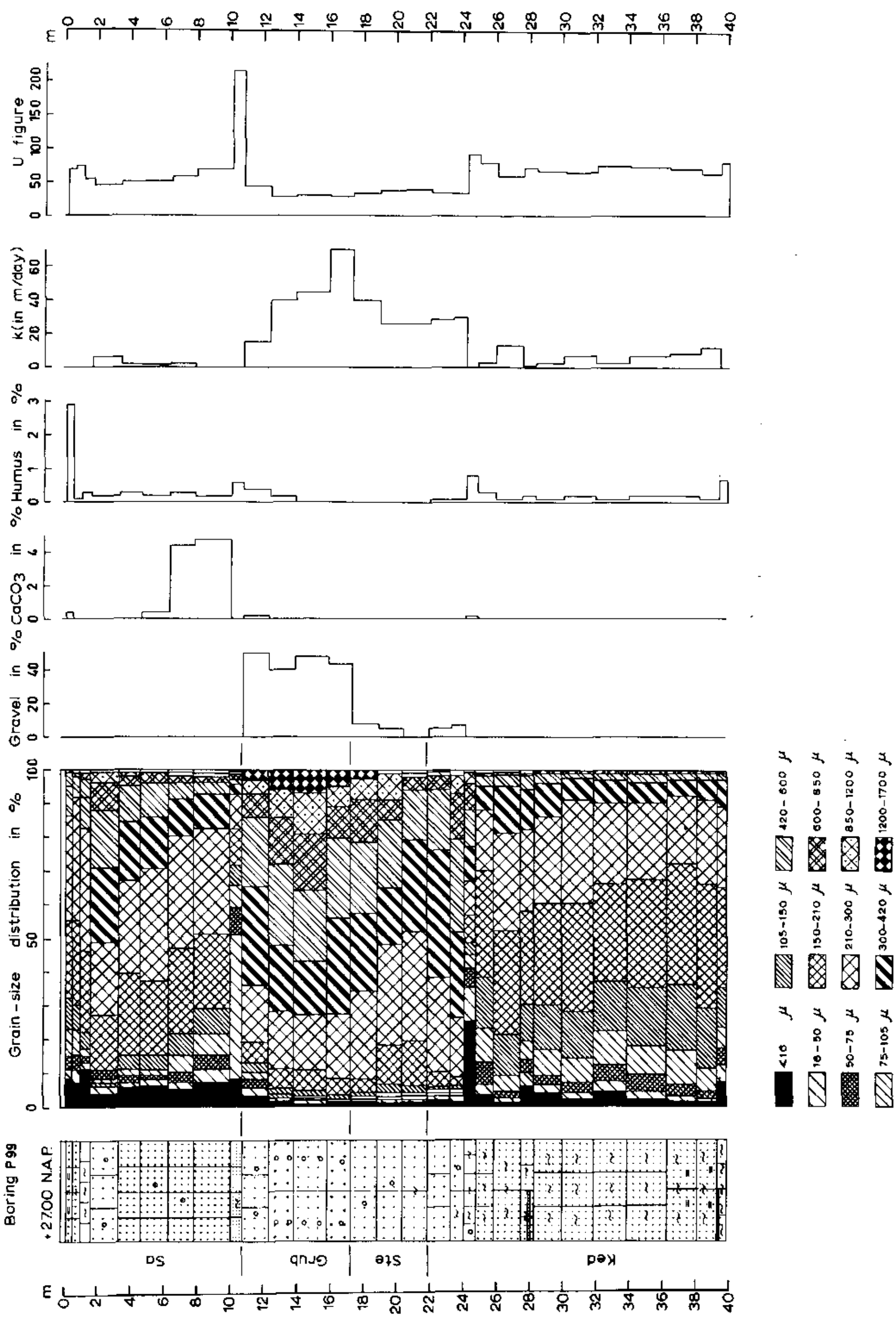
Boring P99
+27.00 N.A.P.
Sa
Grub
Ste
Ked
Grain-size distribution in %
Gravel in %
% CaCO3 in %
% Humus in %
k (in m/day)
U figure
m
<16 μ
16-50 μ
50-75 μ
75-105 μ
105-150 μ
150-210 μ
210-300 μ
300-420 μ
420-600 μ
600-850 μ
850-1200 μ
1200-1700 μ

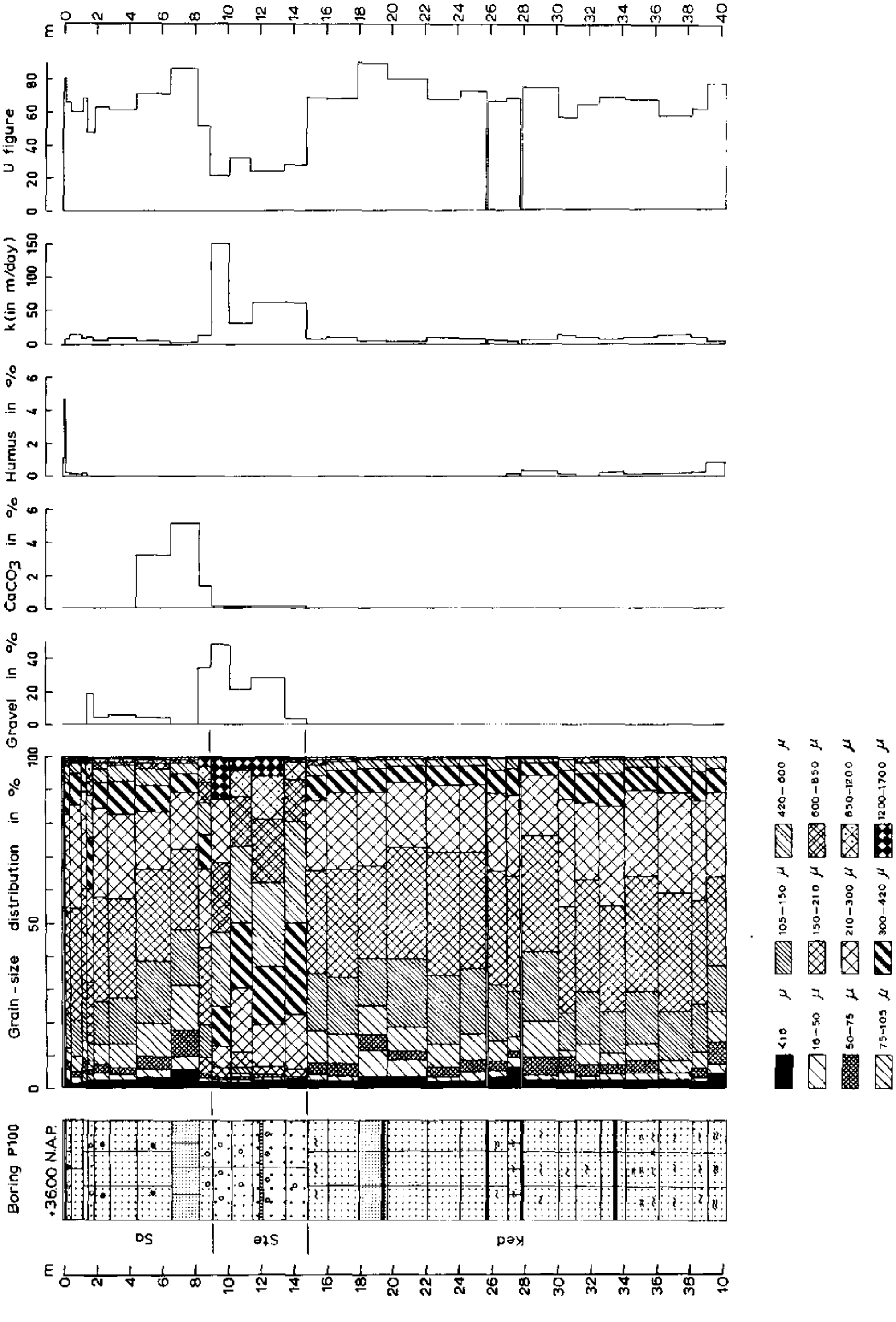

m
U figure
k (in m/day)
Humus in %
CaCO3 in %
Gravel in %
Grain-size distribution in %
Boring P100
+36.00 N.A.P.
Sa
Ste
Ked
<16 μ
16–50 μ
50–75 μ
75–105 μ
105–150 μ
150–210 μ
210–300 μ
300–420 μ
420–600 μ
600–850 μ
850–1200 μ
1200–1700 μ


Boring P101
+42.00 N.A.P.
Grain-size distribution in %
Gravel in %
CaCO3 in %
Humus in %
k(in m/day)
U figure
m
Ste
Praet
<16 µ
16–50 µ
50–75 µ
75–105 µ
105–150 µ
150–210 µ
210–300 µ
300–420 µ
420–600 µ
600–850 µ
850–1200 µ
1200–1700 µ

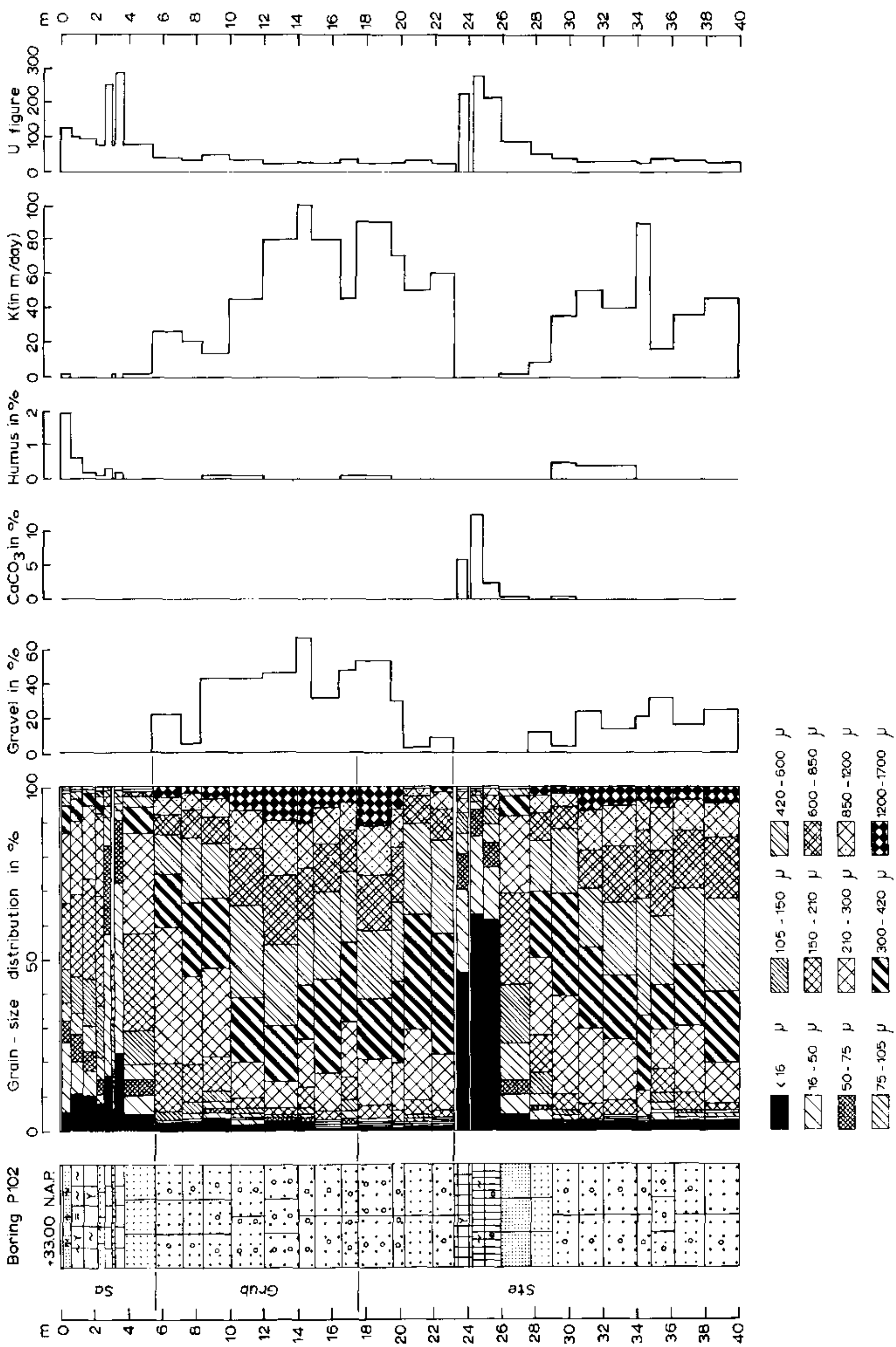

m
U figure
K(in m/day)
Humus in %
$CaCO_3$ in %
Gravel in %
Grain - size distribution in %
Boring P102
+33.00 N.A.P.
Sa
Grub
Ste
< 16 μ
16 - 50 μ
50 - 75 μ
75 - 105 μ
105 - 150 μ
150 - 210 μ
210 - 300 μ
300 - 420 μ
420 - 600 μ
600 - 850 μ
850 - 1200 μ
1200 - 1700 μ

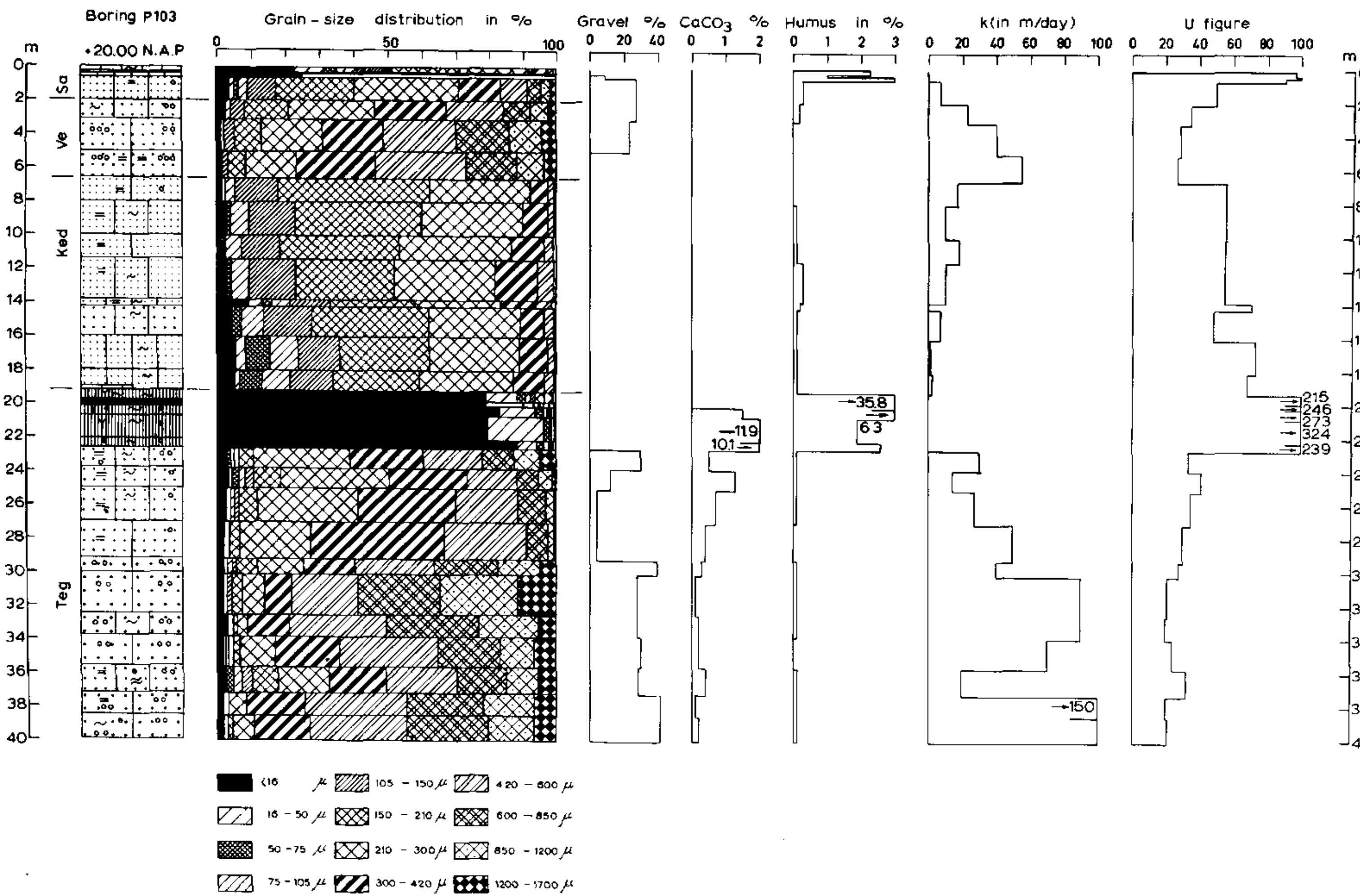

Boring P103
+20.00 N.A.P
Grain - size distribution in %
Gravel %
$CaCO_3$ %
Humus in %
k(in m/day)
U figure
m
Sa
Ve
Ked
Teg
35.8
63
119
101
150
215
246
273
324
239
<16 μ
16 - 50 μ
50 - 75 μ
75 - 105 μ
105 - 150 μ
150 - 210 μ
210 - 300 μ
300 - 420 μ
420 - 600 μ
600 - 850 μ
850 - 1200 μ
1200 - 1700 μ

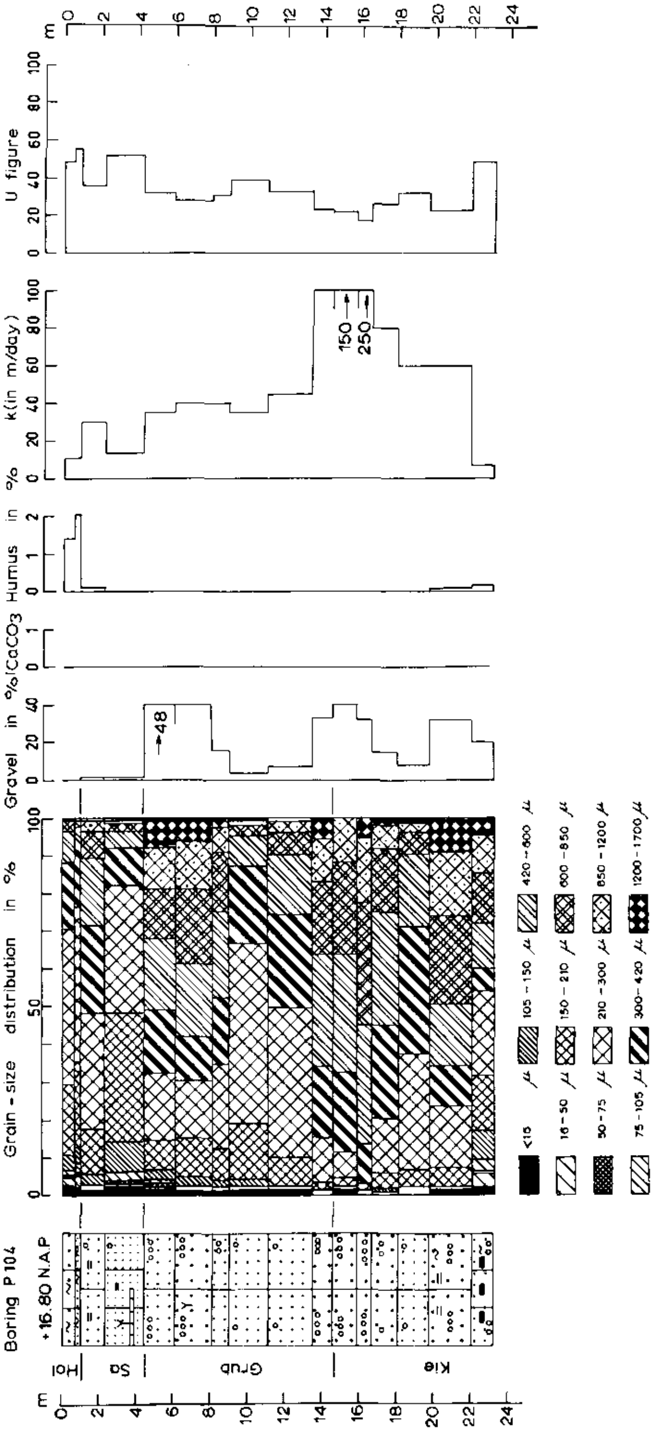
Boring P 104
+16.80 N.A.P
Hol
Sa
Grub
Kie
m
Grain - size distribution in %
Gravel in %
% CaCO3
Humus in %
k (in m/day)
U figure
→48
150→
250→
<16 µ
16 - 50 µ
50 - 75 µ
75 - 105 µ
105 - 150 µ
150 - 210 µ
210 - 300 µ
300 - 420 µ
420 - 600 µ
600 - 850 µ
850 - 1200 µ
1200 - 1700 µ

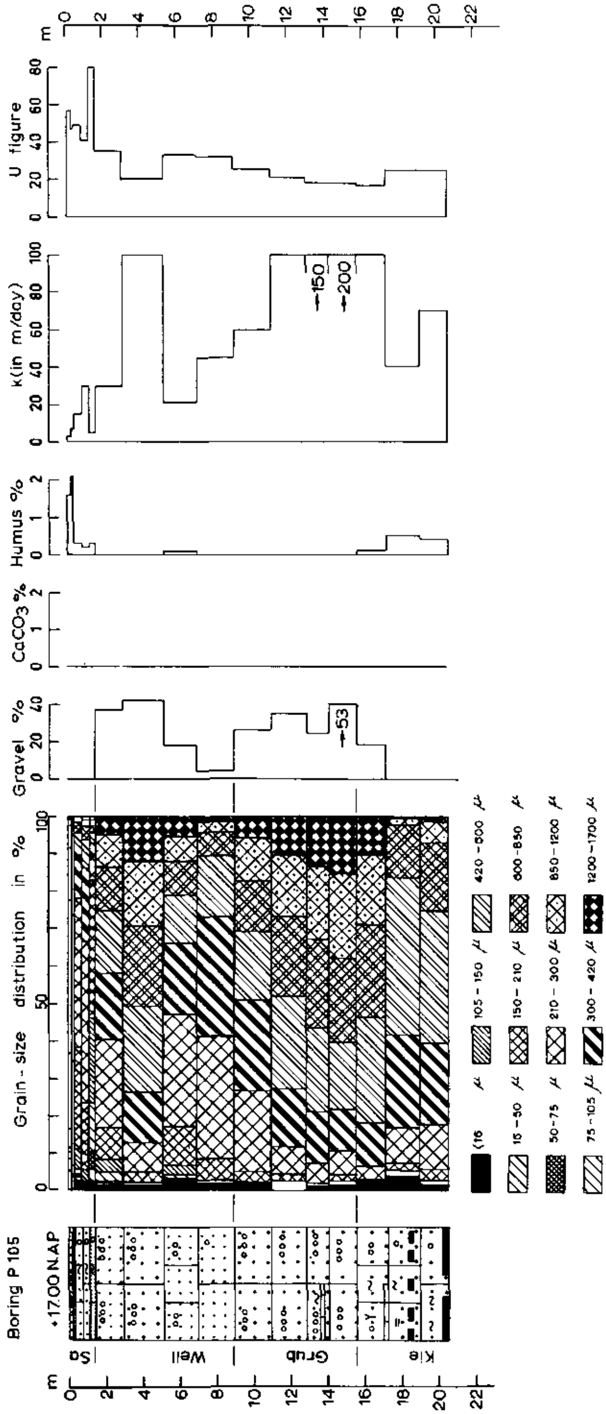
Boring P 105
+17.00 N.A.P
Sa
Well
Grub
Kie
m
Grain - size distribution in %
Gravel %
CaCO3 %
Humus %
k(in m/day)
U figure
150
200
53
<16 μ
16 - 50 μ
50 - 75 μ
75 - 105 μ
105 - 150 μ
150 - 210 μ
210 - 300 μ
300 - 420 μ
420 - 600 μ
600 - 850 μ
850 - 1200 μ
1200 - 1700 μ

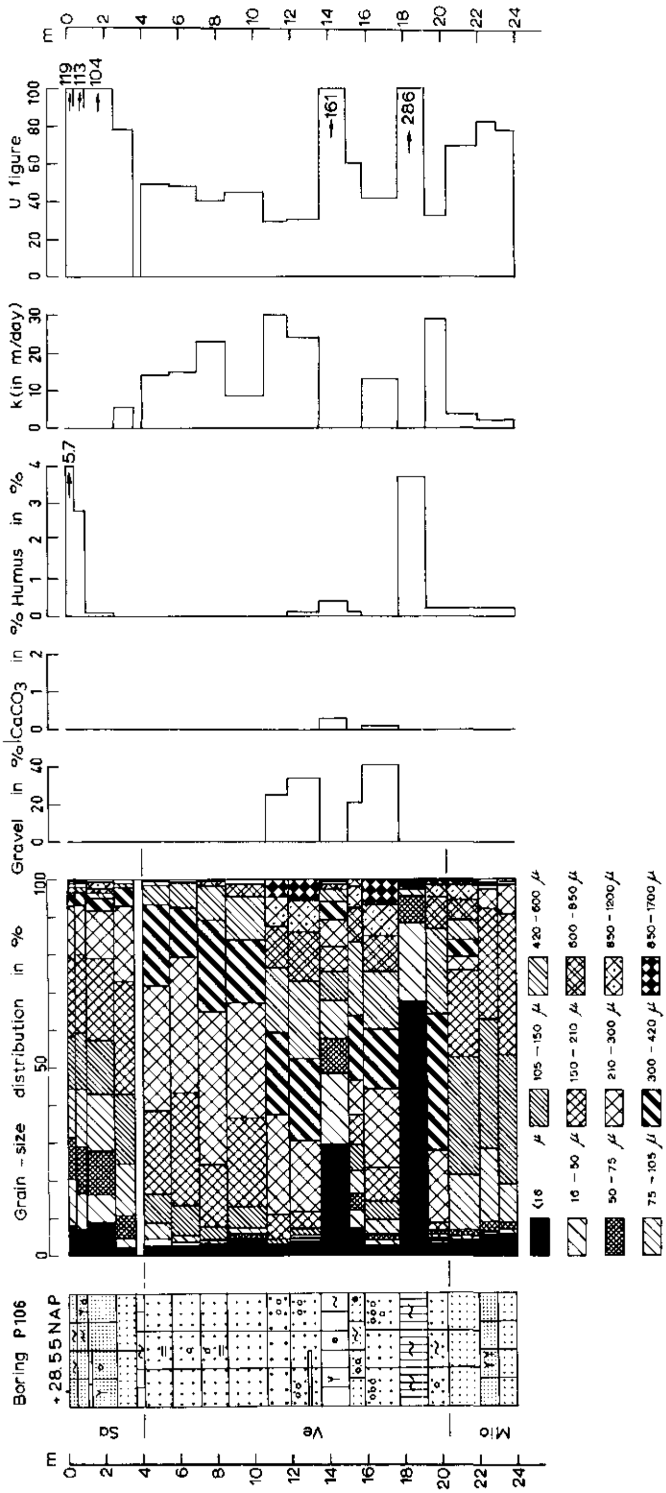

Boring P106
+ 28.55 NAP
Sa
Ve
Mio
Grain - size distribution in %
Gravel in %
% CaCO3 in
% Humus in %
k (in m/day)
U figure
m
<16 μ
16 - 50 μ
50 - 75 μ
75 - 105 μ
105 - 150 μ
150 - 210 μ
210 - 300 μ
300 - 420 μ
420 - 600 μ
600 - 850 μ
850 - 1200 μ
850 - 1700 μ

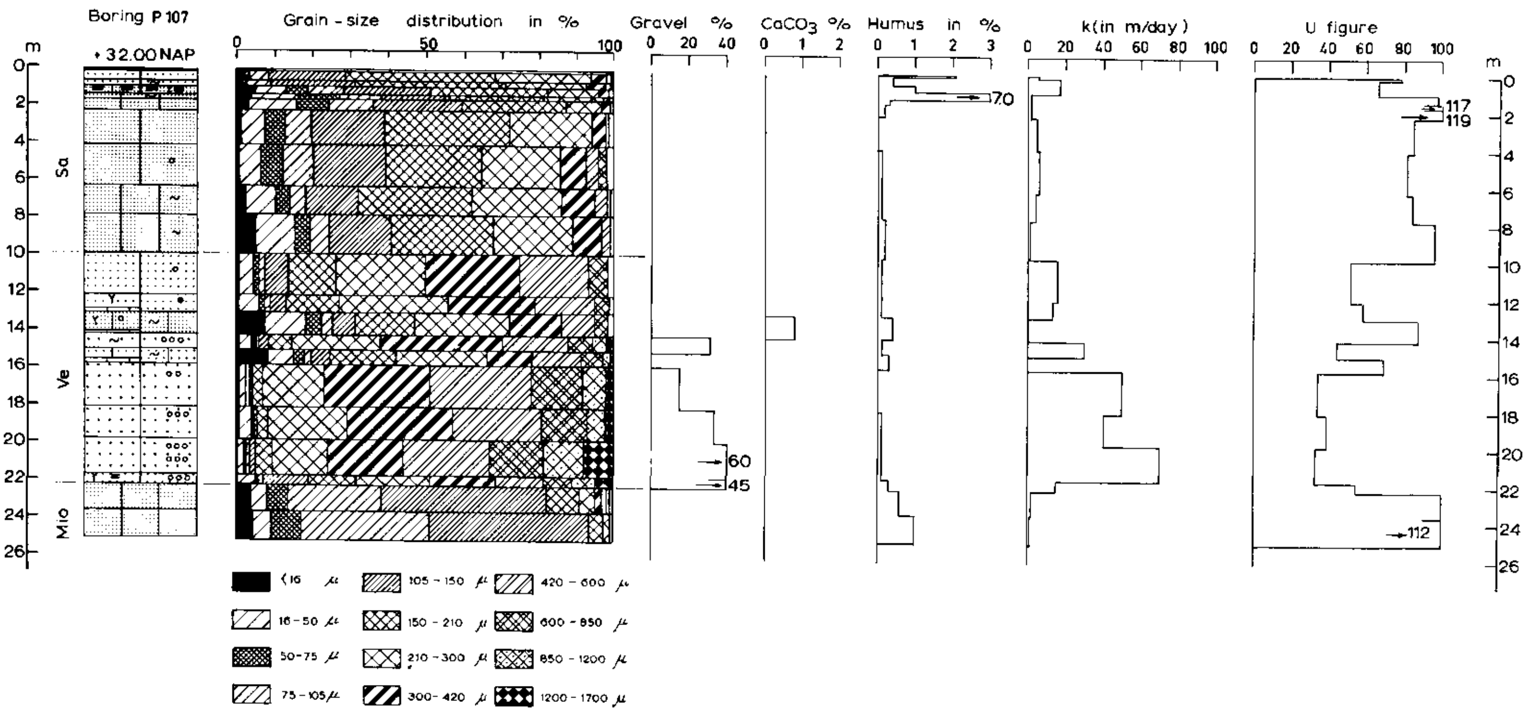
Boring P 107
+ 32.00 NAP
Grain - size distribution in %
Gravel %
CaCO3 %
Humus in %
k (in m/day)
U figure
Sa
Ve
Mio
<16 μ
16 - 50 μ
50 - 75 μ
75 - 105 μ
105 - 150 μ
150 - 210 μ
210 - 300 μ
300 - 420 μ
420 - 600 μ
600 - 850 μ
850 - 1200 μ
1200 - 1700 μ

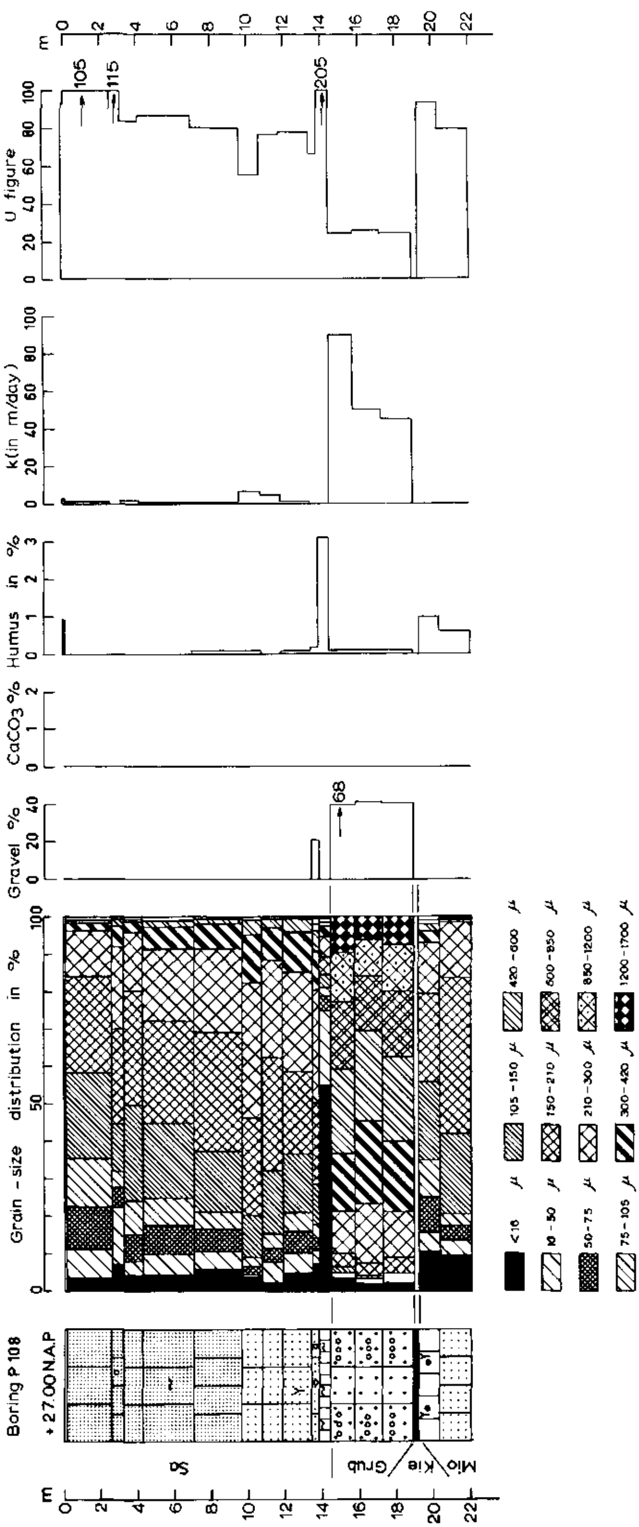
m
Boring P 108
+ 27.00 N.A.P
Sa
Grub
Kie
Mio
Grain - size distribution in %
Gravel %
68
CaCO3 %
Humus in %
k (in m/day)
U figure
105
115
205
< 16 μ
16 - 50 μ
50 - 75 μ
75 - 105 μ
105 - 150 μ
150 - 210 μ
210 - 300 μ
300 - 420 μ
420 - 600 μ
600 - 850 μ
850 - 1200 μ
1200 - 1700 μ

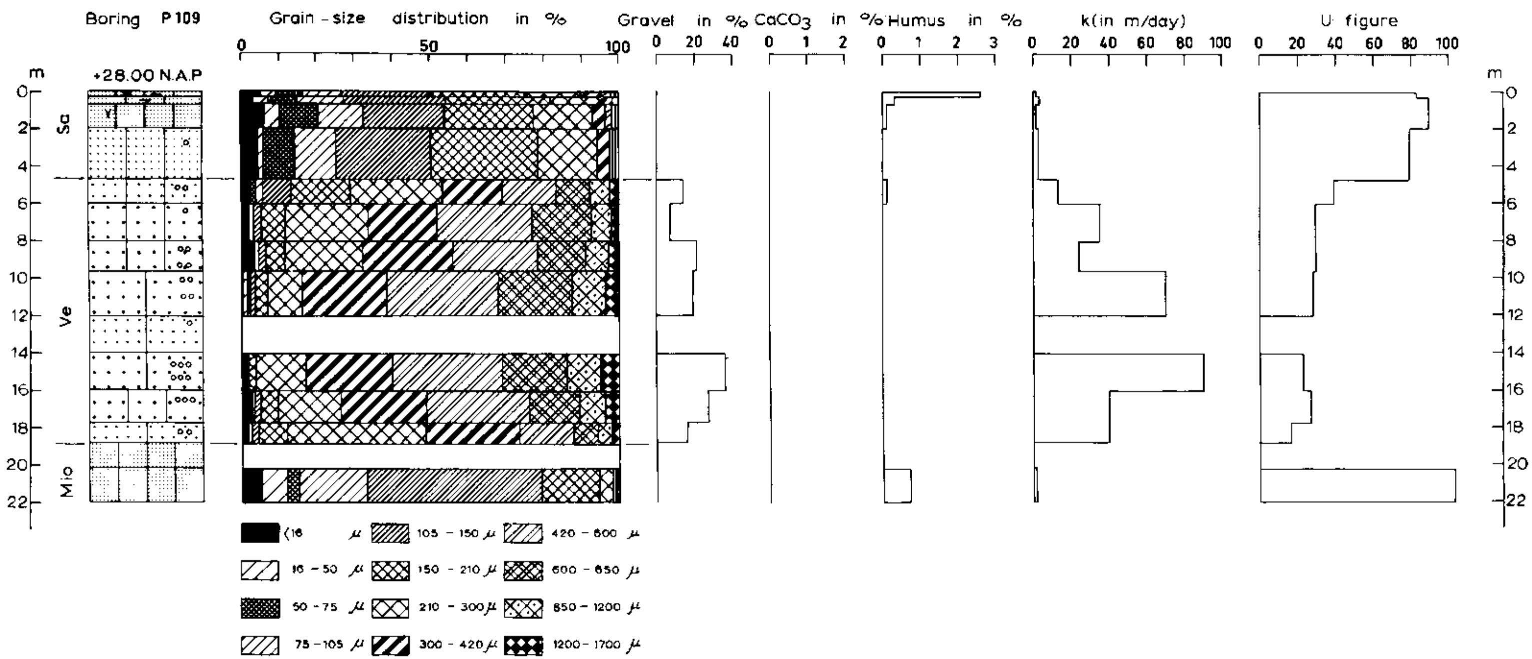

Boring P 109
+28.00 N.A.P
Grain - size distribution in %
Gravel in %
CaCO3 in %
Humus in %
k(in m/day)
U figure
m
Sa
Ve
Mio
<16 μ
16 - 50 μ
50 - 75 μ
75 - 105 μ
105 - 150 μ
150 - 210 μ
210 - 300 μ
300 - 420 μ
420 - 600 μ
600 - 850 μ
850 - 1200 μ
1200 - 1700 μ

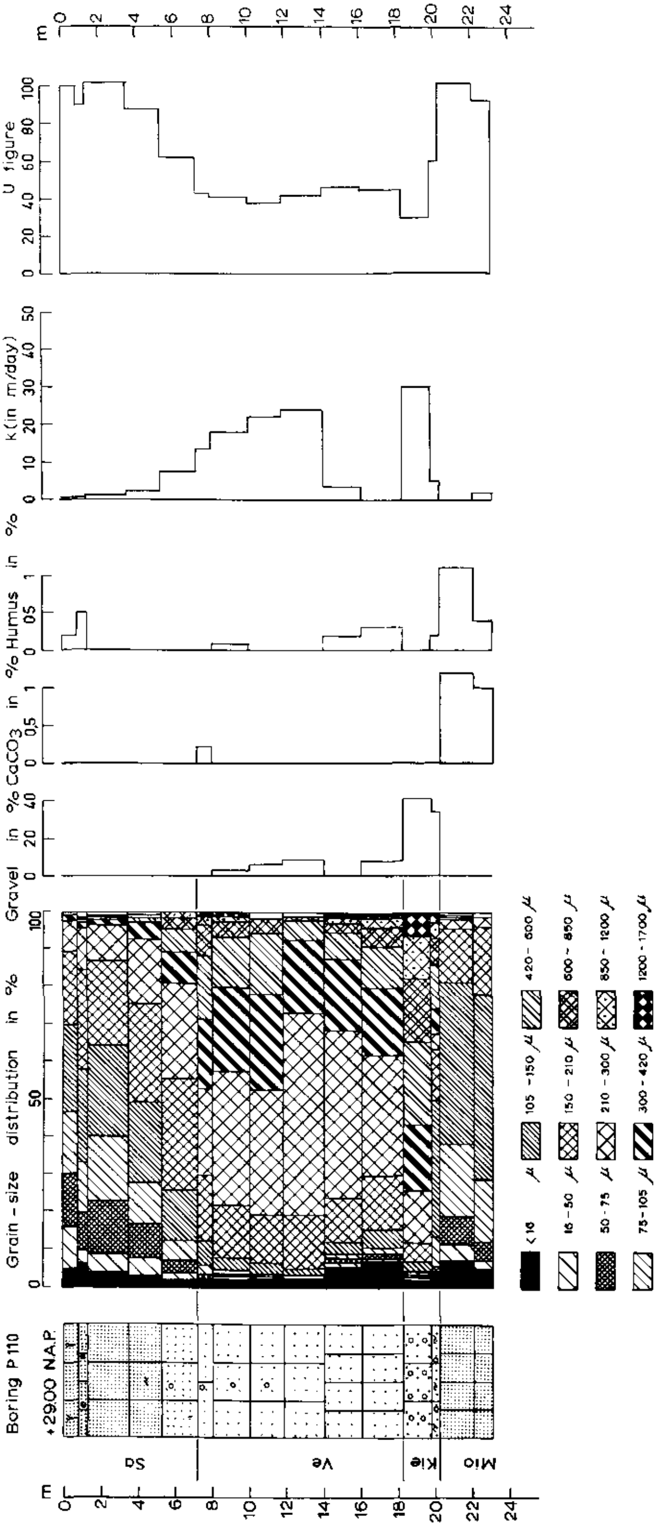

Boring P 110
+29.00 N.A.P.
Sa
Ve
Kie
Mio
Grain - size distribution in %
Gravel in %
CaCO3 in %
Humus in %
k (in m/day)
U figure
m
< 16 μ
16 - 50 μ
50 - 75 μ
75 - 105 μ
105 - 150 μ
150 - 210 μ
210 - 300 μ
300 - 420 μ
420 - 600 μ
600 - 850 μ
850 - 1200 μ
1200 - 1700 μ

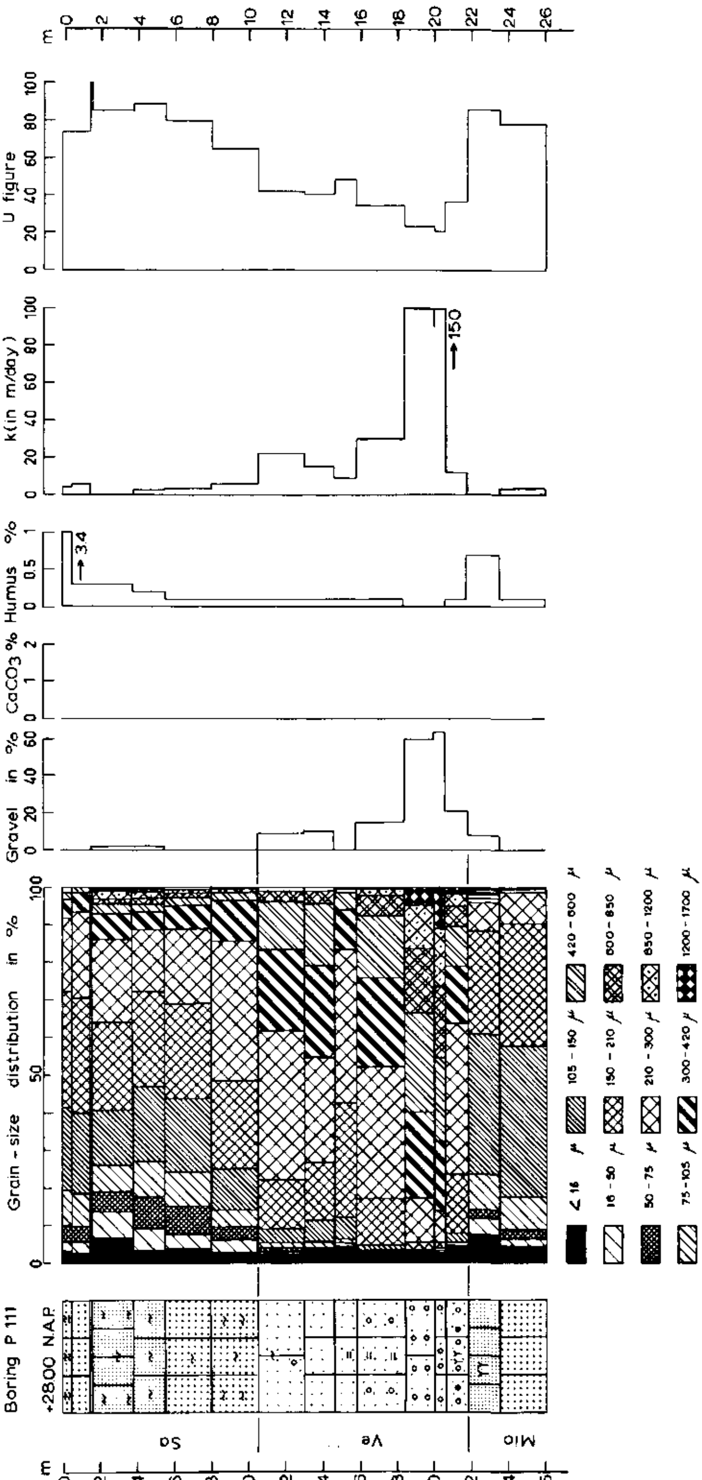
Boring P 111
+2800 NAP
So
Ve
Mio
Grain - size distribution in %
Gravel in %
CaCO3 %
Humus %
→3.4
k(in m/day)
→150
U figure
m
< 16 μ
16 - 50 μ
50 - 75 μ
75 - 105 μ
105 - 150 μ
150 - 210 μ
210 - 300 μ
300 - 420 μ
420 - 600 μ
600 - 850 μ
850 - 1200 μ
1200 - 1700 μ

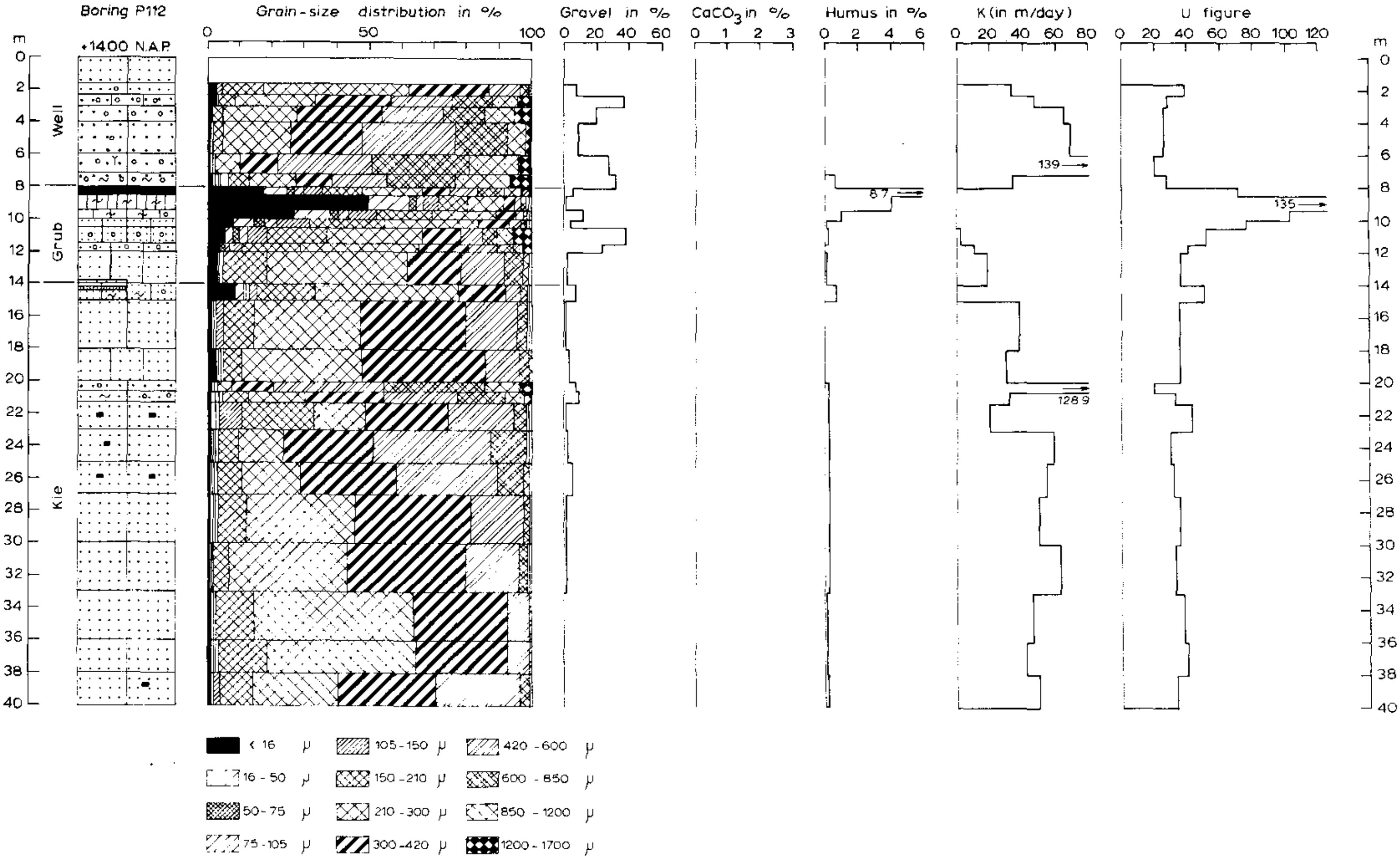
Boring P112
+1400 N.A.P.
Well
Grub
Kie
Grain-size distribution in %
Gravel in %
$CaCO_3$ in %
Humus in %
K (in m/day)
U figure
m
139
8.7
128.9
135
< 16 μ
16 - 50 μ
50 - 75 μ
75 - 105 μ
105 - 150 μ
150 - 210 μ
210 - 300 μ
300 - 420 μ
420 - 600 μ
600 - 850 μ
850 - 1200 μ
1200 - 1700 μ

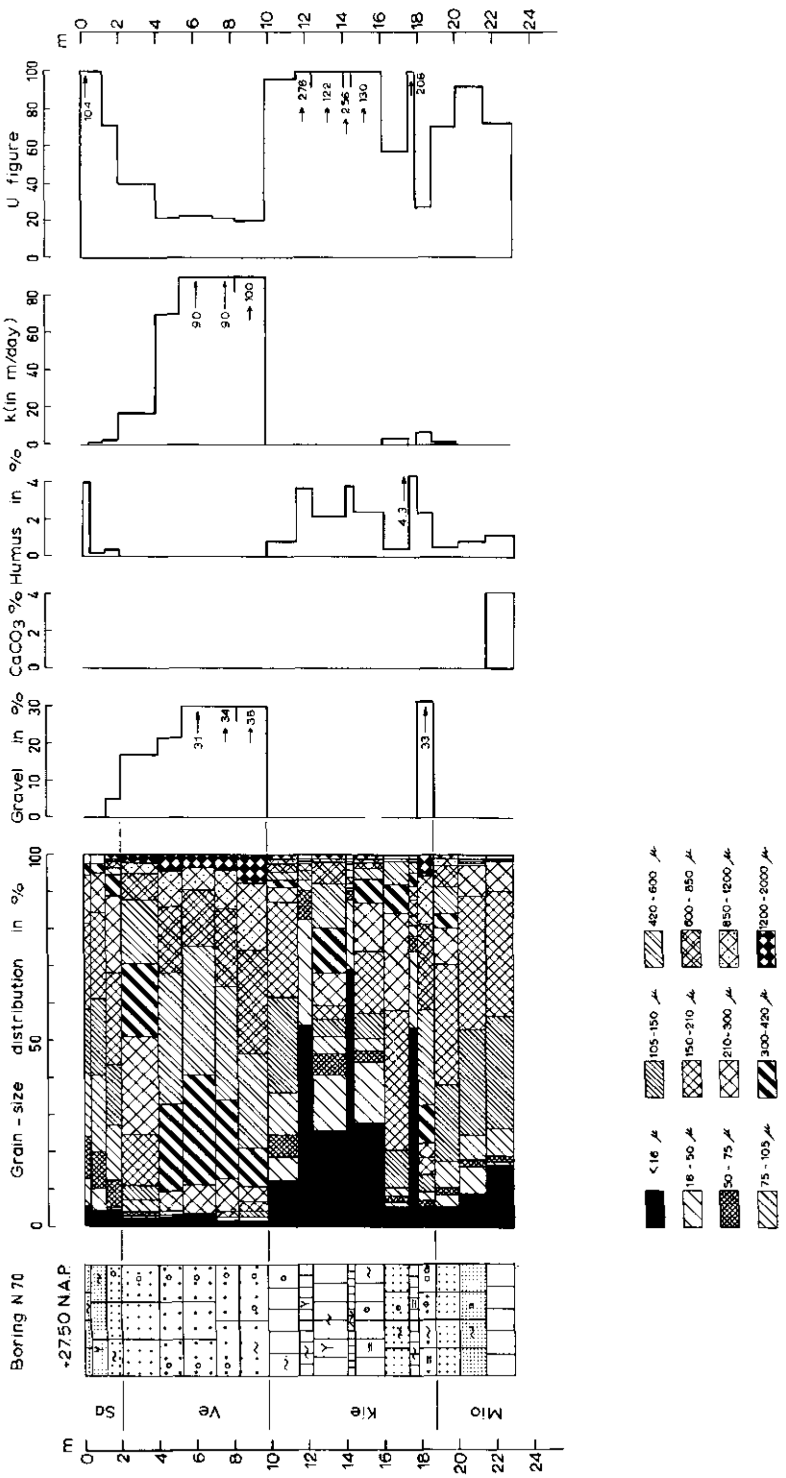
Boring N 70
+27.50 N.A.P.
Sa
Ve
Kie
Mio
m
Grain - size distribution in %
Gravel in %
CaCO3 %
Humus in %
k (in m/day)
U figure
< 16 μ
16 - 50 μ
50 - 75 μ
75 - 105 μ
105 - 150 μ
150 - 210 μ
210 - 300 μ
300 - 420 μ
420 - 600 μ
600 - 850 μ
850 - 1200 μ
1200 - 2000 μ

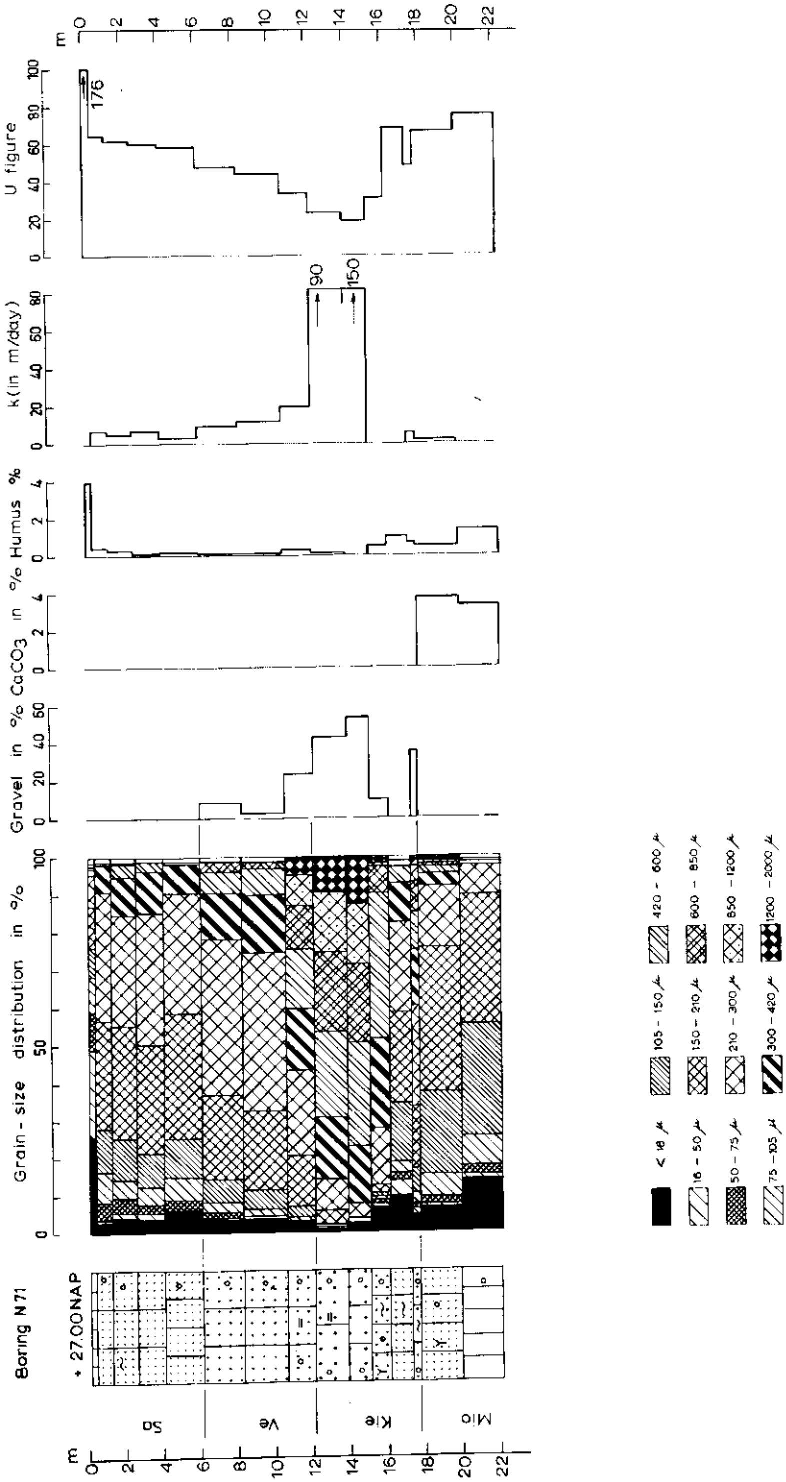

m
U figure
176
k(in m/day)
90
150
Humus %
CaCO3 in %
Gravel in %
Grain - size distribution in %
Boring N 71
+ 27.00 NAP
Sa
Ve
Kie
Mio
< 16 μ
16 - 50 μ
50 - 75 μ
75 - 105 μ
105 - 150 μ
150 - 210 μ
210 - 300 μ
300 - 420 μ
420 - 600 μ
600 - 850 μ
850 - 1200 μ
1200 - 2000 μ

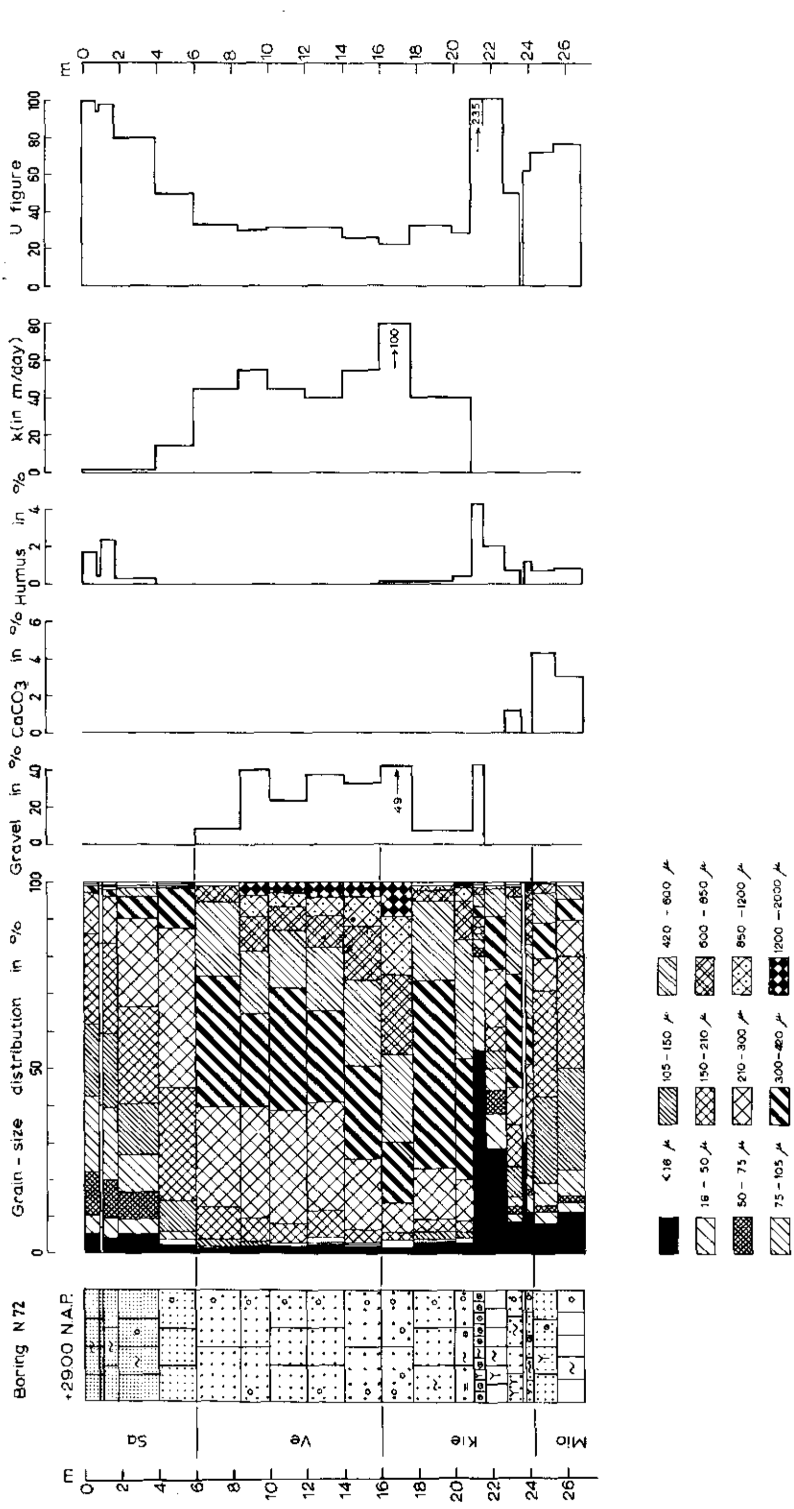
Boring N 72
+2900 N.A.P.
Grain - size distribution in %
Gravel in %
$CaCO_3$ in %
Humus in %
k(in m/day)
U figure
m
Sa
Ve
Kie
Mio
<16 μ
16 - 50 μ
50 - 75 μ
75 - 105 μ
105 - 150 μ
150 - 210 μ
210 - 300 μ
300 - 420 μ
420 - 600 μ
600 - 850 μ
850 - 1200 μ
1200 - 2000 μ
→100
49→
→235

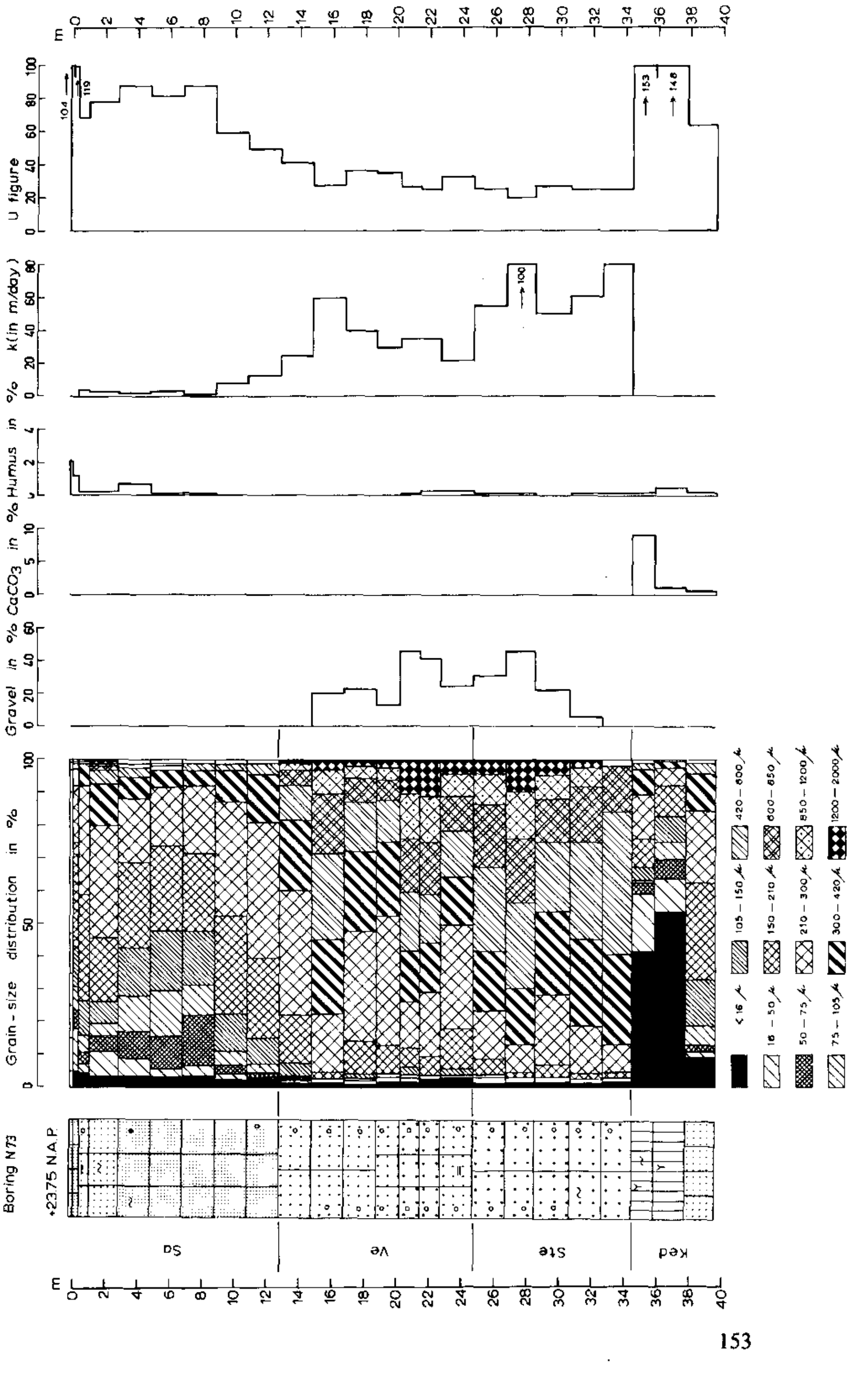

Boring N73
+2375 N.A.P
Sa
Ve
Ste
Ked
Grain - size distribution in %
Gravel in %
CaCO3 in %
Humus in %
% k (in m/day)
U figure
m
< 16 µ
16 – 50 µ
50 – 75 µ
75 – 105 µ
105 – 150 µ
150 – 210 µ
210 – 300 µ
300 – 420 µ
420 – 600 µ
600 – 850 µ
850 – 1200 µ
1200 – 2000 µ

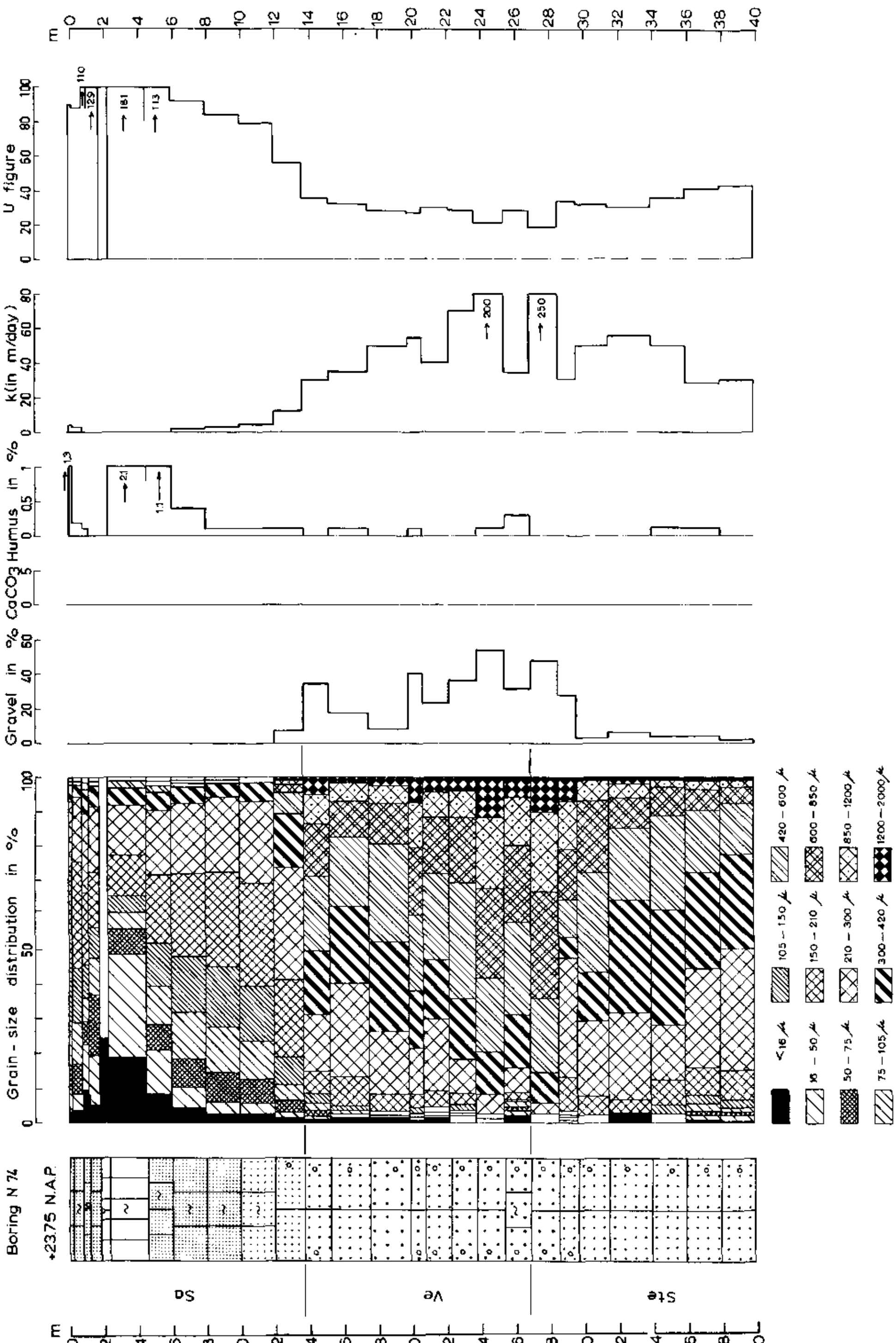

Boring N 74
+23.75 N.A.P.
Grain - size distribution in %
Gravel in %
CaCO3
Humus in %
k(in m/day)
U figure
m
Sa
Ve
Ste
<16 µ
16 - 50 µ
50 - 75 µ
75 - 105 µ
105 - 150 µ
150 - 210 µ
210 - 300 µ
300 - 420 µ
420 - 600 µ
600 - 850 µ
850 - 1200 µ
1200 - 2000 µ

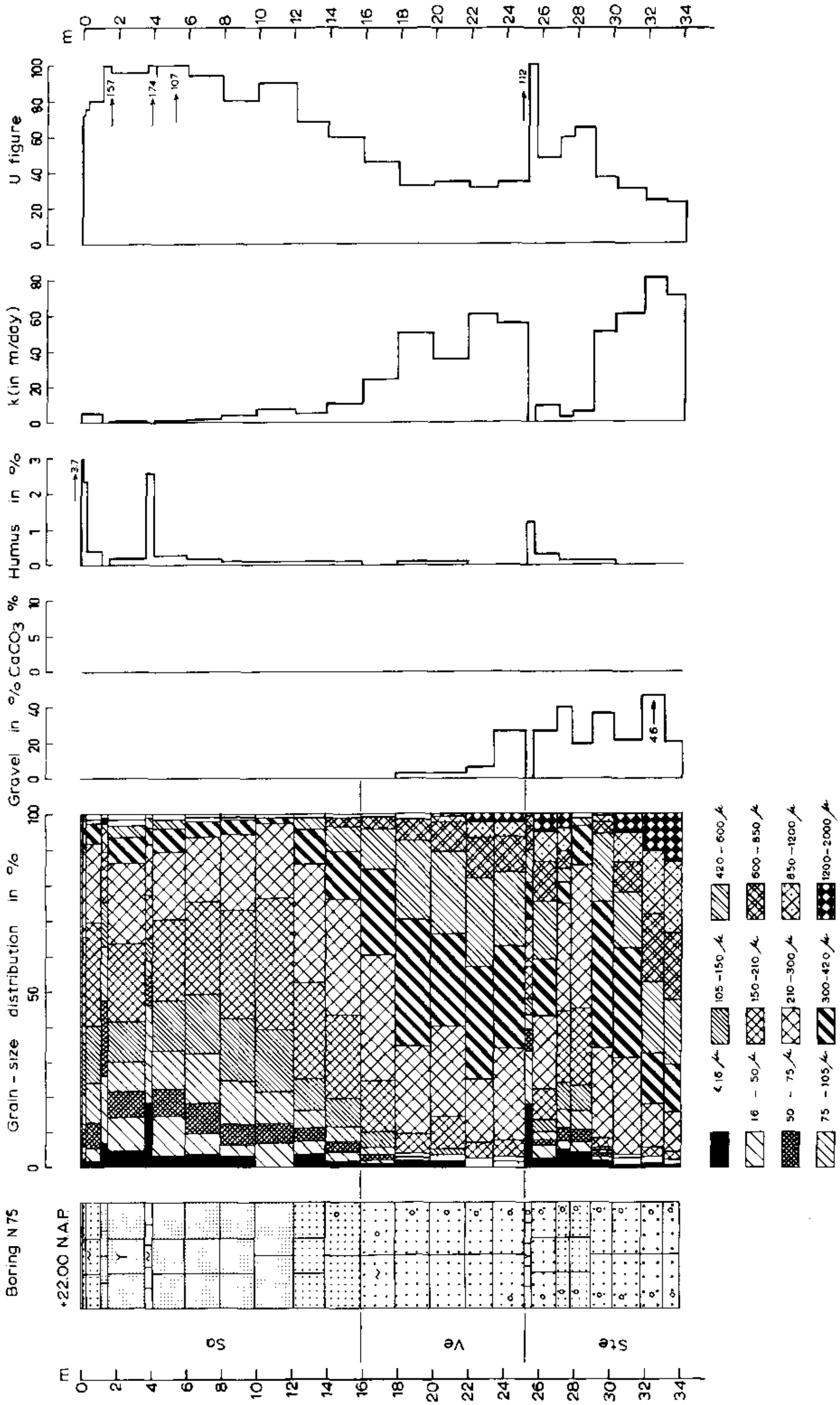

Boring N 75
+22.00 N.A.P.
Grain - size distribution in %
Gravel in %
CaCO3 %
Humus in %
k (in m/day)
U figure
So
Ve
Ste
< 16 μ
16 - 50 μ
50 - 75 μ
75 - 105 μ
105 - 150 μ
150 - 210 μ
210 - 300 μ
300 - 420 μ
420 - 600 μ
600 - 850 μ
850 - 1200 μ
1200 - 2000 μ

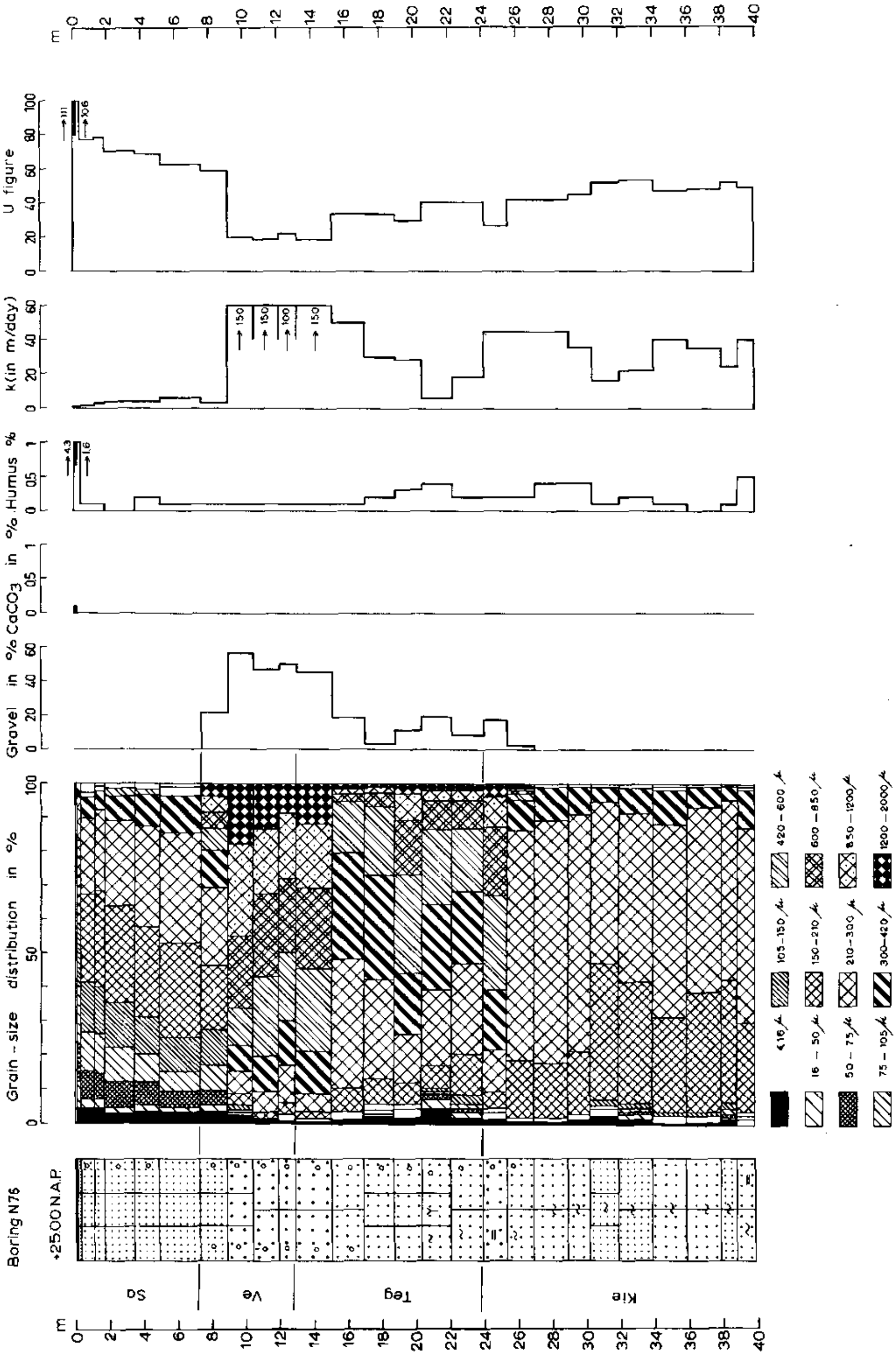
Boring N76
+25.00 N.A.P.
Sa
Ve
Teg
Kie
Grain - size distribution in %
Gravel in %
CaCO3 in %
Humus %
k (in m/day)
U figure
m
<16 μ
16 - 50 μ
50 - 75 μ
75 - 105 μ
105 - 150 μ
150 - 210 μ
210 - 300 μ
300 - 420 μ
420 - 600 μ
600 - 850 μ
850 - 1200 μ
1200 - 2000 μ

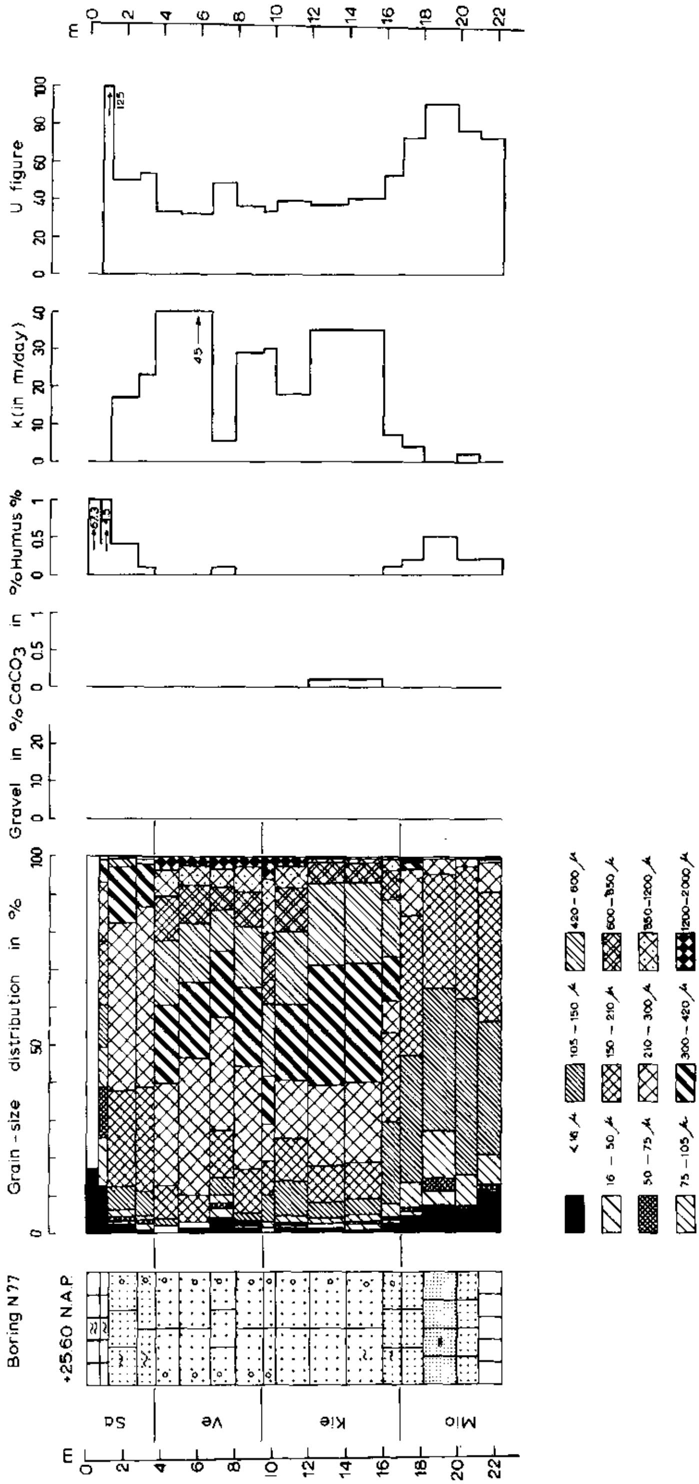
Boring N77
+25.60 N.A.P.
Grain - size distribution in %
Gravel in %
% CaCO3 in
% Humus %
k (in m/day)
U figure
m
Sa
Ve
Kie
Mio
< 16 μ
16 – 50 μ
50 – 75 μ
75 – 105 μ
105 – 150 μ
150 – 210 μ
210 – 300 μ
300 – 420 μ
420 – 600 μ
600 – 850 μ
850 – 1200 μ
1200 – 2000 μ

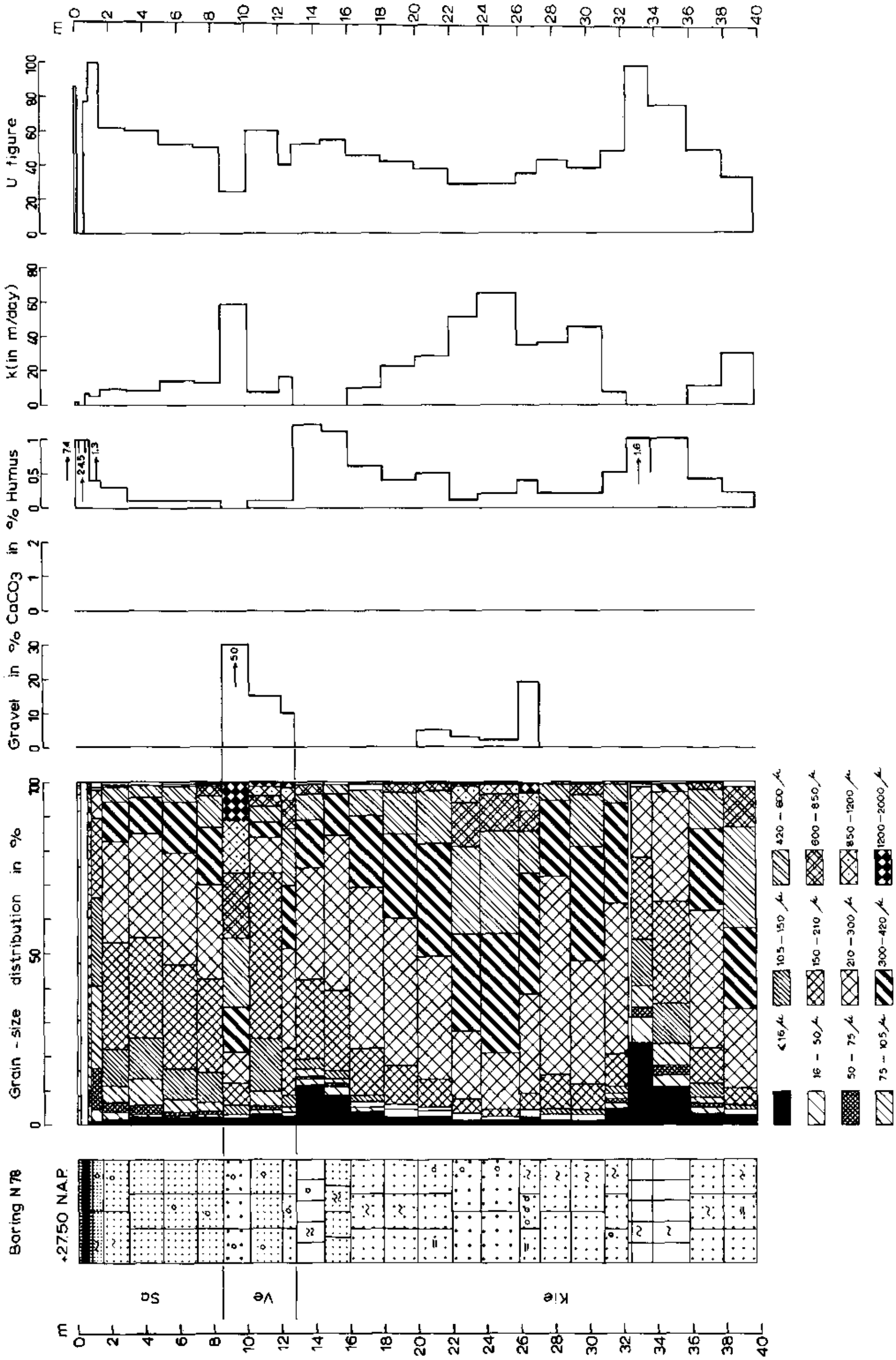
Boring N 78
+27.50 N.A.P.
Sa
Ve
Kie
Grain - size distribution in %
Gravel in %
CaCO3 in %
Humus
k (in m/day)
U figure
m
<16 μ
16 - 50 μ
50 - 75 μ
75 - 105 μ
105 - 150 μ
150 - 210 μ
210 - 300 μ
300 - 420 μ
420 - 600 μ
600 - 850 μ
850 - 1200 μ
1200 - 2000 μ

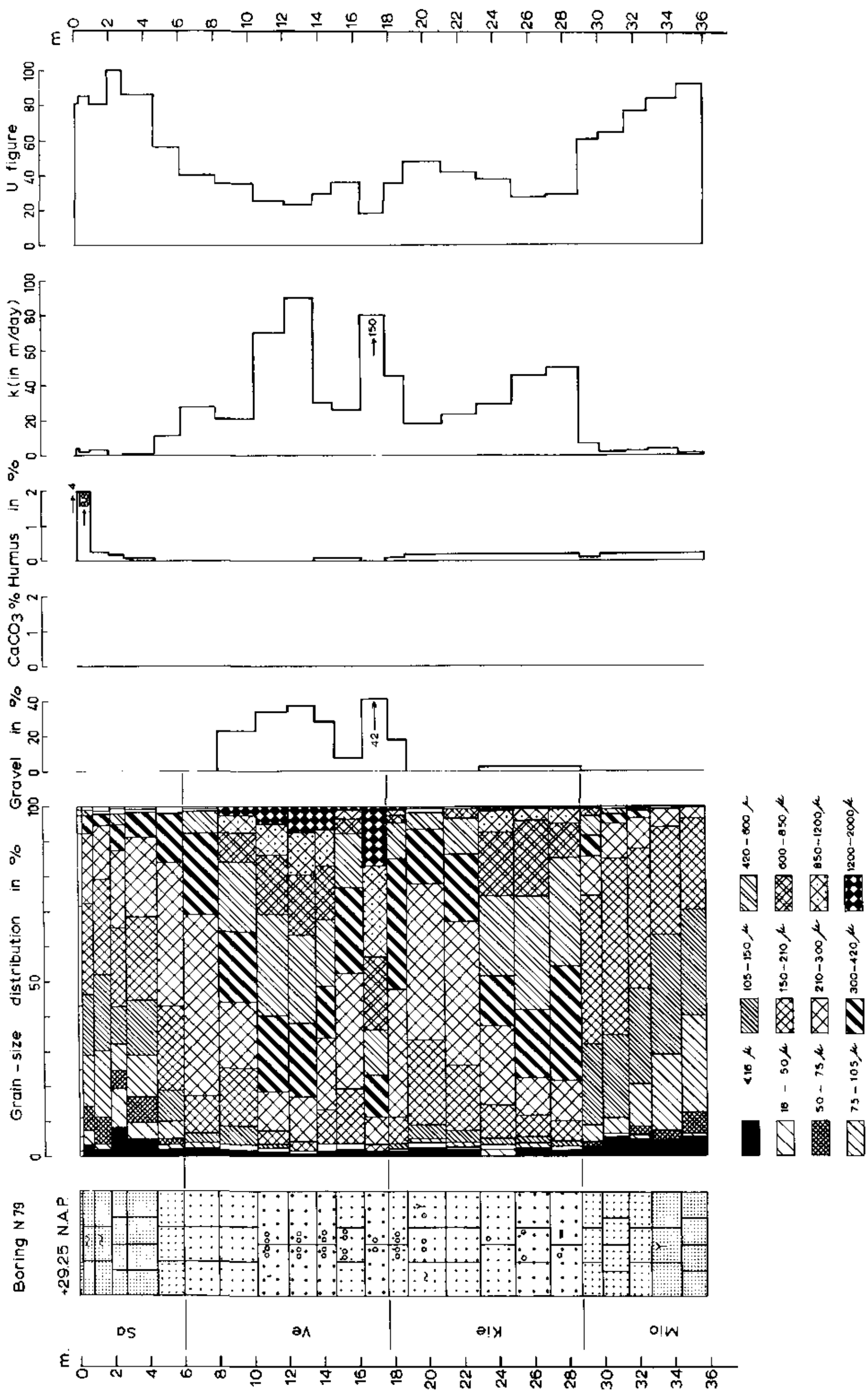
m
U figure
k (in m/day)
→150
Humus in %
4
CaCO3 %
Gravel in %
42
Grain - size distribution in %
Boring N 79
+29.25 N.A.P.
Sa
Ve
Kie
Mio
m.
<16 µ
16 - 50 µ
50 - 75 µ
75 - 105 µ
105 - 150 µ
150 - 210 µ
210 - 300 µ
300 - 420 µ
420 - 600 µ
600 - 850 µ
850 - 1200 µ
1200 - 2000 µ

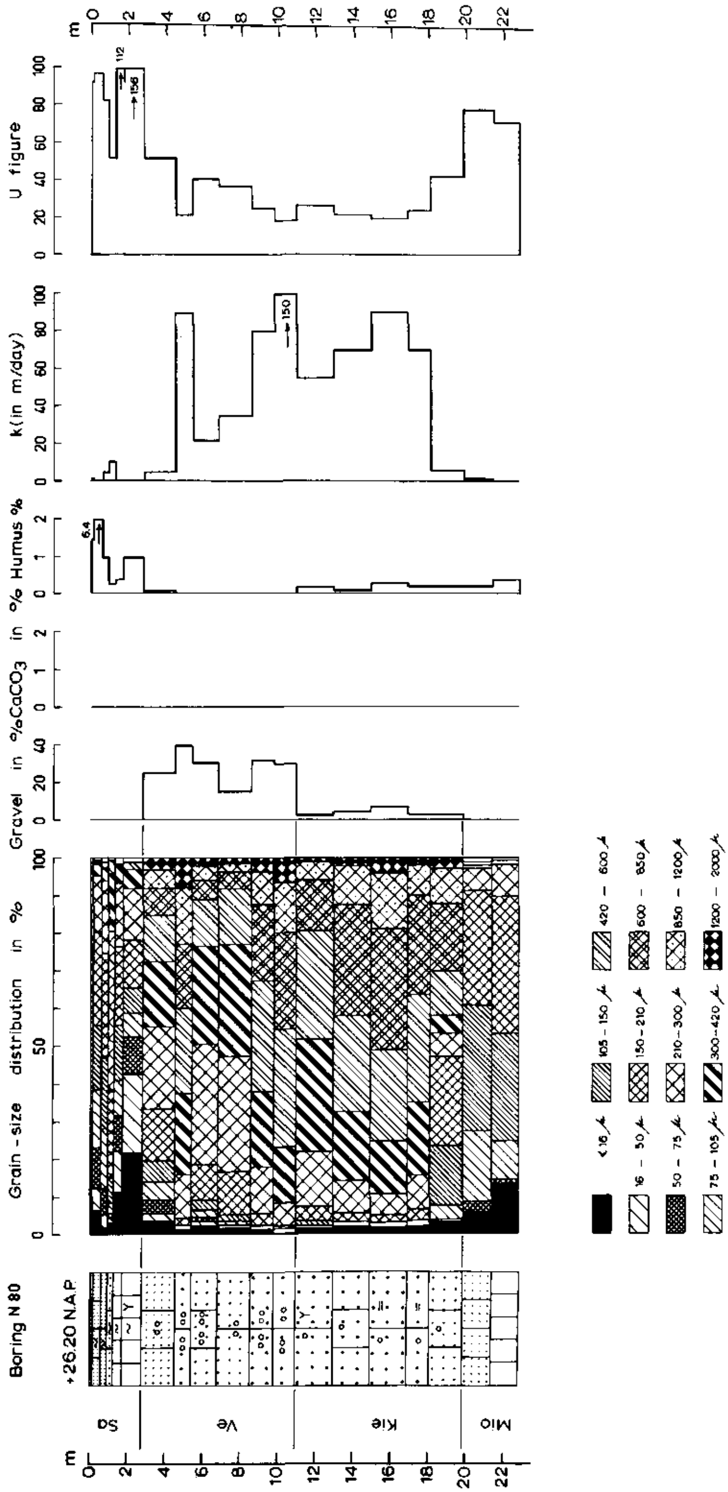
Boring N 80
+26.20 N.A.P.
Sa
Ve
Kie
Mio
m
Grain - size distribution in %
Gravel in %
%CaCO3 in %
Humus %
k (in m/day)
U figure
6.4
150
112
156
<16 μ
16 - 50 μ
50 - 75 μ
75 - 105 μ
105 - 150 μ
150 - 210 μ
210 - 300 μ
300 - 420 μ
420 - 600 μ
600 - 850 μ
850 - 1200 μ
1200 - 2000 μ

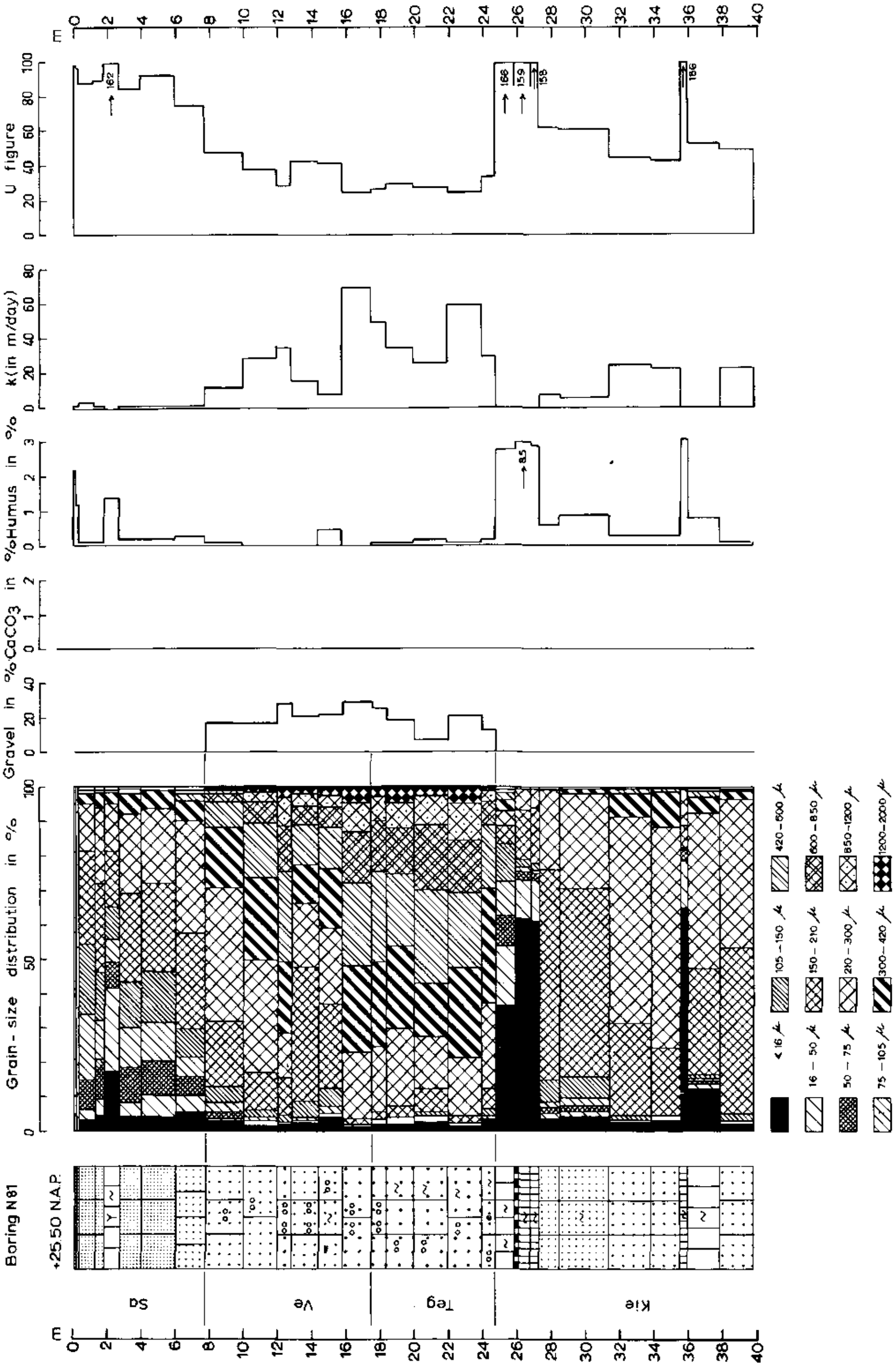
Boring N81
+25.50 N.A.P.
Grain - size distribution in %
Gravel in %
% CaCO3 in %
% Humus in %
k (in m/day)
U figure
m
Sa
Ve
Teg
Kie
< 16 µ
16 – 50 µ
50 – 75 µ
75 – 105 µ
105 – 150 µ
150 – 210 µ
210 – 300 µ
300 – 420 µ
420 – 600 µ
600 – 850 µ
850 – 1200 µ
1200 – 2000 µ

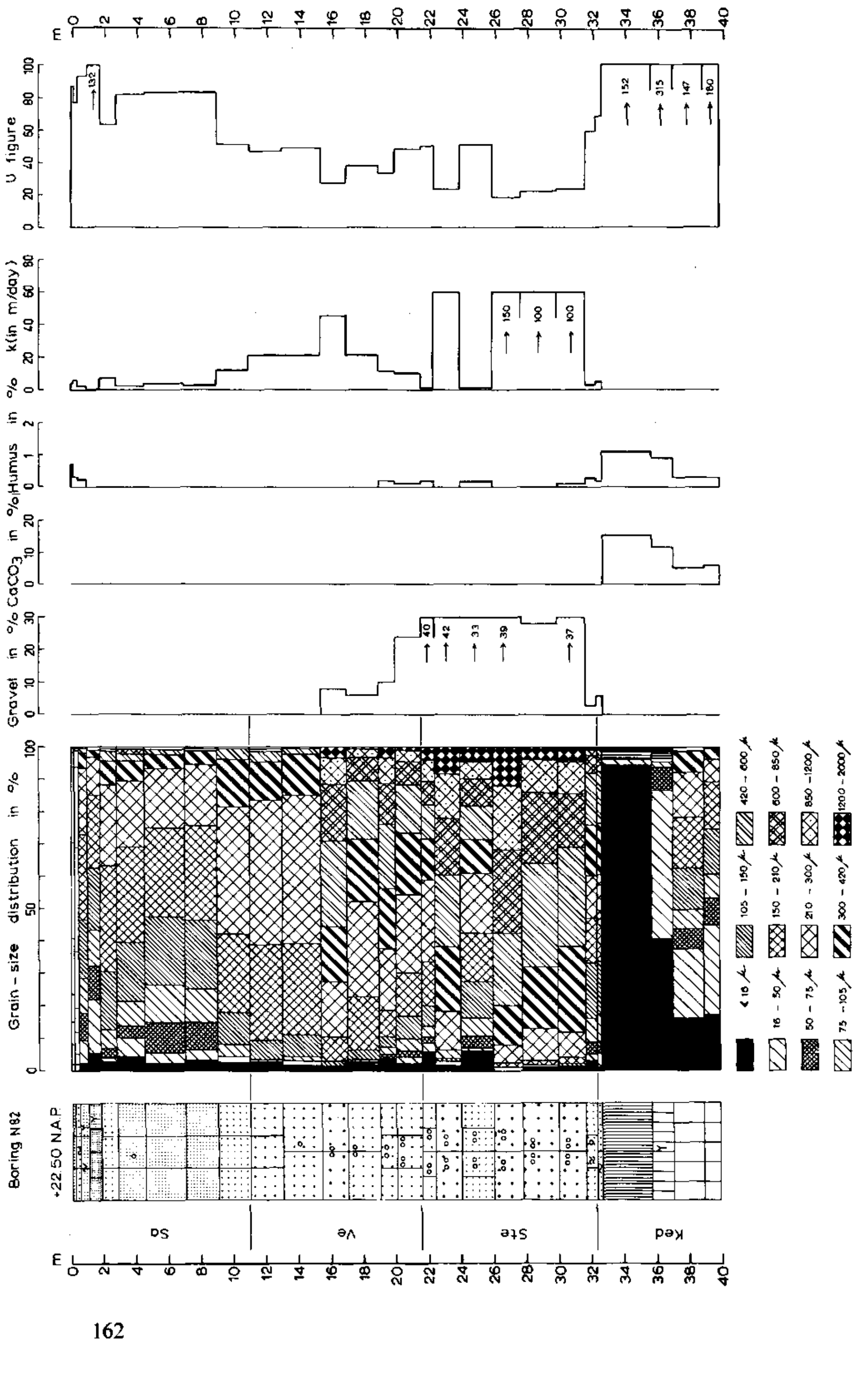
Boring N82
+22.50 N.A.P.
Grain - size distribution in %
Gravel in %
CaCO3 in %
Humus in %
k(in m/day)
U figure
m
Sa
Ve
Ste
Ked
< 16 µ
16 - 50 µ
50 - 75 µ
75 - 105 µ
105 - 150 µ
150 - 210 µ
210 - 300 µ
300 - 420 µ
420 - 600 µ
600 - 850 µ
850 - 1200 µ
1200 - 2000 µ

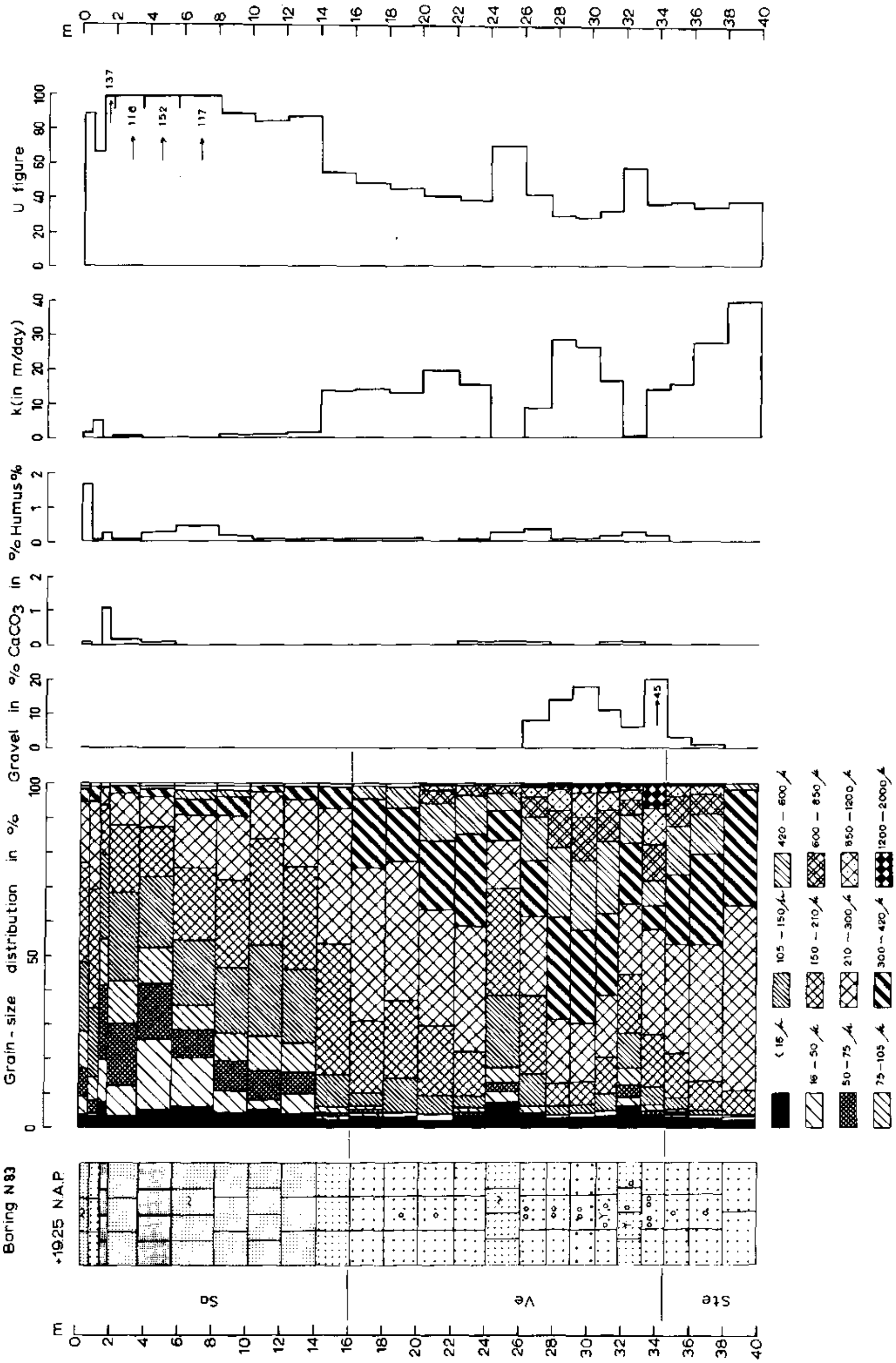
Boring N 83
+1925 N.A.P.
Sa
Ve
Ste
Grain - size distribution in %
Gravel in %
% CaCO3 in %
% Humus %
k (in m/day)
U figure
137
116
152
117
45
m
< 16 μ
16 – 50 μ
50 – 75 μ
75 – 105 μ
105 – 150 μ
150 – 210 μ
210 – 300 μ
300 – 420 μ
420 – 600 μ
600 – 850 μ
850 – 1200 μ
1200 – 2000 μ

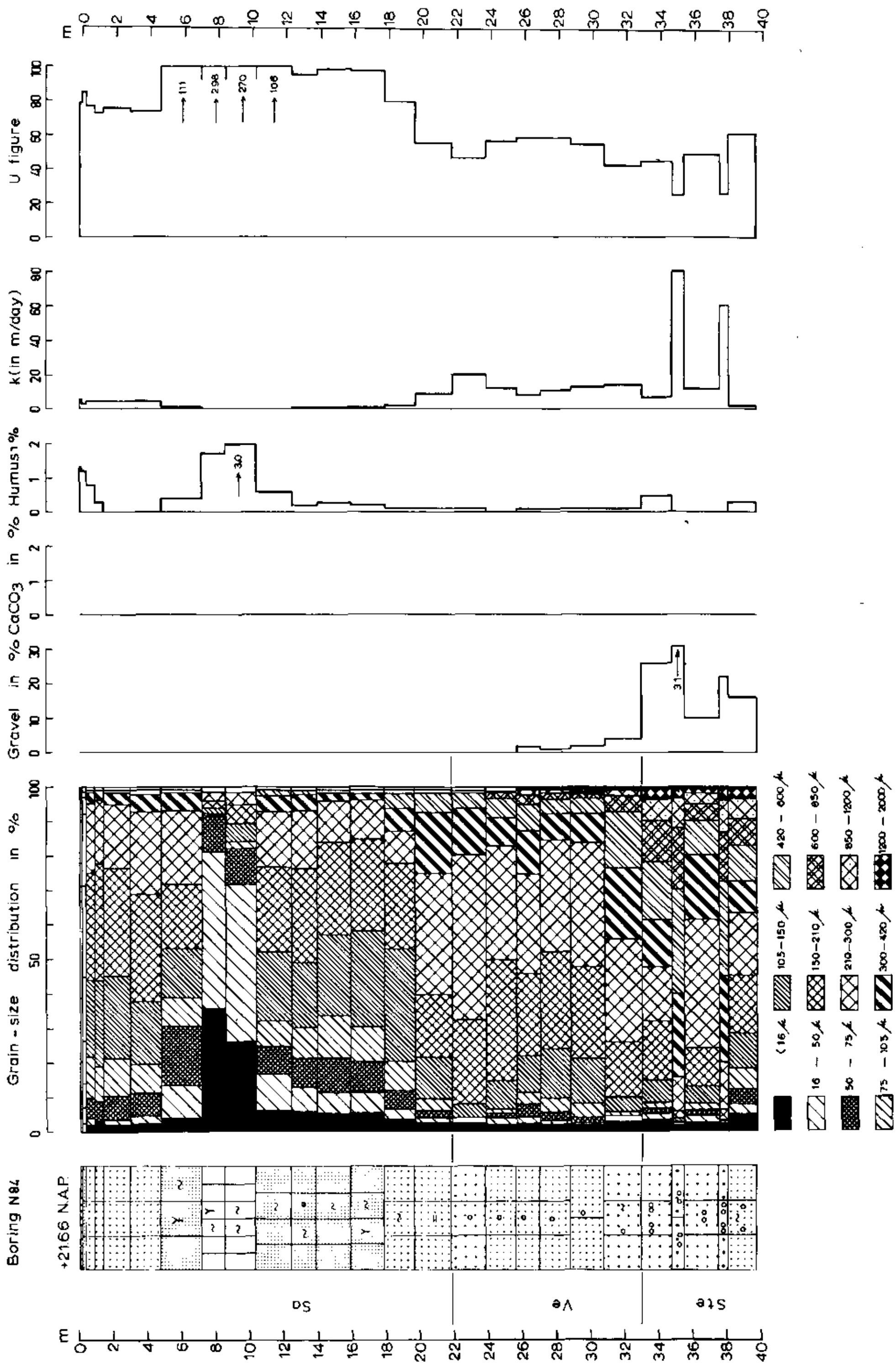
Boring N84
+2166 N.A.P.
Grain - size distribution in %
Gravel in %
CaCO3 in %
Humus in %
k (in m/day)
U figure
m
Sa
Ve
Ste
<16 µ
16 - 50 µ
50 - 75 µ
75 - 105 µ
105-150 µ
150-210 µ
210-300 µ
300-420 µ
420 - 600 µ
600 - 850 µ
850 - 1200 µ
1200 - 2000 µ
111
298
270
106
3.0
31

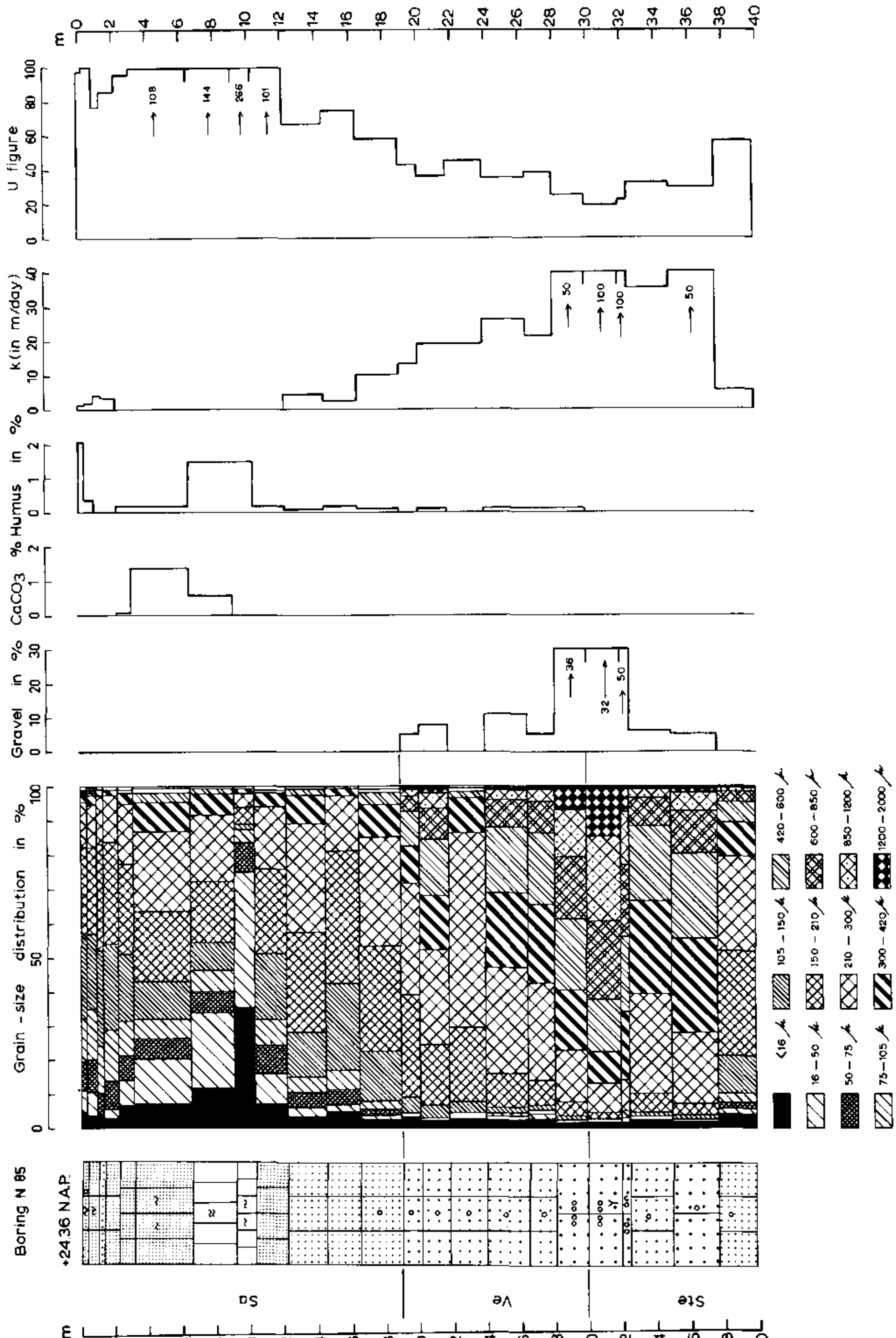

Boring N 85
+24.36 N.A.P.
Grain - size distribution in %
Gravel in %
CaCO3 %
Humus in %
k (in m/day)
U figure
m
Sa
Ve
Ste
<16 μ
16 – 50 μ
50 – 75 μ
75 – 105 μ
105 – 150 μ
150 – 210 μ
210 – 300 μ
300 – 420 μ
420 – 600 μ
600 – 850 μ
850 – 1200 μ
1200 – 2000 μ

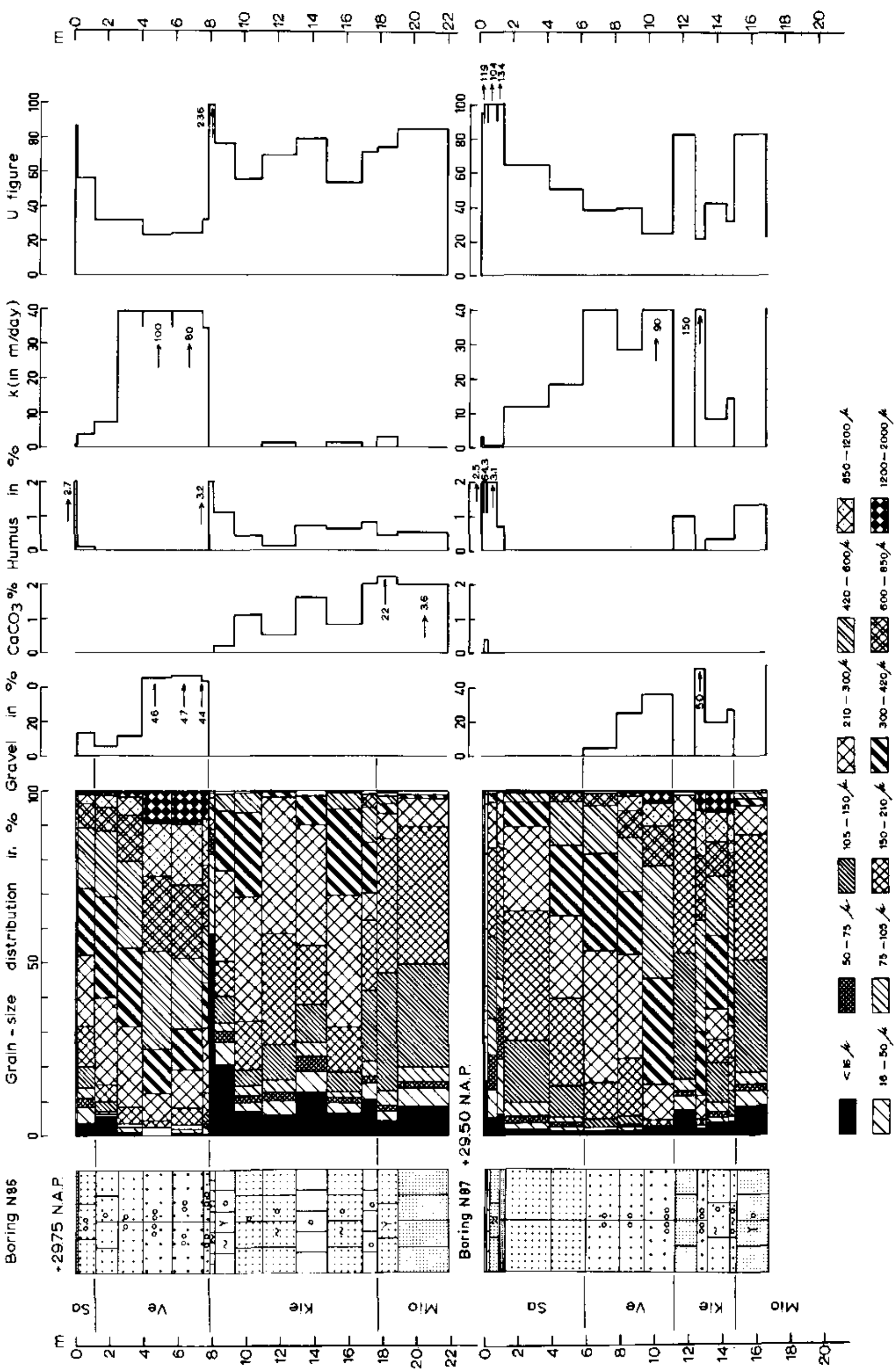
Boring N86
+29.75 N.A.P.
Boring N87
+29.50 N.A.P.
Grain - size distribution in %
Gravel in %
CaCO3 %
Humus in %
k (in m/day)
U figure
Sa
Ve
Kie
Mio
< 16 µ
16 - 50 µ
50 - 75 µ
75 - 105 µ
105 - 150 µ
150 - 210 µ
210 - 300 µ
300 - 420 µ
420 - 600 µ
600 - 850 µ
850 - 1200 µ
1200 - 2000 µ

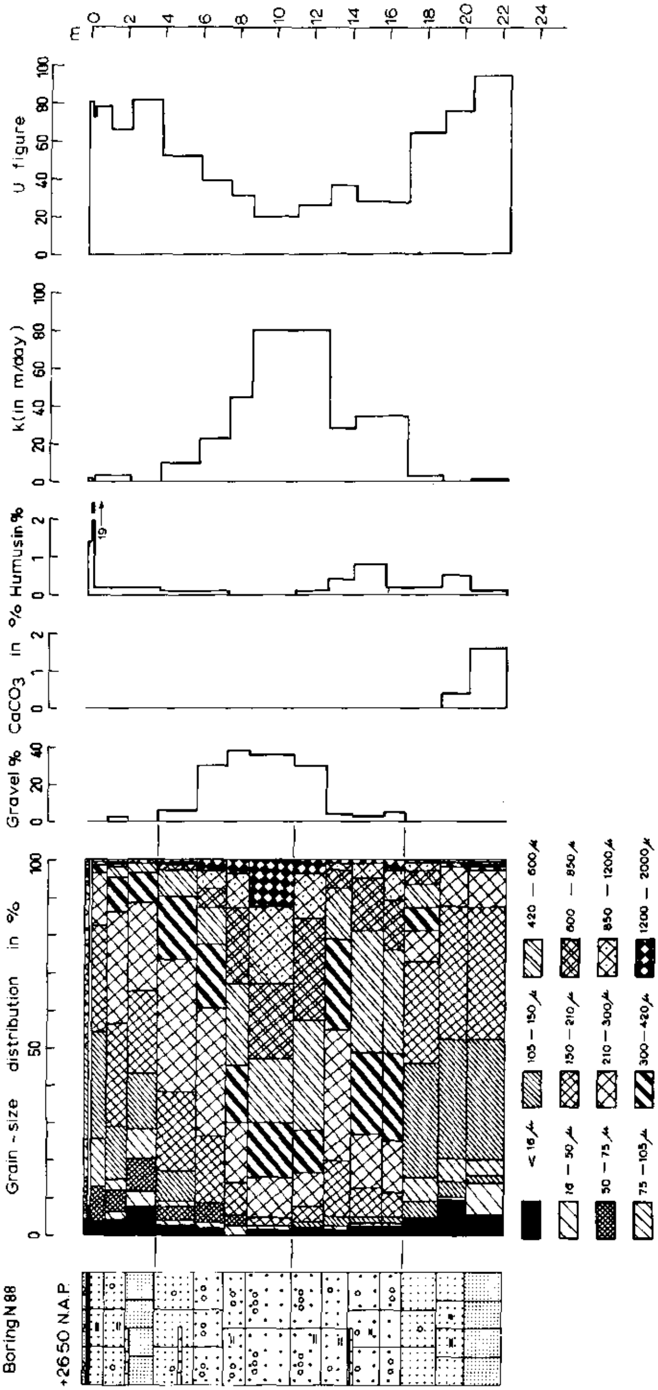
Boring N 88
+26.50 N.A.P.
Sa
Ve
Kie
Mio
m
Grain - size distribution in %
Gravel %
CaCO3 in %
Humus in %
k (in m/day)
U figure
< 16 µ
16 — 50 µ
50 — 75 µ
75 — 105 µ
105 — 150 µ
150 — 210 µ
210 — 300 µ
300 — 420 µ
420 — 600 µ
600 — 850 µ
850 — 1200 µ
1200 — 2000 µ

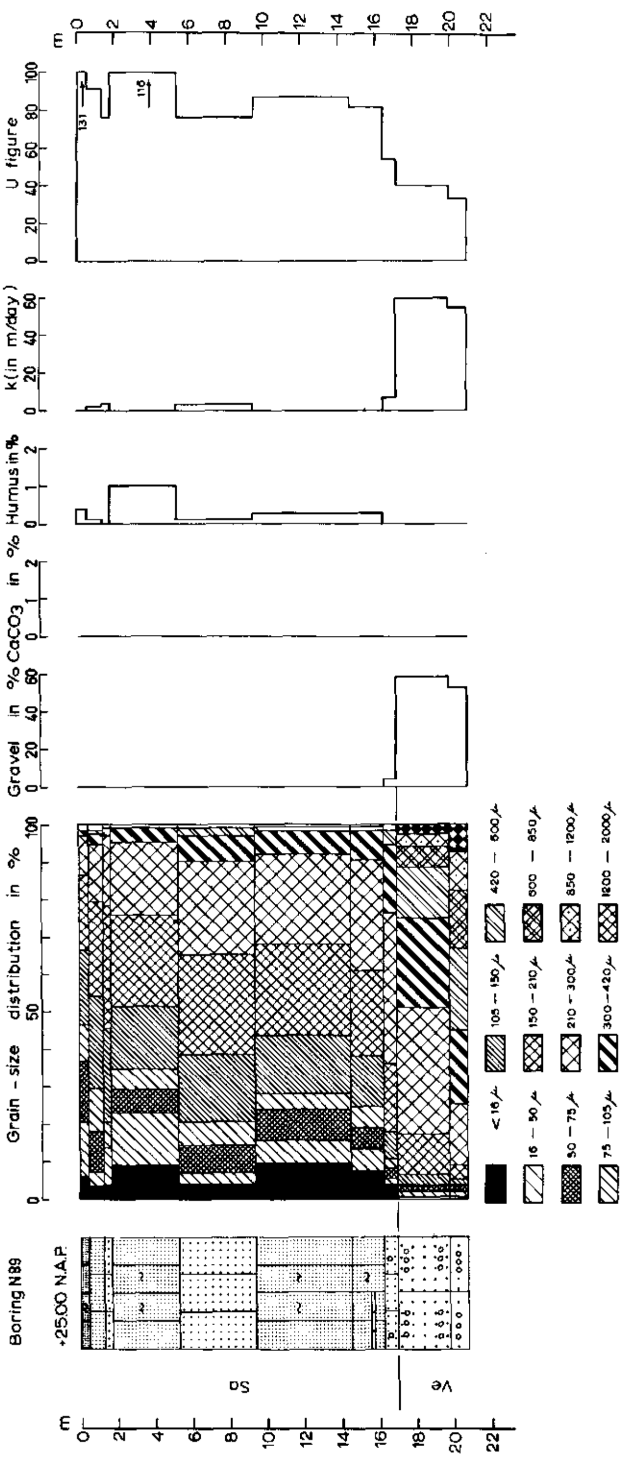
Boring N89
+25.00 N.A.P.
Grain - size distribution in %
Gravel in %
CaCO3 in %
Humus in %
k (in m/day)
U figure
m
Sa
Ve
< 16 µ
16 — 50 µ
50 — 75 µ
75 — 105 µ
105 — 150 µ
150 — 210 µ
210 — 300 µ
300 — 420 µ
420 — 600 µ
600 — 850 µ
850 — 1200 µ
1200 — 2000 µ
131
118

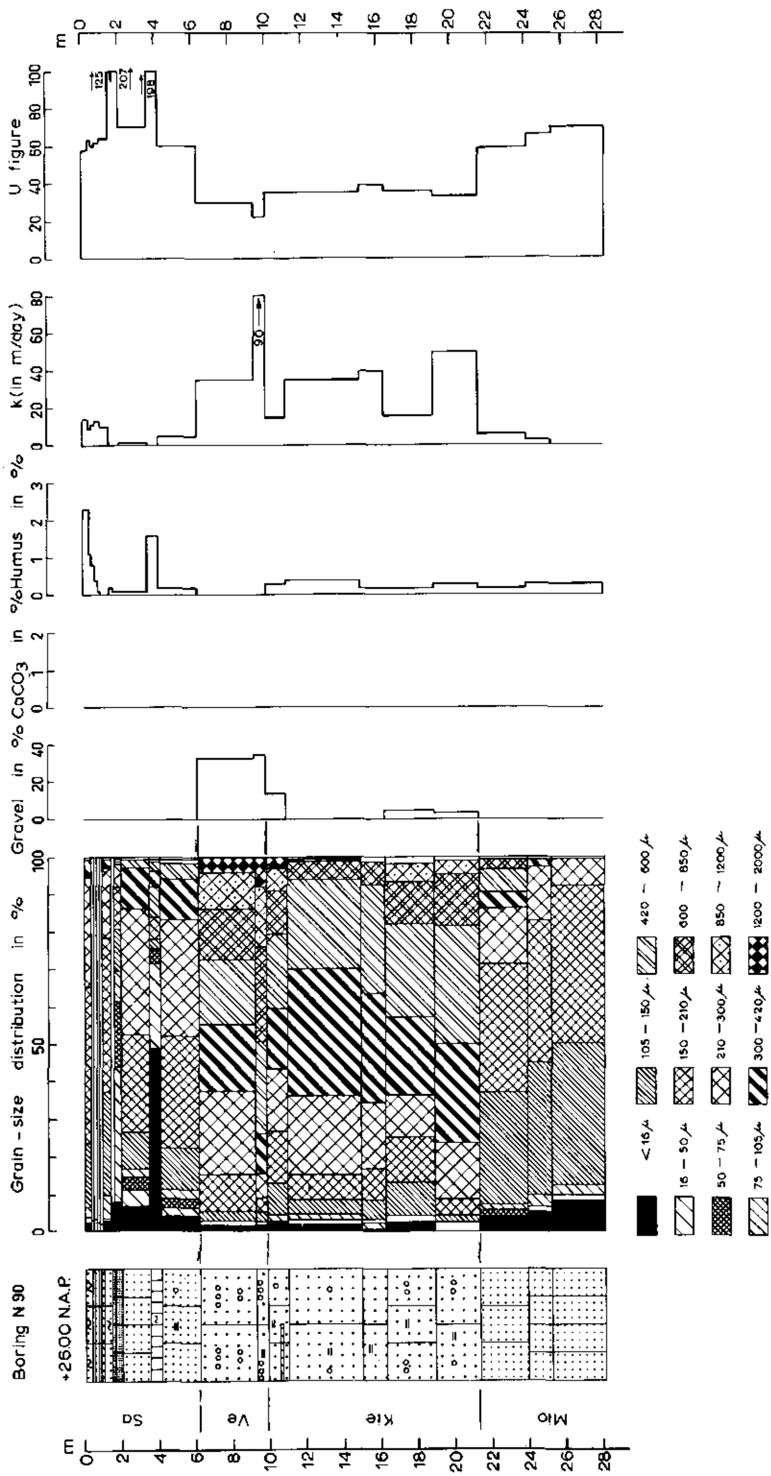

Boring N 90
+26.00 N.A.P.
Sa
Ve
Kie
Mio
m
Grain - size distribution in %
Gravel in %
% CaCO3 in %
% Humus in %
k (in m/day)
U figure
125
207
198
90
< 16 µ
16 – 50 µ
50 – 75 µ
75 – 105 µ
105 – 150 µ
150 – 210 µ
210 – 300 µ
300 – 420 µ
420 – 600 µ
600 – 850 µ
850 – 1200 µ
1200 – 2000 µ

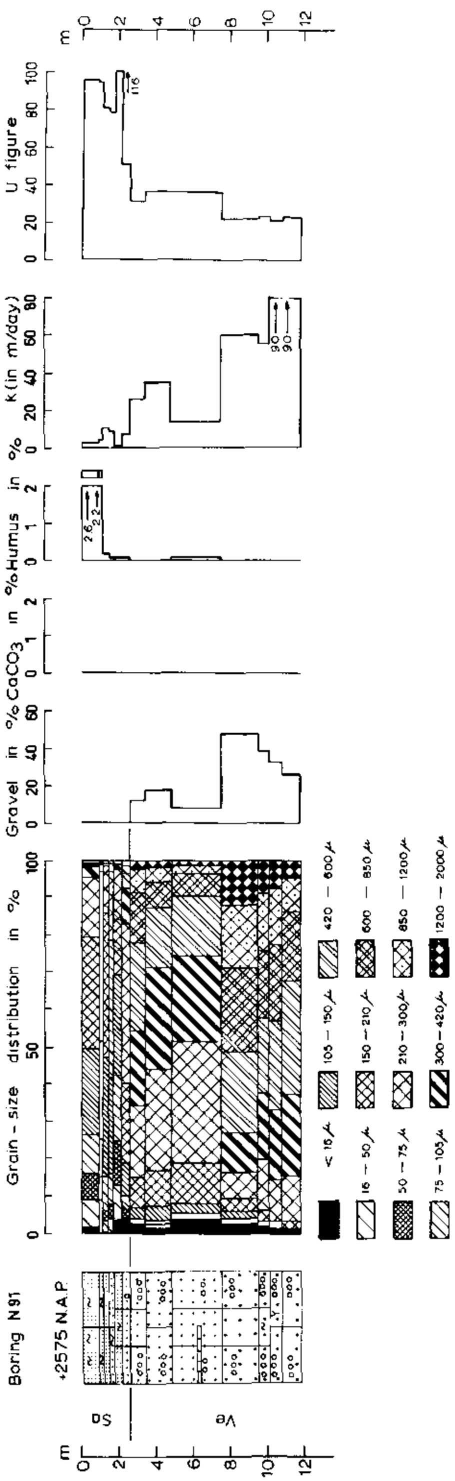

Boring N 91
+2575 N.A.P.
Sa
Ve
m
0
2
4
6
8
10
12
Grain - size distribution in %
0
50
100
Gravel in %
0
20
40
60
CaCO3 in %
0
1
2
% Humus in %
0
1
2
2.6
2.2
% K (in m/day)
0
20
40
60
80
90
90
U figure
0
20
40
60
80
100
116
< 16 μ
16 — 50 μ
50 — 75 μ
75 — 105 μ
105 — 150 μ
150 — 210 μ
210 — 300 μ
300 — 420 μ
420 — 600 μ
600 — 850 μ
850 — 1200 μ
1200 — 2000 μ

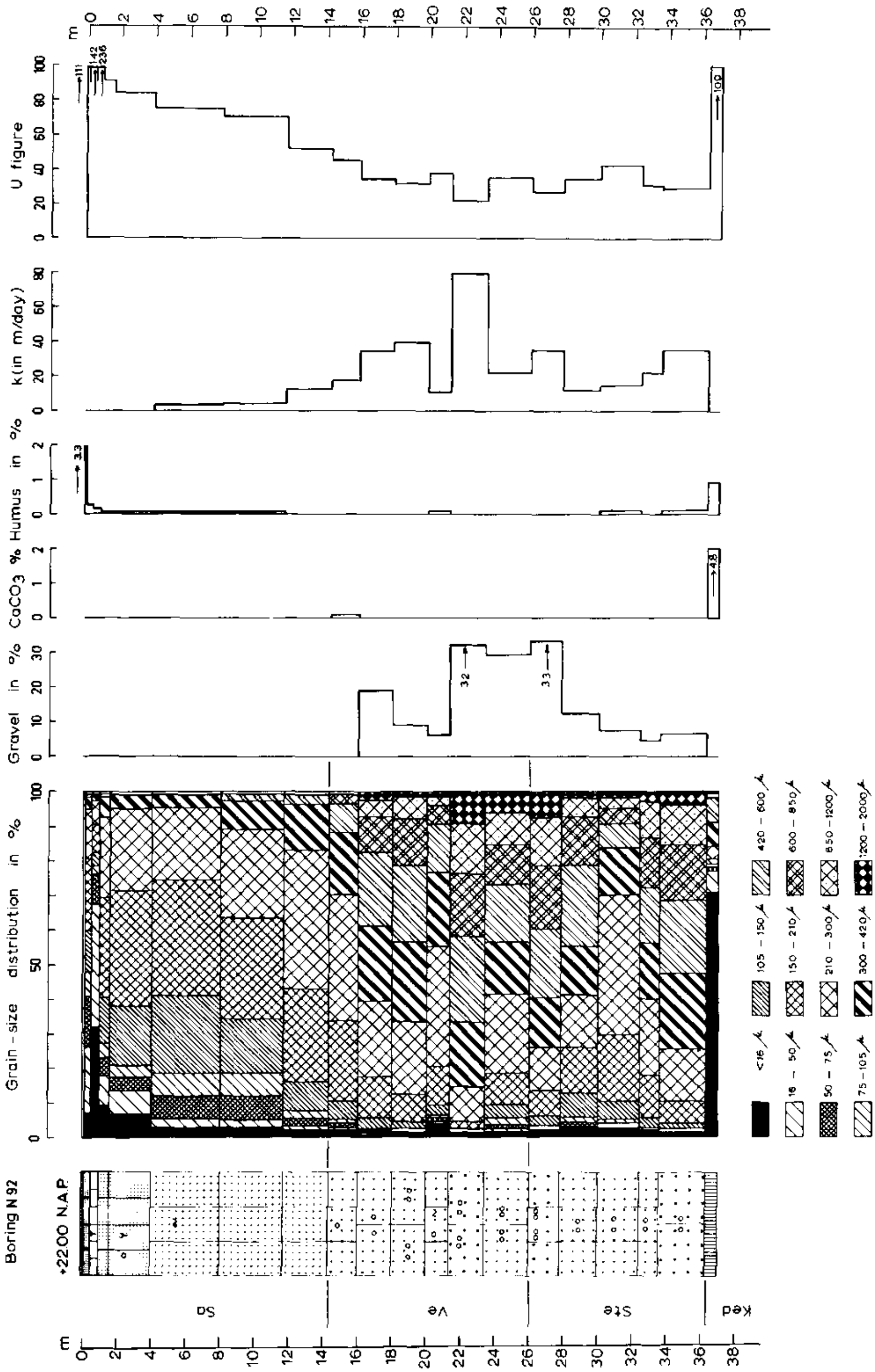
Boring N 92
+22.00 N.A.P.
Grain - size distribution in %
Gravel in %
CaCO3 %
Humus in %
k (in m/day)
U figure
Sa
Ve
Ste
Ked
m
<16 µ
16 - 50 µ
50 - 75 µ
75 - 105 µ
105 - 150 µ
150 - 210 µ
210 - 300 µ
300 - 420 µ
420 - 600 µ
600 - 850 µ
850 - 1200 µ
1200 - 2000 µ

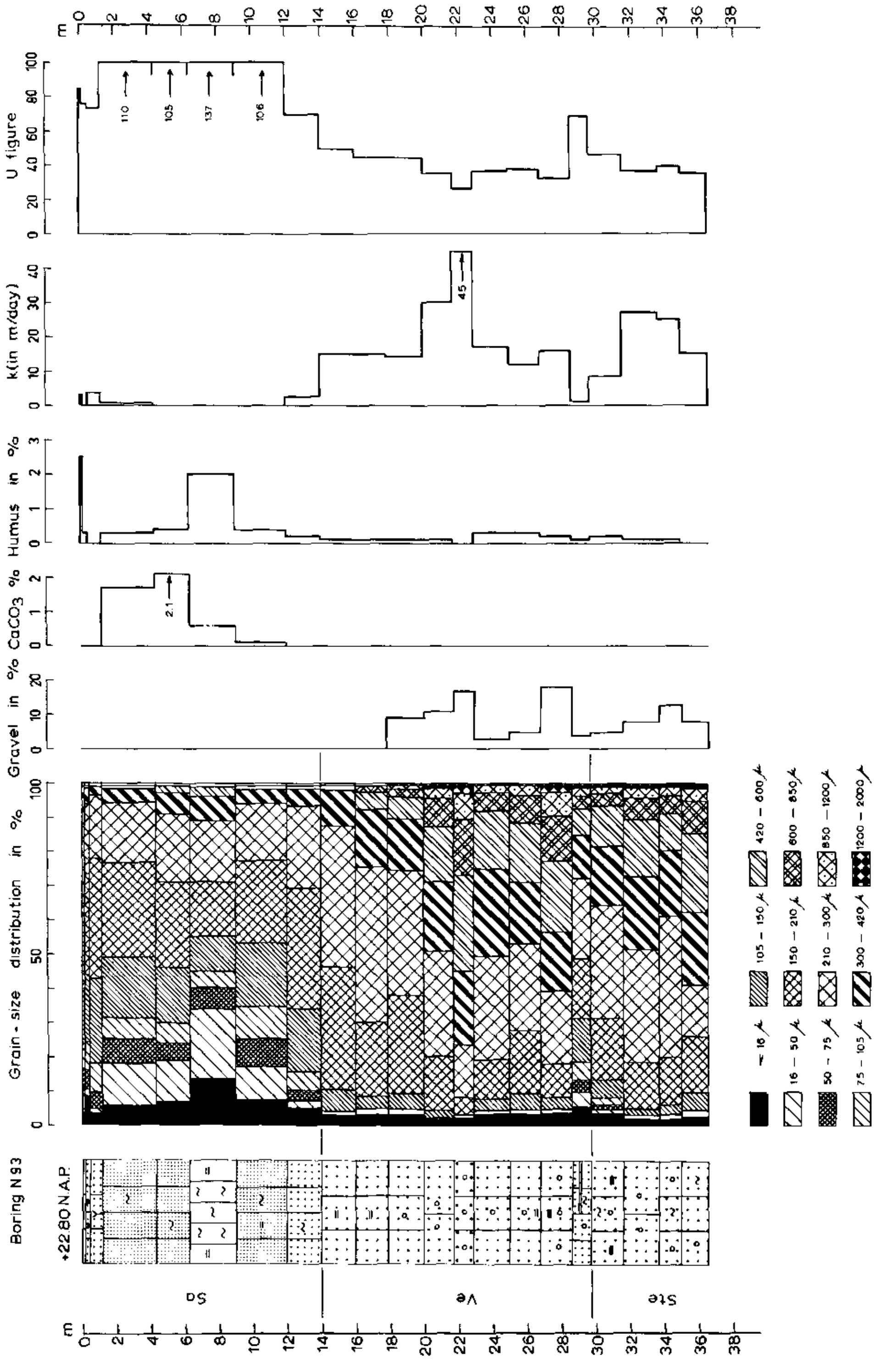
Boring N 93
+22.80 N.A.P.
Grain - size distribution in %
Gravel in %
$CaCO_3$ %
Humus in %
k(in m/day)
U figure
m
Sa
Ve
Ste
110
105
137
106
45
2.1
< 16 µ
16 – 50 µ
50 – 75 µ
75 – 105 µ
105 – 150 µ
150 – 210 µ
210 – 300 µ
300 – 420 µ
420 – 600 µ
600 – 850 µ
850 – 1200 µ
1200 – 2000 µ

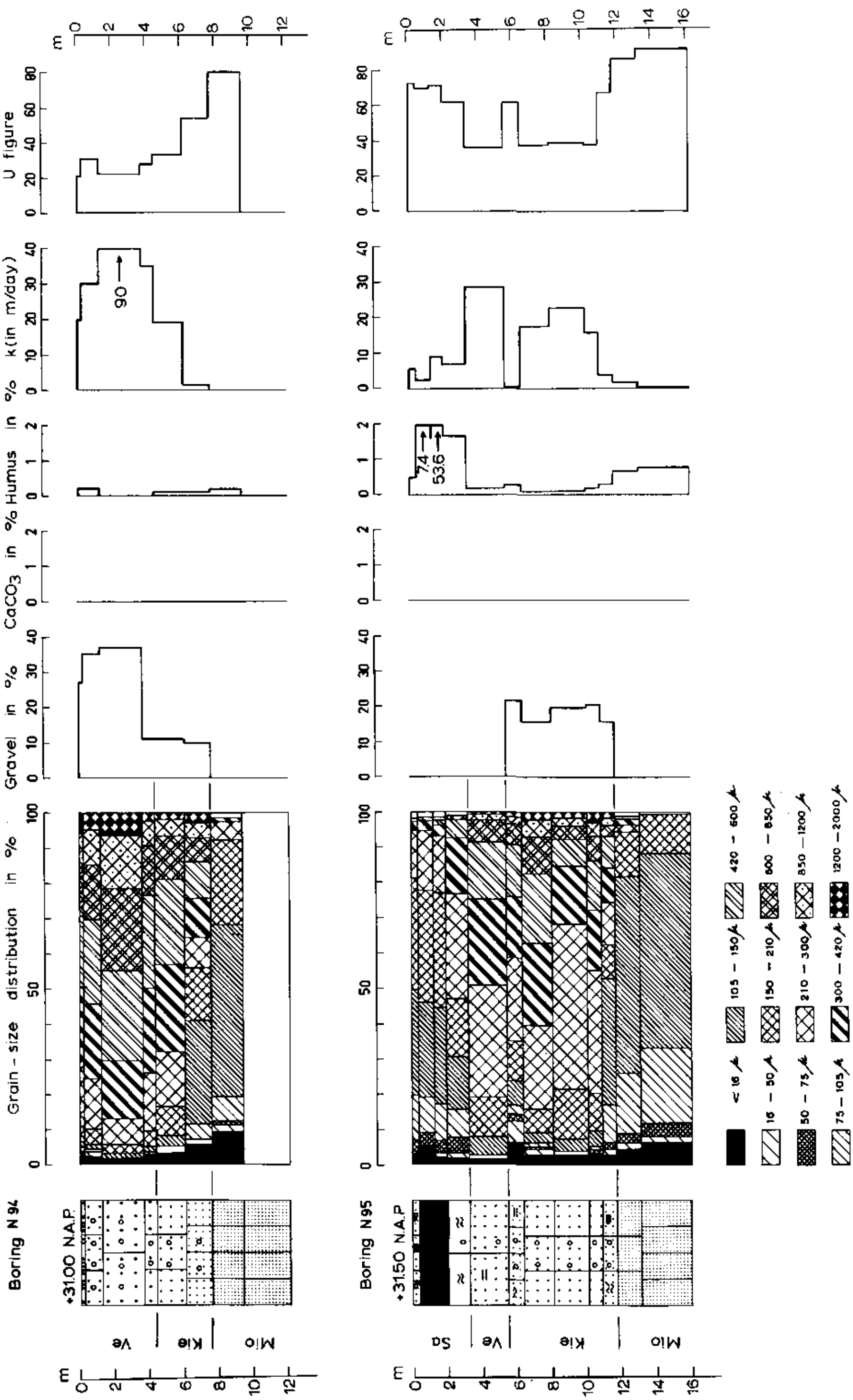
Boring N 94
+31.00 N.A.P.
Boring N 95
+31.50 N.A.P.
Grain - size distribution in %
Gravel in %
CaCO3 in %
% Humus in %
k (in m/day)
U figure
90
7.4
53.6
Sa
Ve
Kie
Mio
m
< 16 μ
16 – 50 μ
50 – 75 μ
75 – 105 μ
105 – 150 μ
150 – 210 μ
210 – 300 μ
300 – 420 μ
420 – 600 μ
600 – 850 μ
850 – 1200 μ
1200 – 2000 μ

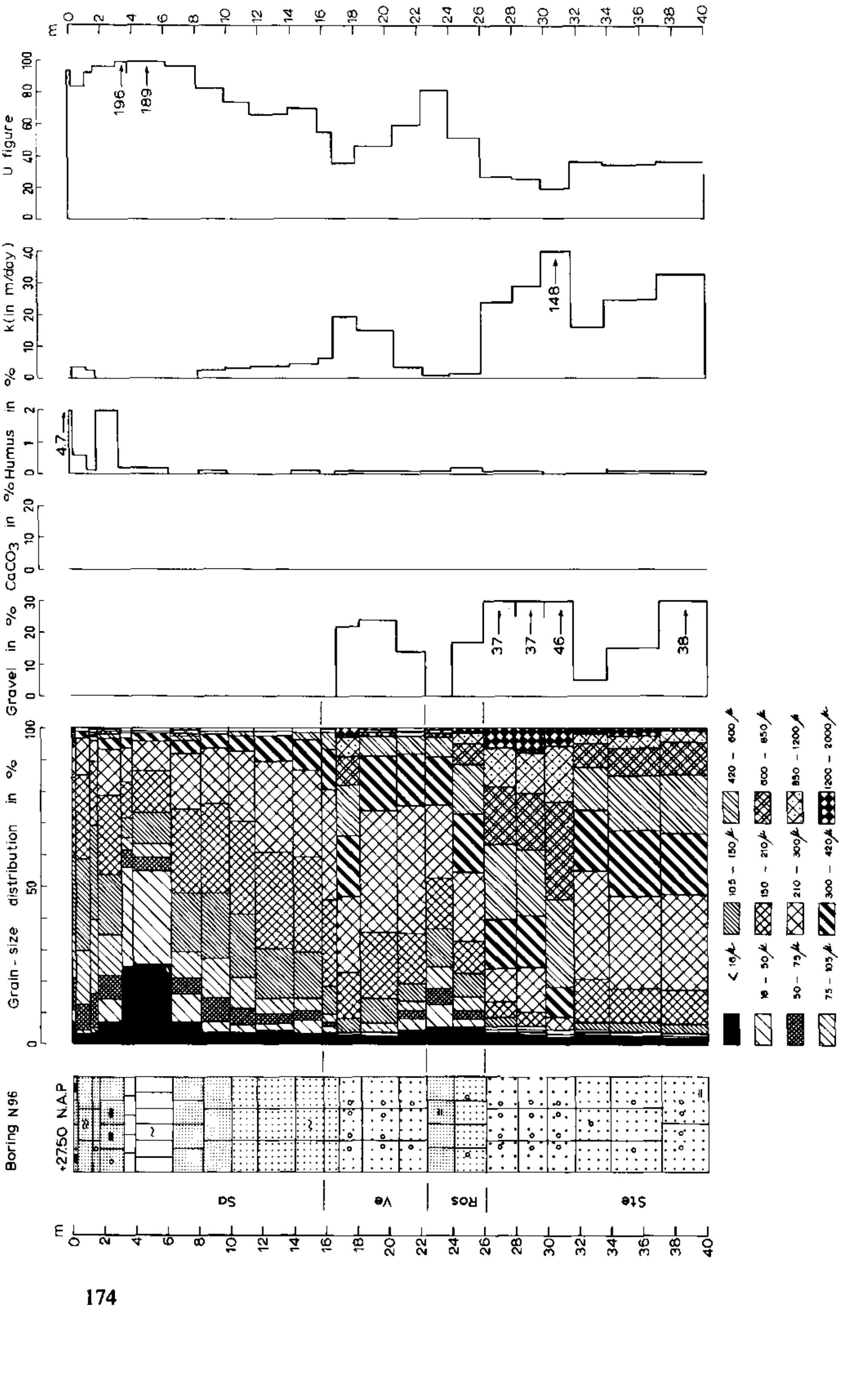
Boring N96
+27.50 N.A.P.
Grain - size distribution in %
Gravel in %
CaCO3 in %
Humus in %
k (in m/day)
U figure
Sa
Ve
Ros
Ste
196
189
148
4.7
37
37
46
38
< 16 μ
16 - 50 μ
50 - 75 μ
75 - 105 μ
105 - 150 μ
150 - 210 μ
210 - 300 μ
300 - 420 μ
420 - 600 μ
600 - 850 μ
850 - 1200 μ
1200 - 2000 μ

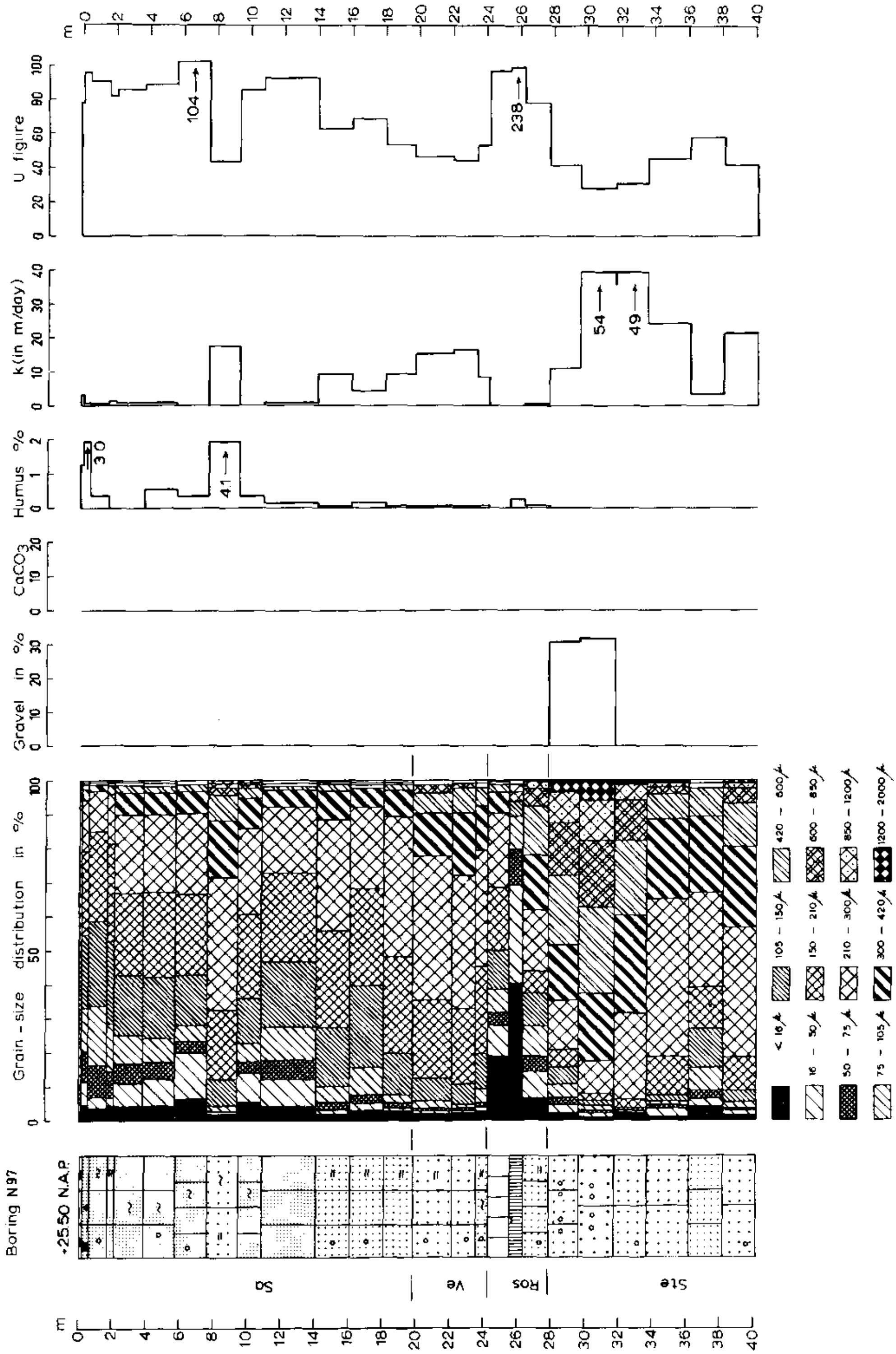

m
U figure
104
238
k (in m/day)
54
49
Humus %
30
41
$CaCO_3$
Gravel in %
Grain - size distribution in %
< 16 µ
16 - 50 µ
50 - 75 µ
75 - 105 µ
105 - 150 µ
150 - 210 µ
210 - 300 µ
300 - 420 µ
420 - 600 µ
600 - 850 µ
850 - 1200 µ
1200 - 2000 µ
Boring N97
+25.50 N.A.P.
Sa
Ve
Ros
Ste

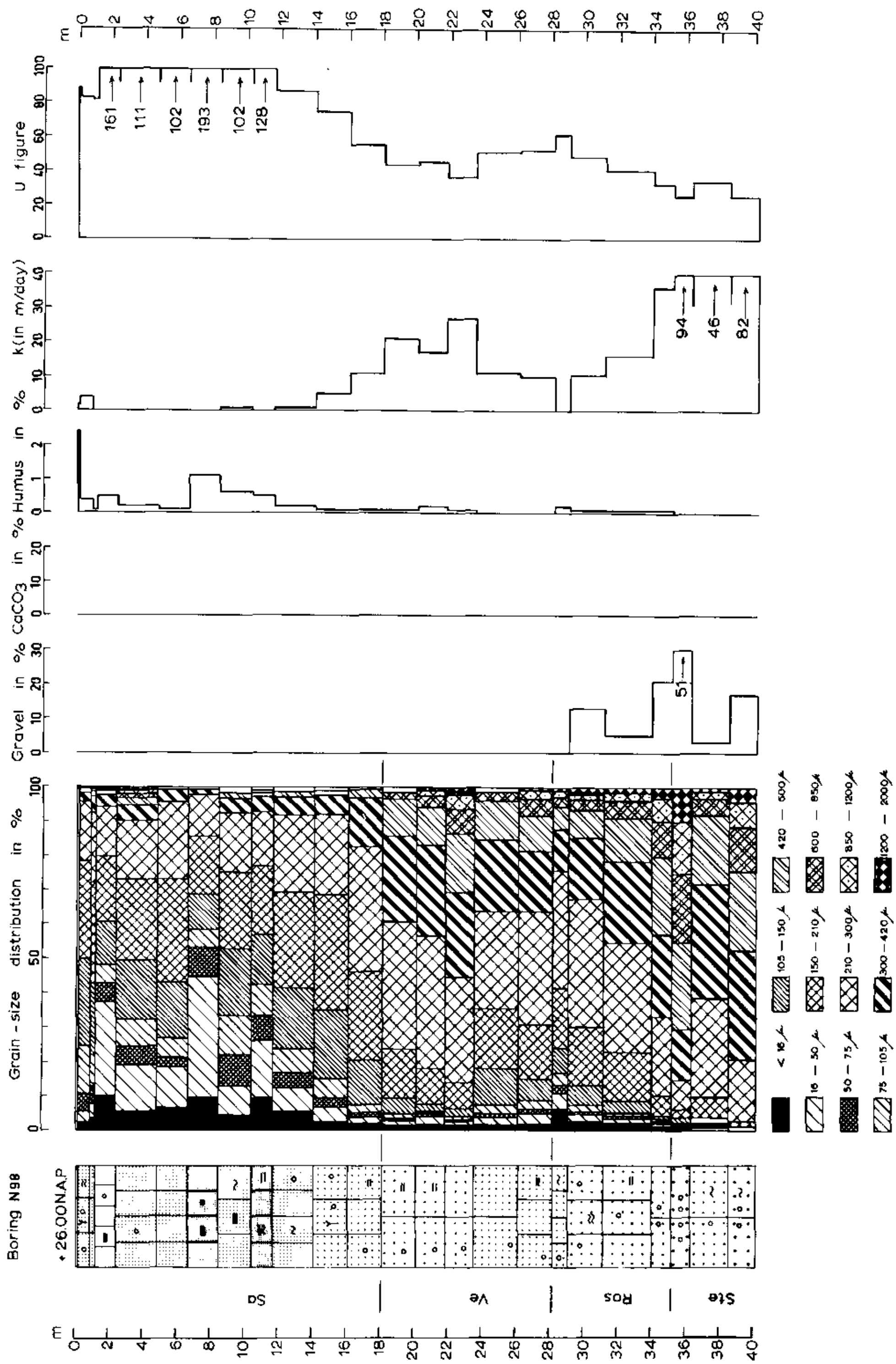
Boring N98
+26.00N.A.P
Sa
Ve
Ros
Ste
Grain - size distribution in %
Gravel in %
CaCO3 in %
Humus in %
k (in m/day)
U figure
161
111
102
193
102
128
94
46
82
51
< 16 µ
16 — 50 µ
50 — 75 µ
75 — 105 µ
105 — 150 µ
150 — 210 µ
210 — 300 µ
300 — 420 µ
420 — 600 µ
600 — 850 µ
850 — 1200 µ
1200 — 2000 µ

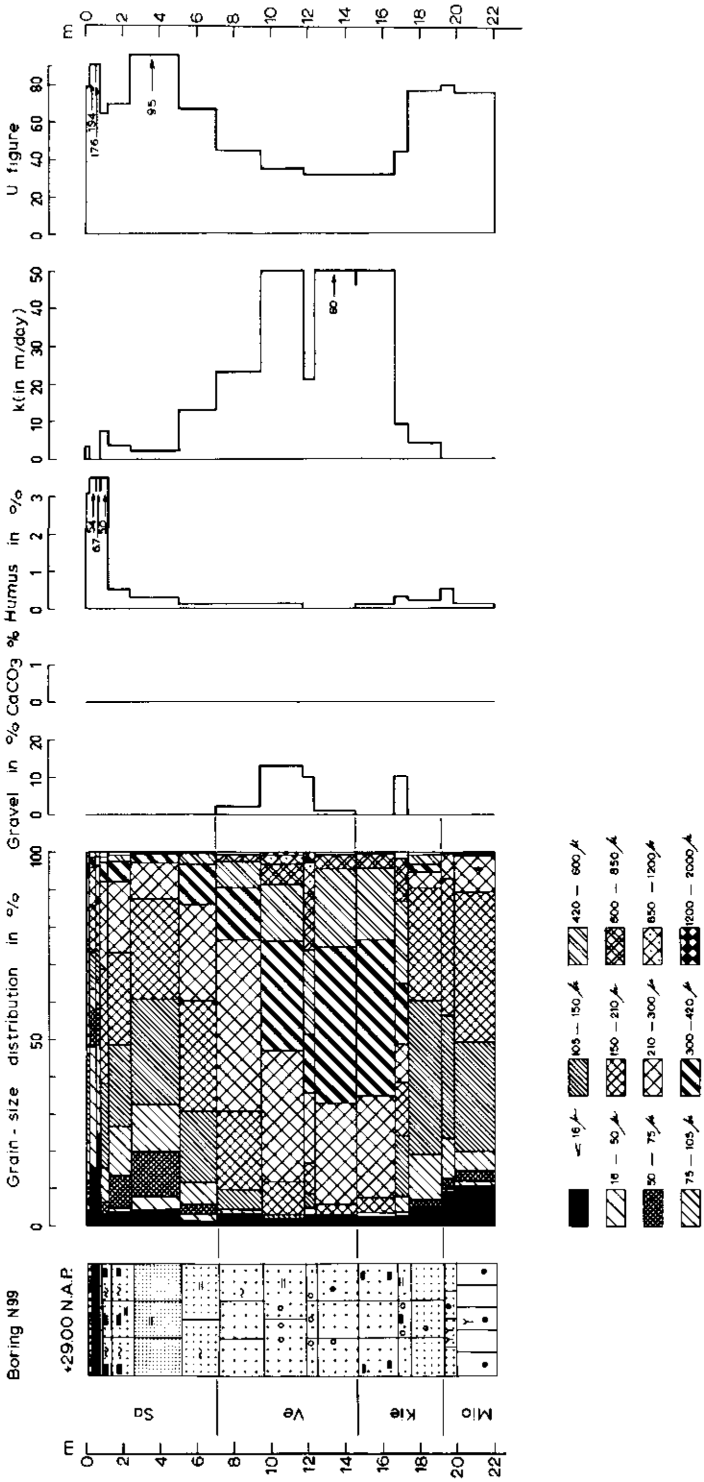

Boring N99
+29.00 N.A.P.
Grain - size distribution in %
Gravel in %
CaCO3 %
Humus in %
k (in m/day)
U figure
m
Sa
Ve
Kie
Mio
< 16 μ
16 — 50 μ
50 — 75 μ
75 — 105 μ
105 — 150 μ
150 — 210 μ
210 — 300 μ
300 — 420 μ
420 — 600 μ
600 — 850 μ
850 — 1200 μ
1200 — 2000 μ